



Introduction of metal-oxo nanostructures associated with ionic liquids for the design of multi-functional polymer materials

Houssem Chabane

► To cite this version:

Houssem Chabane. Introduction of metal-oxo nanostructures associated with ionic liquids for the design of multi-functional polymer materials. Materials. Université de Lyon, 2021. English. NNT : 2021LYSEI042 . tel-03400998

HAL Id: tel-03400998

<https://theses.hal.science/tel-03400998>

Submitted on 25 Oct 2021

HAL is a multi-disciplinary open access archive for the deposit and dissemination of scientific research documents, whether they are published or not. The documents may come from teaching and research institutions in France or abroad, or from public or private research centers.

L'archive ouverte pluridisciplinaire **HAL**, est destinée au dépôt et à la diffusion de documents scientifiques de niveau recherche, publiés ou non, émanant des établissements d'enseignement et de recherche français ou étrangers, des laboratoires publics ou privés.



N° d'ordre NNT : 2021LYSEI042

THESE de DOCTORAT DE L'UNIVERSITE DE LYON

opérée au sein de

L'Institut National des Science Appliquée de Lyon

Ecole Doctorale N° 34

Ecole Doctoral de Matériaux de Lyon

Spécialité de doctorat : Matériaux Polymères et Composites

Discipline : Matériaux

Soutenue publiquement le 09/07/2021, par :

Houssém CHABANE

INTRODUCTION OF METAL-OXO NANOSTRUCTURES ASSOCIATED WITH IONIC LIQUIDS FOR THE DESIGN OF MULTI- FUNCTIONAL POLYMER MATERIALS

Devant le jury composé de :

BONGIOVANNI Roberta

McGRAIL Terry

TOURNILHAC François

DUSKOVA-SMRCKOVA

Miroslava

GERARD Jean-François

DUCHET-RUMEAU Jannick

LIVI Sébastien

Professor (Politecnico di Torino)

Professeur (University of Edinburgh)

Directeur de Recherche CNRS HDR (Paris)

Professeur (Academy of Sciences of the

Czech Republic)

Professeur (INSA de Lyon)

Professeur (INSA de Lyon)

Maitre de Conférences (INSA Lyon)

Examinatrice

Examineur

Rapporteur

Rapportrice

Directeur de thèse

Co-directrice de thèse

Co-directeur de thèse

Département FEDORA – INSA Lyon – Ecole Doctorales

SIGLE	ECOLE DOCTORALE	NOM ET COORDONNEES DU RESPONSABLE
CHIMIE	CHIMIE DE LYON https://www.edchimie-lyon.fr Sec. : Renée EL MELHEM Bât. Blaise PASCAL, 3e étage secretariat@edchimie-lyon.fr	M. Stéphane DANIELE C2P2-CPE LYON-UMR 5265 Bâtiment F308, BP 2077 43 Boulevard du 11 novembre 1918 69616 Villeurbanne directeur@edchimie-lyon.fr
E.E.A.	ÉLECTRONIQUE, ÉLECTROTECHNIQUE, AUTOMATIQUE https://edeea.universite-lyon.fr Sec. : Stéphanie CAUVIN Bâtiment Direction INSA Lyon Tél : 04.72.43.71.70 secretariat.edeea@insa-lyon.fr	M. Philippe DELACHARTRE INSA LYON Laboratoire CREATIS Bâtiment Blaise Pascal, 7 avenue Jean Capelle 69621 Villeurbanne CEDEX Tél : 04.72.43.88.63 philippe.delachartre@insa-lyon.fr
E2M2	ÉVOLUTION, ÉCOSYSTÈME, MICROBIOLOGIE, MODÉLISATION http://e2m2.universite-lyon.fr Sec. : Sylvie ROBERJOT Bât. Atrium, UCB Lyon 1 Tél : 04.72.44.83.62 secretariat.e2m2@univ-lyon1.fr	M. Philippe NORMAND Université Claude Bernard Lyon 1 UMR 5557 Lab. d'Ecologie Microbienne Bâtiment Mendel 43, boulevard du 11 Novembre 1918 69 622 Villeurbanne CEDEX philippe.normand@univ-lyon1.fr
EDISS	INTERDISCIPLINAIRE SCIENCES-SANTÉ http://ediss.universite-lyon.fr Sec. : Sylvie ROBERJOT Bât. Atrium, UCB Lyon 1 Tél : 04.72.44.83.62 secretariat.ediss@univ-lyon1.fr	Mme Sylvie RICARD-BLUM Institut de Chimie et Biochimie Moléculaires et Supramoléculaires (ICBMS) - UMR 5246 CNRS - Université Lyon 1 Bâtiment Raulin - 2ème étage Nord 43 Boulevard du 11 novembre 1918 69622 Villeurbanne Cedex Tél : +33(0)4 72 44 82 32 sylvie.ricard-blum@univ-lyon1.fr
INFOMATHS	INFORMATIQUE ET MATHÉMATIQUES http://edinfomaths.universite-lyon.fr Sec. : Renée EL MELHEM Bât. Blaise PASCAL, 3e étage Tél : 04.72.43.80.46 infomaths@univ-lyon1.fr	M. Hamamache KHEDDOUCI Université Claude Bernard Lyon 1 Bât. Nautibus 43, Boulevard du 11 novembre 1918 69 622 Villeurbanne Cedex France Tél : 04.72.44.83.69 hamamache.kheddouci@univ-lyon1.fr
Matériaux	MATÉRIAUX DE LYON http://ed34.universite-lyon.fr Sec. : Yann DE ORDENANA Tél : 04.72.18.62.44 yann.de-ordenana@ec-lyon.fr	M. Stéphane BENAYOUN Ecole Centrale de Lyon Laboratoire LTDS 36 avenue Guy de Collongue 69134 Ecully CEDEX Tél : 04.72.18.64.37 stephane.benayoun@ec-lyon.fr
MEGA	MÉCANIQUE, ÉNERGÉTIQUE, GÉNIE CIVIL, ACOUSTIQUE http://edmega.universite-lyon.fr Sec. : Stéphanie CAUVIN Tél : 04.72.43.71.70 Bâtiment Direction INSA Lyon mega@insa-lyon.fr	M. Jocelyn BONJOUR INSA Lyon Laboratoire CETHIL Bâtiment Sadi-Carnot 9, rue de la Physique 69621 Villeurbanne CEDEX jocelyn.bonjour@insa-lyon.fr
ScSo	ScSo* https://edsciencessociales.universite-lyon.fr Sec. : Mélina FAVETON INSA : J.Y. TOUSSAINT Tél : 04.78.69.77.79 melina.faveton@univ-lyon2.fr	M. Christian MONTES Université Lumière Lyon 2 86 Rue Pasteur 69365 Lyon CEDEX 07 christian.montes@univ-lyon2.fr

*ScSo : Histoire, Géographie, Aménagement, Urbanisme, Archéologie, Science politique, Sociologie, Anthropologie

Acknowledgements

First and foremost, I would like to thank my supervisors, Prof. Jean-François GERARD, Prof. Jannick DUCHET-RUMEAU, and Dr. Sébastien LIVI for their guidance, confidence in me, advice, and encouragement during the four years of this PhD work. I would like to thank them for always finding time for their PhD student and for always being here to overpass together all the challenges we had to face during this PhD work. I have learnt a lot from them, from their enthusiasm and wisdom. It has been a pleasure and an honor to work with them.

Besides my mentors, I would like to thank the members of the defense committee who accepted to examine this PhD work. I would like to thank Prof. BONGIOVANNI Roberta, and Prof. McGRAIL Terry for examining this manuscript, Prof. DUSKOVA-SMRCKOVA Miroslava, and Prof. TOURNILHAC François for reporting it. Tanks for their time, interest, insightful questions and helpful comments.

I also gratefully acknowledge the Algerian funding grant from the “*École Militaire Polytechnique*” that made my PhD work possible. A sincere thanks to all the teaching staff and officers, doctors and professors of the EMP, each of whom contributed directly or indirectly to this dissertation. These acknowledgements would not be complete without appreciating persons I worked with them in EMP laboratory as Dr. Zitouni SAFIDINE, my first supervisor, for all his support, his sharing and his precious advices. His encouragement was very important to bring me to France. Prof. Amar BOUKERROU and Dr. Abderrazak MOULOUE for helping me to be in contact with Prof. Jean-François GERARD about my thesis. In addition, Ababsa Halima SAADIYA, Dr. Ahmed MEKKI, Fouzia HAYOUNE, and Zakaria B.S. DJELLOUL for helping, pushing me up and teaching me the right way of science.

I would like to thank Dr. Rodolphe SONNIER and Dr. Catherine LADAVIERE for providing their time and giving me the chance to perform fire tests and MALDI TOF spectrometry in their laboratory (IMT Mines-Alès and IMP@Lyon1). I am grateful to them and to Dr. Hynek BENES, Dr. Baris DEMIR, and Dr. Xavier P. Morelle for their collaboration, their discussion, and contribution on my thesis and my papers.

This thesis was conducted in IMP Laboratory, INSA Lyon. Thus, I would like to thank all members of the laboratory for their hospitality, their support, and for their sympathy. I also want

to acknowledge Raphael BRUNEL and Guilhem QUINTARD for performing the trainings for the needed devices. Ahmed BELHADJ for the DSC, TGA; Patrick GOETINCK, Fernande BOISSON and Carlos FERNANDEZ DE ALBA for NMR test; Christelle BOULE for the TEM image at the Centre Technologique des Microstructures CTμ of the University of Lyon, Prof. Jocelyne GALY for the interesting discussions on the epoxy resins and Dr. Sebastien Pruvost for the dielectric measurements. Thanks the secretaries Isabelle POLO and Mallaouia BENGOUA for their kindness and for always being friendly to me. Thank you to all PhD students and postdoc researchers in the lab who spent their time to help me with the equipment and experiments. In addition, I am grateful to Dr. Nour HALAWANI for all her support and sharing in the laboratory, for all the discussions about the preparation of epoxy resins and thanks to her for being my friends in all the time. A special gratitude is addressed to Ahmed BELHADJ and Ismaïl BEN YOUSSEF for all the moments and discussions that we spent together, sharing all the difficulties and happiness in being far away from home, for being as brothers.

My time at IMP was made enjoyable in large part due to the many friends and groups that became a part of my life. I will never forget the PhD students and friends with whom I have shared offices as Emma DELAMARCHE, Marie CROUILLERE, Amel TERRAS, Baptiste GAUMOND, Joris ROUSSEAU, David RUGGI, Luxiao CHAI, and Benoit CAPRIN. Thanks my dear best friends Ting SHI and Alexei RADCHENKO for the scientific discussions, for being my friends instead of colleagues, for interesting talks about everything in life, for the support that I received and for always making me smile. I also appreciate all of their contributions of time and ideas for my PhD experience. Again, thank you Alexei RADCHENKO for teaching me the good ways of synthesizing ionic liquids and for our fruitful collaboration. Personally, I consider them as a sister and brother to whom I can ask for advice and suggestions. And above all, I appreciate all other PhD students and postdocs for spending time with me during my PhD.

Finally, a special thanks to my dears: to my parents for their love, for their phone calls every day just to know if I am OK, for their support and encouragement. To my brother Raphique and my sisters, as well as my grandmothers, my grandfathers and my aunts for telling me to follow my dream. Last but not least, to my wife to always stay by my side when I needed her, to support me and to love me as who I am. I would like to thank them all, for their motivation, patience and support in everything in my life and especially during these four years of PhD work. Their support means a lot and makes always the difference. I would like to thank as well all my

Algerian friends and my students, especially Yazid STATRA, Djamel ATTIA, Abdelmoheiman Zakaria BENBOUZID, Houcine BEKIS, Houssém DOUKHI and Nouredine BOUMDOUHA for their support, for their friendship, for listening to me when I need help and for their encouragements always contribute to the good motivation.

Thank you all and merci beaucoup!

Houssém CHABANE

Lyon / July 2021

Abstract

In recent years, significant advancement in the synthesis, characterization and association with different types of polymers, thermoplastics or reactive (thermosetting) systems of ionic liquids with tunable nature (ammonium, imidazolium, and phosphonium) open up new perspectives in the field of polymers, in particular in one of epoxy networks. It has been shown that ionic liquids (ILs) could contribute to host polymers as they can act as nanostructuring agents, interfacial agents of nanofillers (ionic exchanges with lamellar silicates or grafted onto silica nanofillers), or even as reagent intervening on the polymerization mechanism. Thus, enhanced physical behaviors (mechanical, surface, thermal resistance, etc.) which cannot be obtained with conventional approaches could be achieved. Furthermore, according to numerous studies, it has also been shown that organic-inorganic (O/I) objects such as metal-oxo clusters of the POSS[®] (PolyOligomericSilsexqioxanes) could be incorporated into polymers. In particular, in networks based on epoxy or methacryate, POSS[®] could act as co-monomer and/or self-assemble as O/I nanostructures in order to confer specific functionalities. This thesis work presents the preparation, characterization and modification of epoxy/amine or epoxy IL/amine by IL-modified POSS[®] nanoclusters. The first part of this work is dedicated to study the effect of the grafting of imidazolium ionic liquid onto POSS[®] carrying different organic ligands (isobutyl or phenyl) on the formation of uniform and well-dispersed POSS[®] nanodomains in the epoxy-amine networks. In the second part, the effect of the nanostructuration of IL-g-POSS^{®Ph} within the epoxy/amine network on the properties, including thermal stability, surface properties, mechanical, and fire behavior will be examined. In the last section, new epoxy IL (ILM/IPD) hybrid O/I networks have been implemented. For this, diepoxyde salts (ILMs) were synthesized and then copolymerized with a diamine hardener (IPD) with or without the presence of POSS^{®Ph}-triol or IL-g-POSS^{®Ph}. Such routes were investigated in order to design flexible epoxy IL hybrid networks (ILM/amine/IL-g-POSS^{®Ph}) exhibiting very interesting and multifunctional properties compared to conventional epoxy networks.

Keywords: Ionic Liquid; Polyhedral Oligomeric Silsesquioxane (POSS[®]); Epoxy Network; Organic-Inorganic Nanomaterials, Ionic Liquid Monomer, Nanostructured Network, Shape memory, Fire resistance, Ionic Conductivity.

Résumé

Au cours de ces dernières années, des avancées importantes ont été réalisées dans la synthèse, la caractérisation et l'association avec différents polymères, thermoplastiques ou systèmes réactifs (thermodurcissables) de liquides ioniques de nature divers (ammonium, imidazolium ou phosphonium) ouvrent de nouvelles perspectives dans le domaine des matériaux polymères, en particulier celui des réseaux époxyde. En effet, il a été démontré que les liquides ioniques (LI) pouvaient apporter beaucoup aux polymères en se comportant en tant qu'agents nanostructurants, agents interfaciaux de nanocharges (échanges ioniques avec les silicates lamellaires ou greffés sur des nanocharges de silice) ou encore en tant que co-monomères intervenant sur les mécanismes de polymérisation. Des comportements physiques améliorés (mécanique, de surface, de tenue thermique, etc.) peuvent être ainsi obtenus par des approches conventionnelles. Par ailleurs, au cours de nombreuses études, il a été également démontré que des objets organiques-inorganiques (O/I) comme des clusters de type métal-oxo ou POSS[®] (PolyOligomericSilSexqioxanes) pouvaient être incorporés dans des polymères, en particulier des réseaux de type polyépoxy ou méthacrylates, comme co-monomères et/ou être auto-assemblés sous forme de nanostructures O/I susceptibles de leur conférer des fonctionnalités spécifiques. Ce travail de thèse présente donc la préparation, la caractérisation et la modification de réseaux époxy/amine ou époxy LI/amine avec des POSS[®] modifiés par des LIs. Dans un premier temps, ce travail est dédié à étudier l'effet du greffage des liquides ioniques d'imidazolium sur des POSS[®] porteurs de différents ligands organiques (isobutyle ou phényle) sur la formation de nanodomains POSS[®] uniformément bien dispersés dans des réseaux époxy-amine. Dans la deuxième partie, l'effet de la nanostructuration des LI-g-POSS^{®Ph} sur les propriétés de réseaux époxy/amine, à savoir leur stabilité thermique, leurs propriétés de surface, leur comportement mécanique et leur tenue au feu sera étudié. Dans la dernière section, de nouveaux réseaux époxy-LI hybride O/I ont été mis en œuvre. Pour cela des sels diépoxydés (LIMs) ont été synthétisés puis copolymérisés avec un durcisseur diamine (IPD) avec ou sans la présence de POSS^{®Ph}-triol ou LI-g-POSS^{®Ph} afin de concevoir des réseaux époxy-LI hybride (LIM/amine/LI-g-POSS^{®Ph}) souples présentant des propriétés très intéressantes par rapport des réseaux époxy classiques.

Mots clés : Liquide Ionique; Polyhedral Oligomeric Silsesquioxane (POSS[®]); Epoxy; Nanomatériaux Organiques-Inorganiques, Liquide Ionique Monomère, Réseau Nanostructuré, Mémoire de Forme, Résistance au Feu, Conductivité Ionique.

Tables of contents

Acknowledgements	ii
Abstract	v
Résumé	vi
Tables of contents	vii
Lists of tables	xii
Lists of figures	xiii
General Introduction	1
Résumé Étendu	4
Chapter I: Literature Review	21
Table of contents	22
I.1.What are POSS[®] Compounds?	23
I.1.1. Molecular structure of a Polyhedral Polysilsesquioxane	23
I.1.2. Structure and dimensions of the inorganic core of a POSS [®] -T ₈	25
I.1.3. Organic structure of a POSS [®] -T ₈	25
I.2. Synthesis Strategies of POSS[®] Compounds	26
I.3. Interest of POSS[®] Compound	27
I.4. Macromolecular Structure	29
I.5. Structuration of POSS[®] in Thermosetting Polymers	30
I.6. POSS[®] and Epoxy Nanocomposites	31
I.6.1. Epoxy Networks	31
I.6.2 POSS [®] -modified Epoxy Polymers	34
I.6.2.1. Physical interaction.....	34
I.6.2.2. Epoxide POSS [®] as a precursor.....	37
I.6.2.3. POSS [®] containing curing agent.....	39
I.6.2.4. Influence of the POSS [®] content.....	44
I.6.2.5. Influence of the length of the ligand carrying the reactive function.....	45
I.6.2.6. Influence of nanostructuration.....	47
I.7. Functional Properties of POSS[®]-Modified Epoxy Polymer	48

I.7.1. Fire retardancy and thermal stability.....	49
I.7.2. Mechanical properties	55
I.7.3. Dielectric property.....	58
I.7.4. Conclusion.....	59
I.8. Ionic Liquids and Epoxy Polymers	60
I.8.1. Ionic liquids and their applications	60
I.8.2. ILs-modified epoxy network.....	62
I.8.3. Epoxy resin/imidazolium ILs curing mechanism.....	63
I.8.4. Epoxy/IL composites/nanocomposites.....	66
I.8.5. Conclusion.....	68
I.9. POSS[®] Ionic Liquids.....	68
I.10. Conclusion of chapter I	70
Reference of chapter I.....	71
Chapter II: Synthesis of Modified Ionic Liquid POSSs[®] and Study of Their Dispersions in an Epoxy-amine Matrix	92
Table of contents.....	93
II.1. Introduction	94
II.2. Experimental	96
II.2.1. Materials	96
II.2.2. Synthesis	96
II.2.2.1. Synthesis of the silylated imidazolium ionic liquid (Si-g-Im-Cl).....	96
II.2.2.2. Synthesis of monofunctional ionic liquid monomer (ILM).....	97
II.2.2.3. Synthesis of imidazolium ionic liquid grafted-POSS [®]	99
a. Monofunctional imidazolium ionic liquid grafted-POSS [®]	99
b. Difunctional ionic liquid grafted-POSS [®]	100
II.2.3. Epoxy network preparation.....	101
II.3. Results and discussion	102
II.3.1. Synthesis and characterization of imidazolium ionic liquid grafted-POSS [®]	102
II.3.1.1. Monofunctional imidazolium ionic liquid grafted-POSS [®]	102
a. Synthesis of IL-g-POSS [®]	102
b. Thermal characterization of the IL-g-POSS [®]	108

II.3.1.2. Difunctional imidazolium ionic liquid grafted-POSS [®]	111
a. Synthesis of POSS [®] -N-2IL	111
b. Thermal characterization of the POSS [®] -N-2IL	113
II.3.2. Morphology and glass transition of hybrid O/I networks containing IL-g-POSS [®] or POSS [®] -N-2IL	114
a. Morphology of hybrid O/I networks containing IL-g-POSS [®]	114
b. Morphology of hybrid O/I networks containing POSS [®] -N-2IL	117
c. Glass transition of hybrid O/I networks containing IL-g-POSS [®] or POSS [®] -N-2IL	118
II.4. Conclusion of chapter II	120
Supporting Information of chapter II	121
Reference of chapter II	126
Chapter III: Design and Properties of Nanostructured IL-g-POSS^{®Ph}/Epoxy-amine Hybrid Organic-Inorganic Networks	133
Table of contents.....	134
III.1. Introduction	135
III.2. Materials and characterization methods	138
III.2.1. Materials	138
III.2.2. Anionic exchange procedure of polyhedral oligomeric silsesquioxane (POSS ^{®Ph}) (Chloride Cl ⁻ versus bis(trifluoromethanesulfonyl)imide NTf ₂ ⁻)	139
III.2.3. Epoxy network synthesis	139
III.2.4. Determination of the soluble fraction extractable from hybrid O/I networks	140
III.2.5. Characterization.....	140
III.3. Results and Discussion	143
III.3.1. Curing of epoxy-amine and hybrid O/I networks.....	143
III.3.2. Morphology of hybrid O/I networks	146
III.3.3. Thermomechanical properties of the resulting networks	148
III.3.4. Mechanical properties.....	149
III.3.4.1. Elastic and large strain mechanical properties.....	149
III.3.4.2. Fracture properties.....	150
III.3.5. Surface properties	152
III.3.6. Thermal-oxidative stability.....	153

III.3.7. Fire resistance.....	155
III.3.7.1. Flammability.....	155
III.3.7.2. Fire behavior.....	156
III.4. Conclusion of chapter III.....	163
Supporting Information of chapter III.....	165
References of chapter III.....	169
Chapter IV: New Epoxy Thermosets Organic-Inorganic Hybrid Nanomaterials Derived from Imidazolium Ionic Liquid Monomers and POSS^{®Ph}.....	179
Table of contents.....	180
IV.1. Introduction.....	181
IV.2. Experimental.....	183
IV.2.1. Materials.....	183
IV.2.2. Synthesis of materials.....	184
IV.2.2.1. Synthesis of difunctional ionic liquid monomer (ILM1).....	184
IV.2.2.2. Synthesis of difunctional ionic liquid monomer (ILM2).....	186
IV.2.3. Epoxy network preparation.....	187
IV.2.4. Determination of the soluble fraction extractable from hybrid O/I networks.....	187
IV.2.5. Characterization.....	188
IV.3. Results and discussion.....	190
IV.3.1. Curing behavior of epoxy ILM/IPD: Reactivity study (DSC) and determination of the epoxy conversion (FTIR).....	190
IV.3.2. Thermomechanical properties of ILM/IPD networks.....	194
IV.3.3. Morphology investigation of ILM/IPD networks.....	198
IV.3.4. Thermal stability of ILM/IPD networks.....	199
IV.3.5. Surface energy of DGEBA/IPD and ILM/IPD networks.....	201
IV.3.6. Mechanical properties.....	201
IV.3.7. Shape memory.....	202
IV.3.8. Conclusion.....	205
IV.4. Epoxy hybrid ILM/IPD containing POSS^{®Ph}-triol or IL-g-POSS^{®Ph}.....	205
IV.4.1. Morphology of hybrid O/I networks.....	205
IV.4.2. Epoxy conversion and glass transition.....	208

IV.4.3. Thermo-oxidative stability	210
IV.4.4. Surface properties	213
IV.4.5. Ionic conductivity	215
IV.4.6. Conclusion	223
Supporting information of chapter IV	224
References of chapter IV	228
Chapter V: Conclusions and Perspectives	241

Lists of tables

Table I. 1: Recent works reported on thermal properties of epoxy networks modified by POSS [®] nanoclusters.	53
Table I. 2: Recent works reported on mechanical properties of epoxy networks modified by POSS [®] nanoclusters.	56
Table III. 1: Chemical structures of non-grafted and IL-grafted POSS [®]	138
Table III. 2: Mechanical properties of the neat epoxy-amine and the epoxy hybrid O/I networks measured under uniaxial compression (1 mm.min ⁻¹ ; 25 °C).....	150
Table III. 3: Fracture properties of the neat epoxy-amine and the epoxy hybrid O/I networks.	151
Table III. 4: Determination of dispersive and non-dispersive components of the surface energy of the neat epoxy-amine and the epoxy hybrid O/I networks from contact angles with water and methylene diiodide (at 25 °C).	153
Table III. 5: PCFC data of the neat epoxy-amine and the epoxy hybrid O/I networks.	156
Table III. 6: Cone calorimeter data of the neat epoxy-amine, the epoxy hybrid O/I networks, and the epoxy-amine networks containing IL.	158
Table IV. 1: Chemical formula of chemicals.	183
Table IV. 2: Thermomechanical data of the epoxy DGEBA/IPD and ILM/IPD networks (at 1Hz).....	196
Table IV. 3: Contact angle and surface energy of ILM1 (or ILM2)/IPD networks measured by sessile drop method at 25 °C.	201
Table IV. 4: Determination of dispersive and non-dispersive components of the surface energy on the neat epoxy ILM/IPD and the corresponding hybrid O/I networks from contact angle with water and methylene diiodide at 25 °C.	213
Table IV. 5: Ionic conductivity for the different epoxy ionic liquids networks at different temperatures.	220
Table IV. 6: Arrhenius law applied to ionic conductivity data at room temperature.....	222

Lists of figures

Figure I. 1: Different structures of polysilsesquioxane.....	24
Figure I. 2: Schematic organizations of POSS [®] clusters with respectively 8, 10, and 12 Si atoms.	24
Figure I. 3: Characteristic dimensions of the inorganic core of a T ₈ type POSS [®] (values determined by molecular modeling) ¹	25
Figure I. 4: Main synthesis strategies of POSS [®] ^{1,26}	27
Figure I. 5: Different macromolecular structures possible according to functionality (number of reactive functions carried by POSS [®]).	29
Figure I. 6: Some examples of morphologies obtained for epoxy hybrid O/I networks containing POSS [®] with different non-reactive groups: a) Ph-Gly-POSS [®] ⁴⁵ , b) Phenyl-POSS [®] ⁴⁶ , and c) AH-POSS [®] ⁴⁷	35
Figure I. 7: SEM micrographs of POSS [®] epoxy hybrid O/I networks containing: a) 5 wt. % of octanitrophenyl-POSS [®] and b) 10 wt. % of octaaminophenyl-POSS [®] ⁴⁸	36
Figure I. 8: Synthesis of the isocyanato-propyldinethylsilyl-isobutyl-POSS [®] (IPI-POSS [®])-modified epoxy (IPEP) ⁶¹	39
Figure I. 9: Fracture surfaces of neat epoxy a) and POSS [®] /epoxy nanomaterials containing b) 1 wt. % POSS [®] , and c) 5 wt. % POSS [®] ⁷⁸	42
Figure I. 10: SEM micrographs of resulting morphologies generated in DGEBA-MDEA epoxy networks modified with POSS [®] : a) pre-reacted Gly-iBu POSS [®] , b) pre-reacted Gly-Ph POSS [®] , and c) non-reactive OctaPh POSS [®] ^{45,53}	43
Figure I. 11: Effect of the POSS [®] molar fraction on the glass transition temperature of a) poly(acetoxystyrene) and b) poly(vinylpyrrolidone) ⁸³	45
Figure I. 12: A comparison of heat release rate (HRR) as a function of time for epoxy networks containing: a) Gly-Ph POSS [®] with Gly-IBu POSS [®] and b) Gly-Ph POSS [®] with octaphenyl POSS [®] ⁵³	50
Figure I. 13: Cross sections of cone calorimeter residues of POSS [®] -epoxy hybrid systems: a) neat epoxy-amine matrix, b) 3.7 inorg. wt. % pre-reacted Gly-Ph POSS [®] , and c) 3.7 inorg. wt. % OctaPh POSS [®] ⁵³	51

Figure I. 14: Representative snapshots of UL-94 tests and average residual weights after testing of a) TM, b) TM-POSS [®] , c) TM-POSS [®] -Al, d) MVR, e) MVR-POSS [®] OH, and f) MVR-POSS [®] -Al (the mixture of TGDDM or MVR444 with amine hardener, denoted TM or MVR, respectively) ⁴⁶	52
Figure I. 15: Structure of conventional used cations and anions of IL systems.	61
Figure I. 16: IL-modified clay dispersion in epoxy nanocomposite cured with a) imidazole (intercalation) and b) anhydride (exfoliation) ²⁰⁸	67
Figure I. 17: Epoxy-silica hybrids: a) without ILs and those formed in the presence of b) methyl sulfonate based IL, c) tetrafluoroborate based IL, and d) tetrafluoroborate based IL and hydrochloric acid ²¹⁰	67
Figure I. 18: a) Synthesis of POSS [®] -IL and b) structure of dumbbell-shaped octasilsesquioxanes functionalized with ILs ^{218,219}	69
Figure II. 1: IR spectra of POSS ^{®IB} -triol (upper curve) and IL-g-POSS ^{®IB} (lower curve).	103
Figure II. 2: IR spectra of POSS ^{®Ph} -triol (upper curve) and IL-g-POSS ^{®Ph} (lower curve).	103
Figure II. 3: (A): ²⁹ Si NMR spectra of a) POSS ^{®IB} -triol and b) IL-g-POSS ^{®IB} , (B): ²⁹ Si NMR spectra of a) POSS ^{®Ph} -triol, and b) IL-g-POSS ^{®Ph} . (solide state, 600 MHz)	104
Figure II. 4: Chemical formula of IL-g-POSS [®] obtained by corner-capping reaction from A) POSS ^{®IB} -triol with Si-g-Im-Cl and B) POSS ^{®Ph} -triol with Si-g-Im-Cl.	106
Figure II. 5: ¹ H NMR spectra of a) POSS ^{®IB} -triol and b) IL-g-POSS ^{®IB} (CDCl ₃ , 400 MHz). ..	107
Figure II. 6: ¹³ C NMR spectra of a) POSS ^{®IB} -triol and b) IL-g-POSS ^{®IB} (CDCl ₃ , 400 MHz). ..	107
Figure II. 7: ¹³ C NMR spectra of a) POSS ^{®Ph} -triol and b) IL-g-POSS ^{®Ph} (DMSO-d ₆ , 400 MHz).	108
Figure II. 8: DSC traces for IL-g-POSS [®] : IL-g-POSS ^{®IB} and IL-g-POSS ^{®Ph} (heating rate: 10 K.min ⁻¹).	109
Figure II. 9: TGA traces for: a) IL-g-POSS ^{®IB} with POSS ^{®IB} -triol and b) IL-g-POSS ^{®Ph} with POSS ^{®Ph} -triol (heating rate: 10 K.min ⁻¹ , atmosphere: nitrogen flow).	110
Figure II. 10: IR spectra of POSS [®] -NH ₂ (black curve) and POSS [®] -N-2IL (red curve).	111
Figure II. 11: Positive MALDI-TOF mass spectra of POSS [®] -N-2IL (Dithranol matrix).	112
Figure II. 12: DSC traces for a) POSS [®] -NH ₂ and b) POSS [®] -N-2IL (heating rate: 10 K.min ⁻¹)..	113

Figure II. 13: TGA and DTG traces for POSS [®] -N-2IL compared to the received product POSS [®] -NH ₂ (heating rate: 10 K.min ⁻¹ , atmosphere: nitrogen flow).	114
Figure II. 14: TEM images of the epoxy-amine networks with: a) POSS ^{®IB} -triol, b): IL-g-POSS ^{®IB} at different magnification (b ₁ ; b ₂), c) POSS ^{®Ph} -triol, and d): IL-g-POSS ^{®Ph} at different magnifications (d ₁ ; d ₂).....	115
Figure II. 15: Size distribution of POSS [®] -rich dispersed phase in the epoxy matrix containing a) POSS ^{®IB} -triol, b) IL-g-POSS ^{®IB} , c) POSS ^{®Ph} -triol and d) IL-g-POSS ^{®Ph}	116
Figure II. 16: TEM images of the epoxy-amine networks containing POSS [®] -NH ₂ at different magnifications.	117
Figure II. 17: TEM images of the epoxy-amine networks containing POSS [®] -N-2IL at different magnifications.	118
Figure II. 18: DSC traces of the epoxy-amine network and epoxy hybrid O/I nanomaterials containing a) POSS ^{®IB} -triol, IL-g-POSS ^{®IB} , POSS ^{®Ph} -triol, IL-g-POSS ^{®Ph} , and b) with POSS [®] -N-2IL and POSS [®] -NH ₂ (heating rate: 10 K.min ⁻¹).	119
Figure III. 1: DSC traces of the neat epoxy-amine and the epoxy hybrid O/I reactive systems containing 5 wt. % POSS ^{®Ph} -triol or IL-g-POSS ^{®Ph} functionalized with Cl ⁻ and NTf ₂ ⁻ (heating rate: 10 K.min ⁻¹).	144
Figure III. 2: Conversion of epoxide groups versus reaction time during the curing process of the neat epoxy-amine and the epoxy hybrid O/I networks containing POSS ^{®Ph} -triol and IL-g-POSS ^{®Ph} with different anions (Cl ⁻ and NTf ₂ ⁻).....	145
Figure III. 3: TEM micrographs of the epoxy hybrid O/I networks containing a) POSS ^{®Ph} -triol; b) IL.Cl-g-POSS ^{®Ph} at different magnifications (b ₁ ; b ₂) and c) IL.NTf ₂ -g-POSS ^{®Ph} at different magnifications (c ₁ ; c ₂).	146
Figure III. 4: Size distributions of POSS [®] -rich dispersed phases in the epoxy hybrid O/I networks containing a) POSS ^{®Ph} -triol and b) IL-g-POSS ^{®Ph} with different types of anion (Cl ⁻ and NTf ₂ ⁻).....	147
Figure III. 5: a) Dynamic mechanical spectra and b) shear storage moduli in the rubbery state, G' _c (at 200 °C) of the epoxy-amine and the epoxy hybrid O/I networks containing POSS ^{®Ph} -triol and IL-g-POSS ^{®Ph} (5 wt.%) with different anions (Cl ⁻ and NTf ₂ ⁻) at 1 Hz.	148
Figure III. 6: Stress-strain curves under uniaxial compression of the neat epoxy-amine and the epoxy hybrid O/I networks (1 mm.min ⁻¹).	149

Figure III. 7: SEM images of fractured surfaces of a) the neat epoxy-amine and the epoxy hybrid O/I networks containing b) POSS ^{®Ph} -triol, c) IL.Cl-g-POSS ^{®Ph} , and d) IL.NTf ₂ -g-POSS ^{®Ph}	151
Figure III. 8: a) Weight loss (TGA) and b) derivative of TGA as a function of temperature (DTG) of the neat epoxy-amine and the corresponding epoxy hybrid O/I networks (10 K.min ⁻¹ , atmosphere: air flow).	154
Figure III. 9: PCFC HRR traces of the neat epoxy-amine, the epoxy hybrid O/I networks, and the epoxy-amine networks containing IL.....	156
Figure III. 10: Cone calorimeter HRR curves of the neat epoxy-amine, the epoxy hybrid O/I networks, and the epoxy-amine networks containing IL.	157
Figure III. 11: Cone calorimeter residue of a) the neat epoxy-amine and the epoxy hybrid O/I networks containing b) POSS ^{®Ph} -triol, c) IL.Cl-g-POSS ^{®Ph} , d) IL.NTf ₂ -g-POSS ^{®Ph} . Epoxy networks containing e) IL.Cl and f) IL.NTf ₂	159
Figure III. 12: Pictures from cone calorimeter test of the epoxy hybrid O/I networks containing a) IL.NTf ₂ -g-POSS ^{®Ph} and b) IL.Cl-g-POSS ^{®Ph}	160
Figure III. 13: Temperature curves of the top surface during cone calorimeter tests for epoxy hybrid O/I networks containing IL.Cl-g-POSS ^{®Ph} and IL.NTf ₂ -g-POSS ^{®Ph}	161
Figure III. 14: Pictures obtained using thermal camera from cone calorimeter test of the epoxy hybrid O/I networks containing IL.NTf ₂ -g-POSS ^{®Ph} and IL.Cl-g-POSS ^{®Ph}	162
Figure IV. 1: DSC traces for a first heating run a) ILM1/IPD and b) ILM2/IPD reactive mixtures considering different amino hydrogen-to-epoxy stoichiometric ratios (heating rate: 10 K.min ⁻¹).	190
Figure IV. 2: Epoxy group conversion as a function of the reaction time and during temperature steps from FT-IR for a) DGEBA/IPD, b) ILM1/IPD and c) ILM2/IPD reactive systems.....	193
Figure IV. 3: (A): ¹³ C NMR spectrum of a) ILM1 and HR-MAS ¹³ C NMR spectrum of b) ILM1/IPD network; (B): ¹³ C NMR spectrum of a) ILM2 and HR-MAS ¹³ C NMR spectrum of b) ILM2/IPD network (DMSO-d ₆ , 400 MHz).....	194
Figure IV. 4: Shear storage modulus, G' (black), and loss factor, tan δ, (blue) as a function of temperature at 1 Hz for a) ILM1/IPD and for b) ILM2/IPD networks.	195
Figure IV. 5: DSC thermograms after curing of a) ILM1/IPD and b) ILM2/IPD (heating rate: 10 K.min ⁻¹).	197
Figure IV. 6: TEM images of a) ILM1/IPD and b) ILM2/IPD at different magnifications.	199

Figure IV. 7: a) Weight loss as a function of temperature (TGA) and b) derivative of TGA curves (DTG) of the epoxy-IL networks ILM1 (or ILM2)/IPD and the epoxy-amine DGEBA/IPD (10 K min ⁻¹ , atmosphere: nitrogen flow).....	200
Figure IV. 8: Stress-strain curves under tensile tests of a) ILM1/IPD and b) ILM2/IPD networks (uniaxial tension mode; 1 mm.min ⁻¹).	202
Figure IV. 9: Shape memory test of a) ILM1/IPD and b) ILM2/IPD networks.	204
Figure IV. 10: Remaining deformation vs. time dependence for a) ILM1/IPD and b) ILM2/IPD networks at different temperatures.	204
Figure IV. 11: TEM images of the different epoxy ILMs hybrid O/I networks containing (5 wt. %) POSS ^{®Ph} -triol, IL.Cl-g-POSS ^{®Ph} and IL.NTf ₂ -g-POSS ^{®Ph} respectively, prepared with ILM1 epoxy monomer (a, b, c), and with ILM2 (d, e, f).....	208
Figure IV. 12: DSC traces of the epoxy hybrid O/I networks containing (5 wt. %) POSS ^{®Ph} -triol, IL.Cl-g-POSS ^{®Ph} and IL.NTf ₂ -g-POSS ^{®Ph} respectively, prepared based on epoxy IL monomers a) ILM1, and b) ILM2 (heating rate: 10 K.min ⁻¹).	209
Figure IV. 13: Change of weight loss as a function of the temperature (TGA) and derivative of TGA curves (DTG) for the epoxy hybrid O/I networks containing POSS ^{®Ph} -triol, IL.Cl-g-POSS ^{®Ph} and IL.NTf ₂ -g-POSS ^{®Ph} respectively, prepared based on epoxy monomer a) ILM1, and on b) ILM2. (10 K.min ⁻¹ , atmosphere: air flow)	212
Figure IV. 14: Relative permittivity: a) ϵ'_r and b) ϵ''_r for DGEBA/IPD, ILM/IPD, and their corresponding epoxy hybrid O/I networks as a function of temperature, at 100 Hz.	217
Figure IV. 15: Evolution of AC conductivity as a function of frequency for a) DGEBA/IPD, b) ILM1/IPD, c) ILM2/IPD, d) ILM1/IPD/IL.Cl-g-POSS ^{®Ph} , e) ILM2/IPD/IL.Cl-g-POSS ^{®Ph} , f) ILM1/IPD/IL.NTf ₂ -g-POSS ^{®Ph} , and g) ILM2/IPD/IL.NTf ₂ -g-POSS ^{®Ph}	219
Figure IV. 16: Dependence of DC conductivity with temperature (extrapolated from AC conductivity values at 0.1 Hz). Solid black lines represents a regression to the Arrhenius equation.	222

Lists of schemes

Scheme I. 1: Synthesis of diglycidyl ether of bisphenol A (DGEBA).....	32
Scheme I. 2: Mechanism of addition reactions between epoxy and amino hydrogen groups with k_1 and k_2 reaction rate constants.....	33
Scheme I. 3: Etherification mechanism between epoxy and hydroxyl groups.	33
Scheme I. 4: Chain polymerization of epoxy prepolymer initiated by imidazole.....	34
Scheme I. 5: Proposed mechanism for curing reaction between imidazolium ILs with iodide anion and epoxy prepolymer.	64
Scheme I. 6: Curing mechanism for epoxy networks formation by 1,3-dialkyl imidazolium IL proposed by Spychaj's team ¹⁹⁵	65
Scheme II. 1: Reaction scheme for the synthesis of 1-(3-trimethoxysilylpropyl)-3-methyl-imidazolium chloride (Si-g-Im-Cl).	97
Scheme II. 2: Synthesis of the ILM.	99
Scheme II. 3: Synthesis of mono-functionalized imidazolium ionic liquid grafted POSS [®] (IL-g-POSS [®]).	99
Scheme II. 4: Synthesis of di-functionalized imidazolium ionic liquid grafted POSS [®] (POSS [®] -N-2IL).	100
Scheme III. 1: Synthesis of imidazolium ionic liquid-modified polyhedral oligomeric silsesquioxane (IL.NTf ₂ -g-POSS ^{®Ph}).	139
Scheme III. 2: Compact Tension specimen configuration.....	141
Scheme IV. 1: Synthesis of the ILM1.	185
Scheme IV. 2: Synthesis of the ILM2.	186
Scheme IV. 3: Possible reaction paths of epoxy-functionalized IL with IPD.....	191

General Introduction

The modification of polymer materials by the incorporation of organic/inorganic hybrid clusters and in particular of polyhedral polysilsesquoxanes, denoted POSS[®] attracted a large interest because they lead to organic/inorganic (O/I) materials which combine some excellent features of polymers (low density and easiness of synthesis-processing, high ability to be deformed and electric insulation properties) with the ones of the inorganic materials (high modulus and hardness, flame resistance and gas barrier properties). Nowadays, it is also part of a growing field in the research area of modified epoxy resins.

Epoxies are an important class of thermosetting polymers widely used in structural composite applications such as adhesives coatings and encapsulants for electronics in a wide range of industrial applications matrices. They are considered as high performance thermosetting polymer matrices and generally possess high modulus, low creep, and good adhesion to many substrates, as well as chemical and corrosion resistances. However, they remain brittle as they have a poor resistance to crack propagation and they display a poor intrinsic fire behavior. Strategies for improvement of such properties require the use of different modifiers such as block copolymer, thermoplastics, or inorganic nanoparticles. In fact, inorganic nanoparticles have been shown to enhance the inherent properties of epoxy systems. More precisely, silica filled composites show enhanced modulus and fracture toughness or SWNT (Single wall carbon nanotubes) composites enhanced electrical and thermal conductivity at low contents. GNP (Graphite nanophletelets) composites provide also improvement of modulus and electrical conductivity with a decrease in vapor permeation relative to an unmodified epoxy matrix. The incorporation of POSS[®] clusters leads to epoxy nanocomposites with specific features such as enhanced oxidative and thermal resistances, better flame retardancy, and improved dielectric and mechanical properties. Effective nanoscale dispersion of individual inorganic particles is required for nanocomposites to obtain such improvements of physical properties. Because of this, challenges with polyhedral oligomeric silsesquioxanes, which tend to agglomerate, are still to be addressed during synthesis and processing of nanostructured polymer-based composites.

POSS[®] are O/I hybrid nano-clusters made up of an inorganic core to which are covalently linked organic ligands carrying, or not, polymerizable functions. Not to mention the impact of POSS[®] on the physical properties of polymers, the scientific interests for such a type of clusters

arises essentially from *i*) their nanometric size (≈ 1.5 nanometer in diameter), *ii*) their polyhedral structure, and *iii*) their organic/inorganic hybrid character. Their perfectly defined molecular architecture opens the prospect of controlling the morphology, and therefore the properties, of materials from nanometer scale. Illustratively, we often use the term “nanobric” or “nano-building block” to define these nanoclusters. Thanks to the progress made in their synthesis, the very wide variety of organic ligands, both in terms of chemical nature and reactivity, allow POSS[®] to be introduced into a broad range of polymers covering thermoplastics and thermosets. Depending on the number of polymerizable functions carried by the clusters, they can be introduced as inert nano-objects dispersed in the polymer matrix or linked covalently to the polymer if they carry one or more reactive functions.

Recently, ionic liquids appeared as new reactive additives for epoxy monomers (or oligomers) and epoxy composite/nanocomposite networks. In fact, they can serve both as curing agent and as dispersion aids for epoxy composites/nanocomposites systems to get unprecedented properties. Ionic liquids are known as organic salts with a melting temperature lower than 100 °C. The unique properties of ionic liquids such as non-flammability, great thermal stability, low saturated vapor pressure, and high ionic conductivity gained the attention of both research and industry. However, the application of ionic liquids in the design of epoxy/POSS[®] nanocomposites has not been investigated. Thus, the main goals of this research is to control the structure and morphology of the epoxy-POSS[®] nanomaterials by using ILs as structural modifiers. This work will also analyze how the morphology architecture level is changed and leads to significant modifications of the physical properties of the resulting hybrid nanomaterials. In order to fulfill these objectives, this manuscript is divided into four chapters:

The **first chapter** will deal with a literature survey dedicated to the routes used for modifying conventional epoxy-amine networks. The first section will give a global vision of “POSS[®] technology” from the description of their molecular structure, their synthesis, their incorporation into epoxy polymer materials, and the resulting properties of the POSS[®]-based materials according to the different morphologies which could be generated. The second section will focus on the use of imidazolium ionic liquids in the epoxy networks, *i.e.* on the synthesis and development of new functionalized ILs and the use of ionic liquids as additives or co-monomers to prepare epoxy systems. In particular, this part will be dedicated to know how ionic liquids can be used as a way of dispersing nano-objects in epoxy composites/nanocomposites systems.

The **second chapter** will be dedicated to discover the effect of grafting imidazolium ionic liquid on POSS[®] with different organic ligands (isobutyl or phenyl) on the formation of uniform and well-dispersed POSS[®] nanodomains into epoxy-amine networks. First, two types of ILs based on an imidazolium core containing different counter anions and reactive groups were synthesized and characterized in order to react with POSS[®]. In the second part, the synthesis and characterization of two monofunctionalized imidazolium ionic liquid based-POSS[®], hereafter named IL-g-POSS^{®iB} and IL-g-POSS^{®Ph} starting with a partially condensed POSS[®] named POSS^{®iB}-triol and POSS^{®Ph}-triol, and a difunctionalized imidazolium ionic liquid (POSS[®]-N-2IL) starting from POSS[®] bearing two amino-hydrogen functions (POSS[®]-NH₂). The molecular structure of the resulting IL-g-POSS[®] was determined using ¹H, ¹³C, and ²⁹Si NMR, as well as MALDI-TOF mass spectrometry including its thermal properties (by DSC, and TGA). Finally, the preparation of epoxy nanomaterials based on POSS[®]-triols, POSS[®]-NH₂ and IL-g-POSS[®] will be described. The morphology and thermal properties of hybrid O/I nanomaterials will be investigated by using transmission electron microscopy (TEM).

The **third chapter** will describe the application of IL-g-POSS^{®Ph} with different anions as new additives of epoxy-amine networks and how they can influence their properties. First, the preparation of epoxy nanomaterials based on POSS[®], *i.e.* unmodified POSS[®] (POSS^{®Ph}-triol) and IL-modified POSS^{®Ph} with different anions (Cl⁻ and NTf₂⁻) and their influence on the curing behavior of the epoxy prepolymer will be described. Then, a systematic comparison of properties, *i.e.* morphologies (TEM), thermal properties (DSC), thermomechanical properties (DMA), compressive properties, fracture toughness, surface properties (sessile drop method), thermal stability (TGA), fire and combustion behaviors (pyrolysis-combustion flow calorimetry PCFC and cone calorimetry) for the different hybrid O/I networks will be investigated.

The **final chapter** will discuss the synthesis of two new epoxy-functionalized imidazolium ionic liquid monomers (ILMs) which can substitute bisphenol A diglycidyl ether (DGEBA) as starting material, *i.e.* avoiding the use of highly toxic and carcinogenic bisphenol A and epichlorohydrin products. Networks synthesized from their copolymerization with the isophorone diamine (IPD) will be prepared. This chapter will focus also on the formation of new nanomaterials based on the combination of IL-g-POSS[®] and epoxy ionic liquid monomers (ILMs) in order to design environmentally friendly materials with unprecedented performances.

Résumé Étendu

Introduction générale

La modification des matériaux polymères par l'incorporation des métal-oxo clusters hybrides organiques/inorganiques et en particulier de polysilsesquoxanes polyédriques, ou POSS® (PolyOligomericSilsexqioxanes), suscite un large intérêt grandissant car elle permet de concilier les excellentes caractéristiques de polymères (faible densité et facilité de synthèse-traitement, capacité de déformation, propriétés d'isolation électrique) et leur combinaison avec celles des matériaux inorganiques (important module élastique et dureté élevée, propriétés ignifuges et barrière aux gaz). De nos jours, un domaine en pleine croissance est celui des matériaux thermodurcissables à base d'époxy où des nanoclusters de type POSS® peuvent être incorporés en tant que co-monomères et/ou être auto-assemblés sous forme de nanostructures O/I afin de conférer des fonctionnalités spécifiques aux nanomatériaux résultants.

Les époxydes sont une classe importante de polymères thermodurcissables très utilisés dans un large éventail d'industries depuis les applications au sein de composites structuraux ou les revêtements/adhésifs jusqu'à l'encapsulation pour l'électronique. Ils permettent une application très réversible grâce à leur polyvalence, à leur facilité d'utilisation et leur comportement thermomécanique associés à leur faible densité. Ils sont considérés comme des matrices polymères thermodurcissables de haute performance puisqu'ils possèdent généralement un module élevé, un fluage sous charge limité, une bonne adhérence à de nombreux matériaux de substrat et une excellente tenue diélectrique ainsi qu'une grande résistance aux produits chimiques et à la corrosion. Cependant, ils sont de nature fragile, avec une mauvaise résistance à la propagation des fissures, un mauvais comportement intrinsèque au feu et une faible permittivité relative qui limitent aujourd'hui leurs applications dans certains domaines comme par exemples l'électronique et l'aéronautique. Différents modificateurs tels que : des copolymères à blocs, des thermoplastiques de haute T_g , des élastomères ou des nanoparticules ont été utilisés pour faire face à ces limitations. La recherche sur la solution optimale qui vise à améliorer une propriété sans impact sur une autre est toujours d'actualité. Par exemple, il a été démontré que des nanoparticules de différentes natures améliorent les propriétés inhérentes des systèmes époxy comme dans le cas des composites à base de nanosphère de silice qui présentent

un module et une ténacité à la rupture améliorée. De la même façon, des composites SWNT (Nanotubes de carbone à paroi simple) montrent une conductivité électrique et thermique importante à des faibles taux de charges où des composites GNP (Nanophlételets de graphite) fournissent des augmentations du module et de la conductivité électrique avec une diminution importante de la perméation à la vapeur par rapport à une matrice époxy non modifiée. L'incorporation des clusters POSS[®] dans des polymères à base d'époxy offre des fonctionnalités particulières comme une bonne résistance à l'oxydation et une excellente stabilité thermique et un caractère ignifuge importants combinés à des propriétés diélectriques et mécaniques améliorées. Toutefois, une dispersion nanométrique et homogène individuelle de ces nanoclusters O/I ou de toute charge est requise pour qu'un nanocomposite présente des améliorations de propriétés. En effet, les nanoclusters de type POSS[®] ne sont généralement pas parfaitement répartis de manière homogène au sein des polymères et ont tendance à former des aggrégats. Quant à elle, cette pauvre dispersion, peut-être issue d'une micro séparation de phase qui peut se produire entre le POSS[®] et le monomère avant et pendant la polymérisation en fonction de la nature chimique et de la fonctionnalité des ligands organiques des cages POSS[®]. Pour cette raison, les défis liés à une réduction de cette tendance des silsesquioxanes oligomères polyédriques à s'agglomérer doivent être résolus, soit par la synthèse de nouveaux nanoclusters plus compatibles avec les époxy monomères ou par la recherche d'autres types de ligands organiques qui assureront une meilleure intégration et compatibilité des POSS[®] vis-à-vis la matrice époxy.

Les oligosilsesquioxanes polyédriques, connus sous l'abréviation POSS[®] pour **P**olyhedral **O**ligomeric **S**ilsesquioxane, sont des nano-clusters hybrides O/I constitués d'un cœur inorganique tridimensionnel parfaitement défini composé de silicium et d'oxygène (SiO_{1,5}) auquel sont liés de manière covalente par des ligands organiques porteurs ou non de fonctions polymérisables. Le nom silsesquioxane vient des termes 'sil-oxane' (silice et oxygène) et 'sesqui' (1,5). Sans parler de l'impact des POSS[®] sur les propriétés physiques des polymères, l'effervescence suscitée par ce type de clusters provient essentiellement *i*) de leur taille nanométrique ($\approx 1,5$ nanomètre de diamètre), *ii*) de leur structure polyédrique et *iii*) de leur caractère hybride organique/inorganique. Leur architecture moléculaire parfaitement définie ouvre la perspective de maîtriser la morphologie et donc les propriétés des matériaux à l'échelle nanométrique et ce en lien avec d'autres échelles. À titre d'illustration, nous utilisons souvent le terme « nanobrique » pour

désigner ces nanoclusters. Grâce aux progrès réalisés dans leur synthèse, la très grande variété de ligands organiques, tant en termes de nature chimique que de réactivité, permet d'introduire les POSS[®] dans une large gamme de polymères couvrant les thermoplastiques et thermodurcissables, afin de générer différentes morphologies. En fonction du nombre de fonctions co-polymérisables portées par les clusters, elles peuvent être introduites sous forme de nano-objets inertes dispersés dans une matrice polymère ou liés de manière covalente au polymère s'ils portent une ou plusieurs fonctions polymérisables. L'incorporation de dérivés POSS[®] dans les matériaux polymères peut conduire à améliorer leurs propriétés telles que leurs propriétés mécaniques, leurs inerties chimiques ou leurs stabilité thermique et notamment leurs tenues au feu.

Récemment, les liquides ioniques sont apparus comme de nouveaux additifs réactifs aux réseaux époxy et époxy composite/nanocomposite où ils peuvent être utilisés à la fois comme durcisseur (co-monomère) et comme moyen de dispersion des charges dans les systèmes époxy composites/nanocomposites, permettant d'accéder à des matériaux fonctionnels avec des propriétés sans précédents. Les liquides ioniques sont des sels organiques composés d'un cation organique volumineux associé à un anion organique ou inorganique dont la température de fusion est inférieure à 100 °C. Les propriétés uniques des liquides ioniques telles que leur non-inflammabilité, leur grande stabilité thermique, leur faible pression de vapeur saturante et leur bonne conductivité ionique ont retenu l'attention de la recherche et de l'Industrie. Tous ces éléments font des LI d'excellents candidats pour un grand nombre d'applications dans des domaines aussi variés tels que l'électrochimie, la catalyse, les matériaux polymères ou encore dans la fabrication de nanomatériaux comme agents tensioactifs de silicates lamellaires et silice, des composés du carbone ou d'oxydes métalliques. Cependant, l'application des liquides ioniques pour les nanocomposites époxy/POSS[®] n'a pas été étudiée. Ainsi, les principaux objectifs de cette thèse seront de contrôler la structure et la morphologie des nanomatériaux époxy/POSS[®] et époxy-LI/POSS[®] en utilisant les LIs comme modificateurs structuraux des POSS[®] et par la suite d'étudier l'impact du changement de la morphologie (taille des agrégats et homogénéité de dispersion) sur la cinétique de construction du réseau, les mécanismes de polymérisation et les propriétés globales des nanomatériaux hybride O/I résultants. L'objectif est d'établir un lien avec la structure organique du POSS[®] et du liquide ionique (cation/anion). Afin d'atteindre ces objectifs, ce manuscrit est divisé en quatre chapitres :

Chapitre I : Étude Bibliographique

Le premier chapitre rapportera une étude bibliographique sur deux voies qui sont rapportées pour modifier des réseaux époxy-amines conventionnels. La première partie donnera une vision globale de la « technologie POSS[®] » et comment celle-ci a été mise en oeuvre pour des résines époxy, en s'intéressant à la description de la structure moléculaire de ces clusters, sur les méthodes de synthèse de ces structures ainsi que sur leurs propriétés thermiques mais aussi leur différentes méthode d'incorporation dans les réseaux époxyde et les propriétés qui en découlent en relation avec les différentes morphologies générées (tenue contre le feu, stabilité thermique et résistance à l'oxydation, comportement mécanique, ténacité et comportement diélectrique...). Une attention particulière sera apportée au problème majeur, celui de l'agrégation dans des résines époxyde qui limite le plus souvent l'amélioration des propriétés finales. La deuxième section se concentrera sur l'utilisation des liquides ioniques à bas d'imidazolium dans les réseaux époxy-amine, c'est-à-dire sur la synthèse et le développement de nouveaux LI fonctionnalisés et leur utilisation comme additifs ou co-monomères pour préparer des systèmes époxy réticulés et en particulier, comment les liquides ioniques peuvent être utilisés comme moyen de dispersion de charges dans les systèmes composites époxy/nanocomposites. En fin de chapitre, nous terminerons avec quelques exemples rapportés dans la littérature sur la synthèse des entités POSS[®]-LI et leurs potentiels effets sur les matériaux polymères dans lesquels ils sont introduits.

Chapitre II : Synthèse de Liquide Ionique Modifié POSSs[®] avec l'Étude de leur Dispersion dans une Matrice Époxy-amine

• Introduction

L'objectif de ce chapitre sera le design moléculaire de réseaux d'époxy-amine nanostructurés en utilisant des POSS[®] greffés par un LI comme nano-briques de construction de nanomatériaux organiques-inorganiques. À notre connaissance, il n'y a pas eu d'études rapportant de tels polymères thermodurcissables nanostructurés avec des POSS[®] greffés LI. Dans le présent chapitre divisé en deux parties, nous rapporterons dans une première partie un résumé de toutes les synthèses effectuées dans ce travail de thèse. Plusieurs types de liquide ionique avec différents anions et fonctions, POSS[®] monofonctionnels ou multifonctionnels liquide ionique ont été synthétisés et caractérisés par différentes techniques (RMN- ¹H/ ¹³C/ ²⁹Si/ ¹³P, RMN solide ²⁹Si, spectrométrie de masse MALDI TOF, HR-MS, IRTF, DSC, ATG):

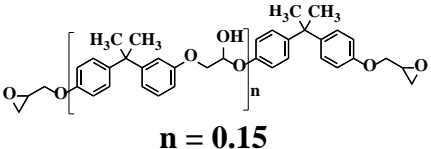
- 1- Liquide ionique silylé à base d'imidazolium (**Si-g-Im-Cl**) visant à être greffé sur des POSS[®]-triol partiellement condensés.
- 2- Liquide ionique monomère monofonctionnel époxy : [2- (oxiran-2-yl) éthyl]-1-phénylimidazolium 1,1,1-trifluoro-N - [(trifluorométhyl) sulfonyl] méthanesulfonamide (**LIM**) visant à être greffé sur des POSS[®] qui portent des fonctions amine-hydrogène (N-H).
- 3- La synthèse et la caractérisation de deux types de POSS[®] monofonctionnels liquides ioniques à base d'imidazolium selon la voie « *corner-capping* », désignés LI-g-POSS^{®iB} et LI-g-POSS^{®Ph} à partir des POSS[®] précurseurs partiellement condensés de types (R₇T₈(OH)₃), désignés POSS^{®iB}-triol et POSS^{®Ph}-triol et des liquides ioniques fonctionnalisés silane.
- 4- La synthèse et la caractérisation d'un POSS[®] difonctionnel liquide ionique à base d'imidazolium (POSS[®]-N-2LI) à partir d'un POSS[®] portant deux fonctions amino-hydrogène (POSS[®]-NH₂) et un liquide ionique qui porte une fonction époxyde (LIM).

La deuxième partie sera dédiée à la préparation des nanomatériaux époxy à base de POSS[®]-triols et de LI-g-POSS[®] avec l'optimisation des différentes conditions opératoires. La morphologie et les propriétés thermiques des nanomatériaux hybrides O/I seront comparées en les étudiant par microscopie électronique à transmission (MET) et calorimétrie différentielle à balayage (DSC).

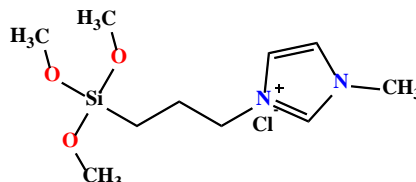
• Matériaux considérés

Toutes les structures chimiques des produits synthétisés et utilisés avec leurs propriétés sont représentées dans le tableau 1.

Tableau 1. Formule chimique des différents composants chimiques utilisés et synthétisés dans ce travail de thèse.

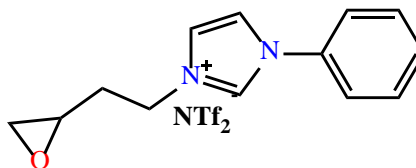
Nom	Structure chimique	Caractéristiques
Diglycidyl ether of bisphénol A (DGEBA)	 <p style="text-align: center;">n = 0.15</p>	<p>M_n = 377 g.mol⁻¹, EEW : (185-192 g/eq)^a, T_g = -13 °C^b, T_d = 330 °C^d CAS No. 1675-54-3 (Hexion)</p>

1-(3-trimethoxysilylpropyl)-3-methyl-imidazolium chloride
(**Si-g-Im-Cl**)



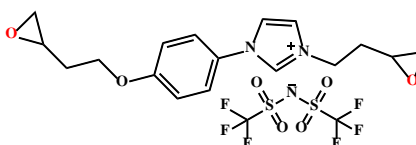
$M = 281 \text{ g.mol}^{-1}$,
 $T_g = -52 \text{ }^{\circ}\text{C}^b$,
 $T_d = 291 \text{ }^{\circ}\text{C}^d$

[2-(oxiran-2-yl) ethyl] -1-phenylimidazolium 1,1,1-trifluoro-N-[(trifluoromethyl) sulfonyl] methanesulphonamide
(**LIM**)



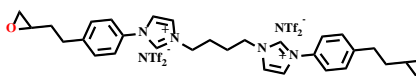
Prepared following the procedure reported in **1**
 $M = 495 \text{ g.mol}^{-1}$,
 $T_g = -46 \text{ }^{\circ}\text{C}^b$,
 $T_d = 437 \text{ }^{\circ}\text{C}^d$

3-[2-(oxiran-2-yl)ethyl]-1-{4-[(2-oxiran-2-yl)ethoxy]phenyl}imidazolium 1,1,1-trifluoro-N-[(trifluoromethyl)sulfonyl]methanesulfonamide (**LIM1**)



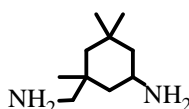
Prepared following the procedure reported in **2**
 $M = 581 \text{ g.mol}^{-1}$
 $T_d = 489 \text{ }^{\circ}\text{C}^b$

3,3'-(1,4-butanediyl)bis[1-(4-(2-oxiran-2-yl)ethyl)phenyl]imidazolium 1,1,1-trifluoro-N-[(trifluoromethyl)sulfonyl]methanesulfonamide (**LIM2**)



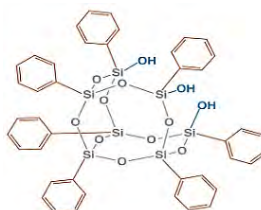
$M = 802 \text{ g.mol}^{-1}$
 $T_f = 71 \text{ }^{\circ}\text{C}^a$
 $T_d = 460 \text{ }^{\circ}\text{C}^b$

Isophoronediamine
(**IPD**)



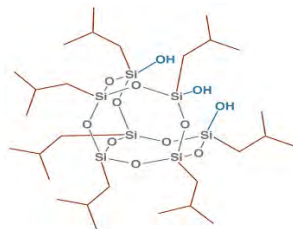
$M = 170,3 \text{ g.mol}^{-1}$
CAS No. 2855-13-2
(Sigma Aldrich)

Heptaphenyl-trisilanol POSS[®]
(**POSS[®]Ph-triol**)



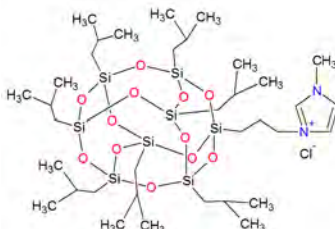
$M = 931,34 \text{ g mol}^{-1}$,
 $T_{f1} = 217 \text{ }^{\circ}\text{C}^a$,
 $T_{f2} = 230 \text{ }^{\circ}\text{C}^a$,
 $T_d = 626 \text{ }^{\circ}\text{C}^b$
CAS No. 444315-26-8
(Hybrid Plastics)

Heptaisobutyl-trisilanol POSS[®]
(POSS[®]iB-triol)



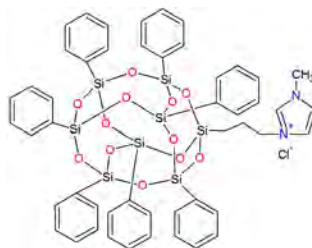
$M = 791,42 \text{ g mol}^{-1}$,
 $T_{f1} = 200 \text{ }^{\circ}\text{C}^a$,
 $T_d = 283 \text{ }^{\circ}\text{C}^b$
CAS No. 307531-92-6
(Hybrid Plastics)

1-methyl-3-propyl heptaisobutyl
octasilesquioxane imidazolium
chloride
(LI.Cl-g-POSS[®]Ph)



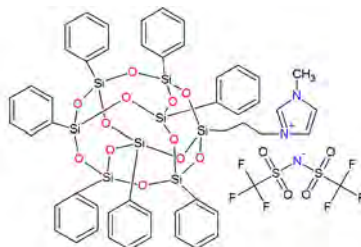
$M = 974,72 \text{ g mol}^{-1}$,
 $T_{f1} = 127 \text{ }^{\circ}\text{C}^a$,
 $T_{f2} = 167 \text{ }^{\circ}\text{C}^a$,
 $T_d = 428 \text{ }^{\circ}\text{C}^b$

1-methyl-3-propyl heptaphenyl
octasilesquioxane imidazolium
chloride
(LI.Cl-g-POSS[®]Ph)



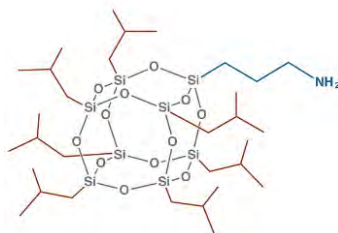
$M = 1116,04 \text{ g mol}^{-1}$,
 $T_{f1} = 127 \text{ }^{\circ}\text{C}^a$,
 $T_{f2} = 168 \text{ }^{\circ}\text{C}^a$,
 $T_d = 632 \text{ }^{\circ}\text{C}^b$

1-methyl-3-propyl heptaphenyl
octasilesquioxane imidazolium
bis(trifluoromethanesulfonyl)imi
date (LI.NTf₂-g-POSS[®]Ph)



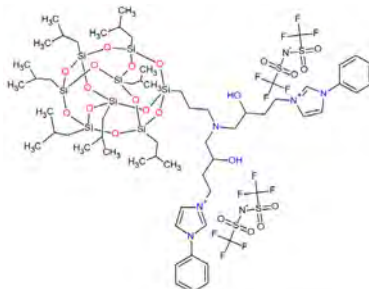
$M = 1360,73 \text{ g mol}^{-1}$,
 $T_{f1} = 135 \text{ }^{\circ}\text{C}^a$,
 $T_{f2} = 158 \text{ }^{\circ}\text{C}^a$,
 $T_d = 534 \text{ }^{\circ}\text{C}^b$

hepta(i-butyl)-aminopropyl
POSS[®]
(POSS[®]-NH₂)



$M = 874,58 \text{ g mol}^{-1}$,
 $T_d = 325 \text{ }^{\circ}\text{C}^b$
CAS No. 444315-15-5
(Hybrid Plastics)

(POSS[®]-N-2LI)



$M = 1864,42 \text{ g mol}^{-1}$,
 $T_d = 462 \text{ }^{\circ}\text{C}^b$

^a T_f : température de fusion, ^b T_d : température de dégradation déterminée au maximum de la dérivée première de la perte de poids en fonction de la température.

• Préparation des réseaux époxy

Pour préparer les réseaux époxy-amine, le prépolymère époxy (DGEBA) et l'isophoronediamine (IPD) utilisés comme co-monomères ont été mélangés sous agitation mécanique avec un rapport stoechiométrique amino-hydrogène/époxy égal à 1.

5 % massique des LI-g-POSS[®], soit LI-g-POSS^{®iB}, LI-g-POSS^{®Ph} ou POSS[®]-N-2LI, ont été pris en compte pour les réseaux époxy modifiés POSS[®]. Tout d'abord, les POSS[®] modifiés LI (LI-g-POSS[®] ou POSS[®]-N-2LI) et IPD ont été pré-mélangés à 60 °C jusqu'à ce qu'un mélange homogène soit obtenu avant d'être ajouté au prépolymère époxy (DGEBA). Ensuite, le mélange a été dégazé et versé dans un moule. Enfin, les réseaux époxy avec et sans LI modifié POSS[®] ont été réticulés pendant 2h à 140 °C et post-polymérisés 8 h à 190 °C.

• Résultats marquants du chapitre [3]

Dans ce chapitre, les deux liquides ioniques ont été synthétisés avec succès, à l'échelle de plusieurs grammes (rendement compris entre 84 et 95 %) et avec une pureté élevée. Deux nouveaux silsesquioxanes oligomères polyédriques à support imidazolium liquide ionique, LI-g-POSS^{iB} et LI-g-POSS^{Ph}, ont également été préparés avec succès. Leurs structures chimiques ont été confirmées par spectrométrie de masse MALDI-TOF, analyses RMN liquide (¹H, ¹³C) et solide du ²⁹Si. Le greffage du LI avec différents anions aux POSS[®]-triol ou POSS[®]-NH₂ a conduit simultanément en une baisse de sa température de fusion mais aussi une amélioration de sa stabilité thermique (400 vs 300 °C). Les rendements de fermeture des POSS[®]-triol ne sont pas de 100 %. Il existe en effet toujours une fraction de POSS[®] portant la fonction liquide ionique mais aussi des groupements hydroxyle (OH) libres (entre 10 et 20 %), phénomène qui a été attribué à l'encombrement stérique des substituants isobutyle et phényle de la cage. Ensuite, 5 % en masse de LI-g-POSS[®] ont été incorporés dans le réseau époxy-amine (DGEBA/IPD) conduisant à la formation de réseaux nanostructurés homogènes. Une excellente dispersion du POSS[®] monofonctionnel LI a été obtenue (voir Figure 1) dans les réseaux, caractérisée par la formation d'agrégats POSS[®]-POSS[®] sphériques ou ellipsoïdaux de tailles nanométriques (de 10 à 80 nm). Alors que la difonctionnalité de POSS[®] avec LI a conduit à deux morphologies composées d'agrégats nanométriques sphériques riches en POSS[®] et une phase co-continue due

probablement à une limite de miscibilité générée par la présence de deux ligands liquide ionique par POSS[®] (Voir Figure 2). De plus, tous les réseaux époxy contenant LI-g-POSS[®] ou POSS[®]-N-2LI conservent une température de transition vitreuse proche de la valeur du réseau époxy-amine de référence (≈ 160 °C). En conclusion, ces résultats prometteurs ouvrent de nouvelles perspectives dans le développement de réseaux époxy-amine organiques-inorganiques nanostructurés et mettent en évidence le rôle du liquide ionique à faibles quantités comme agent interfacial structurant pour conduire aux meilleures dispersions. Des travaux sur l'effet de la nanostructuration des LI-g-POSS[®] dans le réseau époxy-amine sur les différentes propriétés ainsi que les fonctionnalités innovantes que l'on peut en attendre de ces nouveaux additifs (IL-g-POSS[®]) seront présentés dans le troisième et quatrième chapitres.

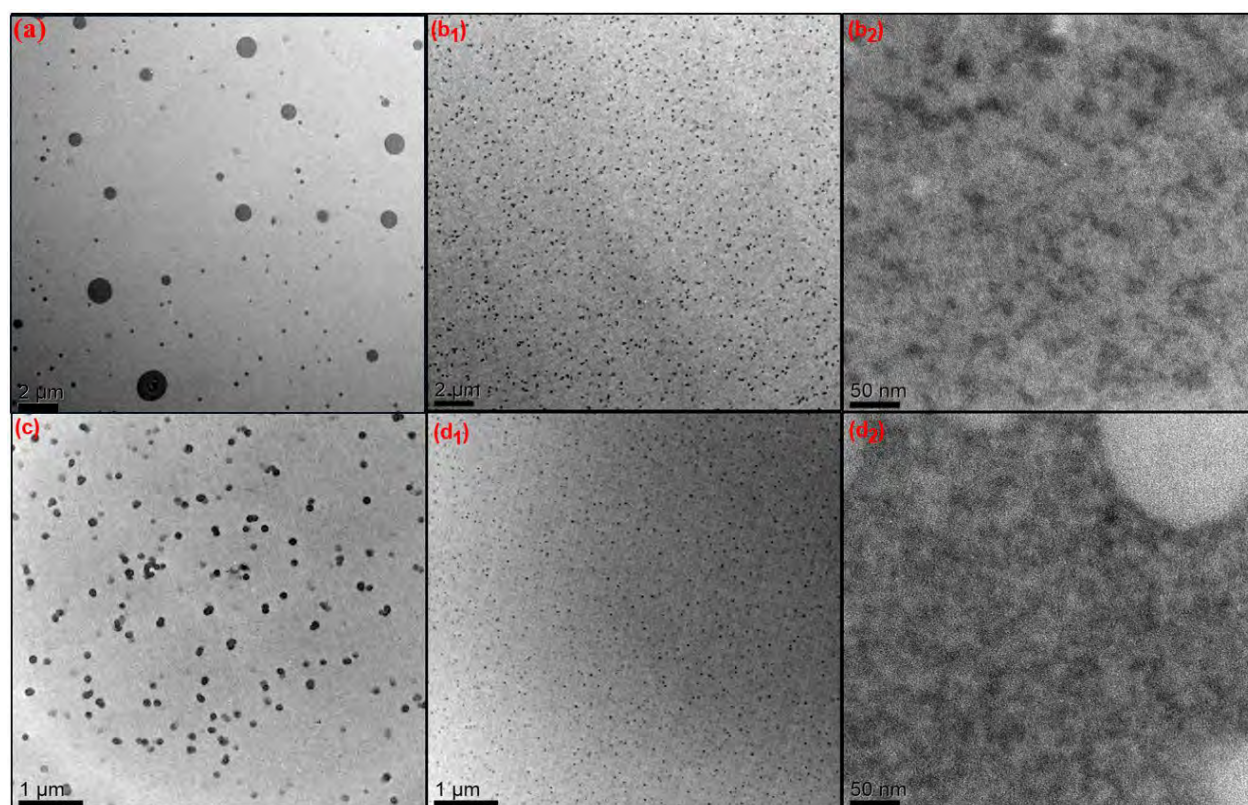


Figure 1 : Micrographies TEM des réseaux époxy-amine contenant (5 % massique): a) POSS^{iB}-triol et b): LI-g-POSS^{iB} à différents grossissements (b₁; b₂), c) POSS^{Ph}-triol et d): LI-g-POSS^{Ph} à différents grossissements (d₁; d₂) [3].

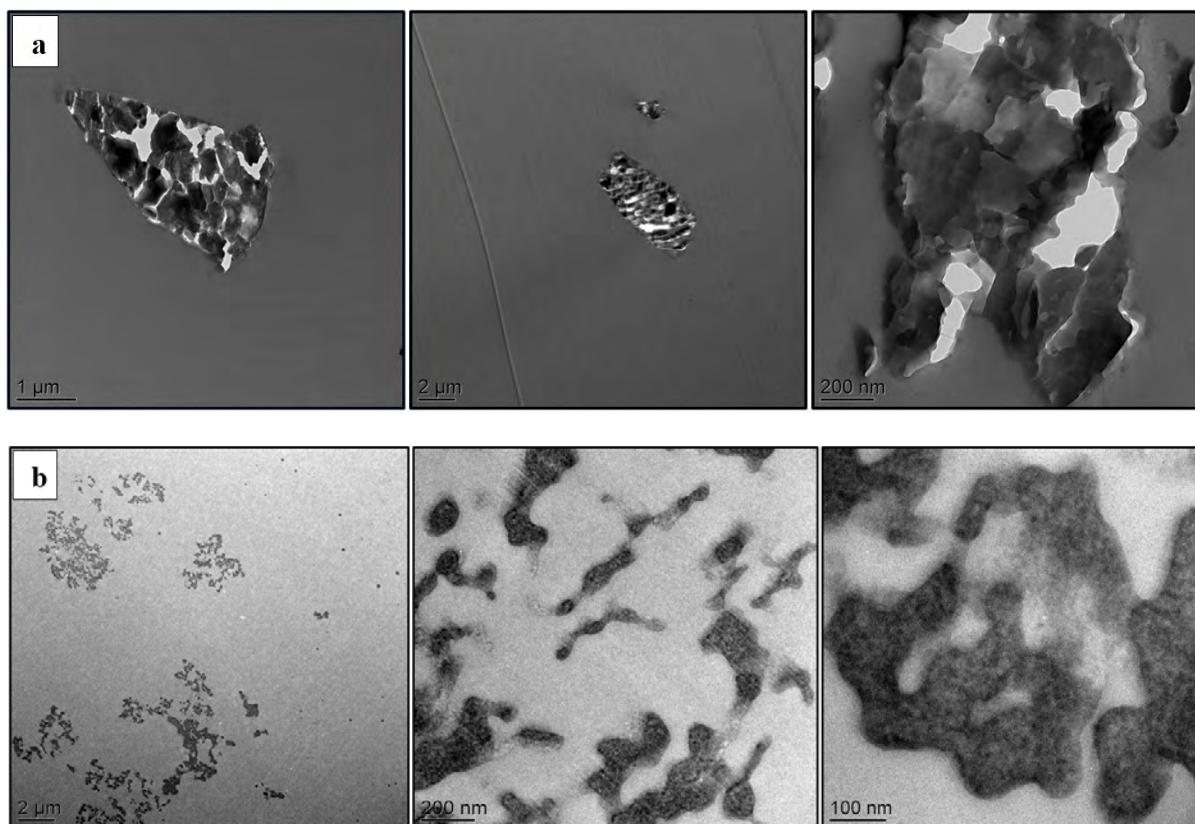


Figure 2: Micrographies TEM des réseaux époxy-amine contenant (5% massique) : a) POSS®-NH₂, et b) POSS®-N-2LI à différents grossissements.

Chapitre III : Conception et Propriétés des Réseaux Hybrides Organiques-Inorganiques IL-g-POSS^{®Ph} / Époxy-amine Nanostructurés

• Introduction

Dans le troisième chapitre, nous dirigerons vers l'application des POSS^{®Ph} monofonctionnels imidazolium liquide ionique (LI-g-POSS^{®Ph}) avec deux différents anions (Cl⁻ et NTf₂⁻) en tant que nouveaux additifs pour nanostructurer des réseaux époxy-amine. Dans un premier temps, la préparation de nanomatériaux époxy à base de POSS[®], c'est-à-dire de POSS[®] non modifiés (POSS^{®Ph}-triol) et POSS^{®Ph} modifié par LI avec différents anions (Cl⁻ et NTf₂⁻) et leur influence sur la cinétique de polymérisation d'époxy ont été étudiées. Par la suite, une comparaison systématique des propriétés avec le système époxy-amine de référence (DGEBA/IPD) : morphologie observée par microscopie électronique en transmission (MET), propriétés thermiques par DSC, propriétés viscoélastique par DMA, les propriétés mécaniques en

compression, ténacité (rupture), propriétés de surface par méthode de goutte sessile, stabilité thermique et résistance à l'oxydation par ATG, comportement au feu et à la combustion par calorimétrie en flux par pyrolyse-combustion (PCFC) et cône calorimètre a été étudiée.

• Résultats marquants du chapitre [4]

Dans ce chapitre, le choix a été orienté vers des POSS[®] portant des groupements phényle avec une fonction LI en présence de deux types d'anions différents chlorure : chlorure (Cl⁻) et bistrifluorométhanesulfonimide (NTf₂⁻). L'effet de l'échange d'anion sur la morphologie ainsi que sur les propriétés finales des réseaux époxy modifiés LI-g-POSS^{®Ph} a été étudié. Les réseaux époxy contenant LI-g-POSS^{®Ph}, quelle que soit la nature d'anion (Cl⁻ ou NTf₂⁻), présentent une forte réactivité vis-à-vis des prépolymères époxy conventionnels (DGEBA) et conduisent à la formation de réseaux polyépoxy avec une conversion des groupements époxy supérieure à 90 %. Une excellente dispersion à l'échelle nanométrique a été obtenue, caractérisée par des agrégats sphériques nanométriques riches en POSS[®] bien dispersées. Un pourcentage de 20 à 30 % de greffage des LI-g-POSS[®] vis-à-vis la matrice a été identifiée par analyse de la fraction soluble extractible des réseaux hybrides O/I. Les réseaux O/I hybrides époxy résultants offrent d'excellentes propriétés telles qu'une transition vitreuse élevée (151 à 161 °C), une bonne stabilité thermique (jusqu'à 400 °C) avec un comportement de surface hydrophobe (23 mJ.m⁻²). De plus, la combinaison de LI aux nanoclusters POSS^{®Ph}-triol avec les deux anions (Cl⁻ ou NTf₂⁻) induit un effet de (nano)renforcement à la rupture combiné avec une rigidité importante (une augmentation du module de Young (3.1 vs 2.3 GPa) et ténacité (1.02 vs 0.61 MPa.m^{1/2})) mais aussi une augmentation importante de la déformation à rupture (40 vs 28 %). De plus, ces réseaux nanostructurés O/I montrent une résistance importante au feu comme montré par analyses de pyrolyse-combustion en flux calorimétrique (PCFC) et cône calorimètre. En effet, l'utilisation de faibles quantités de silsesquioxanes oligomères polyédriques modifiés imidazolium liquide ionique (LI-g-POSS^{®Ph}) induit une réduction significative du pic de taux de dégagement de chaleur (de -53 à -56 %) ainsi qu'une augmentation importante du temps d'ignition (plus de 29 %) avec une production de fumée moins importante que celle du réseau époxy-amine de référence (Voir Figure 2).

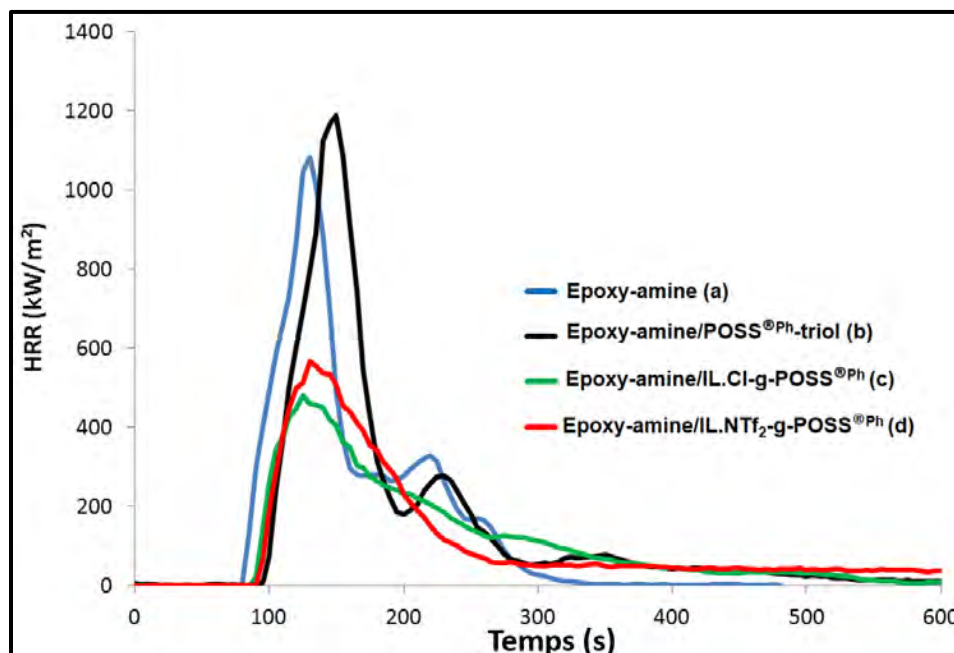


Figure 2 : Courbes HRR de cône calorimètre du l'époxy-amine et des réseaux époxy hybrides O/I [4].

Chapitre IV : Nouveaux Nanomatériaux Hybrides Organiques-Inorganiques Thermodurcissables Époxy Dérivés de Monomères Liquides Ioniques d'Imidazolium et de POSS[®]Ph

• Introduction

Dans le dernier chapitre, nous aborderons la synthèse et la caractérisation de deux nouveaux monomères époxy imidazolium liquides ioniques (LIM1 et LIM2) fonctionnalisés époxyde afin de remplacer le prépolymère DGEBA conventionnel qui est préparé à l'aide de composés toxiques et cancérigènes tels que le bisphénol A et l'épichlorhydrine. Ainsi, sont développés de nouveaux PLIs époxyde, avec copolymérisation avec l'IPD comme diamine. Une étude complète des différentes propriétés et des fonctionnalités de ces PLIs (LIM/IPD) ainsi que de la cinétique et le mécanisme de polymérisation a été menée.

Par la suite, ce chapitre se concentrera sur la formation de nouveaux nanomatériaux sur la base de la combinaison des nanoclusters IL-g-POSS[®]Ph avec deux différents anions (Cl⁻ et NTf₂⁻) et des monomères époxy-LI (LIM1 et LIM2) pour viser à la conception de nanomatériaux hybride innovants respectueux de l'environnement et présentant de nouvelles performances telles que de bonnes conductivité électrique et stabilité thermique.

- **Résultats marquants du chapitre [5, 6]**

Dans ce chapitre, de nouveaux matériaux polymère (multi)fonctionnels ont été développés à partir des sels d'imidazolium porteurs de fonctions époxyde. Ainsi, des réseaux époxy ont été préparés à partir de la copolymérisation de ces monomères (LIM1 et LIM2) avec l'isophorone diamine (IPD). Par la suite, les propriétés de ces nouveaux réseaux polymère à base de liquide ionique époxy (PLIs) ont été étudiées en termes de mécanismes de polymérisation et cinétique de réaction de polyaddition en relation avec leur morphologie et les propriétés finales des réseaux (stabilité thermique, propriétés de surface et performances mécaniques). Dans un premier temps, il est montré que les LIMs présentent une réactivité élevée envers l'amine et que les réseaux de monomères liquides ioniques LIM/IPD époxy obtenus possèdent de bonnes propriétés thermomécaniques, une hydrophobie prononcée (21 mJ.m^{-2}) et une stabilité thermique importante (jusqu'à 450°C) nettement supérieure en comparaison du système époxy-amine de référence. Pour une température de transition vitreuse voisine de 71°C , les performances mécaniques comme le module de Young ($\approx 1,7 \text{ GPa}$) de ces nouveaux réseaux d'époxy (LIM/IPD) sont similaires au réseau époxy-amine (DGEBA/IPD) mais avec un allongement significativement plus important à la rupture (28 %). Ces réseaux ioniques peuvent être qualifiés de matériaux intelligents puisqu'ils montrent une capacité importante à présenter un comportement à mémoire de forme avec une récupération de forme de 100 % juste en quelques minutes à une température modérée (Voir Figure 3 et 4).

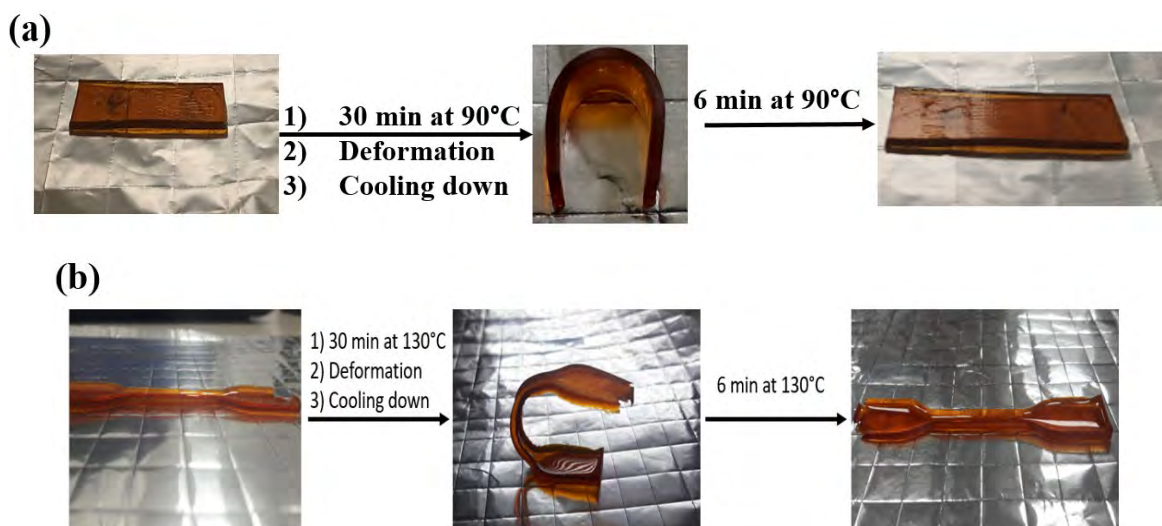


Figure 3: Test de mémoire de forme des réseaux a) LIM1/IPD et b) LIM2/IPD [5].

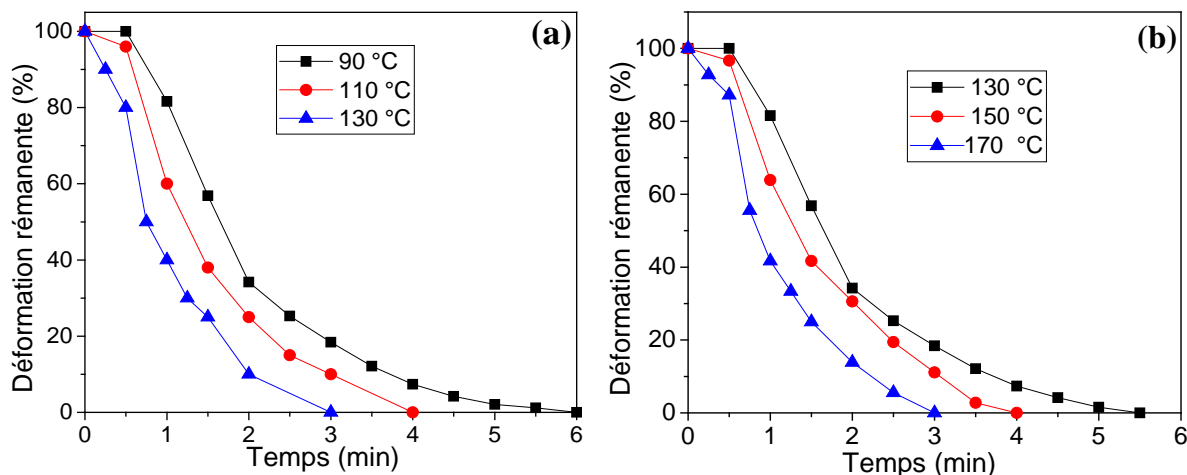


Figure 4: Déformation rémanente en fonction du temps pour les réseaux a) LIM1/IPD et b) LIM2/IPD à différentes températures [5].

Dans une deuxième partie de ce chapitre, de nouveaux nanomatériaux époxy dérivés de monomères liquides ioniques imidazolium (LIMs) ont été modifiés par trois types de POSS^{®Ph} : trisilanol phényl POSS[®] (POSS^{®Ph}-triol) et deux POSS^{®Ph} modifiés par LI ayant deux différentes contre-anions chlorure (Cl⁻) et bis(trifluoromethanesulfonyl)imide (NTf₂⁻). Des POSS^{®Ph} ont été incorporés dans les réseaux LIMs époxy avec une teneur de 5 % massique et copolymérisés avec l'isophorone diamine (IPD) pour concevoir des réseaux PLIs époxy nanostructurés. Les nanomatériaux hybrides organiques-inorganiques ont été préparés par polymérisation *in situ* de monomères époxy LI en présence de POSS^{®Ph}, qui conduisent à des solutions homogènes POSS^{®Ph}/monomères liquides ioniques époxy (LIM1 et LIM2) initialement. Une séparation de phase induite par polymérisation se produit en cours de réaction et de fines nano structures séparées sont obtenues dans lesquelles des agrégats sphériques POSS^{®Ph}-POSS^{®Ph} sont dispersés de manière homogène à l'échelle nanométrique (de 80 à 400 nm) au sein de la matrice époxy. Un pourcentage de greffage des LI-g-POSS^{®Ph} vis-à-vis la matrice LIM/IPD de 16 à 20 % a été mesurée. En conséquence, l'impact des LI-g-POSS^{®Ph} dans les réseaux LIM/IPD se manifeste par une forte diminution de la température de transition vitreuse (45 vs 71 °C) mais une augmentation importante de la stabilité thermique (> 380 °C) avec une haute résistance à l'oxydation. Fait intéressant, les nanomatériaux LIM/IPD/LI-g-POSS^{®Ph} et surtout avec les anions NTf₂⁻ conduisent à une amélioration significative de l'hydrophobicité et de lipophilie avec une énergie de surface très faible (Θ_{Eau} voisine de 120 °, $\Theta_{\text{CH}_2\text{I}_2}$: 92 °, γ_{total} = 18,2 mJ.m⁻²). Cette dernière propriété qui est importante pour l'élaboration de revêtements hydrophobes avec une

aptitude à la non-salis-sue. De plus, tous les PLIs époxy nanostructurés présentent une conductivité ionique élevée (de $9,37 \times 10^{-5}$ à 40°C jusqu'à $6,84 \times 10^{-2} \text{ S.m}^{-1}$ à 100°C) avec une excellente stabilité électrochimique (Voir Figure 5). Pour conclure, le potentiel de ces monomères époxy LIs en tant que nouveaux prépolymères époxy a été clairement mis en évidence.

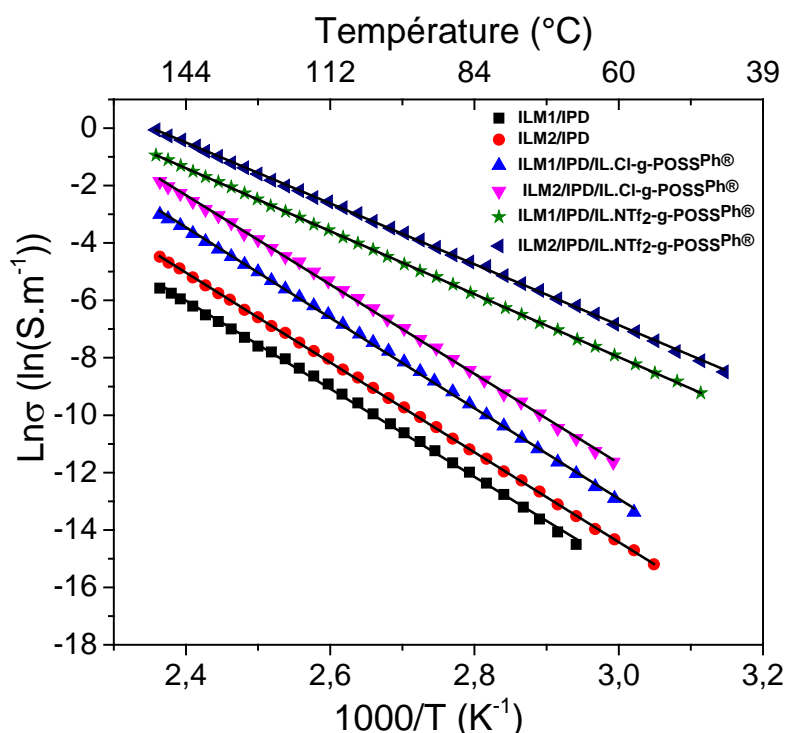


Figure 5: Evolution de la conductivité DC en fonction de la température extrapolée à partir des valeurs de conductivité AC à 0,1 Hz (Les lignes noires pleines représentent une régression vers l'équation d'Arrhenius) [6].

Conclusion et Perspectives

Ce travail de thèse porte sur la synthèse et la caractérisation d'une nouvelle génération de nanomatériaux hybrides organiques/inorganiques basés sur des monomères d'époxy conventionnels comme (DGEBA) ou de types liquides ioniques (LIMs) copolymérisés avec une amine cycloalipatique (IPD) et des nanoclusters du type POSS® (Polyhedral Oligomeric Silsesquioxane) greffés liquide ionique, notés IL-g-POSS®. Ces modifications ont mis en évidence principalement les conclusions suivantes :

- ✓ Le greffage des LI sur des POSS®^{Ph} ouvre de nouvelles perspectives intéressantes dans la maîtrise précise des interactions interfaciales dans des nanocomposites

polymère de ce type et par la suite du contrôle de leurs états de dispersions dans l'époxy. Les ligands liquide ionique gèrent les interactions POSS[®]/POSS[®], POSS[®]/monomère et POSS[®]/époxy, avant et pendant la polymérisation, interactions dont dépend l'organisation des clusters dans le matériau final.

- ✓ Le POSS[®] modifié LI peut être envisagé comme une nouvelle alternative aux additifs retardateurs de flamme conventionnels, puisqu'il conduit non seulement à une capacité de résistance au feu important, mais également améliore les propriétés mécaniques du nanomatériau époxy obtenu.
- ✓ Les monomères liquides ioniques époxydes paraissent comme une nouvelle alternative au prépolymère époxy (DGEBA) puisque leur polymérisation avec une amine conventionnelle donne des propriétés mécaniques similaires mais avec une excellente stabilité thermique et une hydrophobie nettement supérieure.
- ✓ Les réseaux époxy LIM/IPD et leurs réseaux hybrides O/I ont permis d'obtenir des conductivités ioniques élevées avec de larges fenêtres électrochimiques (allant jusqu'à 5 V) indiquant une excellente stabilité électrochimique. Ils amènent de plus une super hydrophobie combinée avec un caractère lipophile important ainsi qu'une stabilité thermique élevée.

Plus globalement, ces résultats ouvrent de nouvelles perspectives dans le développement d'une nouvelle génération de matériaux polymères (multi)fonctionnels dédiés à différents types d'applications telles que celles nécessitant une résistance au feu, associée à des performances mécaniques et à un comportement à mémoire de forme. Ces nouveaux nanomatériaux pourraient être étudiés plus en profondeur pour leurs conductivités ioniques ainsi que leurs propriétés barrière aux gaz pour être utilisés comme électrolytes polymères solides. Pour cela afin d'évaluer leurs domaines d'application potentiels, plusieurs études pourraient être encore entreprises pour mieux approfondir la connaissance de leurs relations structure (à différentes échelles) propriétés physiques:

- Réaction de réticulation entre monomères époxy (DGEBA) ou époxy liquides ioniques (LIM1, LIM2) et diamine en présence de POSS^{®Ph} nécessitent des études plus approfondies afin d'obtenir une compréhension complète des différents mécanismes de la réaction ainsi leur lien avec l'état de dispersion du POSS^{®Ph} au sein de la matrice.

- Le fort caractère hydrophobe est intéressant pour envisager des applications de type revêtements. Des tests de corrosion seraient nécessaires pour évaluer le potentiel de tels monomères époxy liquides ioniques ainsi que des systèmes époxy LIM/amine/POSS^{®Ph} comme revêtements protecteurs pour métal dans des conditions comme par exemple en expositions marines.
- Comme il est bien connu que les liquides ioniques phosphonium présente une forte réactivité vis-à-vis des prépolymères époxy classiques, d'autres associations de liquides ioniques à base d'un cation phosphonium et d'anions phosphinates ou phosphates avec POSS[®] doivent être étudiées pour analyser leur impact sur les différentes propriétés et notamment sur leur tenue au feu.
- Enfin, les monomères époxy LI (LIMs) peuvent présenter une nouvelle voie très attractive pour préparer une nouvelle génération de matériaux époxy liquides ioniques. Ainsi, il serait intéressant de rechercher d'autres types de prépolymères époxy LI avec une plus grande fonctionnalité (en époxyde) et d'explorer une large variété d'anions pour avoir différentes propriétés et ainsi s'ouvrir à une grande diversité d'applications.

Références

1. Chardin, C.; Rouden, J.; Livi, S.; Baudoux, J. Dimethyldioxirane (DMDO) as a valuable oxidant for the synthesis of polyfunctional aromatic imidazolium monomers bearing epoxides. *Green Chemistry* **2017**, *19*, 5054-5059, doi.org/10.1039/C7GC02372C.
2. Livi, S.; Chardin, C.; Lins, L. C.; Halawani, N.; Pruvost, S.; Duchet-Rumeau, J.; Gérard, J. F.; Baudoux, J. r. m. From Ionic Liquid Epoxy Monomer to Tunable Epoxy-Amine Network: Reaction Mechanism and Final Properties. *ACS Sustainable Chemistry & Engineering* **2019**, *7*, 3602-3613.
3. **Chabane, H.**; Livi, S.; Benes, H.; Ladavière, C.; Ecorchard, P.; Duchet-Rumeau, J.; Gérard, J. F. Polyhedral oligomeric silsesquioxane-supported ionic liquid for designing nanostructured hybrid organic-inorganic networks. *Eur. Polym. J.* **2019**, *114*, 332-337.
4. **Chabane, H.**; Livi, S.; Morelle, X. P.; Sonnier, R.; Dumazert, L.; Duchet-Rumeau, J.; Gerard, J. F. Synthesis of New Ionic Liquid-Grafted Metal-Oxo Nanoclusters – Design of Nanostructured Hybrid Organic-Inorganic Polymer Networks. *Polymer* **2021**, *224*, 123721(1-11).
5. Radchenko, A. V.; **Chabane, H.**; Demir, B.; Searles, D. J.; Duchet-Rumeau, J.; Gerard, J. F.; Baudoux, J.; Livi, S. New Epoxy Thermosets Derived from Bisimidazolium Ionic Liquid Monomer: An Experimental and Modelling Investigation. *ACS Sustain. Chem. Eng.* **2020**, *8*, 12208-12221.
6. **Chabane, H.**; Livi, S.; Duchet-Rumeau, J.; Gérard, J. F. New Epoxy Thermosets Organic-Inorganic Hybrid Nanomaterials Derived from Imidazolium Ionic Liquid Monomers and POSS^{®Ph}. *Nanomaterials* **2021**.

Chapter I:

Literature Review

Abstract: This literature review describes two different routes considered to modify conventional epoxy-amine networks. The first section gives a global view of “POSS[®] technology” from the description of the molecular structure of these O/I clusters, their synthesis, their incorporation into epoxy polymer materials, and the properties that result therefrom in relation with the different generated morphologies. The second section focuses on the use of imidazolium ionic liquids in the epoxy networks, *i.e.* on the synthesis and development of new functionalized ILs and the use of ionic liquids as additives or co-monomers, and in particular, on the use of ionic liquids as a mean of dispersing nano-objects in epoxy-based systems.

Graphical abstract of the chapter

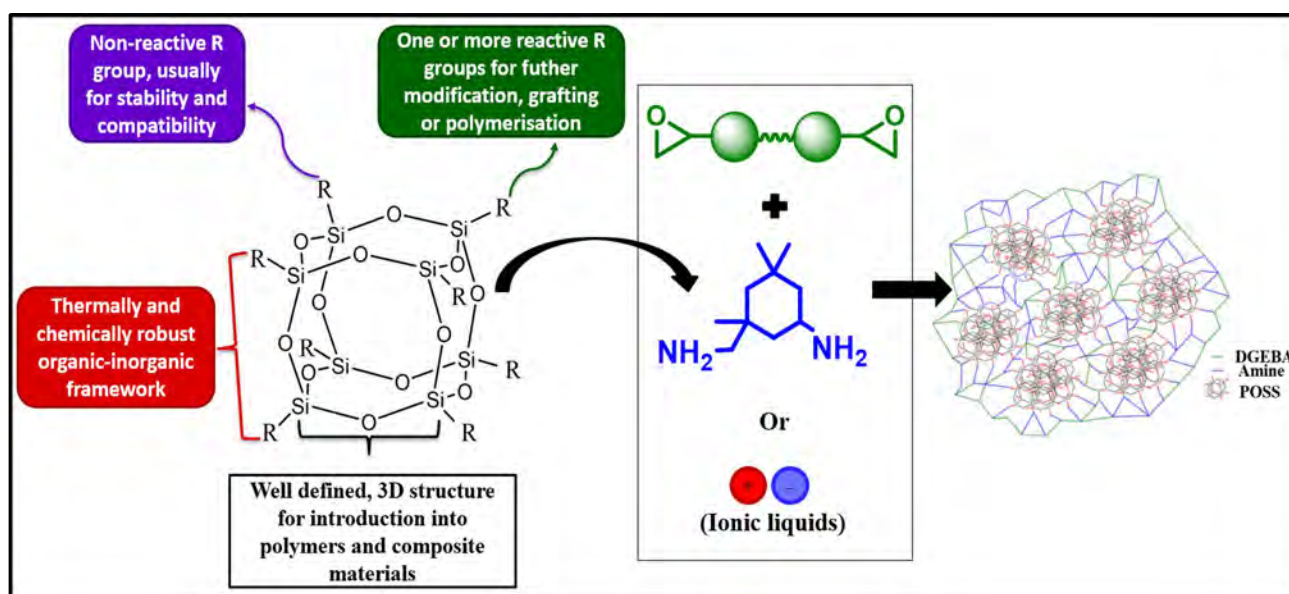


Table of contents

Chapter I – Literature Review	23
I.1. What are POSS[®] Compounds?	23
I.1.1. Molecular structure of a Polyhedral Polysilsesquioxane	23
I.1.2. Structure and dimensions of the inorganic core of a POSS [®] -T ₈	25
I.1.3. Organic structure of a POSS [®] -T ₈	25
I.2. Synthesis Strategies of POSS[®] Compounds	26
I.3. Interest of POSS[®] Compound	27
I.4. Macromolecular Structure	29
I.5. Structuration of POSS[®] in Thermosetting Polymers	30
I.6. POSS[®] and Epoxy Nanocomposites	31
I.6.1. Epoxy Networks	31
I.6.2 POSS [®] -modified Epoxy Polymers	34
I.6.2.1. Physical interaction	34
I.6.2.2. Epoxide POSS [®] as a precursor	37
I.6.2.3. POSS [®] containing curing agent	39
I.6.2.4. Influence of the POSS [®] content	44
I.6.2.5. Influence of the length of the ligand carrying the reactive function	45
I.6.2.6. Influence of nanostructuration	47
I.7. Functional Properties of POSS[®]-Modified Epoxy Polymer	48
I.7.1. Fire retardancy and thermal stability	49
I.7.2. Mechanical properties	55
I.7.3. Dielectric property	58
I.7.4. Conclusion	59
I.8. Ionic Liquids and Epoxy Polymers	60
I.8.1. Ionic liquids and their applications	60
I.8.2. ILs-modified epoxy network	62
I.8.3. Epoxy resin/imidazolium ILs curing mechanism	63
I.8.4. Epoxy/IL composites/nanocomposites	66
I.8.5. Conclusion	68
I.9. POSS[®] Ionic Liquids	68
I.10. Conclusion of chapter I	70
Reference of chapter I	71

Chapter I – Literature Review

In this chapter, the molecular architecture and routes for POSS[®] synthesis will be discussed. In the second part, we will focus on epoxy-based thermosetting polymer materials modified with POSS[®]. It describes the different ways of POSS[®] incorporation within these polymers encountered in the literature, the morphologies generated, and the properties of the resulting materials: fire behavior, thermal stability, mechanical and dielectric properties. Finally, ionic liquids and their effect on the properties of epoxy networks as modifiers will be described. In addition, the use of ionic liquids as dispersion aids or as interfacial agents for epoxy composite/nanocomposite materials are discussed. IL-modified POSS[®] structures reported in the literature and their applications are presented.

I.1. What are POSS[®] Compounds?

I.1.1. Molecular structure of a Polyhedral Polysilsesquioxane

Polysilsesquioxanes or oligosilsesquioxanes are compounds that have $\text{RSiO}_{3/2}$ as a repeat unit. The term “*silsesqui*” refers to the ratio between the silicon and oxygen atoms, *i.e.* $\text{Si}:\text{O} = 1:1.5$. POSS[®] are non-completely oxidized silicate in comparison with SiO_2 . They are obtained from the controlled hydrolysis-condensation of RSiX_3 trifunctional organosilicon monomers, where R is an organic group and X a halogen or alkoxide group, with a mechanism similar to the sol-gel process one. According to their synthesis conditions, different structures are possible (Figure I. 1): a random tridimensional structure, a bi-dimensional structure called “ladder-like”, tridimensional “cage-like” organization, and finally a partially condensed “cage-like” structure¹.

Oligosilsesquioxanes with “cage-like” organizations are better known as POSS[®] (Polyhedral Oligomeric Silsesquioxane) and have been subjected recently to a growing interest from the research community. More than 800 patents and 2300 papers involving POSS[®] are currently available². These clusters have the empirical formula $(\text{RSiO}_{3/2})_n$, where n varies from 6 to 18^{1,3}. They consist of a three-dimensional inorganic core with a perfectly defined architecture, comparable to a polyhedron. The silicon atoms occupy the vertices of the polyhedral cage while the oxygen atoms are in the middle of each edge. For example, Figure I. 2 represents the geometry of POSS[®] for which $n = 8, 10$ and 12 . The inorganic core is surrounded by ligands covalently linked to the silicon atoms. Usually, these ligands are hydrogen or any alkyl, alkylene, aryl, arylene, or organofunctional derivative of alkyl, alkylene, aryl, or arylene groups^{1,3}.

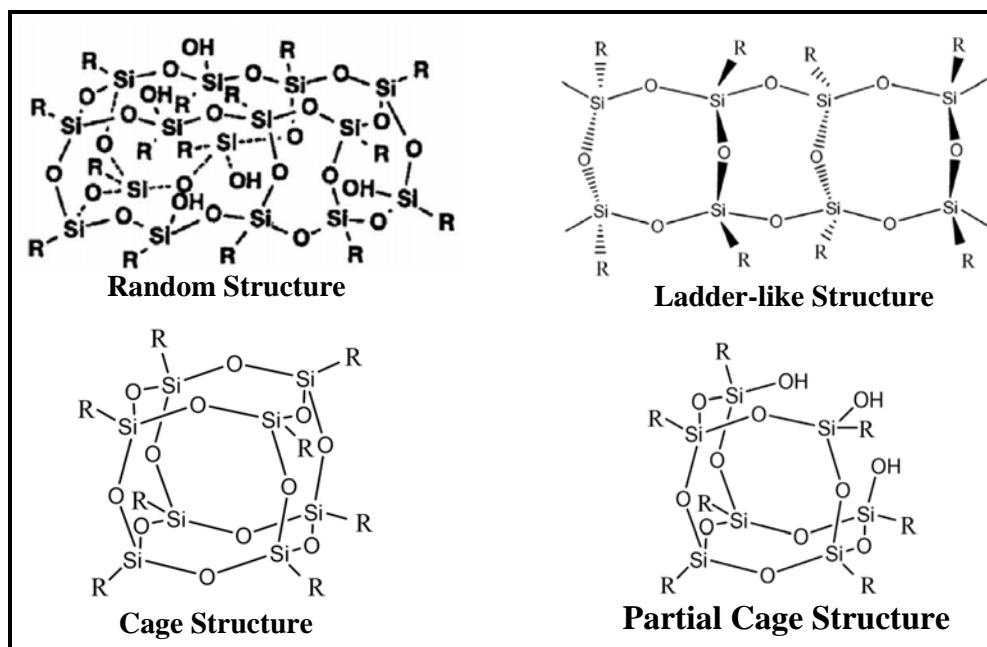


Figure I. 1: Different structures of polysilsesquioxane.

In view of the architectural diversity of the POSS[®], a nomenclature is adopted to define their structure. This one refers to the type of silicon atoms that make up POSS[®], *i.e.* M (R_3SiO), T ($RSiO_3$) or Q (SiO_4) atoms, and their number. Thus, a POSS[®] made up of n atoms of silicon type T is denoted as T_n . In certain cases, the nature of the ligands attached to the silicon atoms is specified. For example, POSS[®] whose eight silicon atoms are linked to hydrogen atoms or dimethylsilyl groups are often denoted as T_8^H and $Q_8M_8^H$ respectively (Figure I. 4). POSS[®] whose inorganic structure is made up of eight silicon atoms are the most widespread. This is why we will focus on this family of POSS[®] to describe their molecular structure ¹.

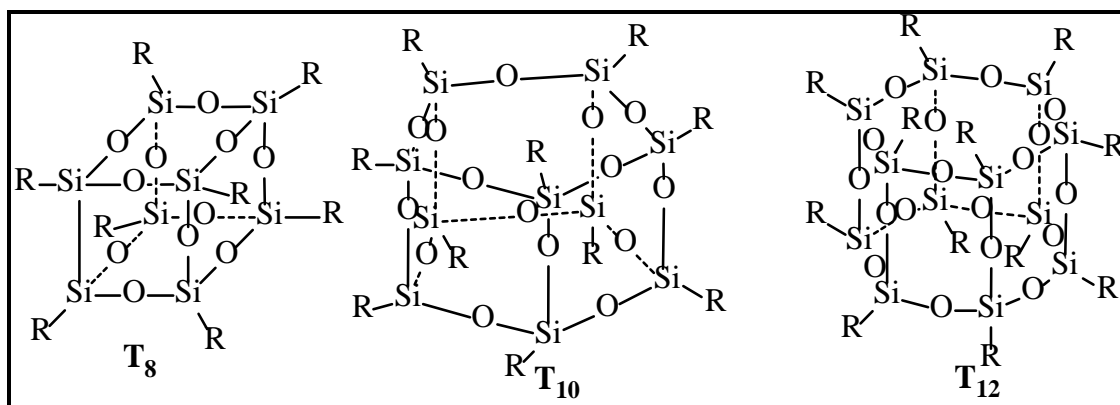


Figure I. 2: Schematic organizations of POSS[®] clusters with respectively 8, 10, and 12 Si atoms.

I.1.2. Structure and dimensions of the inorganic core of a POSS[®]-T₈

Figure I. 3 summarizes the characteristic dimensions of the inorganic cage of a T₈ type POSS[®]. Several remarks can be:

- The distance between two silicon atoms range from three to six Å so that the entire inorganic core thus being inferior to one nanometer.
- The structure has a cubic geometry but rigorously the cage is not a cube since the angles O-Si-O and Si-O-Si differ from 90° and 180°. However, as a first approximation, many authors represent the inorganic core as a perfect cube.
- The closed structure reduces the number of degrees of freedom and restricts the range of motion of the links and angles, which gives it great rigidity.

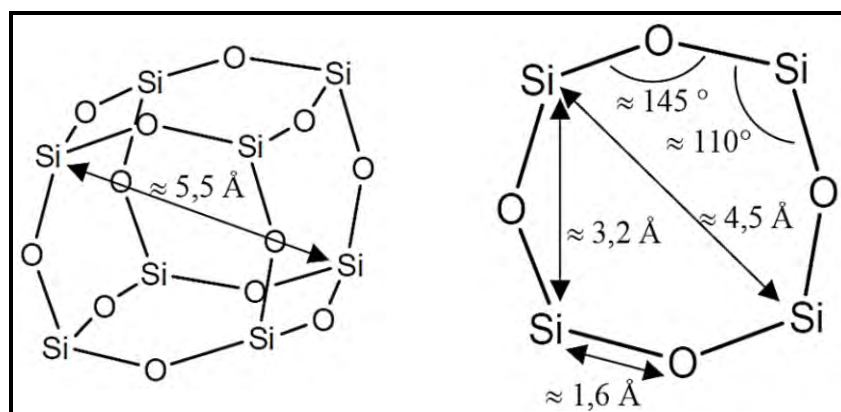


Figure I. 3: Characteristic dimensions of the inorganic core of a T₈ type POSS[®] (values determined by molecular modeling) ¹.

I.1.3. Organic structure of a POSS[®]-T₈

The ligands at the periphery of the inorganic core are generally organic in nature and could be either polar or nonpolar. Thus, the vast majority of POSS[®] has a hybrid organic/inorganic character. The diversity of organic ligands in terms of chemical nature and reactivity offers the opportunity to develop a wide variety of POSS[®]. Currently, many organic groups can be linked to the inorganic core, which allows POSS[®] to be incorporated into a wide range of polymers such as polyolefins ^{4,5}, polymethacrylates ^{6,7}, polystyrene ^{8,9}, polynorbornene ^{10,11}, polyurethanes ^{12,13}, etc. This diversity is also reflected in the functionality of POSS[®]. Depending on the number of carried reactive functions, POSS[®] can be classified into three categories:

- **Non-reactive POSS[®]**: none of the organic groups has a reactive function. POSS[®] are then often referred to as ‘molecular silica’. Generally, the organic ligands are alkyl or phenyl groups.
- **Monofunctional POSS[®]**: from the eight corner silicon atoms, seven are linked to “inert” organic groups and one carries a reactive or co-polymerizable function, *i.e.* the POSS[®] is monofunctional.
- **Multifunctional POSS[®]**: two cases are possible. Either the eight silicon atoms are linked to reactive or polymerizable groups or the POSS[®] has a number of functionalized ligands between two and seven. POSS[®] of intermediate functionality are scarcely reported due to more difficult synthesis conditions. Some examples of such POSS[®] are reported in the literature with two ¹⁴, three ¹⁵, or four ^{16,17} reactive functions. In addition to the diversity of the organic structure, the size of the ligands determines the overall volume of POSS[®]. Depending on the nature of the organic groups, the diameter of POSS[®] can varied from one to three nanometers.

I.2. Synthesis Strategies of POSS[®] Compounds

POSS[®] has attracted tremendous interest of scientists at Air Force labs and other laboratories since the early 1990s. However, the difficulties of synthesis prevented the development of these clusters. Their emergence came as soon as the methods of synthesis made it possible to produce them with significant yields and high purity, in particular thanks to the works of Feher ^{18,19} and Agaskar ²⁰⁻²³. The POSS[®] are derived from the controlled hydrolysis/condensation of a RSiX₃-type precursor where R is hydrogen or an organic group and X is a halogen or an alkoxide ^{3,24,25}. According to Provatas and Cordes ^{1,26}, there are three main synthetic routes which are summarized in Figure I. 4. The first is a direct method which constructs the three-dimensional inorganic core from a pre-functionalized RSiX₃ precursor. The second strategy is a two-step method which consists of *i*) preparing precursor POSS[®] through simple synthesis and then *ii*) functionalizing them without modifying the inorganic structure. The precursor POSS[®] are mainly POSS[®] carrying silane or silanol functions and the silicate anion Si₈O₂₀⁸⁻. From the reactive sites of these POSS[®], organic groups are attached to the vertices of the polyhedron via hydrosilylation or condensation reactions. The last one is the condensation reaction of a trialkoxy or trichlorosilane carrying a reactive function on a POSS[®] which is not fully condensed, *i.e.*

$R_7T_7(OH)_3$. This strategy considers the reactivity of the three silanol groups of $R_7T_7(OH)_3$ POSS[®] with respect to the hydrolysable bonds of an organosilane. This step is often referred to as 'corner-capping' reaction, as the condensation reaction closes the three-dimensional inorganic structure by filling the vacant vertex.

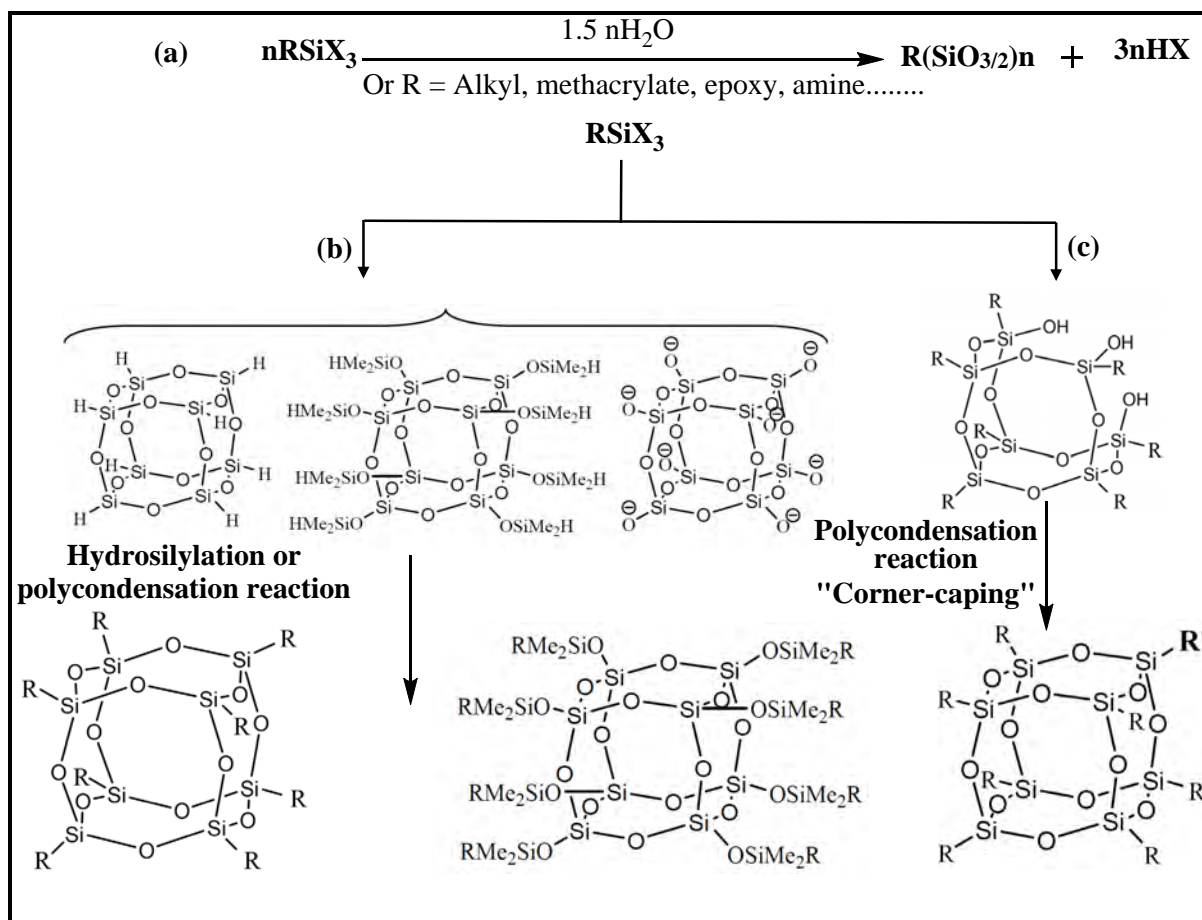


Figure I. 4: Main synthesis strategies of POSS[®] 1,26.

I.3. Interest of POSS[®] Compound

The reason why POSS[®] clusters are so attractive as structural units for hybrid polymers is based on three main considerations:

Nanometric size and isotropy of structure: due to their characteristic dimension close to 1.5 nm, the POSS[®] have an intermediate size compared to a conventional organic molecule (1 - 10 Å) and a macromolecule radius of gyration (\approx 10 - 100 nm). In addition, some features of their geometry make POSS[®] non-conventional objects compared to conventional inorganic nanofillers. In fact, they have size about an order of magnitude smaller than silica nanoparticles (diameter from 7 to

40 nm). Thus, POSS[®] are often considered as ‘the smallest accessible silica particles’. Consequently, if they are dispersed individually within a polymer material, the POSS[®] could act at a molecular scale on the properties of the polymer and the dynamics of the chains. Thus, they could offer the opportunity to generate hybrid O/I materials in the strictest definition of the term. Unlike layered silicate, they display an isotropic geometry with a perfectly defined architecture, which leads to a material with isotropic properties. Finally, conventional nanofillers have a size distributed around an average value while the POSS[®] prepared from the post-functionalization of precursors POSS[®] are isomolecular.

Intrinsic organic/inorganic hybrid character: a distinguished feature of POSS[®] nanoclusters is their intrinsic organic/inorganic hybrid nature. The mass fraction represented by each of the components is variable as a function of the size of the organic groups and of the inorganic core. Due to the intrinsic hybrid nature of POSS[®], the final properties of these clusters result from the combination of the one of each component. The inorganic structure with a chemical composition (O/Si = 3/2) is intermediate between siloxanes one (O/Si = 1) and silica or silicates (O/Si = 2) showing good thermal resistance. Thus, most POSS[®] have degradation temperatures higher than those of organic molecules. As POSS[®] consist of relatively robust siloxane bonds, these are not destroyed during the synthesis or the processing of the polymers as it involves usually heating at high temperatures. Only aggressive conditions, such as hydrofluoric acid treatment, can break these bonds^{27,28}. The organic ligands serve to compatibilize the inorganic core with the surrounding organic medium, *i.e.* to be dissolved in organic solvents or monomers. This intrinsic ability to develop favorable interactions with an organic medium (polymer, solvent) is a huge advantage compared to conventional nanofillers which require surface treatment to render them organophilic. Finally, the cohesion and stability of these hybrid O/I clusters are ensured by covalent silicon-carbon bonds between the organic and inorganic components. These bonds are stable vis-a-vis nucleophilic attacks, unlike other metal clusters based on titanium, aluminum, or zirconium for example, whose metal-carbon bond can easily be broken by certain nucleophilic agents¹.

Versatility of the organic structure: compared to conventional nanofillers, POSS[®] offer the opportunity to "easily shape" their organic architecture by conventional chemical methods, like any organic molecule. Therefore, the POSS[®] offer the possibility of “choosing” the nature of the organic ligands and of tuning them according to the chemical nature of the polymer. Such a

tailoring allows to manage the morphologies and properties leading them to be particularly attractive nanoparticles. The tunability of the organic structure makes it possible to control interactions on a molecular scale. Indeed, the ligands can be chosen according to their polarity and their reactivity to tailor the polymer/POSS[®] interactions and therefore control the state of dispersion and the morphologies generated. In other cases, the ligands can be chosen for their flexibility (or rigidity) to achieve the targeted mechanical or thermomechanical properties ^{1,3}. This ability of POSS[®] to serve as building blocks plays a key role in motivating the study of POSS[®] in polymer matrices.

I.4. Macromolecular Structure

Depending on the number of reactive ligands linked to the silicon atoms of the clusters, *i.e.* the functionality f , POSS[®] could be incorporated following four different pathways within a polymer medium. These are shown in Figure I. 5 ²⁹⁻³¹.

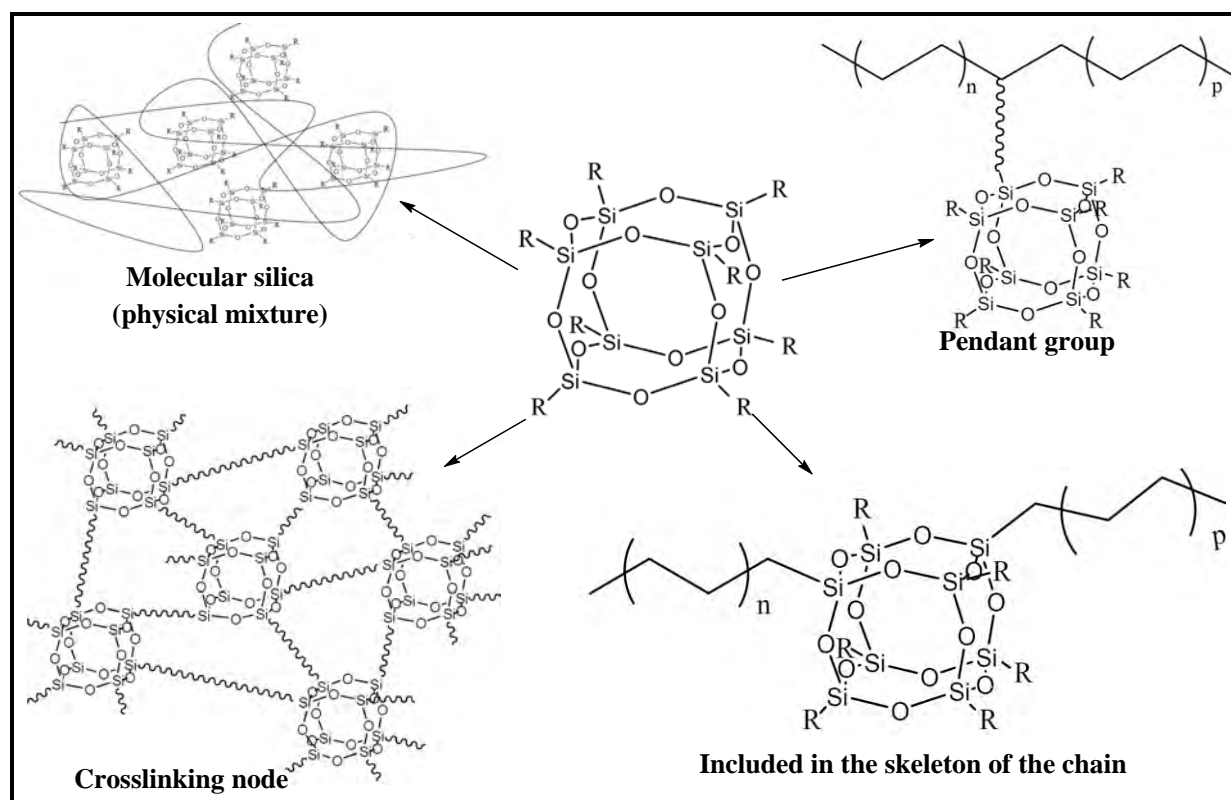


Figure I. 5: Different macromolecular structures possible according to functionality (number of reactive functions carried by POSS[®]).

- Non-reactive POSS[®]: the non-reactive POSS[®] are dispersed within a polymer matrix. They only develop physical interactions with the polymer like any other type of inert nanofillers. The state of dispersion and the morphologies generated depend on “conventional” factors such as the nature of the interactions at the polymer/POSS[®] interface and the conditions of dispersion.
- Monofunctional POSS[®]: a POSS[®] carrying a monovalent polymerizable function is included along the chain by homopolymerization, copolymerization, grafting or in the telechelic position in a macromolecule.
- Multifunctional POSS[®]: generally, a multifunctional POSS[®] is introduced into a polymer as a crosslinking point, but can also be the core of hyperbranched or star polymers. In addition, in the particular case where POSS[®] carries divalent functions on two silicon atoms, it is included in the skeleton of the chain.

I.5. Structuration of POSS[®] in Thermosetting Polymers

The state of dispersion and the size of the aggregates within thermosetting polymers are linked to the miscibility and the crystallinity of POSS[®] in the monomer and in the growing polymer during polymerization. The miscibility of POSS[®] depends on the POSS[®]-POSS[®] and POSS[®]-polymer interactions which are themselves related to the organic structure of POSS[®]. The vertex group of POSS[®] determines the morphology which decides the polarity and interaction with the matrix.

For example, Constable *et al*¹⁵ have shown that the introduction of 20 wt. % of POSS[®] carrying isobutyl ligands in polycyclopentadiene led to the formation of aggregates consisting of three or four POSS[®]. This fine dispersion results from favorable interactions between the isobutyl ligands and the polydicyclopentadiene. Schiraldi *et al*³² used POSS[®] in a series of nanocomposites based on cellulose propionate, polycarbonate, and poly(ethylene-conorbornene). The nanostructured materials stayed amorphous and transparent. Trisilanol isooctyl POSS[®] with cellulose propionate exhibited both high transparency and enhanced thermomechanical properties due to the strong interactions between the POSS[®] nano-objects and the polymer matrix.

On the other hand, Abad *et al*³³ have observed a microphase separation following the introduction of 50 wt. % of a substituted isobutyl POSS[®] in an epoxide-amine network. The formation of microscale POSS[®]-rich aggregates within the polymerized epoxy network comes from the non-miscibility of POSS[®] in the initial mixture due to the poor interactions between the

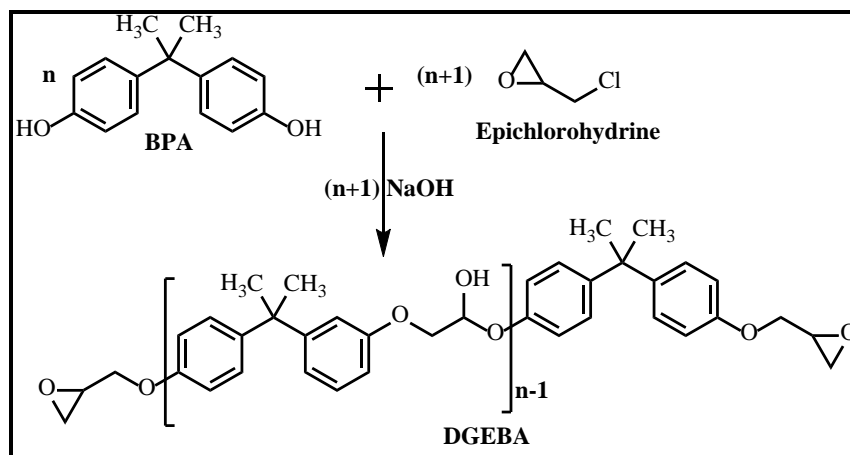
isobutyl ligands and the epoxy prepolymer derived from bisphenol A. In addition, the ability of POSS[®] to crystallize has a significant influence on their dispersion state. For example, Bocek *et al*³⁴ have studied the morphology and the thermomechanical properties of two types of an epoxy-POSS[®] nanocomposite. The mono- and octa-epoxy functionalized POSS[®] (POSS^{®Ph},E1 and POSS[®],E8) were covalently incorporated in the epoxy network DGEBA-3,3-dimethyl-4,4-diaminocyclohexylmethane (Laromin C260) as pendant units or as crosslinks, respectively. While the POSS[®] crosslinks are well dispersed in the hybrid network DGEBA-Laromin/POSS[®],E8 forming small up to 5 - 10 nm sized amorphous domains, the pendant POSS[®] (POSS^{®Ph},E1) aggregate to form large crystalline POSS[®] domains (from 100 nm -to 1 µm). This was explained by the fact that the POSS^{®Ph},E1 is able to crystallize and its crystallinity is kept, even after polymerization as the preserved mobility of the POSS[®] pendent groups is preserved.

Moreover, the tendency of POSS[®] to aggregate is related the mass fraction of POSS[®] and the presence or not of reactive functions. Increasing the volume fraction of POSS[®] contributes to reducing the inter-nanoobject distance and therefore promotes POSS[®]/POSS[®] interactions. Finally, the kinetics of polymerization is also an important factor with regard to the aggregation of POSS[®] in a thermosetting polymer. In fact, the kinetics of polymerization is in competition with the kinetics of aggregation of POSS[®] (microphase separation) and, therefore, promotes or limits the extent of phase separation and further crystallization.

I.6. POSS[®] and Epoxy Nanocomposites

I.6.1. Epoxy Networks

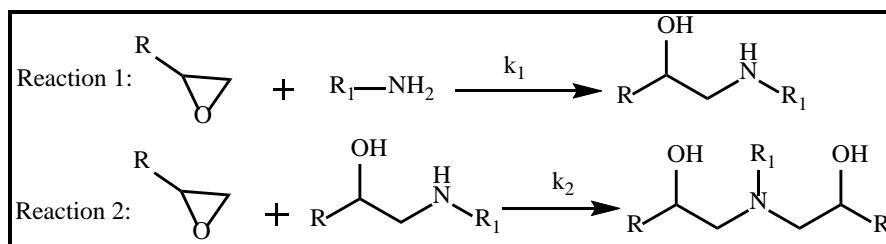
Epoxy networks are important thermosetting materials exhibiting outstanding properties, making them crucial for various applications such as adhesives, paints and coatings, electrical and electronic applications as well as composite matrices in combination with carbon fibers for aerospace applications³⁵. Epoxy networks are developed from epoxy prepolymers which consist of a minimum of two epoxide groups (oxirane rings). The high reactivity of this functional group allows epoxy prepolymers to form stable thermosetting networks. Nowadays, the most commonly used epoxy prepolymer is diglycidyl ether of bisphenol A (DGEBA) produced from the reaction between bisphenol A (BPA) and epichlorohydrin in the presence of sodium hydroxide (Scheme I. 1).



Scheme I. 1: Synthesis of diglycidyl ether of bisphenol A (DGEBA).

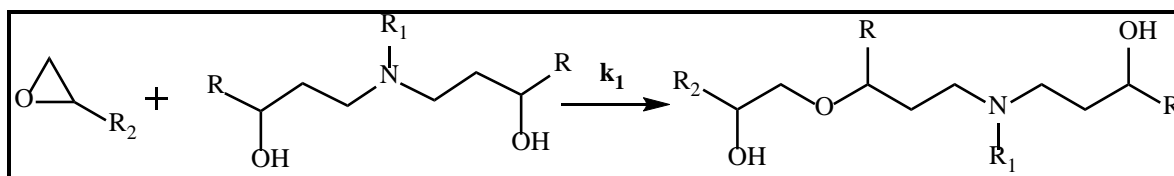
In order to form crosslinked epoxy networks, epoxy prepolymers have to either react with curing agents (amines, phenols, isocyanates, or acids) via polyaddition reactions, or combine with tertiary amines, imidazoles, or ammonium salts which initiate homopolymerization reactions³⁵. Thus, epoxy networks can be formed by step-growth polymerization and/or chain growth polymerization reactions through epoxide groups. In all the cases, the curing reactions are exothermic without emission of volatile products³⁵. The formation of by-products is low and can be controlled by changing the reactive compositions. In addition, low shrinkage is observed for final parts since the reactions are based on the opening of epoxy rings. The structure of epoxy networks depends on prepolymer functionality and molar ratio between reactant as well as the curing protocol.

Step-growth polymerization: Among numerous curing agents for epoxy prepolymers, amines are the most commonly used ones and the most representative for the case of step-growth polymerization. Reaction between epoxide groups and amines are summarized in Scheme I. 2. In fact, primary and secondary amines react with epoxide groups to form secondary and tertiary amine, respectively. The stoichiometric ratio between epoxide groups and active hydrogen of amine groups play an important role in the formation and properties of epoxy-amine networks³⁵. Hydroxyl groups generated during the reaction can facilitate the attack of amino group and epoxy-amine reaction is an autocatalytic process³⁵.



Scheme I. 2: Mechanism of addition reactions between epoxy and amino hydrogen groups with k_1 and k_2 reaction rate constants.

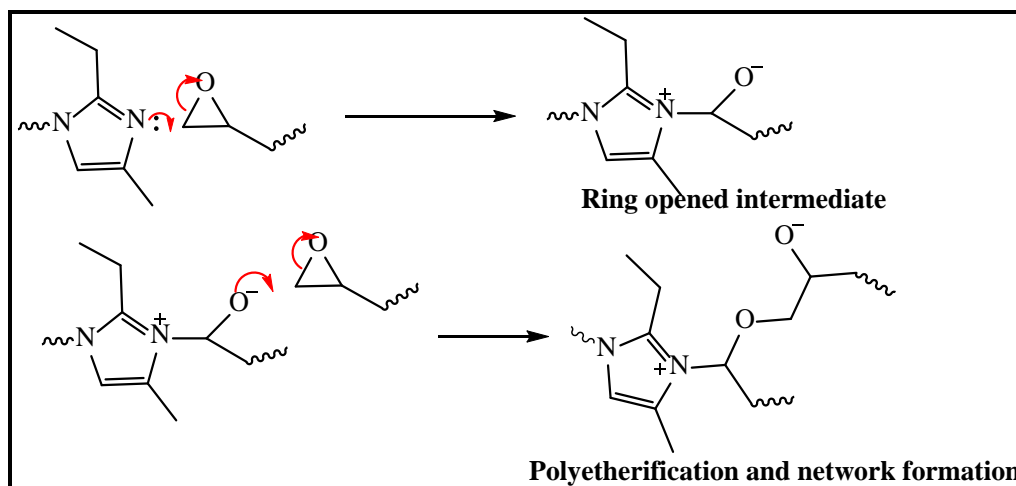
In addition, a side-reaction between epoxy and hydroxyl groups of tertiary amine denoted etherification could participate with the two main reactions (Scheme I. 3). However, this reaction is often negligible as it occurs at high temperature and is favored only in case of excess of epoxide groups ³⁶.



Scheme I. 3: Etherification mechanism between epoxy and hydroxyl groups.

The reactivity of amines which governs the kinetics of curing reactions, depends on their chemical structure ³⁷. Primary amines are more reactive than secondary ones ³⁸. Aliphatic amines are more likely to react than aromatic amines, explaining the fact that aliphatic amines are broadly used for low curing temperature applications ³⁵.

Chain polymerization of epoxy prepolymer: both nucleophilic and electrophilic compounds can react with epoxide groups, so anionic and cationic mechanisms are of great importance in epoxy chemistry. The chain homopolymerization of epoxy prepolymer can be initiated by imidazole ³⁹, tertiary amines ⁴⁰, or ammonium salts for anionic mechanism and by latent cationic catalysts ⁴¹ such as ammonium, iodonium, quinoxalinium, and pyrazinium salts for cationic homopolymerization. Barton *et al.* ³⁹ proposed the anionic reaction mechanism based on the imidazole initiation on epoxy prepolymer (Scheme I. 4). The initiators do not have significant effect on the final properties of epoxy polymers which are mainly determined from the nature of epoxy prepolymers ⁴². Complex chain transfer and termination steps lead to low polymerization degree. The chain polymerization of multifunctional epoxy prepolymers can result in the formation of epoxy networks ³⁵.



Scheme I. 4: Chain polymerization of epoxy prepolymer initiated by imidazole.

I.6.2 POSS[®]-modified Epoxy Polymers

Various researchers have been focused on the preparation of POSS[®]/epoxy hybrid nanomaterials. POSS[®] nanoclusters were mostly used to enhance epoxy properties by incorporating them into the epoxy matrix. Two approaches have been adopted to incorporate POSS[®] clusters into epoxy matrices: *i*) physical mixing of inert POSS[®] (by melt mixing or solvent casting methods) in epoxy matrix, or *ii*) covalent bonding between monofunctional POSS[®] and epoxy or chemical reaction of multifunctional POSS[®] and their contribution to crosslinking of epoxy (reactive mixing). One major difference between the two approaches is that the macroscopic phase separation between the POSS[®] nanoclusters and the polymer matrix that may occur in the former is not possible in the latter due to covalent bonding for POSS[®] copolymers. Here, we will discuss the influence of POSS[®] on the morphology and the properties of the resulting epoxy materials.

I.6.2.1. Physical interaction

The successful dispersion of POSS[®] into polymeric matrices depends on the surface interactions of POSS[®] (*e.g.* van der Waals, strong hydrogen bonding and polar) with polymers. Non-reactive POSS[®] used to modify epoxy polymers has been studied for a decade³³ and the dispersion of POSS[®] was the main challenge to overcome. Physical mixing is an easy method to carry out and has several advantages such as processing, versatility, and being a fast and cost-effective method. Nevertheless, POSS[®] remains poorly dispersed or dispersed inhomogeneously even tending to agglomerate in the mixture with poor interfacial adhesion⁴³. In most cases, such

POSS[®]-based materials have very poor physical properties and a gradient composition over the film thickness. Compared to the bulk material, the surface of POSS[®]-based materials is enriched with POSS[®] cages^{43,44}. The tendency of POSS[®] agglomeration and enrichment in the surface are associated with the poor compatibility of POSS[®] with most of epoxy resins which is due to the nature of the organic ligands (isobutyl, cyclohexyl or phenyl). In fact, the POSS[®] have the tendency to self-assemble (POSS[®]-POSS[®] interactions) in the case of strongly interactive ligands such as phenyl rings⁴⁵ (Figure I. 6a and 6c). As we can see in Figure I. 6, the different micrographs reveals that the dispersion of inserts POSS[®] is not uniform within the epoxy matrix and that there is a large size distribution of aggregates (between 0.5 to 3 μm) having different shapes. It is clearly evidenced that interactions between POSS[®] nanoclusters and epoxy polymer are mediated by ligands which are attached to the POSS[®] nanocluster. As a consequence, ligands play an essential role in influencing the clusters behavior and their spatial distribution.

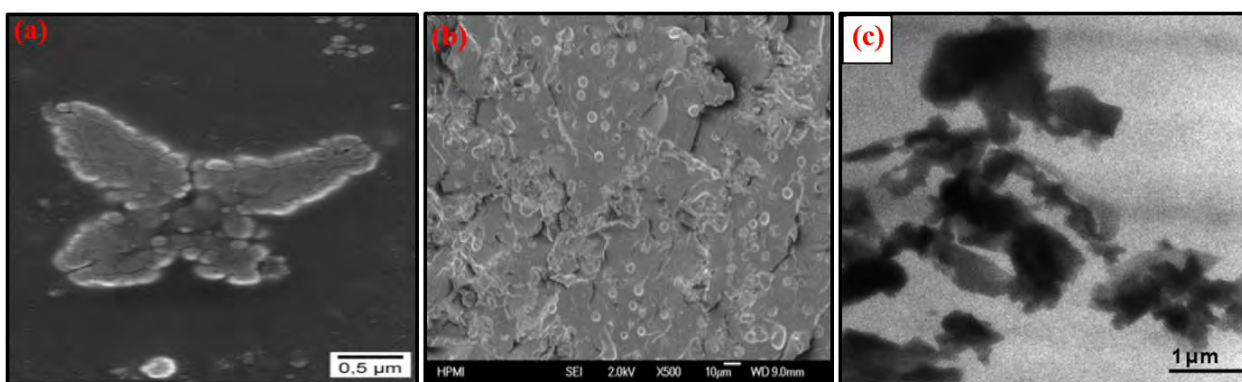


Figure I. 6: Some examples of morphologies obtained for epoxy hybrid O/I networks containing POSS[®] with different non-reactive groups: a) Ph-Gly-POSS[®]⁴⁵, b) Phenyl-POSS[®]⁴⁶, and c) AH-POSS[®]⁴⁷.

For example, two POSS[®] nanoclusters having similar structure such as, octa-aminophenyl-POSS[®] and octanitrophenyl-POSS[®], were prepared and incorporated⁴⁸ into a DGEBA-DDM system (Figure I. 7). All the reactive mixtures before curing are homogenous and transparent. The octanitrophenyl-POSS[®] (ONP) without any ability to form covalent bonding with epoxy matrix (Figure I. 7a), shows uniformly dispersed spherical POSS[®]-rich clusters (from 0.5 to 3 μm in diameter) in the continuous epoxy matrix as ONP is not miscible with DGEBA all along reaction polymerization. The two-phase morphology based on dispersed micro-domains, possesses some of the familiar characteristics of phase separation induced by polymerization. In contrast, the

epoxy hybrids containing octaaminophenyl-POSS[®] (OAP) (Figure I. 7b) remain transparent and the nanoclusters are homogeneously dispersed at nanoscale as OAP remains compatible with the reactive medium all along reaction. The thermostability of epoxy/octaaminophenyl-POSS[®] hybrid is noticed to be higher than epoxy/octanitrophenyl-POSS[®] hybrid one allowing to avoid gaseous fragments as POSS[®] cubes are dispersed at the molecular level. According to the theory of "similarity and intermiscibility", the dispersion of POSS[®] in epoxy matrix depends on the "fit" between vertex group and matrix ³³. Li *et al* investigated the compatibility of epoxy with POSS[®] and found out that the epoxy/POSS[®] blends exhibited good miscibility only at low content (Cyclohexyl-POSS[®] % \leq 10 wt. %), while the blends exhibited phase separation when the POSS[®] content was 15 wt. % ³³.

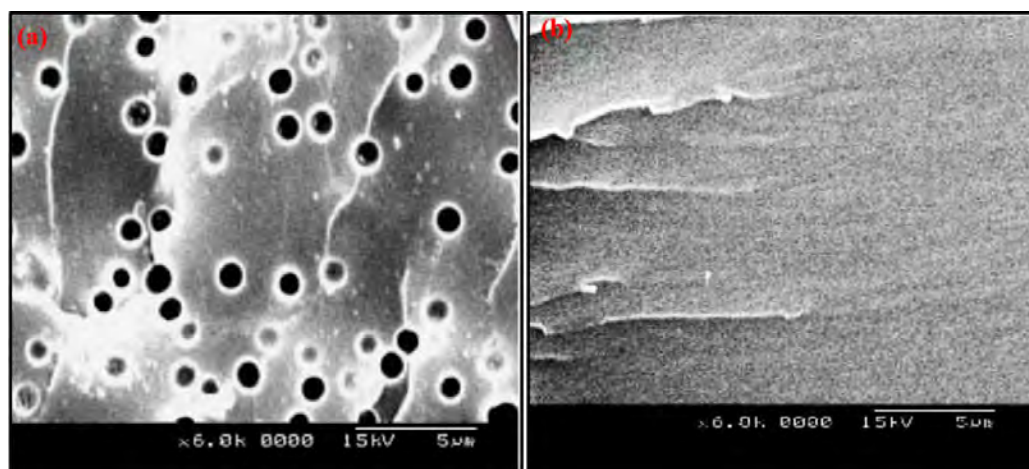


Figure I. 7: SEM micrographs of POSS[®] epoxy hybrid O/I networks containing: a) 5 wt. % of octanitrophenyl-POSS[®] and b) 10 wt. % of octaaminophenyl-POSS[®] ⁴⁸.

With this type of interaction between POSS[®] and epoxy, the nature of the inert ligands has a great influence on the resulting properties of the POSS[®] modified epoxy networks. Commonly, the incorporation of POSS[®] carrying rigid ligands such as cycloalkyls (cp) or phenyl (ph) is accompanied by an increase of the T_g and thermomechanical properties. The introduction of 10 wt. % of a monofunctional POSS[®] provided with cyclohexyl ligands in an epoxy-amine network results in an increase T_g of 8 K ⁴⁹. On the other hand, POSS[®] carrying more flexible aliphatic alkyl ligands cause a reduction of T_g . For example, a polycyclopentadiene modified by 20 wt. % of a POSS[®] which substituted by isobutyl groups has a T_g 15 K lower the one that of the neat matrix ¹⁵. Mishra *et al* ⁵⁰ observed similar effect with the inclusion of glycidyl and methacryl POSS[®] decreased the T_g of the epoxy O/I nanocomposite, while the addition of trisilanol phenyl

POSS[®] increased the T_g . The flexibility of the alkyl groups is therefore a determining factor in the impact of a POSS[®] on the T_g . However, the increase of T_g by POSS[®] contained with cycloalkyls is not systematic. Leu *et al* have shown that the incorporation of POSS[®] carrying cyclopentyl ligands in a polyimide leads to a large decrease of T_g because of the decrease of interchain interactions and increase of free volume ⁵¹. Thus, the influence of inert ligands on the T_g is subtle, as shown by the differences observed between POSS[®] substituted by cycloaliphatic groups such as cyclopentyles or cyclohexyles. In other systems, the influence on the T_g of cyclopentyl and cyclohexyl substituted POSS[®] is reversed. For example, such a different influence on T_g was observed for the poly(4-methyl styrene-co-POSS[®])-based systems studied by Haddad *et al* ⁵². Franchini *et al* ⁵³ obtained similar T_g with epoxy-amine network containing reactive Gly(glycidyl)-POSS[®] clusters and non-reactive OctaPh POSS[®] compared to the epoxy-amine matrix.

1.6.2.2. Epoxide POSS[®] as a precursor

The modification of epoxy resin by the use of reactive POSS[®] is one of the routes developed. Because covalent bonds between POSS[®] and epoxy prepolymer could give rise to an epoxy-philic chain. Then, the POSS[®] would be partially compatible with the epoxy system. As the reaction of the epoxy and the curing agent will take place according to a step polymerization, the reactive POSS[®] will be incorporated into the oligomer of epoxy. As a consequence, it will be easier for POSS[®] hybrid nanoclusters to be dispersed homogeneously at nanoscale level into epoxy matrix ⁵⁴⁻⁵⁶. For such a purpose, there are two types of reactive POSS[®] commonly used: epoxy bearing POSS[®] and ring open reagent POSS[®].

Concerning epoxy bearing POSS[®], they can be classified into two categories. One comes from the synthesis of POSS[®] and the other comes from the grafting of epoxy monomers. POSS[®] can be monofunctional, octafunctional, or multifunctional defining their epoxy functionality. In the works of Zhang *et al.* ⁵⁷, silsesquioxanes were used as synthesis platforms in the functionalization of POSS[®] with epoxy groups. Mya *et al.* ⁵⁸ studied the addition of octafunctional epoxy POSS[®] to a commercial epoxy system. A strong suppression and even a disappearance of the $\tan \delta$ peak, associated to the glass transition, was observed due to the restriction of the segmental chain motions. Huang *et al.* ⁵⁹ used the same type of POSS[®] to synthesize epoxy networks with a glass transition temperature above 400 °C. Gao *et al.* ⁶⁰ synthesized the 3-glycidyloxypropyl-POSS[®] (GM-POSS[®]) based on 3-glycidyloxypropyl-

trimethoxysilane (GTMS) and methyl-triethoxysilane (MTES) by hydrolytic condensation. The product was a mixture of the majority of T₈, T₉, and some T₁₀. GM-POSS[®] which was co-polymerized with bisphenol A epoxy resin (BPA) using 3-methyl-tetrahydrophthalic anhydride (MeTHPA). A homogenous morphology was observed suggesting a complete miscibility between the GM-POSS[®] and the epoxy-anhydride network all along reaction.

It is possible to design the structure of POSS[®] by grafting reaction as it cannot be achieved by hydrolysis route of silane precursors. Chiu *et al.*⁶¹ synthesized a POSS[®] modified DGEBA precursor (denoted as IPEP) from isocyanato-propyldinethylsilyl-isobutyl-POSS[®] (IPI-POSS[®]) and diglycidyl ether of bisphenol A epoxy resin (Figure I. 8). After the addition reaction, the absorption peak at 2,270 cm⁻¹ of the NCO group disappeared and the peaks located at 1,716 and 1,689 cm⁻¹ appeared in FTIR spectrum. The characteristic peaks are related to the C=O bonding and saturated ester group connecting the urethane chain, *i.e.* indicating the successful grafting. The curing activation energies increased slightly as the IPEP content increased. No macroscale aggregation of IPI-POSS[®] was observed. The fracture surface of such materials was smooth indicating a homogeneous phase between the organic epoxy and inorganic POSS[®] segments. Moreover, the POSS[®] phase sizes observed for such IPEP nanomaterials were found to be smaller than 100 nm. Furthermore, Liu *et al.*⁶² indicated that the formation of covalent linkages between the epoxy and POSS[®] domains with diaminodiphenylmethane (DDM) bridges should contribute to keep homogeneous the medium mixture.

Wu *et al.*⁶³ synthesized a functional POSS[®] (NPOSS[®]) with two epoxy ring groups via the reaction between trisilanolisobutyl-POSS[®] and triglycidyl isocyanate which were introduced in an epoxy network. Huang *et al.*⁶⁴ prepared epoxy/POSS[®] nanocomposites from octakis(glycidylsiloxy)octasilsesquioxane (OG) and DGEBA by UV-polymerization at room temperature followed by a thermal treatment at 160 °C for 2 h. T_g increased upon increasing the OG content: for example, T_g with an OG content of 20 phr was 143 °C, *i.e.* significantly higher than that of the neat epoxy (125 °C). The authors attributed this behavior to a significant ‘nano-reinforcement’ effect of the POSS[®] cages within the epoxy network as the nanometer scale POSS[®] cages are supposed restrict the motion of the macromolecular chains. SEM micrographs of these epoxy/POSS[®] hybrid nanomaterials containing 2 phr of OG showed a homogenous dispersion of spherical POSS[®]-rich phases (from 10 to 30 nm). Whereas, for OG content higher than 10 phr, the particle size of the OG-rich phase was 20 to 100 nm due to of the poor

miscibility between OG and the epoxy at the end of polymerization reaction. Recently, Huo *et al.*⁶⁵ investigated thermal, mechanical, and electrical properties of alkyd-epoxy hybrid O/I nanocomposite modified with 3-glycidyloxypropyl-POSS[®] (G-POSS[®]). The results showed that G-POSS[®] increased the impact strength of the hybrid O/I nanomaterials. When 6 wt. % of G-POSS[®] was added to the alkyd resin, a relatively uniform dispersion was observed by TEM combined with an increase (5K) of the T_g and changes in mechanical behavior (impact strength increased up to 53.01 kJ.m⁻² and the tensile strength decreased to 15 MPa).

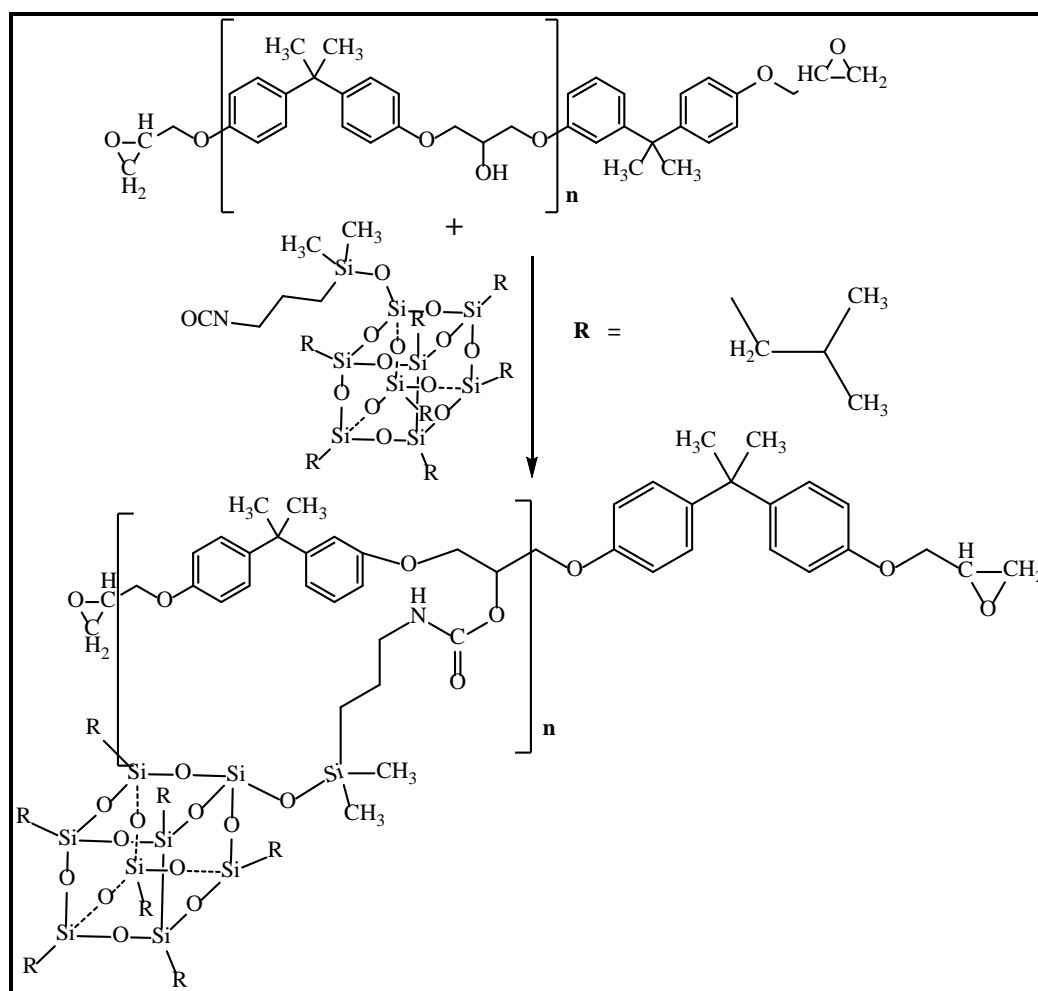


Figure I. 8: Synthesis of the isocyanato-propyldinethylsilyl-isobutyl-POSS[®] (IPI-POSS[®])-modified epoxy (IPEP)⁶¹.

I.6.2.3. POSS[®] containing curing agent

As previously mentioned, the control of the structure and morphology of the epoxy hybrid O/I nanocomposites is governed by adjusting of POSS[®]-polymer and POSS[®]-POSS[®] interactions

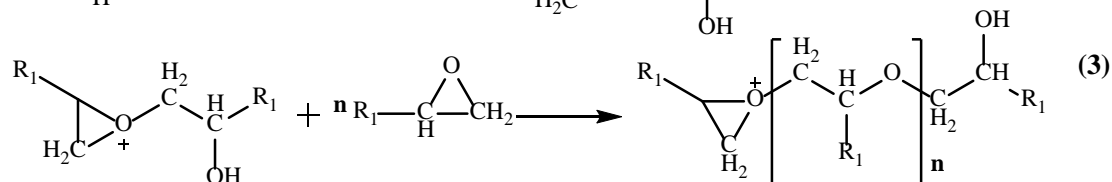
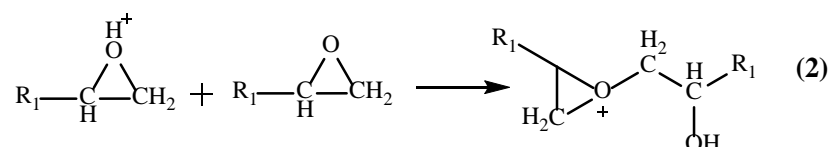
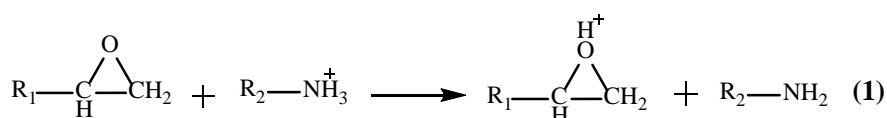
⁶⁶. Matejka *et al.* ^{66,67} studied the distribution of different types of POSS[®] in an epoxy-amine (DGEBA/Jeffamine D2000) network as a function of their content, the nature of curing agent, and POSS[®] type. For example, stoichiometric O/I networks or those with relatively small excess of amine, regularly arranged silsesquioxane cluster junctions interlinked by the organic chains of amine. With an excess of amine, the cylinder-based assembling becomes interconnected and their percolation could be reached to form a silsesquioxane continuum.

Zhang *et al.* ⁶⁸ have used octa(aminopropyl)silsesquioxane (NH₂CH₂CH₂CH₂)₈Si₈O₁₂ (POSS[®]-NH₂), containing eight amine groups as curing agent for an epoxy prepolymer, *i.e.* diglycidyl ether of bisphenol A (DGEBA). After the fracture of the DGEBA/POSS[®] cured network, a river-like structure and the fiber-like pulling out was observed. This POSS[®] *insitu* structuration could sustain large amounts of energy before fracture. As a result, the impact strength was improved. The degradation temperature of DGEBA/POSS[®] network (519 °C) was 160 °C higher than conventional DGEBA-DDS matrix (359 °C) and the char residues for POSS[®]-modified network (30 %) was 17 % higher than that of matrix (13 %).

Liu *et al.* ⁶⁹ prepared benzoxazine-containing silsesquioxanes (SPOSS[®]-BOZ) as a curing agent for epoxy using a thiolene (click) reaction between benzoxazine containing allyl group (BOZ) and mercaptopropylisobutyl POSS[®] (SPOSS[®]) in tetrahydrofuran (THF) solution catalyzed by 4-dimethylaminopyridine (DMPA) under UV irradiation. The crosslinked architectures of the resulting nanocomposites of SPOSS[®]/polybenzoxazine/epoxy showed a homogeneous dispersion of POSS[®] (domain sizes from 80 to 200 nm) with improved thermostability and fire retardancy behavior.

Octa(3-chloroammoniumpropyl)octasilsesquioxane (OCAPS) is a water-soluble quaternary ammonium functionalized POSS[®] synthesized by Perrin *et al.* ⁷⁰ to study its effect on epoxy self-polymerization and epoxy-amine curing. It possesses a latent amine functionality that should be more reactive than the aromatic amino groups of octa(aminophenyl)silsesquioxane. A series of nanomaterials DGEBA-Jeffamine D2000 based on 0, 2, 5, and 7.5 wt. % of OCAPS were prepared for a stoichiometric ratio amino hydrogen - to epoxy equal to 1. Alkyl ammonium ions catalyzed both epoxy homopolymerization ⁷¹ and epoxy-amine reactions ⁷². The mechanism of epoxy homopolymerization is catalyzed by the acidic protons of primary ammonium as shown in equations (1) to (3). As the latent POSS[®] does not react directly to epoxy, a poor compatibility

during the polymerization is observed leading to the aggregation of POSS[®] into the final epoxy network.



POSS[®] containing a mercaptopropyl group (MPOSS[®]) was synthesized by Fu *et al.*⁷³ via the hydrolytic condensation of γ -mercaptopropyl triethoxysilane in an ethanol solution catalyzed in highly acidic conditions. Such a mercaptopropyl-POSS[®] was used to modify epoxy-amine networks via a co-polymerization reaction with DGEBA. The resulting hybrid O/I materials (MPOSS[®]/DGEBA) exhibit homogenous morphologies as no discernable phase separation was observed. This suggests that the MPOSS[®] nano-clusters took part in the formation of crosslinked networks and was well dispersed within the matrix at nanoscale. Xu *et al.*⁴⁷ incorporated monofunctional-anhydride polyhedral oligomeric silsesquioxane (AH-POSS[®]) into epoxy system either pre-reacted or non-reacted using hexahydrophthalic anhydride (HHPA) as curing agent. The result of pre-reaction between AH-POSS[®] and DGEBA was confirmed by SEC, which indicated the formation of higher molar mass compounds and bonding between the AH-POSS[®] to one or two DGEBA molecules. A conventional macrophase separation happened for AH-POSS[®] content lower than 30 wt. % and some “vesicle” structures were formed after curing due to a phase separation mechanism induced by polymerization.

Jothibasur *et al.*⁷⁴ synthesized octa(maleimidophenyl) POSS[®] precursor (OMPS) to develop new nanomaterials for advanced industrial and aerospace applications. When a compound is not a direct curing reagent for epoxy prepolymer, the crosslinking architecture of the networks were predominantly formed between the terminal maleimide double bonds and the amino groups from 4,4'-diaminodiphenylmethane (DDM) through a ‘Michael’ reaction to form aspartimide. For DDM, the residual tail of amine reacted with epoxy which allowed the fine dispersion of OMPS nano-clusters in the epoxy network⁷⁵. As the POSS[®] content of was lower than 5 wt. %, the

nanomaterials showed an enhanced glass transition temperature (T_g) in comparison with the neat epoxy (DGEBA-DDM).

Ni *et al.*⁷⁶ synthesized a reactive POSS[®] bearing hydroxyl and amino group via (γ -aminopropylsilsesquioxane) reacting with n-butyl glycidyl ether. Then, the resulting POSS[®]-BEG nano-clusters were used for improving the mechanical and thermal properties of epoxy resin. The elaborated hybrid networks have shown microphase separation with a dramatic improvement of the impact strength as well as thermal and thermomechanical properties. Compared to the conventional epoxy precursor, the epoxy-functionalized POSS[®] has a lower reactivity due to the introduced steric hindrance. In addition, the phase separation induced by POSS[®] reaction leads to a decrease in conversion and in T_g ⁷⁷. The pre-reaction between the epoxy precursor POSS[®] and the curing agent allowed complete reaction and a homogeneous material with controlled morphologies^{45,77}.

These authors observed that, adding POSS[®] into the epoxy matrix results in a much rougher fracture surface (this effect is emphasized with higher POSS[®] content). Jones *et al.*⁷⁸ also compared the fracture surfaces of neat epoxy (SC-15) with those obtained after incorporation of octaepoxycyclohexyl-POSS[®]. They revealed very different fracture surfaces (Figure I. 9). In fact, the neat epoxy resin displays a relatively smooth fracture surface whereas for the nanomaterials, fracture surfaces are rougher.

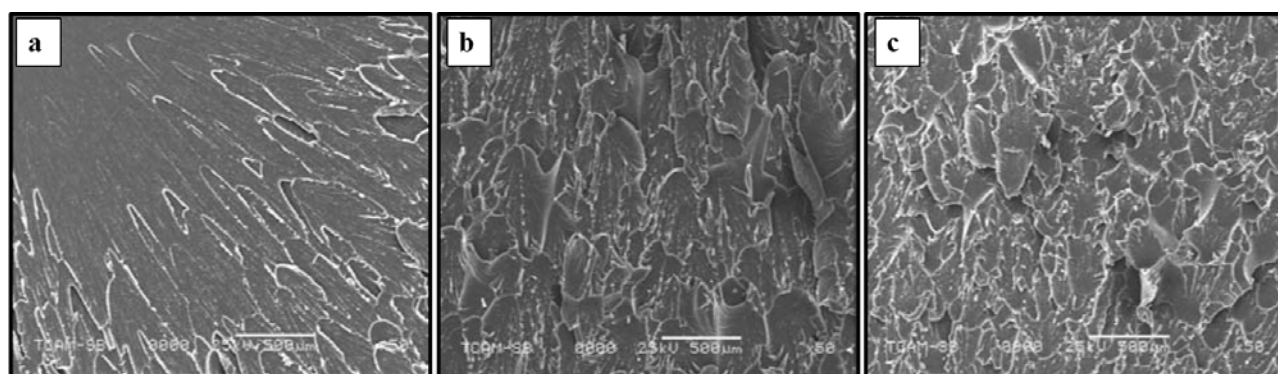


Figure I. 9: Fracture surfaces of neat epoxy a) and POSS[®]/epoxy nanomaterials containing b) 1 wt. % POSS[®], and c) 5 wt. % POSS[®]⁷⁸.

Zucchi *et al.*⁴⁵ and Franchini *et al.*⁵³ compared the phase separation of monofunctionalized epoxide POSS[®] with two other types of inert groups: isobutyl POSS[®] (Gly-iBu POSS[®]) and phenyl POSS[®] (Gly-Ph POSS[®]) incorporated into an epoxy-amine (DGEBA-MDEA) resin. The

Gly-iBu POSS[®] led to the formation of irregular POSS[®] aggregates from POSS[®] self-assembling. Gly-Ph POSS[®]-based material had a more complex morphology composed of smooth areas assigned to the neat epoxy-amine matrix zones, and a large rough area associated with POSS[®]-rich phases. It could be concluded that a better compatibility is obtained between the phenyl ligands with the epoxy-amine components compared with the isobutyl ligands and the pre-reaction of POSS[®] contributed to increase the compatibility of POSS[®] with the epoxy-amine matrix (Figure I. 10).

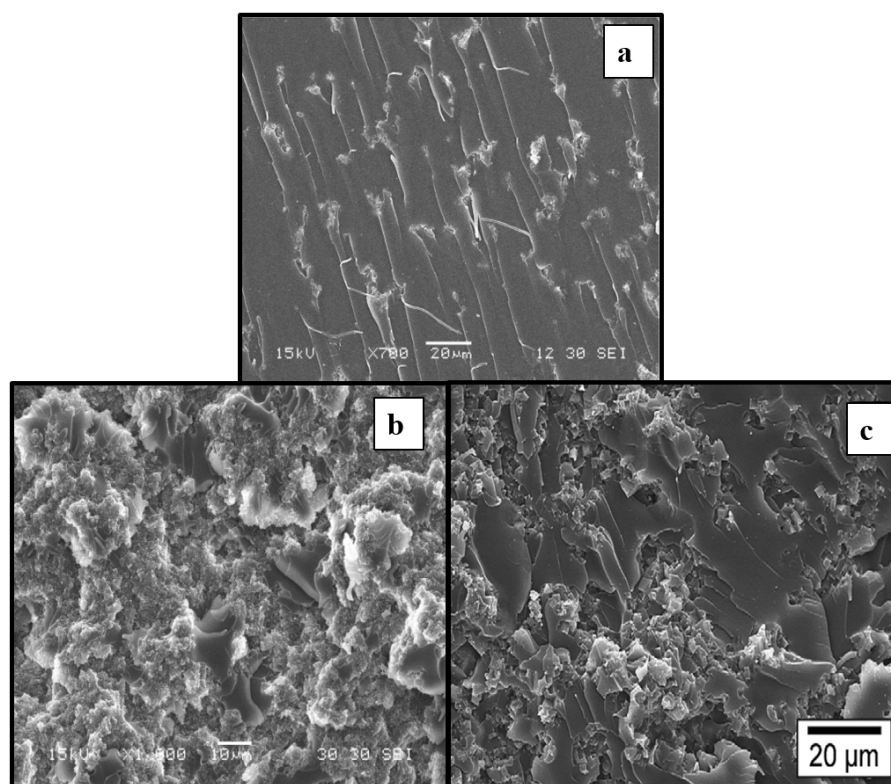


Figure I. 10: SEM micrographs of resulting morphologies generated in DGEBA-MDEA epoxy networks modified with POSS[®]: a) pre-reacted Gly-iBu POSS[®], b) pre-reacted Gly-Ph POSS[®], and c) non-reactive OctaPh POSS[®] ^{45,53}.

The mechanism of phase formation of POSS[®]-modified epoxy could be associated to a liquid-liquid phase separation induced by polymerization (or Reaction Induced Phase Separation RIPS). Recently, Di Luca *et al.* ⁷⁹ prepared conventional (well-known) POSS[®]-epoxy nanomaterials which exhibited a double dispersion of POSS[®] crystal-like platelets and dispersed POSS[®]-rich droplets. The crystal-liquid (C-L) equilibrium between the pure crystalline POSS[®] and the solution was calculated from the conventional equations developed by Flory and

extended to a polydispersal solvent using the ‘Flory-Huggins’ model. Zhang *et al.*⁸⁰ investigated the microscale morphology and mechanical properties of an epoxy resin DGEBA-DDS (EP)/octa(aminopropyl)silsesquioxane (POSS[®]-NH₂) O/I hybrid composite. POSS[®]-NH₂ incorporated into the epoxy network showed good compatibility with the epoxy matrix. Phase separation was not observed even at high POSS[®]-NH₂ content (20 wt.%). The incorporation of POSS[®]-NH₂ nanoclusters into the epoxy network increased the glass transition temperature of the resultant nanocomposites after curing (from 179 to 219 °C). In addition, impact and flexural strengths of the hybrid reached their maximum values (26.4 kJ.m⁻² and 105 MPa) when 10 wt.% content of POSS[®]-NH₂ was introduced.

As a conclusion, one can concluded that the incorporation of reactive POSS[®] nano-clusters influences the T_g of the POSS[®]-modified networks. T_g depends on several factors such as POSS[®] content and POSS[®] organic structure governing POSS[®]-polymer interactions and their dispersion state within the polymer matrix³¹.

I.6.2.4. Influence of the POSS[®] content

Numerous studies have highlighted the influence of the POSS[®] content on the T_g of copolymers based on conventional organic monomers and monofunctional POSS[®]. Haddad *et al.*⁸¹ have prepared a range of copolymers of 4-methylstyrene with heptacycloalkyl POSS[®] of variable compositions ranging from poly(4-methylstyrene) to POSS[®] homopolymer. For these polymers, the thermomechanical glass transition temperature increases with the POSS[®] content. However, above 20 wt. % of POSS[®] homopolymers including the functionalized methacrylate POSS[®], no more glass transition can be evidenced by DSC signing of a strong reduction in the segmental mobilities in the copolymer⁸².

The weight content and volume of POSS[®] as a pendant object have a large influence on the reduction of the mobility of the macromolecular chain. Xu *et al.*⁸³ studied the mechanism of modification of the T_g induced by the incorporation of monofunctional POSS[®] in poly(acetoxy styrene) (PAS-POSS[®]) and poly(vinylpyrrolidone) (PVP-POSS[®]). The influence of the molar fraction of POSS[®] on the T_g of these polymers is shown in Figure I. 11. The increase of the molar fraction of POSS[®] in these polymers leads to a decrease of the T_g up to a critical molar fraction after which the T_g increases. At low concentrations, the POSS[®] reduce the dipole-based interactions between chains, reducing T_g. By increasing the molar fraction in POSS[®], the dipole-dipole interactions between the siloxane cage and the carbonyl groups of the macromolecular

chains as well as the POSS[®]-POSS[®] interactions become preponderant. This results in an increase of the T_g .

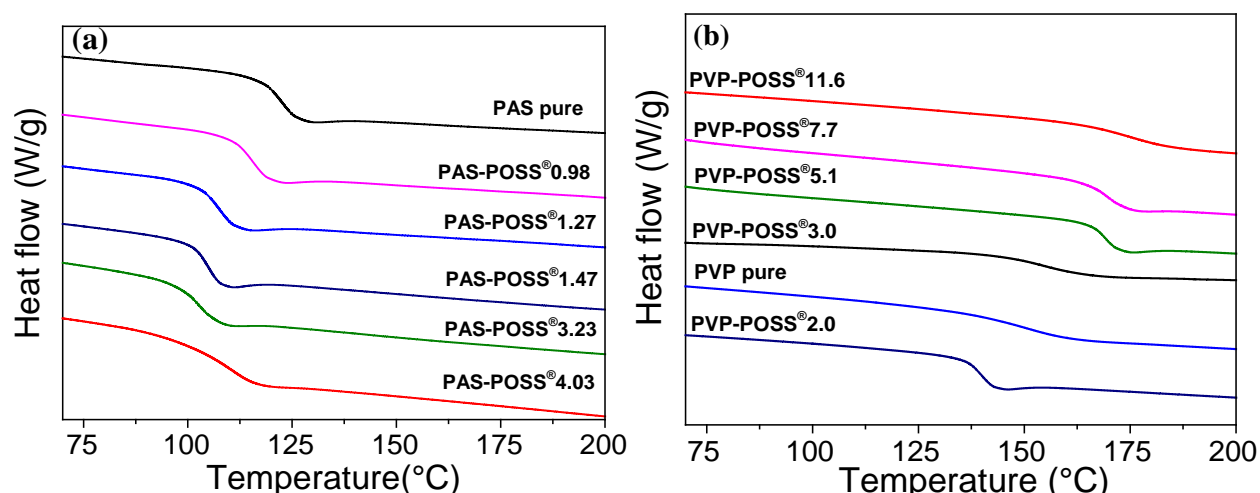


Figure I. 11: Effect of the POSS[®] molar fraction on the glass transition temperature of a) poly(acetoxystyrene) and b) poly(vinylpyrrolidone) ⁸³.

In summary, the influence of POSS[®] content on the glass transition temperature results from the competition between two antagonistic effects: *i*) At low concentrations, the dilution effect of the inter/intramolecular dipole interactions prevails and leads to a decrease of the glass transition temperature; *ii*) At higher concentration, the strong POSS[®]-polymer and POSS[®]-POSS[®] preponderant interactions control the mobility of the macromolecular segments and lead to an increase of the glass transition temperature.

I.6.2.5. Influence of the length of the ligand carrying the reactive function

The length of the functionalized organic vertices determines the distance between the inorganic cage and the skeleton of the macromolecule. Increasing the length of the spacer vertices reduces the mobility of macromolecular segments imposed by the large volume of POSS[®] and, therefore, minimizes its influence on the T_g . This effect has been observed by Haddad *et al.* in the case of copolymers of 4-methylstyrene with POSS[®] carrying an ethyl styrene ($\text{CH}_2=\text{CH}-\text{C}_6\text{H}_4-(\text{CH}_2)_2-$) or styrene ($\text{CH}_2=\text{CH}-\text{C}_6\text{H}_4-$) ligand ⁵². The incorporation of POSS[®] is accompanied by an increase in the T_g of the copolymers compared to poly(4-methylstyrene). However, whatever the composition, the increase of the T_g caused by the functionalized ethyl styrene POSS[®] is less than that produced by the functionalized styrene POSS[®]. The introduction of an ethyl link on the reactive vertices reduces the effect of the cage on the mobility of the polymer skeleton.

With thermosetting resins based on epoxy-amine reactions, the papers considering POSS[®] containing reactive functions such as amine groups report an increase of T_g ^{84,85} whereas POSS[®] containing oxirane groups generally lead to a decrease of T_g ^{86,87}. This difference is due to the fact that amine groups are more reactive with epoxy resin than oxirane with the hardener usually used in epoxy-cured systems. However, the nature of physical interactions of POSS[®] with epoxides are very different numerous. Matejka *et al.*⁶⁶ investigated the effect of POSS[®] bearing reactive function on thermomechanical properties of epoxy-amine (DGEBA-D2000) network. They observed that the incorporation of heptaphenyl-aminopropyl POSS[®] (POSS^{®Ph}-A2) or heptaphenyl-glycidylpropyl POSS[®] (POSS^{®Ph}-E1) as pendant units in the epoxy network leads to an increase of the T_g compared to the neat epoxy (DGEBA-D2000). Li *et al.*³³ considered an aliphatic epoxy combined with a multifunctional epoxy-POSS[®] and found that the epoxy/POSS[®] 75/25 (wt. %) nanomaterial exhibited much lower T_g than the neat epoxy-amine network. These authors argued that the T_g depression could be related to incomplete curing reaction of epoxy due to the incorporation of POSS[®] and low reactivity of the oxirane groups. Choi *et al.*⁸⁸ have used two types of POSS[®] denoted octa(ethylcyclohexylepoxy)dimethylsiloxysilsesquioxane (OC-POSS[®]) and octaglycidyltrimethylsiloxysilsesquioxane (OG-POSS[®]) with a 8 epoxy groups as comonomers with diaminodiphenylmethane (DDM) to synthesize hybrid O/I epoxy-amine networks. The main difference between the two POSS[®] was the flexibility of the organic chains tethered onto the epoxy rings, the OG-POSS[®] being less rigid than the OC-POSS[®] and the nature of the oxirane group (cycloaliphatic versus aliphatic). This latter characteristic has influenced the reactivity of the epoxy rings resulting in different T_g . In particular, it is assumed that each amine group can only react with one OC-POSS[®] while the equivalent groups on OG-POSS[®] can react with one NH₂ group. Thus, the crosslink density of POSS[®]/epoxy networks is controlled by managing POSS[®]-POSS[®] and POSS[®]-epoxy interactions. Moreover, in the case of epoxy containing monofunctional POSS[®], the POSS[®] content is another key parameter. At low content, pendant POSS[®] have a plasticizing effect in the epoxy network whereas at higher content, the aggregated and physically crosslinked POSS[®] can act such fillers and could contribute to the reinforcement.

I.6.2.6. Influence of nanostructuration

As with any nanofillers, the dispersion and nanostructuration of POSS[®] are key factors for tailoring the effect of these nano-objects on thermomechanical properties. Mather and Haddad mainly studied the influence of the nanostructuration of POSS[®] on the T_g for norbornene block copolymers^{10,89,90}. For block copolymers, a phase microseparation occurs between the POSS[®] and norbornene blocks due to the immiscibility of the two blocks. As a consequence, no modification of the glass transition temperature of the norbornene phase has been observed⁸⁹. In contrast, random copolymers nanostructured into a cylinder-based morphology (about a few tens of nanometers)⁹⁰. As mentioned previously, for a given composition, the influence of a POSS[®] on the T_g of poly(norbornene-co-POSS[®]) copolymers is a function of the nature of the organic ligands. The authors attributed the difference of T_g observed between the cyclopentyl and cyclohexyl substituents to the difference in size of the cylinders generated by the two types of POSS[®] as well as to the difference in the organization of POSS[®] within of these aggregates. Indeed, for 50 wt. % content, the cyclopentyl-substituted POSS[®] lead to small aggregates in which they organize themselves in a crystalline manner. Thus, according to the authors⁹⁰, very few polynorbornene segments are trapped within the segregates. Such a feature tends to minimize the effect of this type of POSS[®] on thermomechanical properties of the copolymers. In contrast, the cyclohexyl-functionalized POSS[®] form larger aggregates within which the POSS[®] keep an amorphous organization. Therefore, the authors assumed that a fraction of the polynorbornene segments remains confined within these aggregates, explaining the higher effect on thermomechanical properties for this type of POSS[®].

Pistor *et al.*⁹¹ studied the influence of different concentrations (1, 5, and 10 wt. %) of glycidylisobutyl-POSS[®] on the glass transition temperature of an epoxy resin (DGEBA-cycloaliphatic amine). The T_g measured from the $\tan \delta$, was 76 °C for the neat network. Two relaxation temperature peaks (67 and 93 °C) and (70 and 94 °C) were observed for 1 and 5 wt. % POSS[®]-based networks, respectively (for 10 wt. %, the T_g was again 76 °C). These authors related T_g changes to the effect of heterogeneity of POSS[®] dispersion and to spatial distribution effects as a result of the ability of POSS[®] to form chemical bonds with the epoxy during crosslinking. Zucchi *et al.*⁴⁵ observed a non-complete conversion of POSS[®] which can take place for POSS[®] bearing epoxy groups due to their low reactivity compared with the ones of epoxy precursor. The unreacted epoxy POSS[®] led to a dispersion based on POSS[®]-rich spherical

particles with micrometer sizes due to the incomplete conversion of POSS[®]. Liu *et al.*⁹² reported the preparation of epoxy-amine hybrid O/I nanocomposites with heptaphenyltrisilanol POSS[®] (POSS^{®Ph}-triol) by using a metal complex, *i.e.* aluminum triacetylacetonate (Al). An improvement of thermomechanical properties was observed and has been attributed to the nanoscale dispersion of the POSS^{®Ph}-triol nano-clusters. Bocek *et al.*³⁴, correlated the difference in the properties of the elaborated nanomaterials to the morphology changes. The epoxy-amine nanomaterials with large non-homogeneously dispersed aggregates of pendant heptaphenylglycidyloxypropyl POSS[®] (POSS[®],E1) show the poorest thermal properties, including low T_g and thermal stability, and high dielectric loss factor at higher temperatures. On the opposite, the homogeneous nanocomposites containing octa(glycidyloxypropyl) POSS[®] (POSS[®],E8) dispersed at a molecular scale display improved thermomechanical properties and high thermal stability. Strachota *et al.*⁹³ also have investigated the thermomechanical properties of an epoxy-amine (DGEBA-Jeffamine D2000) modified with different types of POSS[®] as pendant units the network or as crosslinks. They observed that the highest enhancement was achieved for the networks with pendant POSS[®] which self-assemble as crystalline domains and act as physical crosslinks. The POSS[®] skeleton with “soft” flexible ligands, such as octyl groups leads to the formation of weak aggregates which do not contribute to network changes. Therefore, not only the nanostructuration, *i.e.* self-assembling process, is involved but also the ability of POSS[®] to crystallize both have important effects on the properties of final networks.

These studies show that a slight difference in the nature of the organic part of POSS[®] modifies its ability to self-assemble in the polymer medium. In fact, POSS[®] nanoclusters have the capability to form aggregates having different morphologies such as spheres, cylinders, or depending on the processing conditions. In conclusion, the influence of the nature of organic ligands on the glass transition temperature of POSS[®]-modified networks is of great complexity. Multiple parameters such as the intrinsic flexibility of the non-reactive groups, the structure of the reactive ligands, the conformation of macromolecular chains close to the nano-clusters (governed by the POSS[®]-polymer interaction), the resulting state of the POSS[®] dispersion and the nanostructuration of the POSS[®] nanoclusters in the medium all need to be taken into account.

I.7. Functional Properties of POSS[®]-Modified Epoxy Polymer

Epoxy resins are the most commonly used thermoset due to their properties such as high modulus and strength, chemical resistance, and easy processing. As mentioned previously, the

incorporation of POSS[®] units leads to epoxy based nanomaterials with unexpected features such as enhanced thermal stability, chemical and oxidative resistances, improved flame retardancy, and mechanical strength and high isolation.

I.7.1. Fire retardancy and thermal stability

POSS[®] were shown to enhance the properties of polymers or to create new functions such as fire retardancy⁹⁴. Such enhancement primarily depends on the state of dispersion of the POSS[®] cages in the polymer matrix and on the nature of organic substituents on the POSS[®] cage^{1,3}. Much attention has been focused on the use of POSS[®] for partial/total substitution of toxic fire retardants (halogen-type FR) in combination with superior physical properties^{1,3,95,96}. These reported works indicate that POSS[®] bring unusual effects on fire resistance properties of polymers as substituting fire retardants, or as synergistic fire retardants according to fire test requirements imposed by regulations⁹⁴. Numerous studies involving POSS[®] modification consider analyses done using combustion calorimeter to assess fire resistance properties.

Usually, the pHRR (Heat Release Rate) peak is shown to be reduced by the incorporation of POSS[®] whatever the chemical nature of the polymer matrix. From Wu *et al.*⁶³ bearing results, it can be concluded that the incorporation of NPOSS[®] (functional polyhedral oligomeric silsesquioxane bearing two epoxy ring groups) into an epoxy resin (DGEBA-m-PDA) is important for improving the flame retardancy and thermal stability of the epoxy network. The combustion calorimeter results indicated that 10 wt. % of NPOSS[®] in the epoxy-amine network could reduce the peak heat release rate (pHRR) by about 30 %. The nature of the morphology of the POSS[®]-modified material influences the heat release rate (HRR) as a non-halogen fire retardant. The addition of POSS[®] into epoxy resin catalyzes the char formation acting as a barrier for both heat flow and mass transport, *i.e.* reducing the HRR⁶³.

Glycidyl POSS[®] functional groups that can react with the curing agent amino hydrogen groups were often used as fire retardants of epoxy resin^{97,98}. Two reactive POSS[®] containing one tethered glycidyloxypropyl group and bearing either phenyl or isobutyl groups on the other seven silicon atoms were investigated: glycidyloxypropyl-heptaphenyl-POSS[®] (Gly-Ph POSS[®]) and glycidyloxypropyl-heptaisobutyl-POSS[®] (Gly-iBu POSS[®])⁵³. The presence of POSS[®] nanoclusters leads to different reductions of the pHRR depending on the type of POSS[®] as shown in Figure I. 12a. For the Gly-Ph POSS[®] with phenyl groups, the pHRR decreases by 40 % compared to 25 % for isobutyl-based POSS[®] (Gly-iBu POSS[®]) network. This tendency was

confirmed by the UL-94 test (it is a fire test released by Underwriters Laboratories and harmonized via the ASTM standard D3801 with samples of 125 x 13 mm² -thickness can vary) results. As epoxy containing Gly-iBu POSS[®] burnt entirely, *i.e.* showing no improvement as compared to the neat matrix, the Gly-Ph POSS[®] introduction leads to self-extinguishable networks, with a mass residue (96 %). The phenyl groups in the POSS[®] were the reason for a larger improvement, as compared with isobutyl groups.

Furthermore, Franchini *et al.*⁵³ studied the effect of the presence of bonded (or not) phenyl-POSS[®] with the epoxy network on fire behavior. The POSS[®] used were octaphenyl-POSS[®] bounded to eight phenyl groups and gly-Ph POSS[®] with seven phenyl groups and a reactive glycidyl group. Both POSS[®]-modified epoxy networks showed good results for UL-94 tests with self-extinguishing fire behavior and large residues (about 96 %). From the cone calorimeter experiment, a notable reduction in the pHRR was evidenced for both POSS[®]-epoxy networks, with a decrease of 34 %, and 40 % for octaphenyl-POSS[®] and gly-Ph POSS[®], respectively, as shown in Figure I. 12b. Thus, a slightly superior improvement was obtained in the case of the reactive monofunctional POSS[®] compared with the inert POSS[®], but the difference between both epoxy networks was not remarkable.

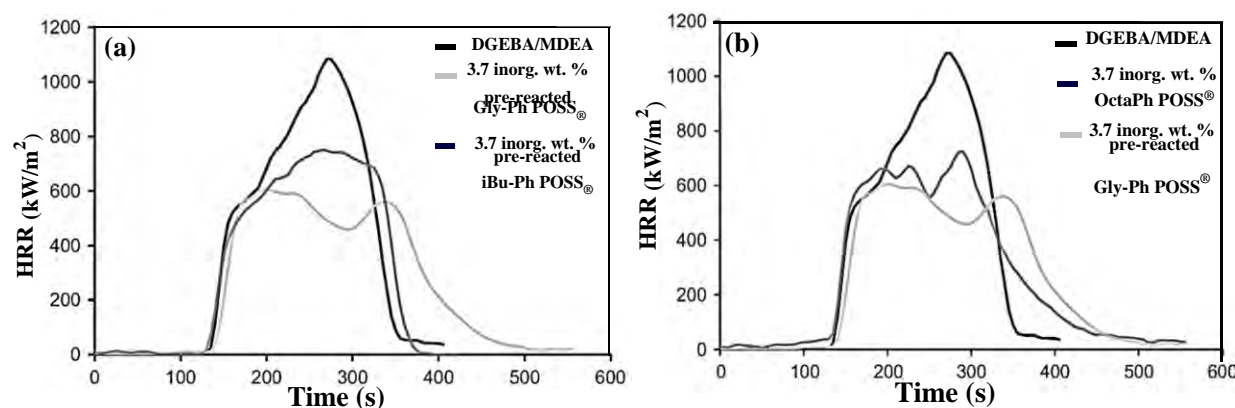


Figure I. 12: A comparison of heat release rate (HRR) as a function of time for epoxy networks containing: a) Gly-Ph POSS[®] with Gly-iBu POSS[®] and b) Gly-Ph POSS[®] with octaphenyl POSS[®].⁵³

Some interesting informations are provided from visual observation of residues (Figure I. 13). On cross sections of the residues, it can be seen that the Gly-Ph POSS[®] nanoclusters formed a solid sponge-like structure during combustion (Figure I. 13b and 13c) that is not generated on

the neat epoxy-amine network (Figure I. 13a) or in the presence of isobutyl containing POSS[®] clusters.

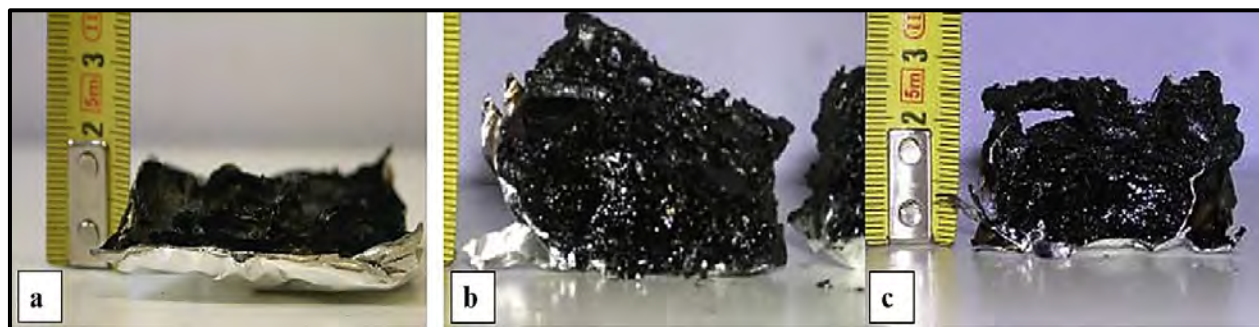


Figure I. 13: Cross sections of cone calorimeter residues of POSS[®]-epoxy hybrid systems: a) neat epoxy-amine matrix, b) 3.7 inorg. wt. % pre-reacted Gly-Ph POSS[®], and c) 3.7 inorg. wt. % OctaPh POSS[®] ⁵³.

Wu *et al.* ⁴⁶ studied the effect of dispersion of POSS[®] in the epoxy-amine matrix on the flame retardancy behavior. They observed that the addition of heptaphenyl-trisilanol-POSS[®] (POSS^{®Ph}-triol) reduced the HRR peak of modified epoxy cured with diethylene toluene diamine (DETDA) (DGEBA-DETDA) from 883 to 777 kW.m⁻². Epoxy-amine/POSS^{®Ph}-triol combined with aluminum acetylacetonate (Al) as an acidic catalyst, leads to a reduction of sizes of POSS[®] aggregate into epoxy network which displays a lower peak release rate (590 kW.m⁻²). Because the presence of Al allowed the formation of a more efficient and thermostable char than for the modification of epoxy-amine with only POSS^{®Ph}-triol and for the neat epoxy networks. As smoke is fatal in the event of a fire, the reduction in smoke production is an important asset. The incorporation of the POSS^{®Ph}-triol, either with or without Al, leads to a decrease of the release of CO and CO₂ in the epoxy-amine/POSS[®] ⁴⁶. These improvements in reducing the toxic components production during combustion are important features for considering POSS[®] as fire retardant candidates. Recently ⁹⁹, similar behavior was observed for epoxy networks based on tetraglycidyl(diaminodiphenyl)methane (TGDDM) from commercial formulation (MVR444), designed for a resin infusion process and combined with POSS^{®Ph}-triol and aluminum-acetylacetonate. Significant improvements with a substantial and effective intumescent-like behavior were observed (Figure I. 14).

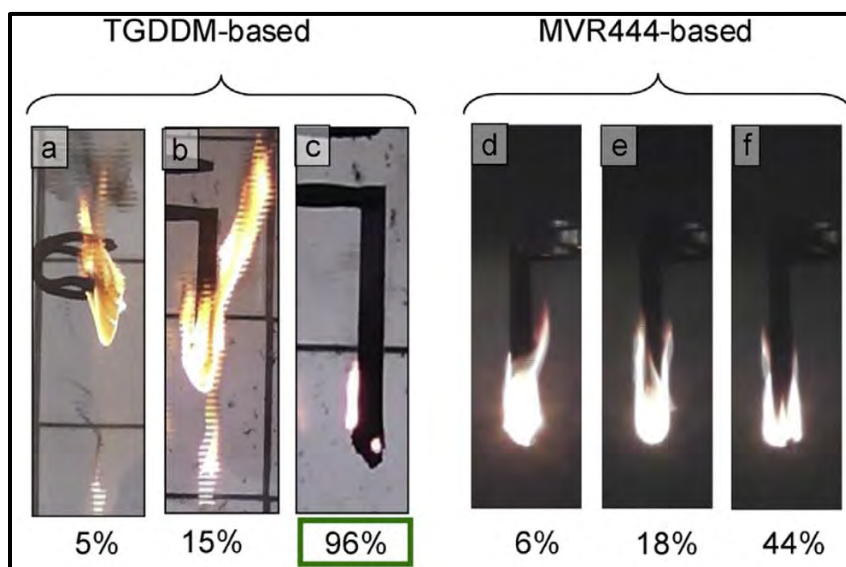


Figure I. 14: Representative snapshots of UL-94 tests and average residual weights after testing of a) TM, b) TM-POSS[®], c) TM-POSS[®]-Al, d) MVR, e) MVR-POSS[®]OH, and f) MVR-POSS[®]-Al (the mixture of TGDDM or MVR444 with amine hardener, denoted TM or MVR, respectively)⁴⁶.

The influence of the non-reactive organic groups surrounding the POSS[®] cage can be an important parameter also for the fire retardancy of the POSS[®]-modified epoxy networks. Depending on the nature of the organic ligands, it is possible to generate different char morphologies, *i.e.* leading to different thermostabilities. Zhang *et al.*¹⁰⁰ studied the combustion of DGEBA-m-PDA networks containing 5 wt. % of octaphenyl-POSS[®] (OPS) and Gérard *et al.*^{101,102} investigated epoxy systems based on DGEBA-DETA with 5 wt. % of octamethyl-POSS[®]. Better dispersion was evidenced in the case of octamethyl-POSS[®] modification where rod-like clusters of about 0.5 - 1 μm were observed, whereas the octaphenyl-POSS[®] forms crystalline phases. The fire analyses by cone calorimeter showed that the addition of octamethyl-POSS[®] to an epoxy network leads reduction of pHRR, whereas the octaphenyl-POSS[®] leads to a higher efficiency by decreasing the pHRR (about 17 % reduction) and reducing the THR (total heat release) (about 10 % reduction). Furthermore, a significant improvement of time to ignition (TTI) caused by octaphenyl-POSS[®] can be observed.

About the thermal stability and thermal oxidative degradation process involved for POSS[®]-modified epoxy-amine systems, POSS[®]-containing epoxy hybrid O/I materials exhibited improved thermal stabilities^{48,86}, which means a slower degradation kinetics by delaying the

motions and scissions of the chains for POSS[®]-modified epoxy-amine networks. The surface functionality of POSS[®] played a crucial role in improving thermal stability of epoxy-based nanomaterials¹⁰³⁻¹⁰⁹. The main findings of recent studies on the thermal properties of epoxy/POSS[®] networks are reported in Table I. 1.

Table I. 1: Recent works reported on the thermal properties of epoxy networks modified by POSS[®] nanoclusters.

POSS [®] used	Results	Reference
POSS[®]-NH₂	POSS-NH ₂ -incorporated in epoxy networks could significantly increase the T _{d5%} and char yield from 290 °C and 20 %, respectively, to 320 °C and 26 %.	Meenaksi and Sudhan. ¹¹⁰
Methacrylisobutyl POSS [®] (MA-POSS[®]) Used from 27.9 wt.% to 42.1 wt.%	The thermal decomposition temperatures (T _{d5%} , T _{d50%}) and char yield of neat epoxy were (263 °C, 393 °C) and 1 %, respectively, while they are improved significantly to (289 °C, 401 °C), and 12 % after incorporation of MA-POSS [®] in epoxy, respectively. The T _g also increased from 96 to 123 °C.	Ma and He. ¹⁰⁵
Aminopropylisobutyl POSS [®] / 9, 10-Dihydroxa-10-phosphaphenanthrene-10-oxide (DOPO) or DOPO tetrabutyltitanate (TBT)	Addition of 5 wt. % TBT + 5 wt. % aminopropylisobutyl POSS [®] -bisDOPO enhanced the T _{d5%} by 22 °C (325 vs 302 °C) and the char residue from 17 to 20 %, respectively. Moreover, the T _g of epoxy network increased from 155 to 161 °C.	Zeng <i>et al.</i> ¹⁰⁷
Octa-(N,N (bis(9,10dihydro-9-oxa10phosphaphenantheny l)methyl)aminopropyl)siles quioxane(ODMAS)	Addition of 15 wt. % of ODMAS decreased the T _{d5%} from 355 °C to 320 °C, and enhanced the char yield at 800 °C from 18 to 26 %. No change on the T _g was observed (≈ 153 °C).	Liu <i>et al.</i> ¹⁰⁴
Octaglycidyl dimethylsilyl POSS [®] (OGPOSS[®])	The initial decomposition temperature - at 1, 2 and 5 % mass loss (T _{d1%} , T _{d2%} , T _{d5%}) - were maximum when the concentration of OGPOSS [®] was 1 wt. % (348 °C vs 342 °C), and thereafter decreased with increasing OGPOSS [®] (to 321 °C). While, The T _g decreased as the content of OGPOSS [®] increased from 167 °C to 137 °C.	Choi <i>et al.</i> ¹¹¹
Aminopropylisobutyl POSS [®] /9, 10-Dihydroxa-10-phosphaphenanthrene-	The incorporation of 2.5 wt. % DOPO + 2.5 wt. % POSS [®] improved the char residue of the network from 16 to 18 %, while 5 wt. % of aminopropylisobutyl POSS [®] increased it to 20 %	Wu <i>et al.</i> ¹⁰⁶

10-oxide (DOPO)	with a slight decrease in thermal stability (348 vs 356 °C) and T_g (155 vs 158 °C).	
Aminopropylisobutyl POSS [®]	The $T_{d5\%}$ for POSS [®] -containing epoxy hybrids decreases from 363 to 359 °C, 347 °C, 350 °C and the T_g from 176 to 163, 144, and 76 °C with respect to epoxy hybrid networks corresponding to 7, 22, and 54 wt. % POSS [®] . While, the char yield increased from 16 % for neat epoxy to 19, 18 and 26 % with the different hybrid O/I epoxy networks.	Sharma <i>et al.</i> ¹¹²
Glycidyl POSS [®] (GPOSS [®])	The temperature at 40 % weight loss of epoxy/polyurethane copolymer increased from 351 to 403 °C, and the char residue from 6 to 20 % by adding 0.2 to 10 wt. % of POSS [®] . While, the T_g increased from 53 to 64 °C by adding 0.2 wt. % of POSS [®] and then decreased with higher loading.	Zhu <i>et al.</i> ¹⁰⁹
OGPOSS [®] /Layered zirconium phenylphosphate (ZrPP)	Addition of 1 wt. % ZrPP + 4 wt. % POSS [®] to epoxy increased the $T_{d50\%}$, T_{dmax} and char residue to 385, 407 °C, and 22 %, respectively, compared to neat epoxy at 364, 383 °C, and 16 %.	Zhou <i>et al.</i> ¹⁰⁸
CLNH ₂ -POSS [®]	Addition of 5 wt. % of CLNH ₂ -POSS [®] to epoxy gives a slight change on the $T_{d5\%}$ (\approx 368 vs 371 °C) and T_{dmax} (\approx 382 vs 380 °C) with an increase on the char residue from 17 to 22 % and T_g from 169 to 171 °C.	Shengnan Li <i>et al.</i> ¹¹³

As seen from Table I. 1, incorporating POSS[®] in the epoxy matrix could increase ¹⁰³⁻¹⁰⁹ or decrease ^{111,112} the thermal stability depending on the dispersion state and the nature of interactions. Rashid *et al.* ¹¹⁴ reported that the epoxy-POSS[®] hybrid O/I materials could sustain higher temperatures prior to decomposition. The coefficient of thermal expansion was also found to increase due to the steric hindrance of the polymer chain due to the presence of bulky POSS[®] side groups ¹¹⁴. Recently, Pistor *et al.* ⁸⁶ have reported the degradation kinetics of epoxy-amine nanocomposites containing different percentage (0.1, 1, 2, and 5 wt. %) of epoxycyclohexyl-POSS[®]. The degradation study showed two distinct stages of weight loss vs temperature and only the first stage, is influenced by the POSS[®] incorporation. The ‘Avrami’ kinetics parameters showed that the incorporation of POSS[®] did not affect the degradation rate constant. However, there is an increase of the time required for the start of the degradation reaction. In addition, an increase of the activation energy is observed for the material containing 5 wt. % of POSS[®].

Similarly, Wu *et al.*⁴⁶ divided the thermo-degradation process into two stages. During the first stage, at low temperatures, the degradation of alkyl group species from the polymer backbone occurs and carbonaceous compounds are produced. A physical barrier is so formed to protect substrates from fire via reducing the energy and mass transfer between substrates and heat source (fire). During the second stage, at high temperatures, the carbonaceous compounds are oxidized, volatilized, and decomposed to form, at the end a silicon dioxide-rich layer. During the second stage the oxidation of the residues formed from thermal decomposition of the resin occurs. Thus, the POSS[®] nano-additives acted as a thermal insulating material, because of their excellent oxidation resistance and reaction to fire¹¹⁵. Wang *et al.*⁹⁶ also studied the thermal degradation behavior of epoxy resin containing octavinyl-POSS[®] (OVPOSS[®]). They proposed that during the oxidation of the epoxy hybrid O/I network (EP/OVPOSS[®]), the vinyl groups are first oxidized to form acetaldehyde before carbon dioxide. The cage of POSS[®], which can be seen as a radical trapper, could react with pyrolysis radicals and form the branched and crosslinked intermediate siloxane products, which are responsible of the thermostability enhancement. For EA/OMP-POSS[®] system¹¹⁵, they suggested that the relatively weak thioether linkages, when heated, should first decompose. Then, POSS[®] cages degradation form a Si-O-Si network inside the char. This ceramic-like protective compound at the surface of the char could prevent further thermal degradation. In addition, the more OMP-POSS[®] was added, the higher the T_{dmax} and the slower rate of mass loss with temperature are. The high char yields also confirm that relatively small amounts of volatile compounds are released during thermal decomposition.

I.7.2. Mechanical properties

Epoxy networks represent an important class of thermoset polymers, widely used in applications from adhesives, paints matrices and coatings in our daily life thanks to their good mechanical properties^{116,117}. However, they are brittle in nature^{35,118} with a poor resistance to crack propagation^{35,118} due to the rigid aromatic and phenyl groups and usually highly crosslinked glassy architecture. Thus, many studies have focused on improving the toughness and on fracture resistance of epoxy resins.

POSS[®] as novel O/I hybrid nanoclusters with unique three-dimensional cage structure, can lead to epoxy networks displaying an enhanced mechanical strength¹¹⁹. In addition, the organic functional groups of the POSS[®] nanoclusters give them the ability to tune mechanical performances of POSS[®]-modified networks¹²⁰. In fact, the addition of monofunctional POSS[®] in

the epoxy matrix makes it possible to design coatings with high tensile strength and Young's modulus. The inorganic part Si-O-Si cage with organic ligands leads to good compatibility and reactivity of POSS[®] nanoclusters allow them to tailor mechanical properties of epoxies. The nature of the organic functional groups attached to POSS[®] and its mass fraction and length are two important factors that influence the fracture toughness. The influence of the functionality, POSS[®] dispersion, and POSS[®] content on the mechanical properties (Young's modulus, yield stress, fracture toughness and elongation at break) recently reported in the literature for epoxy/POSS[®] networks are summarized in Table I. 2.

Table I. 2: Recent works reported on the mechanical properties of epoxy networks modified by POSS[®] nanoclusters.

POSS [®] used	Results	Reference
Glycidyl-POSS [®] (GPOSS [®]) and DodecaPhenyl-POSS [®] (DPHPOSS [®])	The hybrid of 0.5 wt. % MWCNT and 5 wt. % GPOSS [®] improved strength at break of epoxy by about 123 % and elongation at break by about 32 %. However, the hybrid of 0.5 wt. % MWCNT and 5 wt. % DPHPOSS [®] improved strength at break of epoxy by about 82 % and elongation at break by about 50 %.	Barra <i>et al.</i> ¹⁰³
Methacryl-POSS [®] and Glycidyl-POSS [®] and Trisilanol phenyl-POSS [®]	In all three cases, after reaching a maximum value, the fracture toughness starts to decrease on further addition of POSS [®] . In the case of reinforcement by Glycidyl-POSS [®] , the fracture toughness increased by a factor of 2.3 at 5 wt. % loading, while for methacryl- and trisilanol phenyl-POSS [®] at 5 wt. % loading the fracture toughness increased by factors of 1.6 and 1.3, respectively. The Young's modulus remains unchanged with increasing amount of POSS [®] , while yield strength and elongation at break were observed to decrease.	Mishra <i>et al.</i> ⁵⁰
Mono and poly double-decker silsesquioxanes (mono DDSQ and poly DDSQ)	The mono DDSQ showed more flexible structure and toughened the epoxy resin better (at a loading of 8 wt. %, the toughness increased by about 50 % compared to neat epoxy), while the branched poly DDSQ exhibited better thermal resistance.	Cao <i>et al.</i> ¹²¹
Methacrylisobutyl-POSS [®] (MA-POSS [®]) or Aminopropylsibutyl-POSS [®] (NH ₂ -POSS [®])	The introduction of polysiloxane into epoxy matrix is confirmed to create hybrids with strong adhesive strength (1113 N) and high thermostability (T _g = 282 °C, but the flexible PDMS improves PGMA/NH ₂ -PDMS hybrid with much higher storage modulus (519 MPa) than PGMA/NH ₂ -POSS [®] (271 MPa).	Ma <i>et al.</i> ¹²²

Aminopropyl iso-octyl-POSS [®] (AI-POSS [®])	Addition of 1 wt. % AI-POSS [®] + 10 wt. % HBE led to a 229 % increase in fracture toughness and 20 % in Young's modulus, while 5 wt. % of AI-POSS [®] + 10 wt. % HBE increased fracture toughness by about 223 % (1.6 vs 0.5 MPa.m ^{1/2}) and the Young's modulus about 28 % (2.3 vs 1.7 GPa). Slight decrease was observed on the stress and strain Yield.	Misasi <i>et al.</i> ¹²³
Octavinyl-POSS [®] + GO (Graphene oxide) (POSS [®] -GO)	It seen that with increasing GO and POSS [®] -GO, the impact strength of composites achieved a maximum value. Impact strength of epoxy containing POSS [®] -GO enhanced 29 % (22 vs 17 kJ.m ²) compared to that of epoxy containing GO at 0.8 phr and by 54 % compared to neat epoxy (14 kJ.m ²). The bending strength also of GO/epoxy and POSS [®] -GO/epoxy increase by 15 and 33 % to 160 and 185 MPa from 139 MPa of neat epoxy.	Zhang <i>et al.</i> ¹²⁴
Octaammonium POSS [®] (POSS [®] -NH ₂) + the polydopamine (PDA) as modifying agent	The interfacial shear strength of Carbon fiber (CF)-PDA/POSS [®] is 117 vs 72 MPa (64 % increases compared to that of pristine CF).	Yang <i>et al.</i> ¹²⁵
Sulfonated octaphenyl POSS [®] (SOP-POSS [®])	The calculated interfacial shear stress (IFSS) values show that the presence of SOP-POSS [®] absorbed onto the surface of oxidized CF significantly improves the interfacial properties of the corresponding composites by approximately 15 % (without any change on the tensile strength).	Kafi <i>et al.</i> ¹²⁶
Octa(γ-chloropropyl) POSS [®] (hyperbranch hexamethylene diamine)	The IFSS values of the CF-POSS [®] -NH ₂ /epoxy composite is 93 vs 50 MPa in comparison with untreated CF/epoxy composites (about 86 %).	Ma <i>et al.</i> ¹²⁷
CLNH ₂ -POSS [®]	For the epoxy (EP), tensile strength, flexural strength, and flexural modulus were 69.9 ± 5.9 MPa, 99.3 ± 2.4 MPa, and 2.46 ± 0.01 GPa, respectively. By incorporating 3 wt. % of CLNH ₂ -POSS [®] into the epoxy, the tensile strength, flexural strength and flexural modulus increase to 82.8 ± 3.2 MPa, 105.1 ± 1.8 MPa, and 2.50 ± 0.05 GPa, which were increased by ≈ 18 %, ≈ 6 % and ≈ 2 %, respectively, compared to those of neat EP.	Shengnan Li <i>et al.</i> ¹¹³

A significant effect on fracture toughness of epoxy coatings has been reported in the literature from the incorporation of POSS[®] (see Table I. 2) due to their hybrid O/I structure containing an inorganic rigid core and organic flexible pendant groups (non-reactive or reactive).

The inorganic part of POSS[®] can provide a stiff phase that can sustain stress and energy^{128,129}. Toughening for modified epoxies via shear-yielding, crack-bridging, and crack-pinning mechanisms usually reported for this process can be invoked. In addition, the organic groups and reactivity of POSS[®] nanoclusters allow them to be well dispersed in the epoxy matrix with an efficient interphase. As mentioned previously, the bulky structure of POSS[®] cages might improve the mobility of the epoxy chains by increasing the free volume of the network¹³⁰⁻¹³³.

I.7.3. Dielectric property

The main advantages of polyepoxy networks for electrical applications are their low relative permittivity (usually from 3 to 6) and their low dissipation factors, their excellent dielectric strength (which can reach 180 kV/mm in DC) as well as their low conductivity (from 10^{-12} to 10^{-19} S/m). As a result, polyepoxides are widely used and studied as insulating material, cable terminations, and in rotating machines for the high voltage insulation applications^{134,135}. The dielectric behavior of polyepoxides and their composites have been widely discussed in the literature. As composites, they have been associated with conductive^{136,137}, semiconductor¹³⁸ or insulating¹³⁹, organic¹⁴⁰ or inorganic^{136,137} fillers of nanometric¹⁴¹ or micrometric size¹⁴⁰. Addition of hybrid O/I nanoclusters type POSS[®] into epoxy matrices can change significantly their dielectric properties. The enhancement in dielectric properties has been explained by many factors mainly the large particle-polymer interfacial area, the particle-polymer dispersion morphology and the change of the internal electric field (polarity) due to the presence of nanoparticles. Numerous characterization techniques have been used to study their dielectric properties: dielectric spectroscopy, surface and volume conductivity measurements, dielectric strengths in volume and surface (AC and DC), space charge distribution, etc. The main conclusion stated that incorporating POSS[®] into the epoxy could enable high dielectric performances such as of dielectric strength at break and corona resistance¹⁴²⁻¹⁴⁴. Heid *et al.*¹⁴² found that addition of 2.5 wt. % of triglycidylisobutyl-POSS[®] (TGIB-POSS[®]) into epoxy resulted a remarkable increase in dielectric breakdown strength (about 13 % from 215 to 242 kV/mm compared to neat epoxy) and also with a significant increase of thermal conductivity. However, by considering high POSS[®] content, dielectric breakdown strength decreases due to the formation of conductive interfacial layers around aggregated POSS[®] leading to the creation of conductive paths. It was shown by Dhanapal *et al.*¹⁴⁵ that 1.5 wt. % of POSS[®]-NH₂ decreased dielectric constant of epoxy/carbon fiber composite from 4.1 to 2.1 (determined by impedance analyzer)

because of reducing the polarizability of the matrix. Similar results was also obtained by Zhang *et al.*¹⁴⁴ where the dielectric properties were showed to be improved by the incorporation of micro-porous polyhedral oligomeric silsesquioxane bearing benzoxazinyl groups (BZPOSS[®]). The lowest dielectric constant (2.14) was obtained for poly(dicyclopentadiene phenol epoxy resin (DCPD)/BZPOSS[®]) with 20 wt. % BZPOSS[®].

1.7.4. Conclusion

POSS[®] are unusual nano-objects for several reasons: their nanometric size, their perfectly defined molecular architecture, their intrinsic O/I hybrid nature, and the versatility of the nature of organic ligands that can tailor the properties of polymer POSS[®] materials.

In addition, thanks to the synthesis pathways to prepare such nanoclusters, a wide variety of POSS[®] in terms of chemical functionality and structure is now available. As a result, these nano-objects have been introduced into thermoplastics and thermosets as an inert nanofiller, dangling or grafted along the main chain, a crosslinking node or included in the skeleton of the macromolecule. The state of dispersion and the nanostructuration of these objects depend on the nature of the organic ligands, the latter determining the POSS[®]/POSS[®] and POSS[®]/organic medium interactions. In particular, it seems necessary to introduce a polymerizable function to limit the tendency to aggregate.

The incorporation of POSS[®] in epoxy resins has great potential when they are well dispersed for providing materials displaying better flame retardancy and fracture toughness as well as other superior physical properties. Introduction of POSS[®] via chemical crosslinking into epoxy resin can influence the network structure, impart amphiphilicity, and improve mechanical properties, *i.e.* acting as nanofillers. The effect of POSS[®] on the properties of epoxy depends on their nanostructuration within the matrix, the size of POSS[®] agglomerations, the flexibility of the ligands, the number of reactive ligands, and the POSS[®] content. The POSS[®] organic functional groups play a crucial role in controlling properties of POSS[®]-modified epoxy hybrids. The incorporation of POSS[®] nanoclusters into epoxy via physical blending relies on the presence of favorable surface interactions between POSS[®] and polymer. POSS[®] having surface functional groups that can generate favorable interactions can be dispersed uniformly in the epoxy matrix. Uniform dispersion of POSS[®] in an epoxy matrix helps to improve physical properties of the nanomaterials. On the other hand, POSS[®] having organic functional groups not compatible with the epoxy matrix cannot be dispersed uniformly and lead to phase-separated systems with

POSS[®]-rich domains and a polymer-rich phase. Such microphase separated systems cannot provide efficient reinforcement and may even lead to a decrease in certain properties due to their impact on their crosslinking density, *i.e.* large aggregate means a high free volume that gives a lower crosslinking density and subsequently a lower reinforcing effect. For example, the stiffness of a polymer can be increased by incorporating suitable micro-sized fillers, but the resulting composite would lose its toughness.

Emphasis must be put on the fact that the influence of the same POSS[®] on physical properties varies from one system to another depending on the nature of the interactions developed with the matrix which control the generated morphology.

I.8. Ionic Liquids and Epoxy Polymers

I.8.1. Ionic liquids and their applications

Ionic liquid (ILs) are molten organic salts composed of ions, *i.e.* usually an organic cation and a poorly coordinated anion. The cations mainly used to prepare ILs are based on phosphonium, ammonium, imidazolium, or pyridinium, pyrrolidinium, with different functionalization. The anion may be organic or inorganic, such as tetrafluoroborate (BF₄⁻), hexafluorophosphate (PF₆⁻), acetate (CH₃CO₂⁻), nitrate (NO₃⁻), bis(trifluoromethylsulfonyl)imide (CF₃SO₂)₂N⁻), etc. Large variety of cations/anions combination is possible^{146,147}. Typical cations and anions of ILs considered in the literature are shown in Figure I. 15¹⁴⁸.

Ionic liquids show unique properties such as low melting temperature, *i.e.* below 100 °C, with high thermal stability (higher than 300 °C)¹⁴⁹⁻¹⁵¹ as well as non-flammability and non-volatility¹⁵⁰. In addition, their high ionic conductivity and large electrochemical interval offer for applications as electrolytes in electrochemistry¹⁵². Ionic liquids are also considered as “green solvents” due to their capacity to dissolve many substances and their ability to be reused and recycled¹⁵³. Another advantage of ionic liquids comes from their versatile structure, *i.e.* anion and cation type or alkyl chain length, which determines their physico-chemical properties. For instance, a longer alkyl chain favors the Van der Waals force leading to a higher viscosity of ionic liquids¹⁵⁴. The nature of the counter anion plays also a significant role in the IL properties¹⁴⁹. For example, changing of IL anion can be a way to tune their solubility in water, *i.e.* from water-immiscible to water-miscible (Figure I. 15)^{146,147}. The thermal stability of ILs also increases dramatically with changing the nature of the anion, *i.e.* from bromide (Br⁻) to tetra

fluoroborate (BF_4^-) and bistrifluoromethanesulfonimide (NTf_2^-)^{151,155}. Similarly, for the same cation, ILs viscosity is also affected by the nature of anion¹⁵⁴.

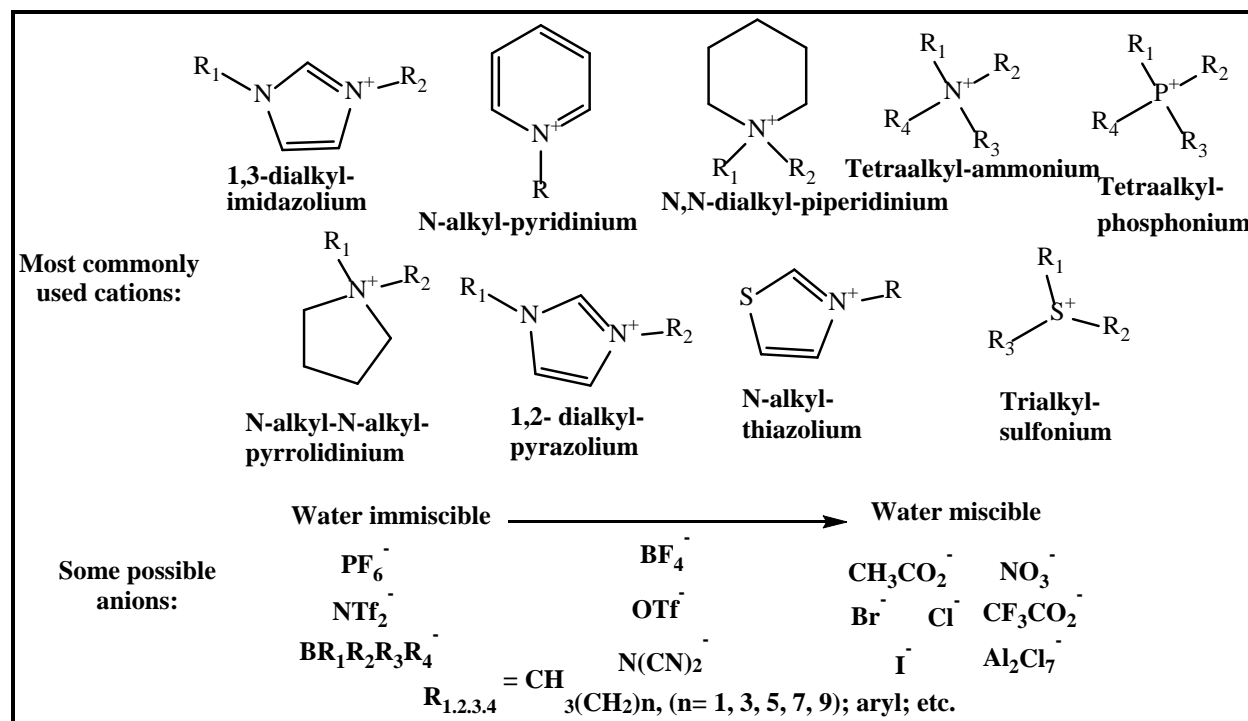


Figure I. 15: Structure of conventional used cations and anions in IL systems.

Ionic liquids are widely used in many fields as solvents^{153,156}, catalysts^{157,158}, analytical chemistry^{159,160}, physical chemistry¹⁶¹, electrochemistry¹⁶², engineering^{163,164}, and biological uses¹⁶⁵. Unprecedented properties have been achieved from the combination of ILs and polymers opening up promising applications. Actually, due to their recyclability, ionic liquids have been extensively used as the solvent medium for polymerization processes¹⁶⁶, especially polycondensation reactions¹⁶⁷ or for radical polymerization¹⁶⁸. Thus, the use of ILs in polymers has developed quickly in recent decades, leading to excellent properties of IL-modified polymers. Diverse uses have been reported in the literature: ionic conducting agents for polymer electrolytes^{169,170}, structuring agents for polymers^{171,172}, adjuvants for dissolving cellulose¹⁷³, etc. For instance, for the dissolution of cellulose in imidazolium based IL, Hameed *et al.* have prepared partially miscible epoxy/cellulose blends in which the IL acts as a coupling agent by forming electron donor acceptor (EDA) complexes with the two polymers¹⁷⁴. They were also considered as compatibilizers for polymer blends^{175,176}, plasticizers for synthetic polymers^{177,178}, and surfactants in the preparation of polymer nanocomposites^{179,180}, etc. Recently, ionic liquids have

gained interest as catalysts and/or curing agents for epoxy resins. These applications will be described in the next section.

I.8.2. ILs-modified epoxy network

More recently, ILs have received attention as new additives for designing epoxy thermosetting material with new functional properties. ILs were used in epoxy networks to develop new polymer electrolytes, anti-corrosive coatings, or for epoxy composite/nanocomposites^{181,182}. According to the literature, two main approaches have been studied to combine ILs with epoxies: *i*) the synthesis and development of new ionic liquids containing epoxy functional group either by the cation or by anion and *ii*) the use of ILs as reactive or non-reactive additives for conventional epoxy systems.

Numerous authors have developed new functionalized ionic liquids to provide better ionic conductivity for the development of polymer electrolytes. Matsumoto *et al.* synthesized ILs carrying epoxy groups, *i.e.* beared by the cation or the anion in order to form epoxy-amine networks^{183,184}. Other authors have synthesized new IL prepolymers to prepare polymeric ionic liquids (PILs) and PIL/IL ion-gels based on epoxy-amine reactions^{185,186}. Ion-gels (PIL/IL) have shown a significant improvement in permeability and selectivity to CO₂¹⁸⁶. McDanel *et al.* developed crosslinked epoxy-amine PILs from the synthesis of bis-epoxide functionalized imidazolium ionic liquids. A free IL (non-reactive) was also incorporated into the PILs up to 75 wt. % to get PIL/IL gel membranes. Recently, our group has reported the formation of epoxy-IL/amine networks from an epoxy-functionalized 1,2,3-triazolium¹⁸⁵ and an epoxy-functionalized imidazolium ionic liquids¹⁸⁷ to prepare networks as potential solid electrolytes. These epoxy-functionalized IL/amine reactive systems have similar curing behavior and properties to a conventional DGEBA-amine system with low glass transition temperature (from 42 to 55 °C) and a moderate value of ionic conductivity (from 2×10^{-7} to 5×10^{-6} S.m⁻¹ at 30 °C).

ILs can also be used as non-reactive additives to modify the properties of conventional epoxy networks. Indeed, the incorporation of a small amount of ionic liquids can lead to an improvement of their curing behavior^{188,189} as well as their resulting thermomechanical properties¹⁹⁰, mechanical behavior¹⁹¹, surface energy¹⁸⁹, ionic conductivity¹⁹², wear and scratch resistance^{193,194}, etc. For example, Sanes *et al.* found an improvement in the wear and scratch resistance of the epoxy-amine networks by using only 1.5 wt. % of imidazolium IL¹⁹³. On the

other hand, Saurin *et al.* have shown that the use of 9 to 12 wt. % of IL in an epoxy-amine system leads to self-healing capability at surface of coatings after abrasion (more than 90 %) ¹⁹⁴.

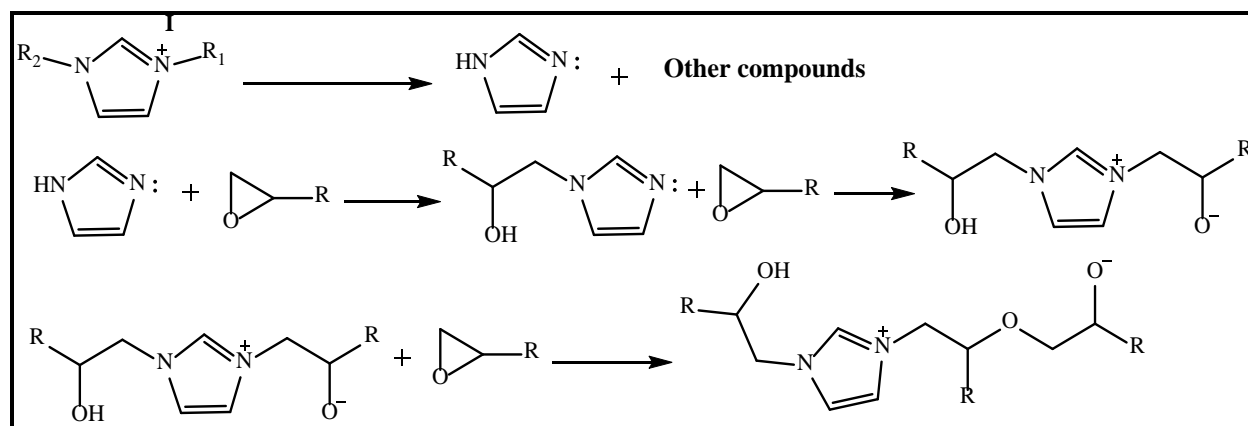
Recently, ILs have also been introduced as curing agents (co-monomers) of epoxy prepolymers ¹⁹⁵⁻¹⁹⁷. In fact, numerous works have shown that ILs containing imidazolium or pyridinium cation can act as initiators or hardeners of DGEBA (bisphenol A diglycidyl ether) from anionic polymerization to form epoxy networks/IL ^{195,196}. For example, Kowalczyk *et al.* have been used 1-butyl 3-methyl imidazolium tetrafluoro borate as hardeners for epoxy prepolymers ¹⁹⁷. The ability of such IL to induce ionic polymerization of epoxide groups has been evidenced by using low IL content (from 0.5 to 5 phr). Furthermore, Rahmathullah *et al.* have used imidazolium ILs combined with dicyanamide anion as latent initiator of epoxy prepolymer ¹⁹⁶. More recently, other authors, as well as our research group, have found that phosphonium ILs combined with different anions are also very good candidates for amine hardner substitution ^{182,198,199}. In fact, the nature of the phosphinate (IL-TMP) and dicyanamide (IL-DCA) anions allows the formation of epoxy/IL networks via anionic polymerization. The authors have also demonstrated that these new epoxy/ILs networks have excellent tunable properties such as high thermal stability (over 400 °C) and a T_g (from 80 to 140 °C) depending on the chemical nature of the anion used. The evidence of nanostructuration was also highlighted due to the miscibility limits between the epoxy prepolymers and the ionic liquids ¹⁹⁸.

I.8.3. Epoxy resin/imidazolium ILs curing mechanism

Referring to the crosslinking reaction of an epoxy resin prepolymer with ILs, possible reaction mechanisms were suggested ^{196,198}. Simplified reaction mechanisms have been also reported ¹⁸⁸. From the analysis of binary mixtures of epoxy prepolymer and imidazolium ILs at different ratios ¹⁸⁸ using Differential Scanning Calorimetry (DSC) measurements, Soares *et al.* demonstrated the ability of ILs to act as curing agents for epoxy systems. In fact, all the epoxy/IL mixtures displayed an exothermic peak, indicating the ability of the imidazolium-based IL to induce the polymerization of the epoxy prepolymer.

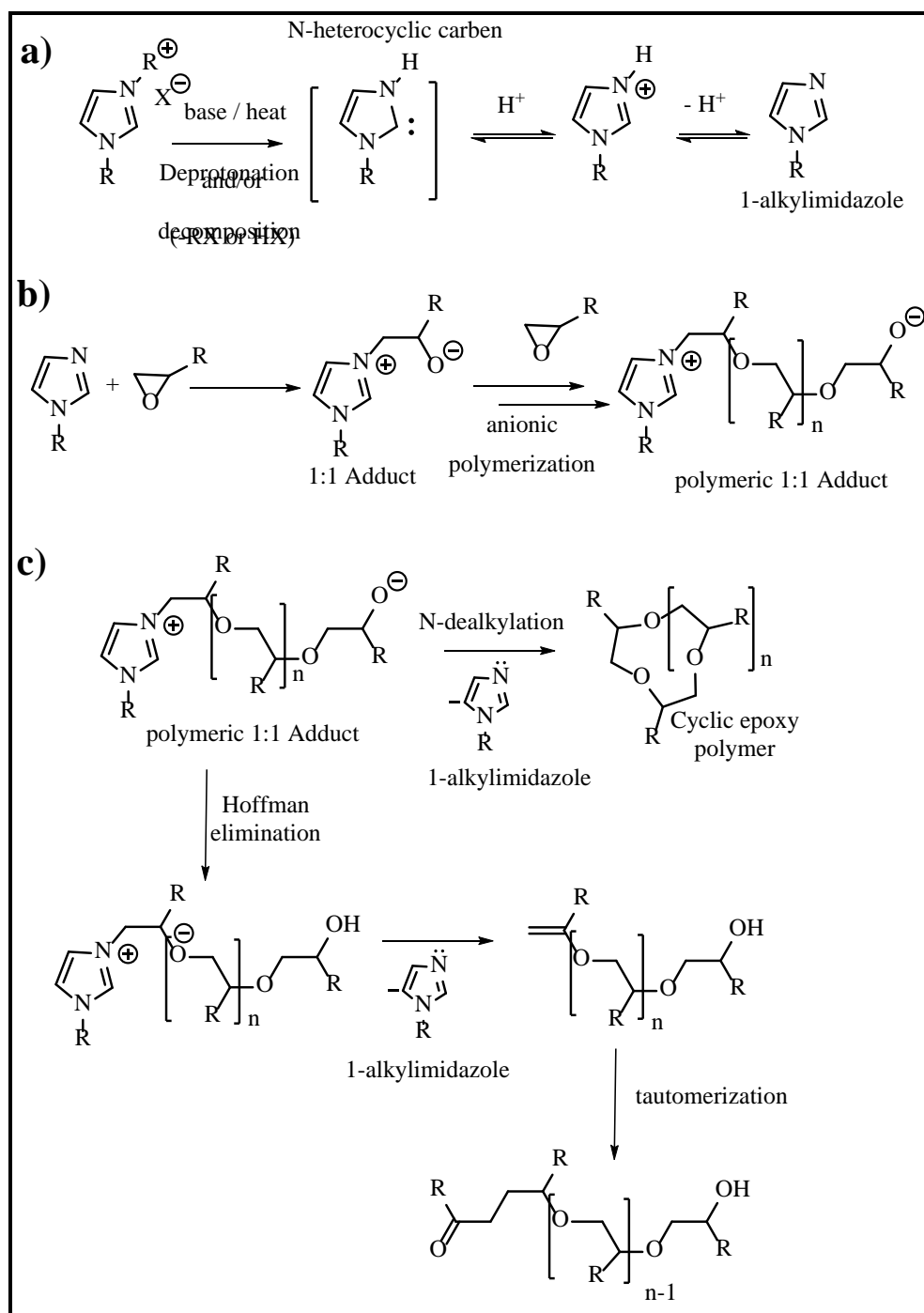
A curing mechanism was suggested based on the formation of imidazole through the decomposition of imidazolium cations (Scheme I. 5). The reaction between ILs and epoxide groups with the epoxy conversion (over 99 % after the curing process) was confirmed by FTIR spectroscopy. The increase in intensity of the 2350 - 2360 cm^{-1} peaks, corresponding to the

stretching vibrations of N^+H ion formed during the curing process, confirmed the proposed mechanism¹⁸⁸.



Scheme I. 5: Proposed mechanism for curing reaction between imidazolium ILs with iodide anion and epoxy prepolymer.

Later, Spychaj's team verified and developed this mechanism from the investigation of a series of ILs differing in imidazolium cation size and anion type, as well as for different IL contents^{195,200,201}. These authors have found that various imidazolium-based ILs are able to react with epoxy perpolymers including those combined with chloride^{195,200}, dicyanamide¹⁹⁵, tetrafluoro borate¹⁹⁵, and thiocyanate²⁰¹. The proposed mechanism for epoxy networks formation by 1,3-dialkyl imidazolium liquids presented in Scheme I. 6 consists of three main steps: *i*) the decomposition of IL into 1-alkyl imidazole *ii*) the formation of imidazole epoxy adduct and the polymerization of epoxy polymer and *iii*) the regeneration of alkyl imidazole and the structuration of final epoxy networks¹⁹⁵. The curing behavior of epoxy/IL mixtures, *i.e.* the reactivity and properties of cured networks depend strongly on the concentration of ILs and the basicity of the anion. Thus, the curing mechanism involving imidazolium cation decomposition is tuned by the basicity of IL counter anion. In fact, as imidazolium ILs are chemically unstable under basic conditions, a higher reactivity of ILs containing more basic counter anion, such as dicyanamide, is observed, and compared to those based on BF_4^- . Handy *et al.* confirmed that anions of imidazolium ILs have strong influence on the conditions which are required for proton exchange during the first step²⁰². The length of alkyl substituent on imidazolium cations has a slight impact on the curing process.



Scheme I. 6: Curing mechanism for epoxy networks formation by 1,3-dialkyl imidazolium IL proposed by Spychaj's team ¹⁹⁵.

Concerning the properties of cured epoxy/IL networks, there is a critical value for IL content (*i.e.* below three phr) in order to provide the highest T_g for epoxy/IL networks ²⁰⁰. For large IL contents, the ILs act the role of plasticizers and decrease the glass transition temperature of cross-

linked epoxy. The use of imidazolium ionic liquid leads also to a significant enhancement of thermal stability of the epoxy networks. In fact, the degradation temperature of the maximum of DTG peak is generally higher (+ 40 to 60 K) compared to conventional epoxies based on DGEBA cured with a diamine^{195,198}.

I.8.4. Epoxy/IL composites/nanocomposites

As ILs are effective solvents, epoxy/IL networks have attracted significant attention as matrices for composites and nanocomposites since ILs could be considered as dispersing agents of nanofillers. ILs allow to efficiently produce monodispersed epoxy nanocomposites of silica nanoparticles at the nanoscale level²⁰³. They can be arranged as a percolating phase that provides electrostatic and steric ionic layer around nanoparticles preventing their agglomeration^{204,205}. Throckmorton *et al.* reported a good dispersion of epoxy/imidazolium IL/silica nanocomposites with a simultaneous increase of mechanical properties and fracture toughness. For single-wall carbon nanotubes (SWNT) and graphite nanoplatelets (GNP), the introduction of ILs led to low electrical percolation threshold at low fillers contents (0.0086 and 1.7 vol % for SWNT and GNP, respectively,) with uniform dispersion at the nanoscale level²⁰³. Gholami *et al.* found that the use of 15 wt. % of choline chloride-based IL facilitated the dispersion of carbon nanotubes (CNTs) and prevented their aggregation in the epoxy networks resulting in a large increase of electrical conductivity of CNT-epoxy nanocomposite (up to 50 times higher than the nanocomposites without ILs)²⁰⁶.

Recently, Maka *et al.* studied both imidazolium and phosphonium-based ILs combined with different anions as dispersion agents for carbon nanofillers and curing agents of epoxy prepolymers in order to prepare high performance nanocomposites. An enhancement in electrical volume resistivity and flame retardancy was found for these nanocomposites at low contents of both fillers and ILs^{184,201}. Similarly, Guo *et al.* have observed the separation of expanded graphite from stacked sheets to thinner sheets in DGEBA-Jeffamine D230 with the addition of 1-butyle-3-methyl-imidazolium hexafluorophosphate ILs²⁰⁷. In the works of Hou *et al.*, rectorite treated with alkyl-imidazolium bromide ILs was well-dispersed into epoxy matrix with a resulting morphology going from intercalation to exfoliation depending on the curing agents types and improved thermal stabilities and mechanical properties (Figure I. 16)^{208,209}.

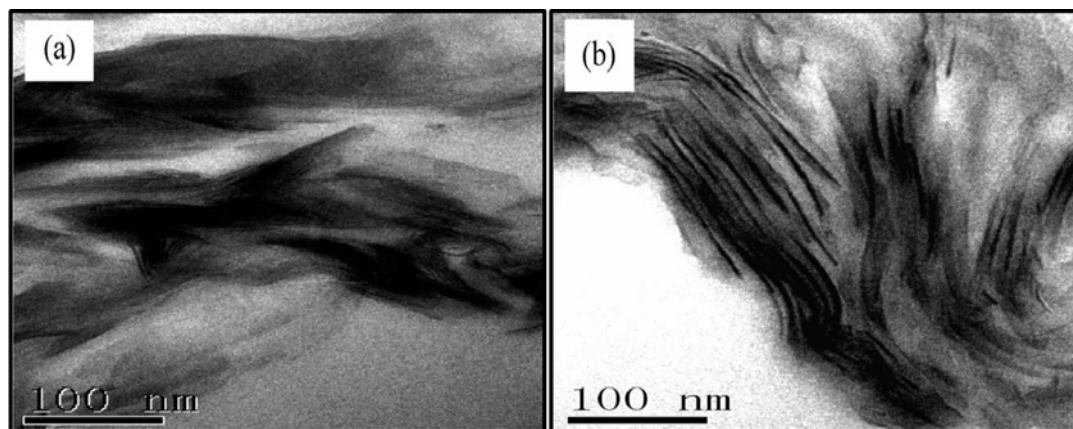


Figure I. 16: IL-modified clay dispersion in epoxy nanocomposite cured with a) imidazole (intercalation) and b) anhydride (exfoliation) ²⁰⁸.

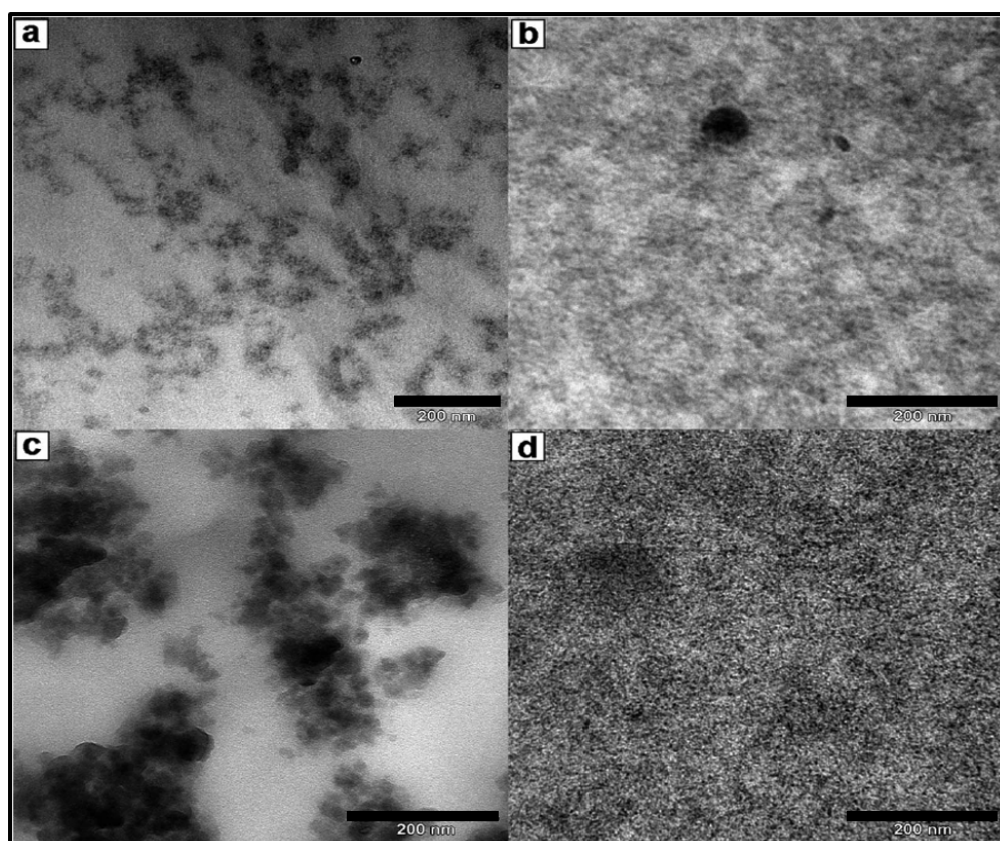


Figure I. 17: Epoxy-silica hybrids: a) without ILs and those formed in the presence of b) methyl sulfonate based IL, c) tetrafluoroborate based IL, and d) tetrafluoroborate based IL and hydrochloric acid ²¹⁰.

In addition, the influence of imidazolium-based ILs chemical nature on the morphology of epoxy-amine/silica nanocomposites has been demonstrated by Donato *et al.* ^{210,211}. These authors

observed that the silica dispersion changed from clusters having a size of about 200 nm without ILs to finer dispersion state with particles of 10 nm using only 0.6 wt. % of ILs (Figure I. 17)²¹⁰. In addition, the introduction of ILs leads to an improvement of the mechanical modulus of nanocomposites. In fact, the use of ILs combined with a coupling agent led to a remarkable compromise between toughness and stiffness of epoxy silica nanocomposites, *i.e.* six times higher for modulus and 10 times higher for energy at break²¹¹. Generally, ILs are promising candidates for conventional curing agents in epoxy networks due to their latent character associated with the good thermal and mechanical properties of the corresponding networks. Epoxy/IL based systems with tunable properties could be designed for various engineering purposes.

I.8.5. Conclusion

This literature section highlighted the benefits and the properties of ionic liquids, such as their excellent thermal stability, large temperature liquid domain, non-flammability, very low vapor pressure, tunable solubility of organic and inorganic molecules, and multiple combinations of cations/anions. These many advantages make them suitable for uses in the development of multifunctional epoxy thermosetting materials. The role of ionic liquids in the epoxy networks have been highlighted through the synthesis of ILs containing epoxide groups, the use of ILs as modifiers or co-monomers of epoxy networks, and as dispersing agents in the preparation of epoxy/IL composites and nanocomposites. No papers are reported in a literature about IL modified-POSS[®] incorporated into epoxy thermoset polymers.

Recently, regarding the good properties of ionic liquids and their different possible applications, different authors try to make a new design of POSS[®] with ionic liquids and to study their impact on the properties of polymer materials (morphology and functionality).

I.9. POSS[®] Ionic Liquids

This section reports the few results about IL modified-POSS[®] and related modified-polymer nanomaterials found in the literature. These papers concern POSS[®]-IL particles incorporated physically or participating in the chemical cross-linking.

POSS[®] can serve as a building block for new types of ILs²¹²⁻²¹⁹. Tanaka *et al.*²¹⁷ synthesized a stable room-temperature ionic liquid consisting of an octacarboxy polyhedral oligomeric silsesquioxane (POSS[®]) anion and an imidazolium cation. 1-methyl-3-propylhepta (i-butyl)

octasilsesquioxaneimidazoliumiodide (MePrIm⁺I⁻ IB₇ T₈ POSS[®]) was synthesized by Colovic *et al.*²¹³ to be used as an electrolyte for hybrid electrochromic devices. Moreover, a series of POSS[®]-IL have been synthesized to be used as potential solid polymer electrolytes (SPs) with different polymers^{214,216,219} based on polyethylene oxide, propylene carbonate and lithium imide bis(trifluoromethanesulfonyl), or poly (vinylidene fluoride-hexafluoropropylene). For example, Yang *et al.* reported a series (dendritic POSS[®]-IL, Figure I .18a; dumbbell-shaped POSS[®]-IL and Figure I .18b) of IL-tethered POSS[®]^{218,219} synthesized by grafting ILs and oligoethylene glycol chains to the POSS[®] cages and a coupling reaction.

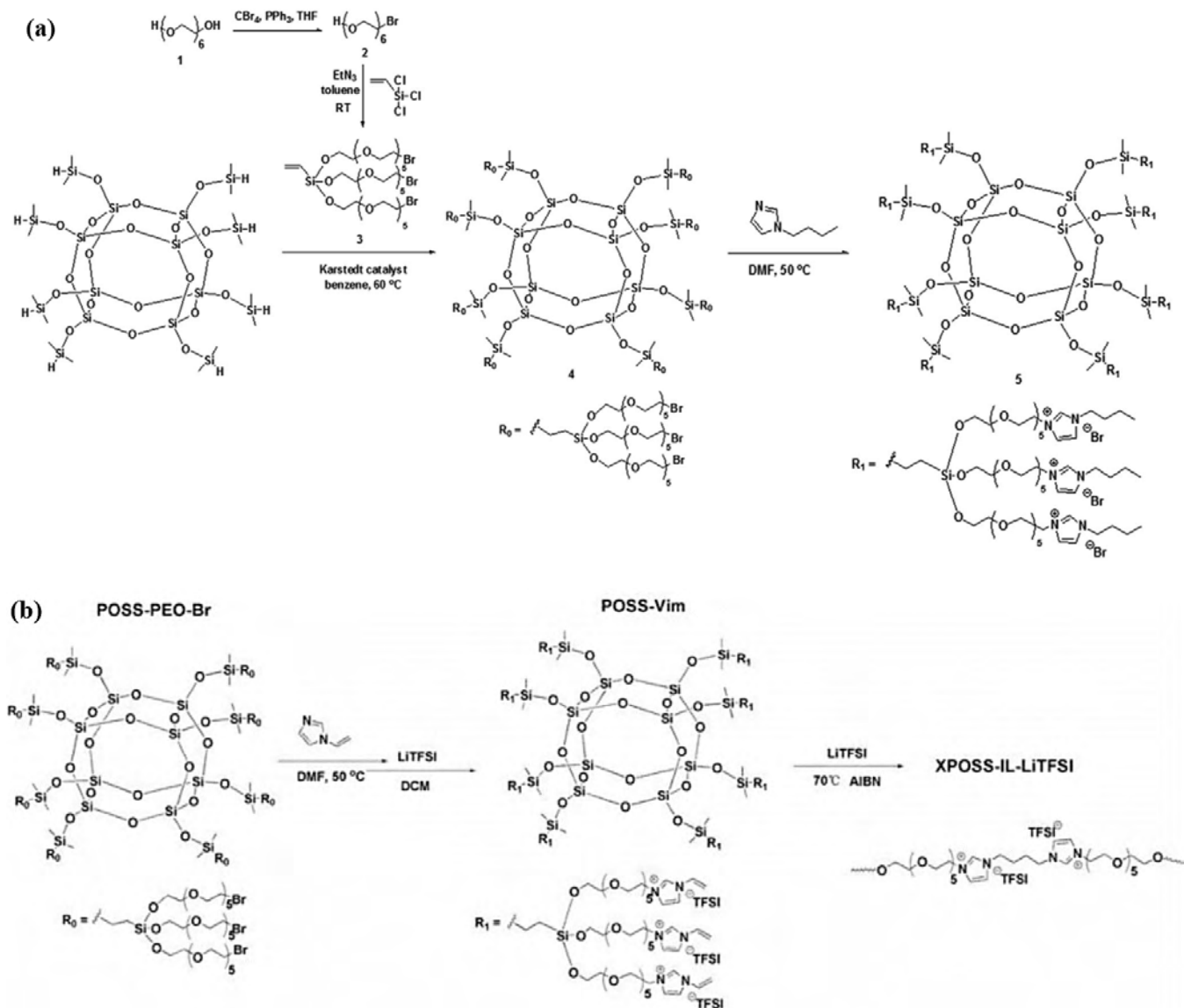


Figure I. 18: a) Synthesis of POSS[®]-IL and b) structure of dumbbell-shaped octasilsesquioxanes functionalized with ILs^{218,219}.

These dendritic POSS[®]-IL with TFSI anion (Figure I. 18) are amorphous and have a high charge density. They have a good electrochemical stability and good mechanical integrity. In addition, the imidazolium rings at the end of the branches could generate more interactions with TFSI (NTf₂⁻) anions and Li⁺ cations could be also released. Thus, such compounds could contribute to the improvement of the conductivity, σ , at room temperature. Compared to the control material without grafted POSS[®]-IL, σ , for POSS[®]-IL-TFSI was found to be significantly higher (4.8×10^{-4} S/cm at 25 °C).

I.10. Conclusion of chapter I

In the last few years, polymer/POSS[®] nanomaterials show a great potential to design materials displaying enhanced fire retardancy together with superior physical properties while maintaining other important characteristics such as mechanical and thermal properties. Recently, numerous studies have shown the interest of using the POSS[®] nanoclusters for processing fire retardant epoxy resins. It was learned from the literature that the POSS[®] content, the dispersive state, and the aggregation level of POSS[®] in an epoxy matrix have prominent roles in determining ultimate properties of resulting epoxy materials. In fact, higher POSS[®] contents lead to non-homogeneous dispersion as POSS[®] tend to agglomerate at micro scale in the epoxy-amine matrix. (Micro)phase separation frequently occurs between POSS[®] and epoxy systems before and/or during polymerization depending on the chemical nature and functionality of the organic ligands of POSS[®] cages. The ideal morphology of POSS[®]-modified networks, *i.e.* with POSS[®] nanoclusters homogeneously dispersed in the matrix at nanometrics scale, is often desired. However, such morphologies are not achieved in practice due to the lack of compatibility of POSS[®] with the epoxy matrix and the strong POSS[®]-POSS[®] interactions. The literature about epoxy networks including the formation, reaction mechanism, and resulting properties with the addition of imidazolium ionic liquids was summarized. Ionic liquids have become new multi-functional additives for polymers as modifiers or co-monomers of epoxy to synthesize networks. When ILs are used as curing agents and/or dispersion aids for epoxy composite/nanocomposites, they could lead to nanostructured morphologies with relevant properties. Thus, additional studies are required to answer the following questions: Could the presence of ionic liquids as a new ligand grafted onto POSS[®] nano-clusters or as epoxy monomers (ILM) contribute to their dispersion into an epoxy matrix? How will the use of such ionic compounds influence the physical properties of epoxy networks?

Reference of chapter I

- (1) Cordes, D. B.; Lickiss, P. D.; Rataboul, F. Recent developments in the chemistry of cubic polyhedral oligosilsesquioxanes. *Chemical Reviews* **2010**, *110*, 2081-2173.
- (2) Hybrid Plastics Company. "POSS[®] User's Guide". <http://www.hybridplastics.com/docs/user-v2.06.pdf>. Accessed: **2014**.
- (3) Li, G.; Wang, L.; Ni, H.; Pittman, C. U. Polyhedral oligomeric silsesquioxane (POSS[®]) polymers and copolymers: a review. *Journal of Inorganic and Organometallic Polymers* **2001**, *11*, 123-154.
- (4) Qin, Y.; Dong, J. Preparation of nano-compounded polyolefin materials through in situ polymerization technique: status quo and future prospects. *Chinese Science Bulletin* **2009**, *54*, 38-45.
- (5) Zheng, L.; Farris, R. J.; Coughlin, E. B. Synthesis of polyethylene hybrid copolymers containing polyhedral oligomeric silsesquioxane prepared with ring-opening metathesis copolymerization. *Journal of Polymer Science Part A: Polymer Chemistry* **2001**, *39*, 2920-2928.
- (6) Lichtenhan, J. D.; Noel, C. J.; Bolf, A. G.; Ruthi, P. N. Thermoplastic hybrid materials: polyhedral oligomeric silsesquioxane (POSS[®]) reagents, linear polymers, and blends. *MRS Online Proceedings Library Archive* **1996**, 435.
- (7) Pyun, J.; Matyjaszewski, K.; Wu, J.; Kim, G. M.; Chun, S. B.; Mather, P. T. ABA triblock copolymers containing polyhedral oligomeric silsesquioxane pendant groups: synthesis and unique properties. *Polymer* **2003**, *44*, 2739-2750.
- (8) Romo-Uribe, A.; Mather, P.; Haddad, T.; Lichtenhan, J. Viscoelastic and morphological behavior of hybrid styryl-based polyhedral oligomeric silsesquioxane (POSS[®]) copolymers. *Journal of Polymer Science Part B: Polymer Physics* **1998**, *36*, 1857-1872.
- (9) Yu, B.; Yuen, A. C. Y.; Xu, X.; Zhang, Z. C.; Yang, W.; Lu, H.; Fei, B.; Yeoh, G. H.; Song, P.; Wang, H. Engineering MXene Surface with POSS[®] for Reducing Fire Hazards of Polystyrene with Enhanced Thermal Stability. *Journal of Hazardous Materials* **2020**, 123342.

-
- (10) Mather, P. T.; Jeon, H. G.; Romo-Uribe, A.; Haddad, T. S.; Lichtenhan, J. D. Mechanical relaxation and microstructure of poly (norbornyl-POSS[®]) copolymers. *Macromolecules* **1999**, *32*, 1194-1203.
- (11) Pan, R.; Xiao, L.; He, S.; Qiu, S. Effect of spacer lengths on the interplay of intrachain and interchain in polynorbornene homopolymers embedded with polyhedral oligomeric silsesquioxane (POSS[®]): A molecular simulation approach. *Computational Materials Science* **2020**, *182*, 109779.
- (12) Fu, B. X.; Hsiao, B.; Pagola, S.; Stephens, P.; White, H.; Rafailovich, M.; Sokolov, J.; Mather, P.; Jeon, H.; Phillips, S. Structural development during deformation of polyurethane containing polyhedral oligomeric silsesquioxanes (POSS[®]) molecules. *Polymer* **2001**, *42*, 599-611.
- (13) Knott, R.; Dutta, N. K.; Choudhury, N. R. Molecular structure development in silsesquioxane-urethane thin film hybrids: A small-angle neutron scattering investigation. *Journal of Applied Polymer Science* **2020**, *137*, 48772.
- (14) Lichtenhan, J. D.; Vu, N. Q.; Carter, J. A.; Gilman, J. W.; Feher, F. J. Silsesquioxane-siloxane copolymers from polyhedral silsesquioxanes. *Macromolecules* **1993**, *26*, 2141-2142.
- (15) Constable, G. S.; Lesser, A. J.; Coughlin, E. B. Morphological and mechanical evaluation of hybrid organic-inorganic thermoset copolymers of dicyclopentadiene and mono-or tris (norbornenyl)-substituted polyhedral oligomeric silsesquioxanes. *Macromolecules* **2004**, *37*, 1276-1282.
- (16) Sellinger, A.; Laine, R. M. Silsesquioxanes as synthetic platforms. 3. Photocurable, liquid epoxides as inorganic/organic hybrid precursors. *Chemistry of Materials* **1996**, *8*, 1592-1593.
- (17) Sellinger, A.; Laine, R. M. Silsesquioxanes as synthetic platforms. Thermally curable and photocurable inorganic/organic hybrids. *Macromolecules* **1996**, *29*, 2327-2330.
- (18) Feher, F. J.; Budzichowski, T. A.; Blanski, R. L.; Weller, K. J.; Ziller, J. W. Facile syntheses of new incompletely condensed polyhedral oligosilsesquioxanes: [(c-C₅H₉)₇Si₇O₉ (OH)₃], [(c-C₇H₁₃)₇Si₇O₉ (OH)₃], and [(c-C₇H₁₃)₆Si₆O₇ (OH)₄]. *Organometallics* **1991**, *10*, 2526-2528.
- (19) Feher, F. J.; Newman, D. A.; Walzer, J. F. Silsesquioxanes as models for silica surfaces. *Journal of the American Chemical Society* **1989**, *111*, 1741-1748.

-
- (20) Agaskar, P.; Day, V.; Klemperer, W. A new route to trimethylsilylated spherosilicates. Synthesis and structure of $[\text{Si}_{12}\text{O}_{18}](\text{OSiMe}_3)_{12}$, $\text{D}_{3h}\text{-}[\text{Si}_{14}\text{O}_{21}](\text{OSiMe}_3)_{14}$, and $\text{C}_{2v}\text{-}[\text{Si}_{14}\text{O}_{21}](\text{OSiMe}_3)_{14}$. *Journal of the American Chemical Society* **1987**, *109*, 5554-5556.
- (21) Agaskar, P. A. Facile, high yield synthesis of functionalized spherosilicates: precursors of novel organolithic macromolecular materials. *Inorganic Chemistry* **1990**, *29*, 1603-1603.
- (22) Agaskar, P. A. New synthetic route to the hydridospherosiloxanes $\text{Oh-H}_8\text{Si}_8\text{O}_{12}$ and $\text{D}_{5h}\text{-H}_{10}\text{Si}_{10}\text{O}_{15}$. *Inorganic Chemistry* **1991**, *30*, 2707-2708.
- (23) Agaskar, P. A.; Klemperer, W. G. The higher hydridospherosiloxanes: synthesis and structures of $\text{H}_n\text{Si}_n\text{O}_{1.5n}$ ($n = 12, 14, 16, 18$). *Inorganica Chimica Acta* **1995**, *229*, 355-364.
- (24) Baney, R. H.; Itoh, M.; Sakakibara, A.; Suzuki, T. Silsesquioxanes. *Chemical Reviews* **1995**, *95*, 1409-1430.
- (25) Ye, Q.; Zhou, H.; Xu, J. Cubic polyhedral oligomeric silsesquioxane based functional materials: synthesis, assembly, and applications. *Chemistry-An Asian Journal* **2016**, *11*, 1322-1337.
- (26) Provatas, A.; Matisons, J. Silsesquioxanes: synthesis and applications. *Trends in Polymer Science* **1997**, *10*, 327-332.
- (27) Feher, F. J. Controlled cleavage of $\text{R}_8\text{Si}_8\text{O}_{12}$ frameworks: a revolutionary new method for manufacturing precursors to hybrid inorganic-organic materials. *Chemical Communications* **1998**, 399-400.
- (28) Feher, F. J.; Soulivong, D.; Lewis, G. T. Facile framework cleavage reactions of a completely condensed silsesquioxane framework. *Journal of the American Chemical Society* **1997**, *119*, 11323-11324.
- (29) Ayandele, E.; Sarkar, B.; Alexandridis, P. Polyhedral oligomeric silsesquioxane (POSS[®])-containing polymer nanocomposites. *Nanomaterials* **2012**, *2*, 445-475.
- (30) Bizet, S.; Galy, J.; Gérard, J. F. Structure-property relationships in organic-inorganic nanomaterials based on methacryl-POSS[®] and dimethacrylate networks. *Macromolecules* **2006**, *39*, 2574-2583.
- (31) Matejka, L. 'POSS[®] and other Hybrid Epoxy Polymers. Chapter 8 in *Epoxy Polymers: New materials and Innovations*. Ed by Jean-Pierre Pascault and Ronerto j. j. Williams. WILEY-VCH Verlag GmbH & Co-KGaA, Weinheim, **2010**, 137.

-
- (32) Schiraldi, D. A.; Abu-Ali, A.; Iyer, S.; Detweiler, A. Transparent nanocomposites of polyhedral oligomeric silsesquioxanes (POSS®). *Polymer Preprints Amer.* **2004**, *45*, 642-643.
- (33) Li, G. Z.; Wang, L.; Toghiani, H.; Daulton, T. L.; Koyama, K.; Pittman, C. U. Viscoelastic and mechanical properties of epoxy/multifunctional polyhedral oligomeric silsesquioxane nanocomposites and epoxy/ladder-like polyphenylsilsesquioxane blends. *Macromolecules* **2001**, *34*, 8686-8693.
- (34) Boček, J.; Matějka, L.; Mentlík, V.; Trnka, P.; Šlouf, M. Electrical and thermomechanical properties of epoxy-POSS® nanocomposites. *European Polymer Journal* **2011**, *47*, 861-872.
- (35) Pascault, J. P.; Williams, R. J. in *Epoxy Polymers: New Materials and Innovations*; John Wiley & Sons, **2009**.
- (36) Riccardi, C. C.; Williams, R. J. A kinetic scheme for an amine-epoxy reaction with simultaneous etherification. *Journal of Applied Polymer Science* **1986**, *32*, 3445-3456.
- (37) Grillet, A.; Galy, J.; Pascault, J.; Bardin, I. Effects of the structure of the aromatic curing agent on the cure kinetics of epoxy networks. *Polymer* **1989**, *30*, 2094-2103.
- (38) Wang, X.; Gillham, J. K. Competitive primary amine/epoxy and secondary amine/epoxy reactions: Effect on the isothermal time-to-vitrify. *Journal of Applied Polymer Science* **1991**, *43*, 2267-2277.
- (39) Barton, J. M.; Buist, G. J.; Hamerton, I.; Howlin, B. J.; Jones, J. R.; Liu, S. Preparation and characterization of imidazole-metal complexes and evaluation of cured epoxy networks. *Journal of Materials Chemistry* **1994**, *4*, 379-384.
- (40) Galante, M.; Vázquez, A.; Williams, R. Macro-and microgelation in the homopolymerization of diepoxides initiated by tertiary amines. *Polymer Bulletin* **1991**, *27*, 9-15.
- (41) Park, S. J.; Jin, F. L.; Lee, J. R.; Shin, J. S. Cationic polymerization and physicochemical properties of a biobased epoxy resin initiated by thermally latent catalysts. *European Polymer Journal* **2005**, *41*, 231-237.
- (42) Petrie, E. in *Epoxy Adhesive Formulations*. New York, Chicago, San Francisco, Lisbon, London, Madrid, Mexico City, Milan, New Delhi, San Juan. McGraw-Hill Professional, **2006**.

-
- (43) Weickmann, H.; Delto, R.; Thomann, R.; Brenn, R.; Döll, W.; Mülhaupt, R. PMMA nanocomposites and gradient materials prepared by means of polysilsesquioxane (POSS®) self-assembly. *Journal of Materials Science* **2007**, *42*, 87-92.
- (44) Misra, R.; Fu, B. X.; Morgan, S. E. Surface energetics, dispersion, and nanotribomechanical behavior of POSS®/PP hybrid nanocomposites. *Journal of Polymer Science Part B: Polymer Physics* **2007**, *45*, 2441-2455.
- (45) Zucchi, I. A.; Galante, M. J.; Williams, R. J.; Franchini, E.; Galy, J.; Gérard, J. F. Monofunctional epoxy-POSS® dispersed in epoxy-amine networks: Effect of a prereaction on the morphology and crystallinity of POSS domains. *Macromolecules* **2007**, *40*, 1274-1282.
- (46) Wu, Q.; Zhang, C.; Liang, R.; Wang, B. Combustion and thermal properties of epoxy/phenyltrisilanol polyhedral oligomeric silsesquioxane nanocomposites. *Journal of Thermal Analysis and Calorimetry* **2010**, *100*, 1009-1015.
- (47) Xu, Y.; Ma, Y.; Deng, Y.; Yang, C.; Chen, J.; Dai, L. Morphology and thermal properties of organic-inorganic hybrid material involving monofunctional-anhydride POSS® and epoxy resin. *Materials Chemistry and Physics* **2011**, *125*, 174-183.
- (48) Ni, Y.; Zheng, S.; Nie, K. Morphology and thermal properties of inorganic-organic hybrids involving epoxy resin and polyhedral oligomeric silsesquioxanes. *Polymer* **2004**, *45*, 5557-5568.
- (49) Lee, A.; Lichtenhan, J. D. Viscoelastic responses of polyhedral oligosilsesquioxane reinforced epoxy systems. *Macromolecules* **1998**, *31*, 4970-4974.
- (50) Mishra, K.; Pandey, G.; Singh, R. P. Enhancing the mechanical properties of an epoxy resin using polyhedral oligomeric silsesquioxane (POSS®) as nano-reinforcement. *Polymer Testing* **2017**, *62*, 210-218.
- (51) Leu, C. M.; Chang, Y. T.; Wei, K. H. Synthesis and dielectric properties of polyimide-tethered polyhedral oligomeric silsesquioxane (POSS®) nanocomposites via POSS®-diamine. *Macromolecules* **2003**, *36*, 9122-9127.
- (52) Haddad, T.; Choe, E.; Lichtenhan, J. Hybrid styryl-based polyhedral oligomeric silsesquioxane (POSS®) polymers. *MRS Online Proceedings Library Archive* **1996**, *435*.

-
- (53) Franchini, E.; Galy, J.; Gerard, J. F.; Tabuani, D.; Medici, A. Influence of POSS[®] structure on the fire retardant properties of epoxy hybrid networks. *Polymer Degradation and Stability* **2009**, *94*, 1728-1736.
- (54) Kausar, A. State-of-the-Art overview on polymer/POSS[®] nanocomposite. *Polymer-Plastics Technology and Engineering* **2017**, *56*, 1401-1420.
- (55) Matějka, L.; Strachota, A.; Pleštil, J.; Whelan, P.; Steinhart, M.; Šlouf, M. Epoxy networks reinforced with polyhedral oligomeric silsesquioxanes (POSS[®]). Structure and morphology. *Macromolecules* **2004**, *37*, 9449-9456.
- (56) Tucker, S. J.; Fu, B.; Kar, S.; Heinz, S.; Wiggins, J. S. Ambient cure POSS[®]-epoxy matrices for marine composites. *Composites Part A: Applied Science and Manufacturing* **2010**, *41*, 1441-1446.
- (57) Zhang, C.; Laine, R. M. Silsesquioxanes as synthetic platforms. II. Epoxy-functionalized inorganic-organic hybrid species. *Journal of Organometallic Chemistry* **1996**, *521*, 199-201.
- (58) Mya, K. Y.; He, C.; Huang, J.; Xiao, Y.; Dai, J.; Siow, Y. P. Preparation and thermomechanical properties of epoxy resins modified by octafunctional cubic silsesquioxane epoxides. *Journal of Polymer Science Part A: Polymer Chemistry* **2004**, *42*, 3490-3503.
- (59) Huang, J.; He, C.; Liu, X.; Xu, J.; Tay, C. S.; Chow, S. Y. Organic-inorganic nanocomposites from cubic silsesquioxane epoxides: direct characterization of interphase, and thermomechanical properties. *Polymer* **2005**, *46*, 7018-7027.
- (60) Gao, J.; Kong, D.; Li, S. Preparation of BPA epoxy resin/POSS[®] nanocomposites and nonisothermal co-curing kinetics with MeTHPA. *International Journal of Polymeric Materials* **2008**, *57*, 940-956.
- (61) Chiu, Y. C.; Riag, L.; Chou, I. C.; Ma, C. C. M.; Chiang, C. L.; Yang, C. C. The POSS[®] side chain epoxy nanocomposite: Synthesis and thermal properties. *Journal of Polymer Science Part B: Polymer Physics* **2010**, *48*, 643-652.
- (62) Liu, Y. L.; Chang, G. P.; Wu, C. S.; Chiu, Y. S. Preparation and properties of high performance epoxy-silsesquioxane hybrid resins prepared using a maleimide-alkoxysilane compound as a modifier. *Journal of Polymer Science Part A: Polymer Chemistry* **2005**, *43*, 5787-5798.

- (63) Wu, K.; Song, L.; Hu, Y.; Lu, H.; Kandola, B. K.; Kandare, E. Synthesis and characterization of a functional polyhedral oligomeric silsesquioxane and its flame retardancy in epoxy resin. *Progress in Organic Coatings* **2009**, *65*, 490-497.
- (64) Huang, J. M.; Huang, H. J.; Wang, Y. X.; Chen, W. Y.; Chang, F. C. Preparation and characterization of epoxy/polyhedral oligomeric silsesquioxane hybrid nanocomposites. *Journal of Polymer Science Part B: Polymer Physics* **2009**, *47*, 1927-1934.
- (65) Huo, L.; Wu, X.; Tian, C.; Gao, J. Thermal, mechanical, and electrical properties of alkyd-epoxy resin nanocomposites modified with 3-glycidyloxypropyl-POSS[®]. *Polymer-Plastics Technology and Engineering* **2018**, *57*, 371-379.
- (66) Matějka, L.; Murias, P.; Pleštil, J. Effect of POSS[®] on thermomechanical properties of epoxy-POSS[®] nanocomposites. *European Polymer Journal* **2012**, *48*, 260-274.
- (67) Matějka, L.; Dukh, O. Organic-inorganic hybrid networks. in *Macromolecular Symposia*; Wiley Online Library, **2001**; Vol. 171, p 181-188.
- (68) Zhang, Z.; Wang, X.; Xie, J.; Liang, G. Using octa (aminopropyl) silsesquioxane as the curing agent for epoxy resin. *Journal of Reinforced Plastics and Composites* **2007**, *26*, 1665-1670.
- (69) Liu, B.; Wang, H.; Guo, X.; Yang, R.; Li, X. Effects of an organic-inorganic hybrid containing allyl benzoxazine and POSS[®] on thermal properties and flame retardancy of epoxy resin. *Polymers* **2019**, *11*, 770.
- (70) Perrin, F.; Chaoui, N.; Margaillan, A. Effects of octa (3-chloroammoniumpropyl) octasilsesquioxane on the epoxy self-polymerisation and epoxy-amine curing. *Thermochimica Acta* **2009**, *491*, 97-102.
- (71) Nakas, G. I.; Kaynak, C. Use of different alkylammonium salts in clay surface modification for epoxy-based nanocomposites. *Polymer Composites* **2009**, *30*, 357-363.
- (72) Mohan, T.; Ramesh Kumar, M.; Velmurugan, R. Rheology and curing characteristics of epoxy-clay nanocomposites. *Polymer International* **2005**, *54*, 1653-1659.
- (73) Fu, J.; Shi, L.; Chen, Y.; Yuan, S.; Wu, J.; Liang, X.; Zhong, Q. Epoxy nanocomposites containing mercaptopropyl polyhedral oligomeric silsesquioxane: Morphology, thermal properties, and toughening mechanism. *Journal of Applied Polymer Science* **2008**, *109*, 340-349.

- (74)Jothibas, S.; Premkumar, S.; Alagar, M.; Hamerton, I. Synthesis and characterization of a POSS[®]-maleimide precursor for hybrid nanocomposites. *High Performances Polymers* **2008**, *20*, 67-85.
- (75)Ni, Y.; Zheng, S. Epoxy resin containing octamaleimidophenyl polyhedral oligomeric silsesquioxane. *Macromolecular Chemistry and Physics* **2005**, *206*, 2075-2083.
- (76)Ni, C.; Ni, G.; Zhang, S.; Liu, X.; Chen, M.; Liu, L. The preparation of inorganic/organic hybrid nanomaterials containing silsesquioxane and its reinforcement for an epoxy resin network. *Colloid and Polymer Science* **2010**, *288*, 469-477.
- (77)Teo, J. K. H.; Teo, K. C.; Pan, B.; Xiao, Y.; Lu, X. Epoxy/polyhedral oligomeric silsesquioxane (POSS[®]) hybrid networks cured with an anhydride: Cure kinetics and thermal properties. *Polymer* **2007**, *48*, 5671-5680.
- (78)Jones, I.; Zhou, Y.; Jeelani, S.; Mabry, J. Effect of polyhedral-oligomeric-sil-sesquioxanes on thermal and mechanical behavior of SC-15 epoxy. *Express Polymer Letters* **2008**, *2*, 494-501.
- (79)Di Luca, C.; Soule, E.; Zucchi, I.; Hoppe, C.; Fasce, L.; Williams, R. In-situ generation of a dispersion of POSS[®] crystalline platelets in an epoxy matrix induced by polymerization. *Macromolecules* **2010**, *43*, 9014-9021.
- (80)Zhang, Z.; Liang, G.; Wang, J.; Ren, P. Epoxy/POSS[®] organic-inorganic hybrids: viscoelastic, mechanical properties and micromorphologies. *Polymer composites* **2007**, *28*, 175-179.
- (81)Haddad, T. S.; Lichtenhan, J. D. Hybrid organic-inorganic thermoplastics: Styryl-based polyhedral oligomeric silsesquioxane polymers. *Macromolecules* **1996**, *29*, 7302-7304.
- (82)Lichtenhan, J. D.; Otonari, Y. A.; Carr, M. J. Linear hybrid polymer building blocks: methacrylate-functionalized polyhedral oligomeric silsesquioxane monomers and polymers. *Macromolecules* **1995**, *28*, 8435-8437.
- (83)Xu, H.; Kuo, S. W.; Lee, J. S.; Chang, F. C. Preparations, thermal properties, and T_g increase mechanism of inorganic/organic hybrid polymers based on polyhedral oligomeric silsesquioxanes. *Macromolecules* **2002**, *35*, 8788-8793.
- (84)Pistor, V.; Barbosa, L. G.; Soares, B. G.; Mauler, R. S. Relaxation phenomena in the glass transition of epoxy/N-phenylaminopropyl-POSS[®] nanocomposites. *Polymer* **2012**, *53*, 5798-5805.

-
- (85)Pistor, V.; Soares, B. G.; Mauler, R. S. Influence of different concentrations of N-phenylaminopropyl-POSS[®] on the thermodynamic fragility of the cured epoxy resin. *Polymer* **2013**, *54*, 2292-2298.
- (86)Pistor, V.; Ornaghi, F. G.; Ornaghi Jr, H. L.; Zattera, A. J. Degradation kinetic of epoxy nanocomposites containing different percentage of epoxycyclohexyl-POSS[®]. *Polymer Composites* **2012**, *33*, 1224-1232.
- (87)Strachota, A.; Whelan, P.; Kříž, J.; Brus, J.; Urbanová, M.; Šlouf, M.; Matějka, L. Formation of nanostructured epoxy networks containing polyhedral oligomeric silsesquioxane (POSS[®]) blocks. *Polymer* **2007**, *48*, 3041-3058.
- (88)Choi, J.; Yee, A. F.; Laine, R. M. Organic/inorganic hybrid composites from cubic silsesquioxanes. Epoxy resins of octa-(dimethylsiloxylethylcyclohexylepoxy) silsesquioxane. *Macromolecules* **2003**, *36*, 5666-5682.
- (89)Haddad, T. S.; Mather, P. T.; Jeon, H. G.; Chun, S. B.; Phillips, S. H. "Hybrid Inorganic/Organic Diblock Copolymers. Nanostructure in Polyhedral Oligomeric Silsesquioxane Polymorborenes. *Materials Research Society Symposium Proceedings*, **2000**, 628, CC2.6.1-CC2.6.7.
- (90)Jeon, H. G.; Mather, P. T.; Haddad, T. S. Shape memory and nanostructure in poly (norbornyl-POSS[®]) copolymers. *Polymer International* **2000**, *49*, 453-457.
- (91)Pistor, V.; Puziski, L.; Zattera, A. J. Influence of different concentrations of glycidylisobutyl-POSS[®] on the glass transition of cured epoxy resin. *Journal of Applied Polymer Science* **2015**, *132*, 41453 (1-8).
- (92)Pan, R.; Shanks, R.; Wang, L. Trisilanolisobutyl POSS[®]/polyurethane hybrid composites: preparation, WAXS and thermal properties. *Polymer Bulletin* **2014**, *71*, 2453-2464.
- (93)Strachota, A.; Kroutilová, I.; Kovářová, J.; Matějka, L. Epoxy networks reinforced with polyhedral oligomeric silsesquioxanes (POSS[®]). Thermomechanical properties. *Macromolecules* **2004**, *37*, 9457-9464.
- (94)Zhang, W.; Camino, G.; Yang, R. Polymer/polyhedral oligomeric silsesquioxane (POSS[®]) nanocomposites: An overview of fire retardance. *Progress in Polymer Science* **2017**, *67*, 77-125.

-
- (95) Gnanasekaran, D.; Madhavan, K.; Reddy, B. Developments of polyhedral oligomeric silsesquioxanes (POSS[®]), POSS[®] nanocomposites and their applications: A review. *Journal of Scientific and Industrial Research* **2009**, 68, 437-464.
- (96) Wang, X.; Hu, Y.; Song, L.; Xing, W.; Lu, H. Thermal degradation behaviors of epoxy resin/POSS[®] hybrids and phosphorus-silicon synergism of flame retardancy. *Journal of Polymer Science Part B: Polymer Physics* **2010**, 48, 693-705.
- (97) Liu, Y. L.; Chang, G. P.; Hsu, K. Y.; Chang, F. C. Epoxy/polyhedral oligomeric silsesquioxane nanocomposites from octakis (glycidyl dimethylsiloxy) octasilsesquioxane and small-molecule curing agents. *Journal of Polymer Science Part A: Polymer Chemistry* **2006**, 44, 3825-3835.
- (98) Zhang, J.; Zhang, W.; Guan, D. Preparation and properties of epoxy resin/polyhedral oligomeric silsesquioxane hybrid materials. *Polymer Bulletin* **2016**, 73, 113-123.
- (99) Laik, S.; Galy, J.; Gérard, J. F.; Monti, M.; Camino, G. Fire behaviour and morphology of epoxy matrices designed for composite materials processed by infusion. *Polymer Degradation and Stability* **2016**, 127, 44-55.
- (100) Zhang, W.; Li, X.; Li, L.; Yang, R. Study of the synergistic effect of silicon and phosphorus on the blowing-out effect of epoxy resin composites. *Polymer Degradation and Stability* **2012**, 97, 1041-1048.
- (101) Gérard, C.; Fontaine, G.; Bellayer, S.; Bourbigot, S. Reaction to fire of an intumescent epoxy resin: Protection mechanisms and synergy. *Polymer Degradation and Stability* **2012**, 97, 1366-1386.
- (102) Zhang, W.; Li, X.; Jiang, Y.; Yang, R. Investigations of epoxy resins flame-retarded by phenyl silsesquioxanes of cage and ladder structures. *Polymer Degradation and Stability* **2013**, 98, 246-254.
- (103) Barra, G.; Vertuccio, L.; Vietri, U.; Naddeo, C.; Hadavinia, H.; Guadagno, L. Toughening of epoxy adhesives by combined interaction of carbon nanotubes and silsesquioxanes. *Materials* **2017**, 10, 1131.
- (104) Liu, C.; Chen, T.; Yuan, C.; Chang, Y.; Chen, G.; Zeng, B.; Xu, Y.; Luo, W.; Dai, L. Highly transparent and flame-retardant epoxy composites based on a hybrid multi-element containing POSS[®] derivative. *RSC advances* **2017**, 7, 46139-46147.

-
- (105) Ma, Y.; He, L. POSS[®]-pendanted in epoxy chain inorganic-organic hybrid for highly thermo-mechanical, permeable and hydrothermal-resistant coatings. *Materials Chemistry and Physics* **2017**, *201*, 120-129.
- (106) Wu, H.; Li, Y.; Zeng, B.; Chen, G.; Wu, Y.; Chen, T.; Dai, L. A high synergistic P/N/Si-containing additive with dandelion-shaped structure deriving from self-assembly for enhancing thermal and flame retardant property of epoxy resins. *Reactive and Functional Polymers* **2018**, *131*, 89-99.
- (107) Zeng, B.; Liu, Y.; Yang, L.; Zheng, W.; Chen, T.; Chen, G.; Xu, Y.; Yuan, C.; Dai, L. Flame retardant epoxy resin based on organic titanate and polyhedral oligomeric silsesquioxane-containing additives with synergistic effects. *RSC Advances* **2017**, *7*, 26082-26088.
- (108) Zhou, T.; Wu, T.; Xiang, H.; Li, Z.; Xu, Z.; Kong, Q.; Zhang, J.; Li, Z.; Pan, Y.; Wang, D. Simultaneously improving flame retardancy and dynamic mechanical properties of epoxy resin nanocomposites through synergistic effect of zirconium phenylphosphate and POSS[®]. *Journal of Thermal Analysis and Calorimetry* **2019**, *135*, 2117-2124.
- (109) Zhu, G. L.; Han, D.; Yuan, Y.; Chen, F.; Fu, Q. Improving damping properties and thermal stability of epoxy/polyurethane grafted copolymer by adding glycidyl POSS[®]. *Chinese Journal of Polymer Science* **2018**, *36*, 1297-1302.
- (110) Meenakshi, K. S.; Sudhan, E. P. J. Development of novel TGDDM epoxy nanocomposites for aerospace and high performance applications-Study of their thermal and electrical behaviour. *Arabian Journal of Chemistry* **2016**, *9*, 79-85.
- (111) Choi, C.; Kim, Y.; Kumar, S. K. S.; Kim, C. G. Enhanced resistance to atomic oxygen of OG POSS[®]/epoxy nanocomposites. *Composite Structures* **2018**, *202*, 959-966.
- (112) Sharma, A. K.; Sloan, R.; Ramakrishnan, R.; Nazarenko, S. I.; Wiggins, J. S. Structure-property relationships in epoxy hybrid networks based on high mass fraction pendant POSS[®] incorporated at molecular level. *Polymer* **2018**, *139*, 201-212.
- (113) Li, S.; Zhao, X.; Zhang, Y.; Yang, X.; Yu, R.; Zhang, Y.; Deng, K.; Huang, W. A facile approach to prepare cage-ladder-structure phosphorus-containing amino-functionalized POSS for enhancing flame retardancy of epoxy resins. *Journal of Applied Polymer Science* **2021**, *138*, 49870.

- (114) Abd Rashid, E. S.; Ariffin, K.; Kooi, C. C.; Akil, H. M. Preparation and properties of POSS[®]/epoxy composites for electronic packaging applications. *Materials & Design* **2009**, *30*, 1-8.
- (115) Wang, X.; Wang, X.; Song, L.; Xing, W.; Tang, G.; Hu, W.; Hu, Y. Preparation and thermal stability of UV-cured epoxy-based coatings modified with octamercaptopropyl POSS[®]. *Thermochimica acta* **2013**, *568*, 130-139.
- (116) Aliakbari, M.; Jazani, O. M.; Sohrabian, M.; Jouyandeh, M.; Saeb, M. R. Multi-nationality epoxy adhesives on trial for future nanocomposite developments. *Progress in Organic Coatings* **2019**, *133*, 376-386.
- (117) Bayat, S.; Jazani, O. M.; Molla-Abbasi, P.; Jouyandeh, M.; Saeb, M. R. Thin films of epoxy adhesives containing recycled polymers and graphene oxide nanoflakes for metal/polymer composite interface. *Progress in Organic Coatings* **2019**, *136*, 105201.
- (118) Akbari, V.; Jouyandeh, M.; Paran, S. M. R.; Ganjali, M. R.; Abdollahi, H.; Vahabi, H.; Ahmadi, Z.; Formela, K.; Esmaeili, A.; Mohaddespour, A. Effect of Surface Treatment of Halloysite Nanotubes (HNTs) on the kinetics of epoxy resin cure with amines. *Polymers* **2020**, *12*, 930.
- (119) Li, Y.; Dong, X.-H.; Guo, K.; Wang, Z.; Chen, Z.; Wesdemiotis, C.; Quirk, R. P.; Zhang, W. B.; Cheng, S. Z. Synthesis of shape amphiphiles based on POSS[®] tethered with two symmetric/asymmetric polymer tails via sequential “grafting-from” and thiol-ene “click” chemistry. *ACS Macro Letters* **2012**, *1*, 834-839.
- (120) Li, Y.; Dong, X. H.; Zou, Y.; Wang, Z.; Yue, K.; Huang, M.; Liu, H.; Feng, X.; Lin, Z.; Zhang, W. Polyhedral oligomeric silsesquioxane meets “click” chemistry: Rational design and facile preparation of functional hybrid materials. *Polymer* **2017**, *125*, 303-329.
- (121) Cao, J.; Fan, H.; Li, B. G.; Zhu, S. Synthesis and evaluation of Double-Decker silsesquioxanes as modifying agent for epoxy resin. *Polymer* **2017**, *124*, 157-167.
- (122) Ma, Y.; He, L.; Jia, M.; Zhao, L.; Zuo, Y.; Hu, P. Cage and linear structured polysiloxane/epoxy hybrids for coatings: Surface property and film permeability. *Journal of Colloid and Interface Science* **2017**, *500*, 349-357.
- (123) Misasi, J. M.; Jin, Q.; Knauer, K. M.; Morgan, S. E.; Wiggins, J. S. Hybrid POSS[®]-Hyperbranched polymer additives for simultaneous reinforcement and toughness improvements in epoxy networks. *Polymer* **2017**, *117*, 54-63.

-
- (124) Zhang, C.; Li, T.; Song, H.; Han, Y.; Dong, Y.; Wang, Y.; Wang, Q. Improving the thermal conductivity and mechanical property of epoxy composites by introducing polyhedral oligomeric silsesquioxane-grafted graphene oxide. *Polymer Composites* **2018**, *39*, E1890-E1899.
- (125) Ci, J.; Cao, C.; Kuga, S.; Shen, J.; Wu, M.; Huang, Y. Improved performance of microbial fuel cell using esterified corncob cellulose nanofibers to fabricate air-cathode gas diffusion layer. *ACS Sustainable Chemistry & Engineering* **2017**, *5*, 9614-9618.
- (126) Kafi, A.; Li, Q.; Chaffraix, T.; Khoo, J.; Gengenbach, T.; Magniez, K. J. C. Surface treatment of carbon fibres for interfacial property enhancement in composites via surface deposition of water soluble POSS[®] nanowhiskers. *Polymer* **2018**, *137*, 97-106.
- (127) Ma, L.; Zhu, Y.; Wang, M.; Yang, X.; Song, G.; Huang, Y. Enhancing interfacial strength of epoxy resin composites via evolving hyperbranched amino-terminated POSS[®] on carbon fiber surface. *Composites Science and Technology* **2019**, *170*, 148-156.
- (128) Kim, G. M.; Qin, H.; Fang, X.; Sun, F.; Mather, P. Hybrid epoxy-based thermosets based on polyhedral oligosilsesquioxane: Cure behavior and toughening mechanisms. *Journal of Polymer Science Part B: Polymer Physics* **2003**, *41*, 3299-3313.
- (129) Mishra, K.; Singh, R. P. Reinforcement of epoxy resins with POSS[®] for enhancing fracture toughness at cryogenic temperature. in *Composite Materials and Joining Technologies for Composites, Volume 7*; Springer, **2013**, p 179-187.
- (130) Hao, N.; Böhning, M.; Schönhals, A. Dielectric properties of nanocomposites based on polystyrene and polyhedral oligomeric phenethyl-silsesquioxanes. *Macromolecules* **2007**, *40*, 9672-9679.
- (131) Ke, F.; Zhang, C.; Guang, S.; Xu, H. POSS[®] Core star-shape molecular hybrid materials: Effect of the chain length and POSS[®] content on dielectric properties. *Journal of Applied Polymer Science* **2013**, *127*, 2628-2634.
- (132) Tang, L. C.; Wang, X.; Wan, Y. J.; Wu, L. B.; Jiang, J. X.; Lai, G. Q. Mechanical properties and fracture behaviors of epoxy composites with multi-scale rubber particles. *Materials Chemistry and Physics* **2013**, *141*, 333-342.
- (133) Zhang, W.; Wang, S.; Li, X.; Yuan, J.; Wang, S. Organic/inorganic hybrid star-shaped block copolymers of poly (L-lactide) and poly (N-isopropylacrylamide) with a polyhedral

- oligomeric silsesquioxane core: Synthesis and self-assembly. *European Polymer Journal* **2012**, 48, 720-729.
- (134) Qi, L.; Lee, B. I.; Chen, S.; Samuels, W. D.; Exarhos, G. J. High-dielectric-constant silver-epoxy composites as embedded dielectrics. *Advanced Materials* **2005**, 17, 1777-1781.
- (135) Singha, S.; Thomas, M. J. Dielectric properties of epoxy nanocomposites. *IEEE Transactions on Dielectrics and Electrical Insulation* **2008**, 15, 12-23.
- (136) Fréchette, M. F.; Zribi, E.; Vanga-Bouanga, C.; David, E. Effect of various parameters on the dielectric behavior of an epoxy composite containing 10 wt. % of carbon black. in *IEEE International Conference on Dielectrics (ICD)*; IEEE, **2016**; 1, 10-14.
- (137) Zhang, M.; Zhai, Z.; Li, M.; Cheng, T.; Wang, C.; Jiang, D.; Chen, L.; Wu, Z.; Guo, Z. Epoxy nanocomposites with carbon nanotubes and montmorillonite: Mechanical properties and electrical insulation. *Journal of Composite Materials* **2016**, 50, 3363-3372.
- (138) Singha, S.; Thomas, M. J. Influence of filler loading on dielectric properties of epoxy-ZnO nanocomposites. *IEEE Transactions on Dielectrics and Electrical Insulation* **2009**, 16, 531-542.
- (139) Halawani, N.; Auge, J. L.; Pruvost, S.; Gain, O. Epoxy composites for insulating properties. In *2015 IEEE Electrical Insulation Conference (EIC)*; IEEE, **2015**, p 547-550.
- (140) Gu, H.; Ma, C.; Gu, J.; Guo, J.; Yan, X.; Huang, J.; Zhang, Q.; Guo, Z. An overview of multifunctional epoxy nanocomposites. *Journal of Materials Chemistry C* **2016**, 4, 5890-5906.
- (141) Abdelkader, K.; Pascal, R.; Olivier, L.; Céline, R. Dielectric relaxation and ionic conduction in 66% Silica/CW229-3/HW229-1 microcomposite polymer. *Composites Part B: Engineering* **2015**, 78, 488-496.
- (142) Heid, T.; Fréchette, M.; David, E. Nanostructured epoxy/POSS[®] composites: high performance dielectrics with improved corona resistance and thermal conductivity. In *2014 IEEE Electrical Insulation Conference (EIC)*; IEEE, **2014**, p 316-319.
- (143) Peng, W.; Xu, S.; Li, L.; Zhang, C.; Zheng, S. Organic-inorganic nanocomposites via self-assembly of an amphiphilic triblock copolymer bearing a Poly (butadiene-g-POSS[®]) subchain in epoxy thermosets: morphologies, surface hydrophobicity, and dielectric properties. *The Journal of Physical Chemistry B* **2016**, 120, 12003-12014.

- (144) Zhang, S.; Li, X.; Fan, H.; Fu, Q.; Gu, Y. Epoxy nanocomposites: Improved thermal and dielectric properties by benzoxazinyl modified polyhedral oligomeric silsesquioxane. *Materials Chemistry and Physics* **2019**, *223*, 260-267.
- (145) Dhanapal, D.; Srinivasan, A. K.; Ramalingam, N. Role of POSS[®] as coupling agent for DGEBA/GF reinforced nanocomposites. *Silicon* **2018**, *10*, 537-546.
- (146) Castner Jr, E. W.; Margulis, C. J.; Maroncelli, M.; Wishart, J. F. Ionic liquids: Structure and photochemical reactions. *Annual Review of Physical Chemistry* **2011**, *62*, 85-105.
- (147) Singh, G.; Kumar, A. Ionic liquids: Physico-chemical, solvent properties and their applications in chemical processes. *Indian Journal of Chemistry-Section A* **2008**, *47A*, 495-503.
- (148) Hayes, R.; Warr, G. G.; Atkin, R. Structure and nanostructure in ionic liquids. *Chemical Reviews* **2015**, *115*, 6357-6426.
- (149) Awad, W. H.; Gilman, J. W.; Nyden, M.; Harris Jr, R. H.; Sutto, T. E.; Callahan, J.; Trulove, P. C.; DeLong, H. C.; Fox, D. M. Thermal degradation studies of alkyl-imidazolium salts and their application in nanocomposites. *Thermochimica Acta* **2004**, *409*, 3-11.
- (150) Lu, J.; Yan, F.; Texter, J. Advanced applications of ionic liquids in polymer science. *Progress in Polymer Science* **2009**, *34*, 431-448.
- (151) Ngo, H. L.; LeCompte, K.; Hargens, L.; McEwen, A. B. Thermal properties of imidazolium ionic liquids. *Thermochimica acta* **2000**, *357*, 97-102.
- (152) Plechkova, N. V.; Seddon, K. R. Applications of ionic liquids in the chemical industry. *Chemical Society Reviews* **2008**, *37*, 123-150.
- (153) Earle, M. J.; Seddon, K. R. Ionic liquids. Green solvents for the future. *Pure and Applied Chemistry* **2000**, *72*, 1391-1398.
- (154) Hapiot, P.; Lagrost, C. Electrochemical reactivity in room-temperature ionic liquids. *Chemical Reviews* **2008**, *108*, 2238-2264.
- (155) Scheuermeyer, M.; Kusche, M.; Agel, F.; Schreiber, P.; Maier, F.; Steinrück, H. P.; Davis, J. H.; Heym, F.; Jess, A.; Wasserscheid, P. Thermally stable bis (trifluoromethylsulfonyl) imide salts and their mixtures. *New Journal of Chemistry* **2016**, *40*, 7157-7161.
- (156) Huddleston, J. G.; Willauer, H. D.; Swatoski, R. P.; Visser, A. E.; Rogers, R. D. Room temperature ionic liquids as novel media for 'clean' liquid-liquid extraction. *Chemical Communications* **1998**, 1765-1766.

- (157) Baudequin, C.; Baudoux, J.; Levillain, J.; Cahard, D.; Gaumont, A. C.; Plaquevent, J. C. Ionic liquids and chirality: opportunities and challenges. *Tetrahedron: Asymmetry* **2003**, *14*, 3081-3093.
- (158) Welton, T. Room-temperature ionic liquids. Solvents for synthesis and catalysis. *Chemical Reviews* **1999**, *99*, 2071-2084.
- (159) Ho, T. D.; Zhang, C.; Hantao, L. W.; Anderson, J. L. Ionic liquids in analytical chemistry: fundamentals, advances, and perspectives. *Analytical Chemistry* **2014**, *86*, 262-285.
- (160) Pandey, S. Analytical applications of room-temperature ionic liquids: A review of recent efforts. *Analytica Chimica Acta* **2006**, *556*, 38-45.
- (161) Endres, F.; El Abedin, S. Z. Air and water stable ionic liquids in physical chemistry. *Physical Chemistry Chemical Physics* **2006**, *8*, 2101-2116.
- (162) McFarlane, D.; Sun, J.; Golding, J.; Meakin, P.; Forsyth, M. High conductivity molten salts based on the imide ion. *Electrochimica Acta* **2000**, *45*, 1271-1278.
- (163) Bermúdez, M. D.; Jiménez, A. E.; Sanes, J.; Carrión, F. J. Ionic liquids as advanced lubricant fluids. *Molecules* **2009**, *14*, 2888-2908.
- (164) Somers, A. E.; Howlett, P. C.; MacFarlane, D. R.; Forsyth, M. A review of ionic liquid lubricants. *Lubricants* **2013**, *1*, 3-21.
- (165) Tan, S. S. Y.; MacFarlane, D. R. Ionic liquids in biomass processing. in *Ionic liquids*; Springer, **2009**, p 311-339.
- (166) Kubisa, P. Ionic liquids as solvents for polymerization processes-Progress and challenges. *Progress in Polymer Science* **2009**, *34*, 1333-1347.
- (167) Vygodskii, Y. S.; Lozinskaya, E. I.; Shaplov, A. S.; Lyssenko, K. A.; Antipin, M. Y.; Urman, Y. G. Implementation of ionic liquids as activating media for polycondensation processes. *Polymer* **2004**, *45*, 5031-5045.
- (168) Strehmel, V.; Laschewsky, A.; Wetzel, H.; Görnitz, E. Free radical polymerization of n-butyl methacrylate in ionic liquids. *Macromolecules* **2006**, *39*, 923-930.
- (169) Ohno, H. Molten salt type polymer electrolytes. *Electrochimica Acta* **2001**, *46*, 1407-1411.
- (170) Susan, M. A. B. H.; Kaneko, T.; Noda, A.; Watanabe, M. Ion gels prepared by in situ radical polymerization of vinyl monomers in an ionic liquid and their characterization as polymer electrolytes. *Journal of the American Chemical Society* **2005**, *127*, 4976-4983.

-
- (171) Livi, S.; Duchet-Rumeau, J.; Gérard, J. F. Nanostructuration of ionic liquids in fluorinated matrix: Influence on the mechanical properties. *Polymer* **2011**, *52*, 1523-1531.
- (172) Yang, J.; Pruvost, S.; Livi, S.; Duchet-Rumeau, J. Understanding of versatile and tunable nanostructuration of ionic liquids on fluorinated copolymer. *Macromolecules* **2015**, *48*, 4581-4590.
- (173) Swatloski, R. P.; Holbrey, J. D.; Spear, S. K.; Rogers, R. D. Ionic liquids for the dissolution and regeneration of cellulose. in *ECS Proceedings Conference* **2002**, *19*, 155-164.
- (174) Hameed, N.; Bavishi, J.; Parameswaranpillai, J.; Salim, N.; Joseph, J.; Madras, G.; Fox, B. Thermally flexible epoxy/cellulose blends mediated by an ionic liquid. *RSC Advances* **2015**, *5*, 52832-52836.
- (175) Lins, L. C.; Livi, S.; Duchet-Rumeau, J.; Gérard, J. F. Phosphonium ionic liquids as new compatibilizing agents of biopolymer blends composed of poly (butylene-adipate-co-terephthalate)/poly (lactic acid)(PBAT/PLA). *RSC advances* **2015**, *5*, 59082-59092.
- (176) Yousfi, M.; Livi, S.; Duchet-Rumeau, J. Ionic liquids: A new way for the compatibilization of thermoplastic blends. *Chemical Engineering Journal* **2014**, *255*, 513-524.
- (177) Park, K.; Ha, J. U.; Xanthos, M. Ionic liquids as plasticizers/lubricants for polylactic acid. *Polymer Engineering & Science* **2010**, *50*, 1105-1110.
- (178) Rahman, M.; Brazel, C. S. Ionic liquids: New generation stable plasticizers for poly (vinyl chloride). *Polymer Degradation and Stability* **2006**, *91*, 3371-3382.
- (179) Livi, S.; Duchet-Rumeau, J.; Gérard, J. F. Supercritical CO₂-ionic liquid mixtures for modification of organoclays. *Journal of Colloid and Interface Science* **2011**, *353*, 225-230.
- (180) Livi, S.; Dufour, C.; Gaumont, A. C.; Levillain, J.; Pham, T. N. Influence of the structure of the onium iodide salts on the properties of modified montmorillonite. *Journal of Applied Polymer Science* **2013**, *127*, 4015-4026.
- (181) Mąka, H.; Spychaj, T.; Zenker, M. High performance epoxy composites cured with ionic liquids. *Journal of Industrial and Engineering Chemistry* **2015**, *31*, 192-198.
- (182) Silva, A. A.; Livi, S.; Netto, D. B.; Soares, B. G.; Duchet, J.; Gérard, J. F. New epoxy systems based on ionic liquid. *Polymer* **2013**, *54*, 2123-2129.

-
- (183) Matsumoto, K.; Endo, T. Synthesis of ion conductive networked polymers based on an ionic liquid epoxide having a quaternary ammonium salt structure. *Macromolecules* **2009**, *42*, 4580-4584.
- (184) Matsumoto, K.; Endo, T. Design and synthesis of ionic-conductive epoxy-based networked polymers. *Reactive and Functional Polymers* **2013**, *73*, 278-282.
- (185) Ly Nguyen, T. K.; Obadia, M. M.; Serghei, A.; Livi, S.; Duchet-Rumeau, J.; Drockenmuller, E. 1, 2, 3-triazolium-based epoxy-amine networks: Ion-conducting polymer electrolytes. *Macromolecular Rapid Communications* **2016**, *37*, 1168-1174.
- (186) McDanel, W. M.; Cowan, M. G.; Barton, J. A.; Gin, D. L.; Noble, R. D. Effect of monomer structure on curing behavior, CO₂ solubility, and gas permeability of ionic liquid-based epoxy-amine resins and ion-gels. *Industrial & Engineering Chemistry Research* **2015**, *54*, 4396-4406.
- (187) Livi, S.; Chardin, C.; Lins, L. C.; Halawani, N.; Pruvost, S.; Duchet-Rumeau, J.; Gérard, J. F.; Baudoux, J. From Ionic Liquid Epoxy Monomer to Tunable Epoxy-Amine Network: Reaction Mechanism and Final Properties. *ACS Sustainable Chemistry & Engineering* **2019**, *7*, 3602-3613.
- (188) Soares, B. G.; Livi, S.; Duchet-Rumeau, J.; Gerard, J. F. Synthesis and characterization of epoxy/MCDEA networks modified with imidazolium-based ionic liquids. *Macromolecular Materials and Engineering* **2011**, *296*, 826-834.
- (189) Soares, B. G.; Silva, A. A.; Pereira, J.; Livi, S. Preparation of epoxy/Jeffamine networks modified with phosphonium based ionic liquids. *Macromolecular Materials and Engineering* **2015**, *300*, 312-319.
- (190) Soares, B. G.; Livi, S.; Duchet-Rumeau, J.; Gerard, J. F. Preparation of epoxy/MCDEA networks modified with ionic liquids. *Polymer* **2012**, *53*, 60-66.
- (191) Soares, B. G.; Silva, A. A.; Livi, S.; Duchet-Rumeau, J.; Gerard, J. F. New epoxy/Jeffamine networks modified with ionic liquids. *Journal of Applied Polymer Science* **2014**, *131*, 39834 (1-6).
- (192) Leclère, M.; Livi, S.; Maréchal, M.; Picard, L.; Duchet-Rumeau, J. The properties of new epoxy networks swollen with ionic liquids. *RSC Advances* **2016**, *6*, 56193-56204.

-
- (193) Sanes, J.; Carrión, F.; Bermúdez, M. Effect of the addition of room temperature ionic liquid and ZnO nanoparticles on the wear and scratch resistance of epoxy resin. *Wear* **2010**, 268, 1295-1302.
- (194) Saurín, N.; Sanes, J.; Carrión, F.; Bermúdez, M. Self-healing of abrasion damage on epoxy resin controlled by ionic liquid. *RSC Advances* **2016**, 6, 37258-37264.
- (195) Maka, H.; Spychaj, T.; Pilawka, R. Epoxy resin/ionic liquid systems: the influence of imidazolium cation size and anion type on reactivity and thermomechanical properties. *Industrial & Engineering Chemistry Research* **2012**, 51, 5197-5206.
- (196) Rahmathullah, M. A. M.; Jeyarajasingam, A.; Merritt, B.; VanLandingham, M.; McKnight, S. H.; Palmese, G. R. Room temperature ionic liquids as thermally latent initiators for polymerization of epoxy resins. *Macromolecules* **2009**, 42, 3219-3221.
- (197) Kowalczyk, K.; Spychaj, T. Ionic liquids as convenient latent hardeners of epoxy resins. *Polimery* **2003**, 48, 833-835.
- (198) Livi, S.; Silva, A. A.; Thimont, Y.; Nguyen, T. K. L.; Soares, B. G.; Gérard, J. F.; Duchet-Rumeau, J. Nanostructured thermosets from ionic liquid building block-epoxy prepolymer mixtures. *RSC Advances* **2014**, 4, 28099-28106.
- (199) Mąka, H.; Spychaj, T.; Pilawka, R. Epoxy resin/phosphonium ionic liquid/carbon nanofiller systems: Chemorheology and properties. *Express Polymer Letters* **2014**, 8, 723-732.
- (200) Maka, H.; Spychaj, T. Epoxy resin crosslinked with conventional and deep eutectic ionic liquids. *Polimery* **2012**, 57, 456-462.
- (201) Mąka, H.; Spychaj, T.; Kowalczyk, K. Imidazolium and deep eutectic ionic liquids as epoxy resin crosslinkers and graphite nanoplatelets dispersants. *Journal of Applied Polymer Science* **2014**, 131, 40401 (1-7).
- (202) Handy, S. T.; Okello, M. The 2-position of imidazolium ionic liquids: Substitution and exchange. *The Journal of Organic Chemistry* **2005**, 70, 1915-1918.
- (203) Throckmorton, J. A.; Watters, A. L.; Geng, X.; Palmese, G. R. Room temperature ionic liquids for epoxy nanocomposite synthesis: Direct dispersion and cure. *Composites Science and Technology* **2013**, 86, 38-44.

-
- (204) Hu, J.; Yang, Q.; Yang, L.; Zhang, Z.; Su, B.; Bao, Z.; Ren, Q.; Xing, H.; Dai, S. Confining noble metal (Pd, Au, Pt) nanoparticles in surfactant ionic liquids: Active non-mercury catalyss for hydrochlorination of acetylene. *ACS Catalysis* **2015**, *5*, 6724-6731.
- (205) Liu, Y.; Qiao, L.; Xiang, Y.; Guo, R. Adsorption behavior of low-concentration imidazolium-based ionic liquid surfactant on silica nanoparticles. *Langmuir* **2016**, *32*, 2582-2590.
- (206) Gholami, H.; Arab, H.; Mokhtarifar, M.; Maghrebi, M.; Baniadam, M. The effect of choline-based ionic liquid on CNTs' arrangement in epoxy resin matrix. *Materials & Design* **2016**, *91*, 180-185.
- (207) Guo, B.; Wan, J.; Lei, Y.; Jia, D. Curing behaviour of epoxy resin/graphite composites containing ionic liquid. *Journal of Physics D: Applied Physics* **2009**, *42*, 145307.
- (208) Hou, L.; Liu, Y. Morphology and thermal/mechanical properties of alkyl-imidazolium-treated rectorite/epoxy nanocomposites. *Journal of Applied Polymer Science* **2012**, *126*, 1572-1579.
- (209) Li, W.; Hou, L.; Zhou, Q.; Yan, L.; Loo, L. S. Curing behavior and rheology properties of alkyl-imidazolium-treated rectorite/epoxy nanocomposites. *Polymer Engineering & Science* **2013**, *53*, 2470-2477.
- (210) Donato, R. K.; Matějka, L.; Schrekker, H. S.; Pleštil, J.; Jigounov, A.; Brus, J.; Šlouf, M. The multifunctional role of ionic liquids in the formation of epoxy-silica nanocomposites. *Journal of Materials Chemistry* **2011**, *21*, 13801-13810.
- (211) Donato, R. K.; Donato, K. Z.; Schrekker, H. S.; Matějka, L. Tunable reinforcement of epoxy-silica nanocomposites with ionic liquids. *Journal of Materials Chemistry* **2012**, *22*, 9939-9948.
- (212) Chabane, H.; Livi, S.; Benes, H.; Ladavière, C.; Ecorchard, P.; Duchet-Rumeau, J.; Gérard, J. F. Polyhedral oligomeric silsesquioxane-supported ionic liquid for designing nanostructured hybrid organic-inorganic networks. *European Polymer Journal* **2019**, *114*, 332-337.
- (213) Čolović, M.; Jerman, I.; Gaberšček, M.; Orel, B. POSS[®] based ionic liquid as an electrolyte for hybrid electrochromic devices. *Solar Energy Materials and Solar Cells* **2011**, *95*, 3472-3481.

-
- (214) Fu, J.; Lu, Q.; Shang, D.; Chen, L.; Jiang, Y.; Xu, Y.; Yin, J.; Dong, X.; Deng, W.; Yuan, S. A novel room temperature POSS[®] ionic liquid-based solid polymer electrolyte. *Journal of Materials Science* **2018**, *53*, 8420-8435.
- (215) Lv, K.; Zhang, W.; Zhang, L.; Wang, Z. S. POSS[®]-based electrolyte for efficient solid-state dye-sensitized solar cells at sub-zero temperatures. *ACS Applied Materials & Interfaces* **2016**, *8*, 5343-5350.
- (216) Shang, D.; Fu, J.; Lu, Q.; Chen, L.; Yin, J.; Dong, X.; Xu, Y.; Jia, R.; Yuan, S.; Chen, Y. A novel polyhedral oligomeric silsesquioxane based ionic liquids (POSS[®]-ILs) polymer electrolytes for lithium ion batteries. *Solid State Ionics* **2018**, *319*, 247-255.
- (217) Tanaka, K.; Ishiguro, F.; Chujo, Y. POSS[®] ionic liquid. *Journal of the American Chemical Society* **2010**, *132*, 17649-17651.
- (218) Yang, G.; Chanthad, C.; Oh, H.; Ayhan, I. A.; Wang, Q. Organic-inorganic hybrid electrolytes from ionic liquid-functionalized octasilsesquioxane for lithium metal batteries. *Journal of Materials Chemistry A* **2017**, *5*, 18012-18019.
- (219) Yang, G.; Fan, B.; Liu, F.; Yao, F.; Wang, Q. Ion Pair Integrated Organic-Inorganic Hybrid Electrolyte Network for Solid-State Lithium Ion Batteries. *Energy Technology* **2018**, *6*, 2319-2325.

Chapter II:

Synthesis of Modified Ionic Liquid POSSs[®] and Study of Their Dispersions in an Epoxy-amine Matrix

ABSTRACT: In this work, different polyhedral oligomeric silsesquioxane-supported mono or difunctional imidazolium ionic liquids have been successfully synthesized and used as organic-inorganic hybrid nano-objects in order to design nanostructured epoxy-amine networks. In fact, two partially condensed POSS[®] and POSS[®]-NH₂ covalently grafted with an ionic liquid-functionalized silane and ionic liquid functionalized epoxy monomer (ILM) were synthesized. The thermal properties of the ionic liquid (IL)-modified POSS[®] have highlighted a significant enhancement of the thermal stability (400 vs 300 °C) and an important decrease of their melting temperature. Then, these hybrid organic-inorganic nano-objects (5 wt. %) have been incorporated into a conventional epoxy prepolymer (diglycidyl ether of bisphenol A) which was copolymerized with the isophorone diamine in order to prepare nanostructured networks. An excellent dispersion of the mono IL-functionalized POSS[®] was obtained in the networks, characterized by the formation of spherical or ellipsoidal inorganic-rich phases with nanoscale size (from 10 to 80 nm). On the other hand, the difunctionalized IL-g-POSS[®] induced a multi-scale morphology composed of POSS[®]-rich particle with sizes of 40 to 80 nm and co-continuous phases.

Graphical abstract of the chapter

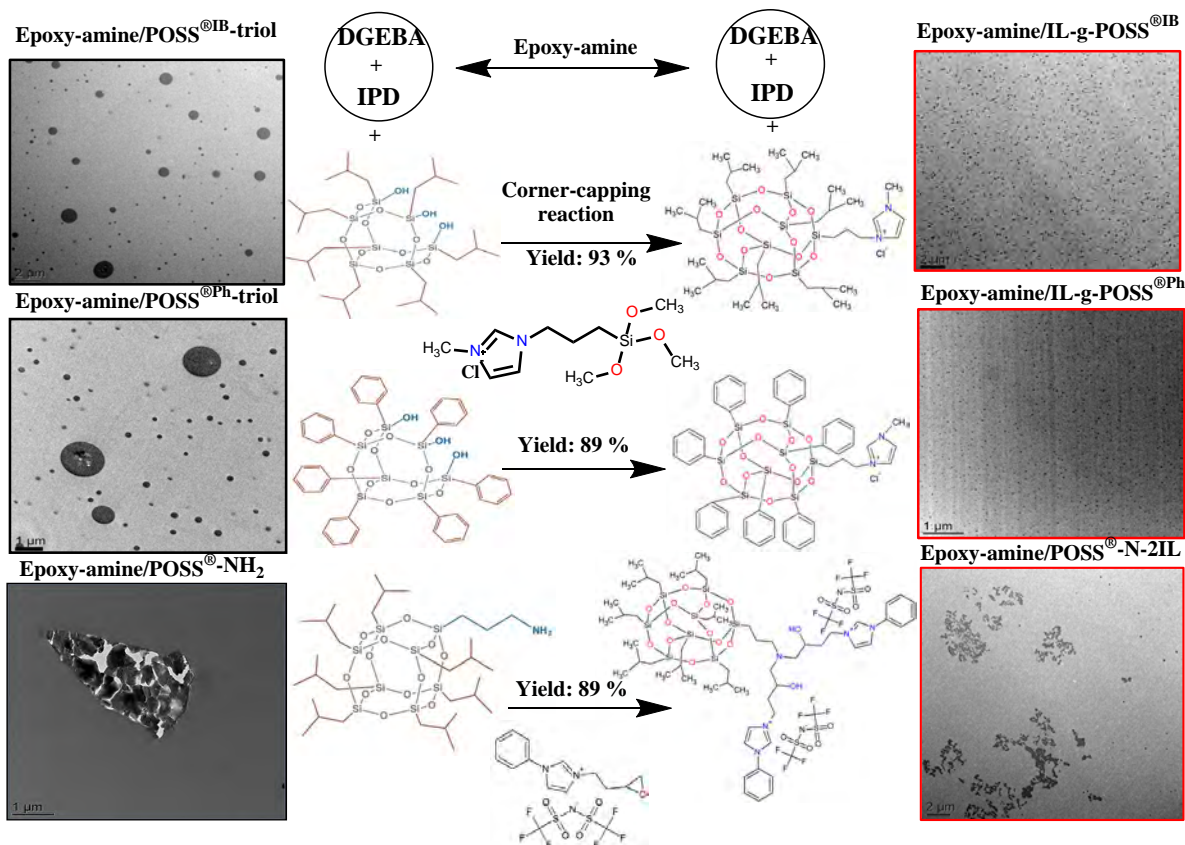


Table of contents

II.1. Introduction	94
II.2. Experimental	96
II.2.1. Materials	96
II.2.2. Synthesis of materials	96
II.2.2.1. Synthesis of the silylated imidazolium ionic liquid (Si-g-Im-Cl)	96
II.2.2.2. Synthesis of monofunctional ionic liquid monomer (ILM)	96
II.2.2.3. Synthesis of imidazolium ionic liquid grafted-POSS [®]	99
a. Monofunctional imidazolium ionic liquid grafted-POSS [®]	99
b. Difunctional ionic liquid grafted-POSS [®]	100
II.2.3. Epoxy network preparation	100
II.3. Results and discussion	102
II.3.1. Synthesis and characterization of imidazolium ionic liquid grafted-POSS [®]	102
II.3.1.1. Monofunctional imidazolium ionic liquid grafted-POSS [®]	102
a. Synthesis of IL-g-POSS [®]	102
b. Thermal characterization of the IL-g-POSS [®]	108
II.3.1.2. Difunctional imidazolium ionic liquid grafted-POSS [®]	111
a. Synthesis of POSS [®] -N-2IL	111
b. Thermal characterization of the POSS [®] -N-2IL	113
II.3.2. Morphology and glass transition of hybrid O/I networks containing IL-g-POSS [®] or POSS [®] -N-2IL	114
a. Morphology of hybrid O/I networks containing IL-g-POSS [®]	114
b. Morphology of hybrid O/I networks containing POSS [®] -N-2IL	117
c. Glass transition of hybrid O/I networks containing IL-g-POSS [®] or POSS [®] -N-2IL	118
II.4. Conclusion of chapter II	120
Supporting Information of chapter II	121
Reference of chapter II	126

II.1. Introduction

In materials science, the ability to create and design new polymer-based materials with unprecedented improvements in their final properties is a crucial challenge. Nanoscale materials often exhibit physical and chemical properties that are dramatically different from their neat counterparts. During the last two decades, polymer nanocomposites were designed from the introduction of nanofillers (*e.g.*, nanoparticles, nanoplatelets, nanotubes) in order to develop high performance coatings, reinforced polymers and barrier films. The design of functional nanomaterials requires the control of the diffusion and structuration at different scales, *i.e.* from the individual nanoscale objects to micrometer scale ^{1,2}. As consequence, tailoring structures and morphologies at various length scales is the key challenge to propre advanced functionalities ³.

Polyhedral oligomeric silsesquioxanes (POSS[®]) are well-known to be used as nanobuilding blocks for achieving such functional nanomaterials ^{4,5}. They could be considered as organic-inorganic hybrid nano-objects according to their cage structure having different geometries and symmetries (about 1 to 3 nm in size) ⁶. As a general feature, the molecular structure of these compounds consists of silicon atoms bonded to one and-a-half oxygen (“sesqui-”) and hydrocarbon (“-ane”) moieties, such as alkyl, aryl, or any of their derivatives (herein denoted as R), leading to an O/I hybrid nano-objects with a chemical composition (RSiO_{1.5})_n bond units, where n is equal to 6, 8, 10, and 12. These substituents can be simply alkyl groups or functionalized organic ligands. The most common POSS[®] are cubic-like with a general formula R₈Si₈O₁₂ ⁷. Besides fully condensed polyhedral silsesquioxanes, open-corner POSS[®] compounds, structurally related to cubic systems where a Si vertex is removed leaving incompletely condensed silanol groups (with general formula R₇Si₇O₉(OH)₃) offer the possibility to be corner-capped in order to design specific functionalities via the reaction with organosilane and hetero-element precursors. In particular, partially condensed POSS[®] can react with a large variety of trialkoxy- or trichloro-silanes (RSiY₃, Y = OEt, OMe, Cl, etc.) leading to fully condensed POSS[®] (T₈-POSS[®]) ⁸⁻¹⁰.

Nowadays, ionic liquids (ILs) offer a new route for designing polymer-based materials. Their unique characteristics, *i.e.* high thermal stability, low saturation vapor pressure, low flammability, dispersant capabilities, and high ionic conductivity make them very attractive ^{11,12}. Consequently, not only their molecular features but also their morphologies that they could form have a great potential to introduce advanced functions that are very different from those of conventional small

organic molecules^{13,14}. According to the literature, the main relevant studies have focused on the use of a multitude of combinations (cation/anion) of ILs or the design of ionic liquid monomer (ILM) backbones based on imidazolium¹⁵⁻¹⁷ units with polymerizable groups such as alkene, silane, alkyne and amine¹⁸ or bearing aromatic rings and epoxy functions¹⁹⁻²¹. Thus, they offer a real opportunity to design new smart and (multi)functional-dedicated polymer materials with enhanced properties such as thermal stability^{22,23}, mechanical performance^{24,25}, gas or water barrier properties²⁶, antibacterial^{27,28}, and self-healing properties²⁹. Recently, ILs based-POSS[®] have attracted much attention as versatile platforms for developing and designing multifunctional polymer nanomaterials. Incorporated directly in the polymer, bulk ILs can generate nanostructures from nano-phase separation phenomena³⁰⁻³³. These ionic salts are also ideal candidates for tailoring the surface properties of fillers and tuning the physico-chemical and mechanical properties of polymer composites³⁴. ILs can also participate in the polymerization process as they can initiate the opening of epoxy groups and lead to the formation of cross-linked polymers^{13,14,16,25}. The incorporation of IL-based POSS[®] in a variety of polymers brings significant modifications of their physical properties, such as the enhancement of thermal and mechanical stability, toughness improvement, and modifications in optical properties, dielectric constant, and solubility³⁵⁻³⁷. Such hybrid O/I nanomaterials could be used as a high-performance electrolyte, due to their unique internal nano structures which can enhance the ion transport capability³⁸. Monofunctional imidazolium-based POSS[®], which can self-assemble into lamellar nanostructures, is also used as an organic modifier for clays³⁹. Dapeng *et al.* outlined that by using of imidazolium-based POSS[®], solid electrolytes for lithium ion batteries could be developed with a high ionic conductivity and a broad electrochemical windows⁴⁰. Orel *et al.* also reported that POSS[®]-imidazolium/iodide ILs could be successfully used as electrolytes for fuel cells⁴¹.

The aim of this chapter is the molecular design of nanostructured epoxy-amine networks by using IL-grafted POSS[®] as organic-inorganic nano-building blocks. To the best of our knowledge, no works have been reported on nanostructured thermosets polymers using IL-grafted POSS[®] as nanobuilding blocks. In this work, we report first the use of two types of ILs based on imidazolium core combined with different counter anions and reactive groups in order to react with POSS[®]: silylated ionic liquid based on imidazolium cation, denoted **Si-g-Im-Cl**, and [2-(oxiran-2-yl) ethyl] -1-phenylimidazolium 1,1,1-trifluoro-N-[(trifluoromethyl) sulfonyl]

methanesulphonamide denoted **ILM**. The Si-g-Im-Cl will be grafted onto partially condensed POSSs[®]-triol by corner capping reaction. The ILM will be used to specifically react with POSS[®]-NH₂. Secondly, the synthesis and characterization of two monofunctionalized imidazolium ionic liquid based POSS[®], hereafter named IL-g-POSS^{®iB} and IL-g-POSS^{®Ph}, starting from a partially condensed POSS[®] named POSS^{®iB}-triol and POSS^{®Ph}-triol. A difunctionalized imidazolium ionic liquid (POSS[®]-N-2IL) will be made from POSS[®] bearing two amino-hydrogen functions (POSS[®]-NH₂). The molecular structures of the resulting IL-g-POSS[®] were determined using ¹H, ¹³C, and ²⁹Si NMR, as well as MALDI-TOF mass spectrometry. Its thermal properties were investigated by DSC and TGA. In the last part of this chapter, the preparation of epoxy nanomaterials based on POSS[®]-triols and IL-g-POSS[®] is described. The morphology and the glass transition temperature of the different obtained hybrid O/I nanomaterials are comparatively investigated based on transmission electron microscopy (TEM) and differential scanning calorimetry (DSC).

II.2. Experimental

II.2.1. Materials

All reagents were purchased from Sigma Aldrich, Alfa Aesar, or TCI and were used as received. Solvents were used in RPE grade without further purification. Anhydrous solvents were obtained from a Puresolv SPS400 apparatus developed by Innovative Technology Inc. A commercial epoxy prepolymer based on diglycidyl ether of bisphenol A (DGEBA) (Epon 828 trademark) was supplied from Hexion. The diamine hardener, *i.e.* isophorone diamine (IPD), provided by Aldrich, was used as co-monomer of the DGEBA epoxy monomer. The diamine was incorporated into the DGEBA in a stoichiometric ratio, *i.e.* amino hydrogen-to-epoxy, equal to 1. The two incompletely condensed POSS[®] bearing isobutyl or phenyl ligands, denoted POSS^{®iB}-triol and POSS^{®Ph}-triol, and the aminopropylisobutyl POSS[®] denoted POSS[®]-NH₂, were provided from Hybrid Plastics and used as received.

II.2.2. Synthesis

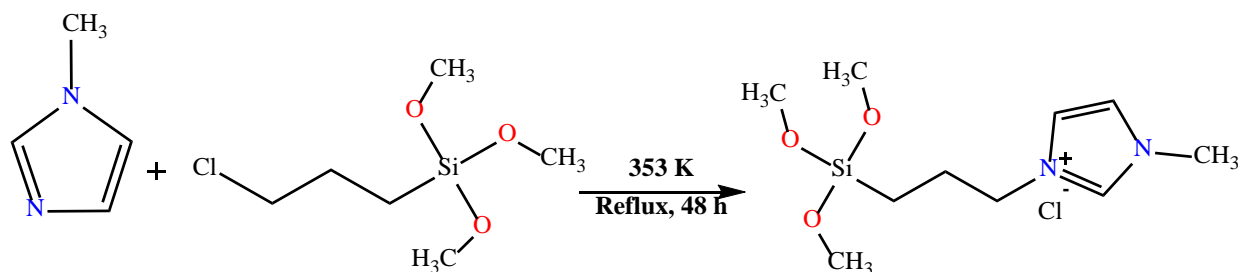
II.2.2.1. Synthesis of the silylated imidazolium ionic liquid (Si-g-Im-Cl)

The silylated imidazolium ionic liquid, denoted Si-g-Im-Cl, was synthesized in one step from 1-methylimidazole and 3-chloropropyltrimethoxysilane. Under argon atmosphere, 1 equiv. of 1-

methylimidazole (2.05 g; 25 mmol) and 1 equiv. of 3-chloropropyltrimethoxysilane (5.12 g; 25 mmol) were added to a 100 mL flask. The mixture was allowed to react at 80 °C for 48 h and its composition was regularly monitored by ^1H -NMR. A viscous oil was obtained. Then, the product was washed repeatedly with dried diethyl ether (5 x 10 mL) in order to remove unreacted species. The product was dried at 60 °C for 24 h. In this case, silylated imidazolium IL was obtained with an excellent yield (96 %) and its purity was confirmed by FTIR, $^1\text{H}/^{13}\text{C}$ -NMR, and HR-MS where the assignment of resonance peaks are reported below:

^1H NMR (400 MHz, CDCl_3 , 25 °C, ppm): 10.69 (1H, s, $-\text{NCHN}-$), 7.6 and 7.40 (2H, $-\text{NCHCHN}-$), 4.33 (2H, t, $-\text{CH}_2\text{N}-$), 4.14 (3H, s, $-\text{NCH}_3$), 3.51 (9H, s, $-\text{OCH}_3$), 2.02 (2H, m, $-\text{SiCH}_2\text{CH}_2\text{CH}_2\text{N}-$), 0.64 (2H, t, $-\text{SiCH}_2-$). **^{13}C NMR** (100 MHz, CDCl_3 , 25 °C, ppm): 6.01 - 7.34 (SiCH_2), 24.19 (SiCH_2CH_2), 36.59 (CH_2N), 50.74 (OCH_3), 51.75 (NCH_3), 122.03; 123.89 ($=\text{CN}$), 137.8 ($\text{N}-\text{C}=\text{N}$). **IR (neat, cm^{-1})**: 3139, 3047, 2944, 2840, 1636, 1570, 1459, 1251, 1153, 1068, 916, 880, 807, 773, 648, 623. **HR-MS m/z (ESI)**: calcd. for $\text{C}_{10}\text{H}_{21}\text{N}_2\text{O}_3\text{Si}$ $[\text{M}]^+$: 245.1316, found: 245.1316. **M** = 281 $\text{g}\cdot\text{mol}^{-1}$. **T_g** : -52 °C.

In addition, the formation of the following molecule was confirmed by MALDI-TOF mass spectrometry (see Figure S2.1 in the SI of chapter II). The general procedure for the synthesis of the imidazolium IL silane is given in Scheme II. 1:



Scheme II. 1: Reaction scheme for the synthesis of 1-(3-trimethoxysilylpropyl)-3-methylimidazolium chloride (Si-g-Im-Cl).

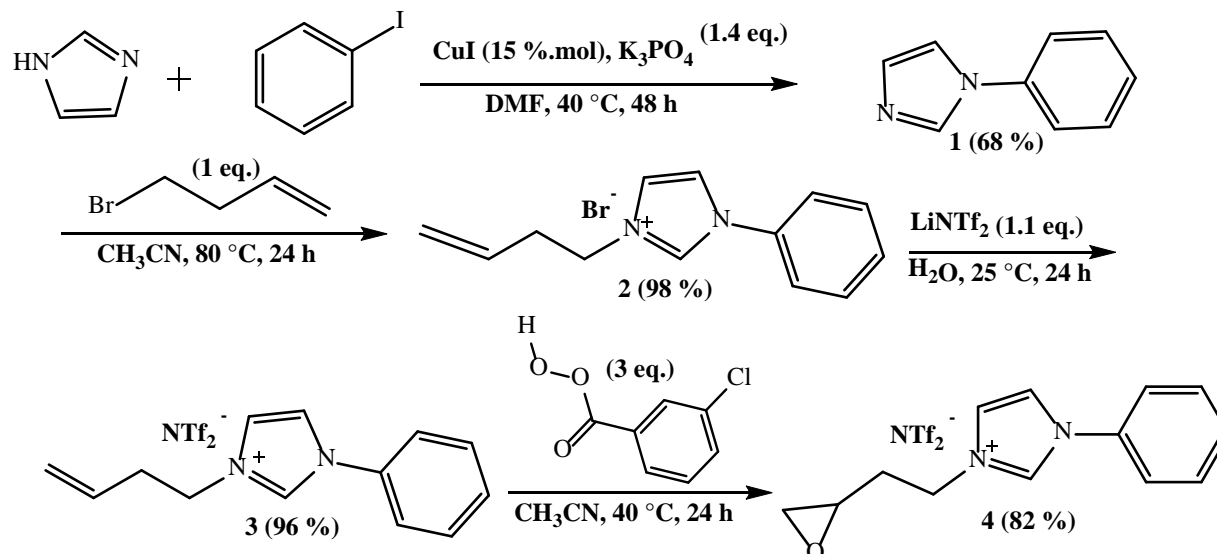
II.2.2.2. Synthesis of monofunctional ionic liquid monomer (ILM)

As previously described by our research group, the imidazolium salt **4** containing one epoxy function, denoted ILM, was synthesized in 4 steps from imidazole (Scheme II. 2). The first step (Ullman reaction) proceeded from a mixture of imidazole (1.0 equiv.), CuI (0.15 equiv.), and K_3PO_4 (1.4 equiv.) in DMF (45 mL) and iodobenzene (1 equiv.). The reaction mixture was stirred

at 40 °C for 48 h under argon, diluted with 40 mL of ethyl acetate, filtered through a plug of celite, and washed with ethyl acetate. The solution was then concentrated *under vacuum*. The crude product was purified over a silica gel column using ethyl acetate/cyclohexane (9/1). The product **1** was obtained as colorless oil (68 %). The compound **2** was prepared by nucleophilic substitution reaction between 1-phenylimidazole (1 equiv.) in CH₃CN and 4-bromo-butene (1 equiv.). The mixture was then refluxed at 80 °C and regularly monitored by ¹H-NMR. After complete conversion of the starting material (24 h), the mixture was cooled to room temperature. Evaporation of volatile compounds under reduced pressure afforded the imidazolium salt **2** as a yellow oil (98 %). Then, for the anionic exchange, LiNTf₂ (1.1 equiv.) was added to a solution of imidazolium bromide (1 equiv) in H₂O (100 mL). The solution was stirred at room temperature for 24 h and then extracted with dichloromethane. The organic layer was washed several times with water, dried over MgSO₄ and concentrated under reduced pressure to obtain the product **3** under the form of yellow oil (96 %). Finally, from a Prilezhaev reaction, the compound **4** was prepared from compound **3** (1.0 equiv.) in CH₃CN (200 mL) and 3-Chloroperbenzoic acid (mCPBA: 3.0 equiv.). The reaction mixture was stirred at 40 °C for 24 h (¹H-NMR monitoring). The crude product was evaporated under reduced pressure and washed with diethyl ether to extract the excess of mCPBA and 3-chlorobenzoic acid. The product **4** was obtained as a brown oil (18.10 g, 82 %) with high purity confirmed by FTIR, ¹H/¹³C/¹⁹F-NMR, and HR-MS (the assignment of resonance peaks are reported below) and DSC analysis:

¹H NMR (400 MHz, CDCl₃, 25 °C, ppm): 9.08 (s, 1H), 7.55-7.62 (m, 7H), 4.51 (t, J = 6.8 Hz, 2H), 3.04-3.08 (m, 1H), 2.75-2.77 (m, 1H), 2.40-2.53 (m, 2H), 1.87-1.96 (m, 1H). **¹³C NMR** (100 MHz, CDCl₃, 25 °C, ppm): 134.4, 134.3, 130.7, 130.6, 123.8, 123.5, 122.2, 121.6, 115.0 (q, JCF = 322.4 Hz), 49.2, 48.0, 46.3, 32.4. **¹⁹F NMR** (376 MHz, CDCl₃, 25 °C, ppm): -78.95. **IR (neat) cm⁻¹**: 3147, 3106, 1733, 1598, 1554, 1497, 1464, 1418, 1347, 1329, 1178, 1132, 1051, 917, 843, 789, 761, 739, 690, 652, 611, 599, 569. **HR-MS m/z (ESI)**: calcd. for C₁₃H₁₅N₂O [M]⁺: 215.1179, found: 215.1179 and Calcd. for C₂F₆NO₄S₂ [M]⁻: 279.9188, found: 279.9178. **M** = 495 g.mol⁻¹. **T_g**: -46 °C.

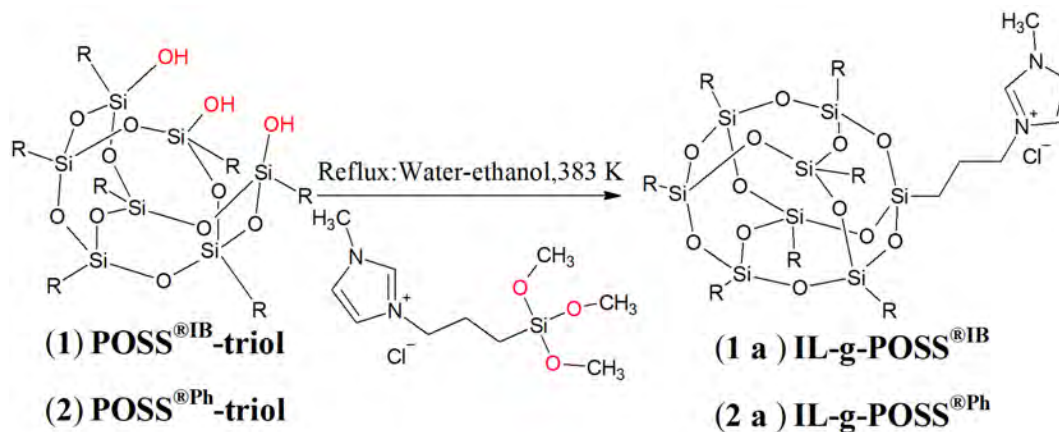
In addition, the formation of the **ILM** was confirmed by MALDI-TOF mass spectrometry (see Figure S2.2 in the SI of chapter II).



Scheme II. 2: Synthesis of the ILM.

II.2.2.3. Synthesis of imidazolium ionic liquid grafted-POSS[®]

a. Monofunctional imidazolium ionic liquid grafted-POSS[®]



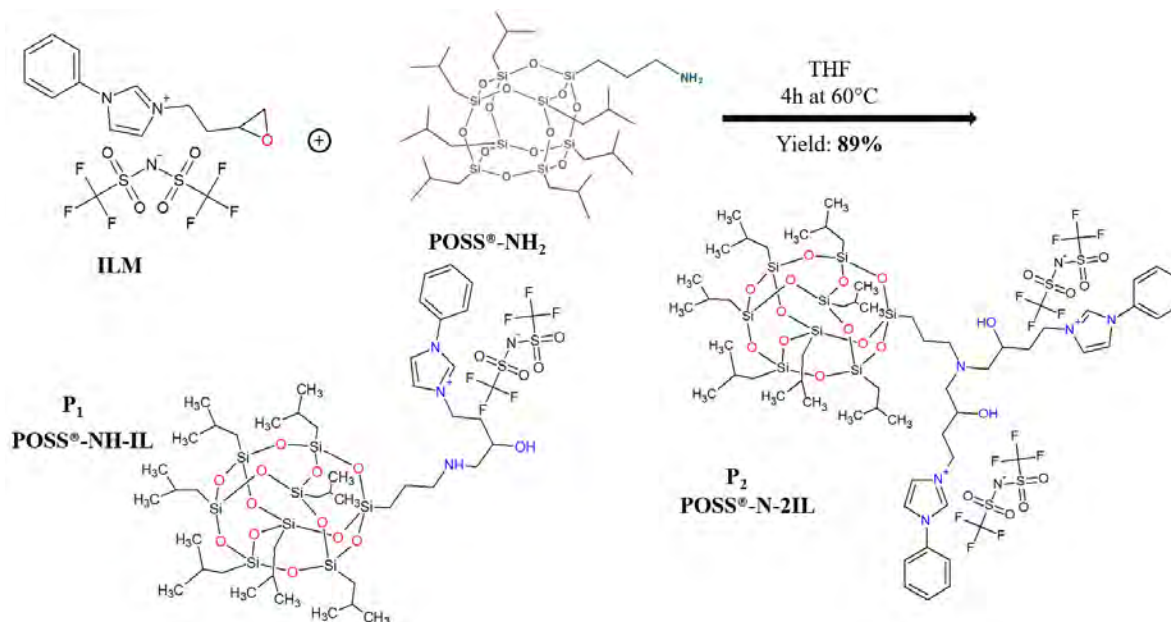
Scheme II. 3: Synthesis of mono-functionalized imidazolium ionic liquid grafted POSS[®] (IL-g-POSS[®]).

Under dry argon atmosphere, the imidazolium ionic liquid modified POSS[®] (IL-g-POSS[®]) was synthesized by a corner-capping reaction between POSS[®]-triol bearing isobutyl or phenyl ligands and Si-g-Im-Cl IL in two steps. First, in a 500 mL flask, 1 equiv. of Si-g-Im-Cl (0.71 g, 2.53 mmol) in water/ethanol (20 / 80, v:v) was added drop wise to 1 equiv. of POSS[®]-triol (2 g, 2.53 mmol) in water/ethanol under vigorous stirring at 40 °C for 6 h. Then, the mixture was heated to 110 °C and stirred overnight. The product was filtered and washed repeatedly with

ethanol (2 x 30 mL) in order to remove unreacted reagents. The solvent was removed under vacuum and the final product was dried at 80 °C for 48 h. In both cases, independently on the POSS[®] nature (1 vs 2), a white powder was obtained with very satisfactory yields, 93 % for IL-g-POSS^{®iB} (1a) and 89 % for IL-g-POSS^{®Ph} (2a). The follow up of the different reaction steps, the purity, and the chemical composition of the final product were investigated by ²⁹Si, ¹H and ¹³C-NMR (Figures II. 3, II. 5, II. 6 and II. 7) as well as by MALDI-TOF (Figure S2.3 in the SI of chapter II) mass spectroscopy. The general procedure for the synthesis of IL-g-POSS[®] is detailed in Scheme II. 3.

b. Difunctional ionic liquid grafted-POSS[®]

Under dry argon atmosphere, an amount of POSS[®]-NH₂ (1 equiv.) was dissolved in 50 ml of THF at 60 °C and stirred for 2 h. A mixture of ILM (2 equiv.) with 10 ml of THF was added dropwise into the above system, and the reaction was carried out at the same temperature, *i.e.* 60°C for 4 h. The product was washed with diethyl ether three times and dried under vacuum at 80 °C for 48 h to obtain a yellow powder (yield 89 %). The chemical structure of the final product was investigated by FTIR, ¹H and ¹³C-NMR (Figures II. 10, S2.4 and S2.5 in the SI of chapter II) as well as by MALDI-TOF mass spectroscopy (Figure II. 11). The general procedure for the synthesis of POSS[®]-N-2IL is detailed in Scheme II. 4.



Scheme II. 4: Synthesis of di-functionalized imidazolium ionic liquid grafted POSS[®] (POSS[®]-N-2IL).

II.2.3. Epoxy network preparation

To prepare epoxy-amine networks, epoxy prepolymer (DGEBA) and isophoronediamine (IPD) used as co-monomers were mixed under mechanical stirring with a stoichiometric ratio of amino hydrogen-to-epoxy equal to one. 5 wt. % of IL-g-POSS[®], either IL-g-POSS^{®iB}, IL-g-POSS^{®Ph}, or POSS[®]-N-2IL were considered for POSS[®]-modified epoxy networks. First, IPD and IL-modified POSS[®] (IL-g-POSS[®] or POSS[®]-N-2IL) were premixed at 60 °C until a homogeneous mixture is obtained before adding to the epoxy prepolymer. Then, the mixture was degassed and poured into molds. Finally, epoxy networks without and with IL modified POSS[®] were cured for 2 h at 140 °C and post-cured 8 h at 190 °C.

II.2.4. Characterization methods

Fourier Transform Infrared Spectroscopy (FT-IR) spectra were recorded on a Nicolet Magna 550 spectrometer at room temperature (25 °C) with Golden Gate (ATR). The spectra were collected in 32 scans with a spectral resolution of 4 cm⁻¹ from 4,000 to 525 cm⁻¹.

Single pulse ²⁹Si solid-state NMR measurements were performed using a JEOL 600 MHz NMR spectrometer operating at 14.1 T (119.2 MHz for ²⁹Si) equipped with 3.2 mm rotors and for a rotation of 5 kHz. The relaxation delay was 60 s for POSS^{®iB}-triol (or POSS^{®Ph}-triol) and 90 s for IL-g-POSS^{®iB} (or IL-g-POSS^{®Ph}).

¹H-, ¹³C-, ¹⁹F-NMR spectra were recorded on a Bruker Avance II 400 MHz spectrometer. Samples were dissolved in an appropriate deuterated solvent (CDCl₃ and DMSO) at 25 °C. The chemical shifts (δ) are expressed in ppm relative to internal tetramethylsilane for ¹H and ¹³C nuclei, and coupling constants are indicated in Hz. Abbreviations for signal coupling are as follows: s=singlet; d=doublet; dd=doublet of doublets; t=triplet; q=quartet; quin=quintet; m=multiplet; br=broad signal.

MALDI-TOF mass spectra were acquired using a Voyager-DE STR (Absciex, USA) and were obtained using a nitrogen laser emitting at 337 nm with 3 ns pulses. The instrument operated in the linear or reflectron modes. Ions were accelerated under a final potential of 20 kV. The positive ions were detected in all cases. Mass spectra are the sum of 300 shots and an external mass calibration of mass analyzer was used (mixture of peptides from SequazymeTM standards kit, Absciex, Life Sciences Holdings France SAS, France). The matrix used for all analyses is dithranol purchased from Sigma Aldrich used without further purification. The solid matrix and

samples were dissolved at 10 mg.mL⁻¹ in chloroform. A volume of 9 µL matrix solution was then mixed with 1 µL of sample solution. An aliquot of 0.5 µL of resulting solution was spotted onto the MALDI sample plate and air-dried at room temperature.

Differential scanning calorimetry (DSC) analysis was performed on a Q10 DSC calorimeter from TA instrument in a dynamic mode at heating rate of 10 K.min⁻¹ from 0 to 250 °C for the synthesized hybrid O/I nanoclusters and from -70 to 300 °C for the resulted hybrid O/I networks. The equipment was regularly calibrated using Indium standard. About 1 to 3 mg of samples were sealed in hermetic aluminum pans and heated under nitrogen atmosphere.

Thermogravimetric analyses (TGA) was achieved using a Q500 TGA from TA Instrument Inc. with a platinum pan. The samples (about 5 to 10 mg) were heated from ambient temperature up to 900 °C under 50 mL.min⁻¹ nitrogen flow at a heating rate of 20 K.min⁻¹.

Transmission electron microscopy (TEM) was performed at the Technical Center of Microstructures (University of Lyon) using a Phillips CM 120 microscope operating at 80 kV to characterize the dispersion of the inorganic-rich components in the resulting epoxy networks. 60 nm-thick ultrathin sections of samples were obtained using an ultramicrotome equipped with a diamond knife and then set on copper grids for observation.

II.3. Results and discussion

II.3.1. Synthesis and characterization of imidazolium ionic liquid grafted-POSS[®]

II.3.1.1. Monofunctional imidazolium ionic liquid grafted-POSS[®]

a. Synthesis of IL-g-POSS[®]

The occurrence of the corner-capping reaction of the open cage POSS[®] was monitored by FTIR spectroscopy. The IR spectrum of the IL-g-POSS[®] (1a, 2a) samples was compared to the profile of the reactant POSS[®]-triols (1, 2) (Figure II. 1 and II. 2). The compounds after and before the reaction show very similar IR features in the region of the stretching and bending modes of the ligands (isobutyl or phenyl) chains and the ν_{as} (Si-O-Si) of the cage framework (1,500 - 1,100 cm⁻¹). This is proof that the POSS[®] cage structure was essentially preserved from the chemical point of view during the corner-capping reaction. The most important differences between the two samples fall in the 3,500 - 3,000 cm⁻¹ and 1,000 - 500 cm⁻¹ IR ranges. In particular, the vibrational profile of samples 1 and 2 before the reaction shows two absorptions at 888 and 3,250

cm⁻¹ related to the stretching modes of Si-OH and O-H groups ⁴², respectively. These are almost completely absent in 1a or 2a after the reaction as the cage is completely condensed ⁴³. The presence of additional bands, *i.e.* at, 1,570, 928 cm⁻¹ (imidazolium ring mode) and the corresponding C-H stretching ring modes at 3,140 and 3,054 cm⁻¹ evidenced the presence of the imidazolium ring ⁴⁴. IR analyses have been confirmed by ¹H, ¹³C, ²⁹Si-NMR spectroscopy and MALDI-TOF mass spectrometry.

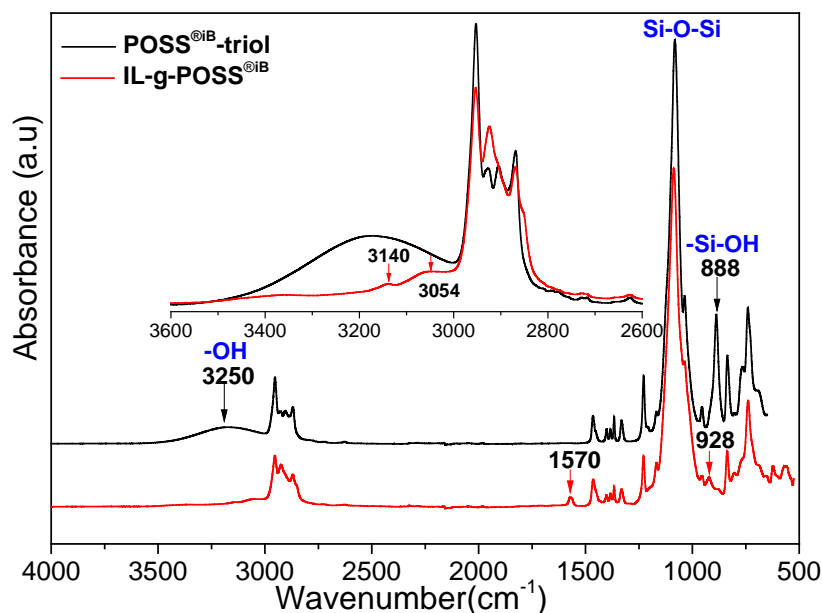


Figure II. 1: IR spectra of POSS^{iB}-triol (upper curve) and IL-g-POSS^{iB} (lower curve).

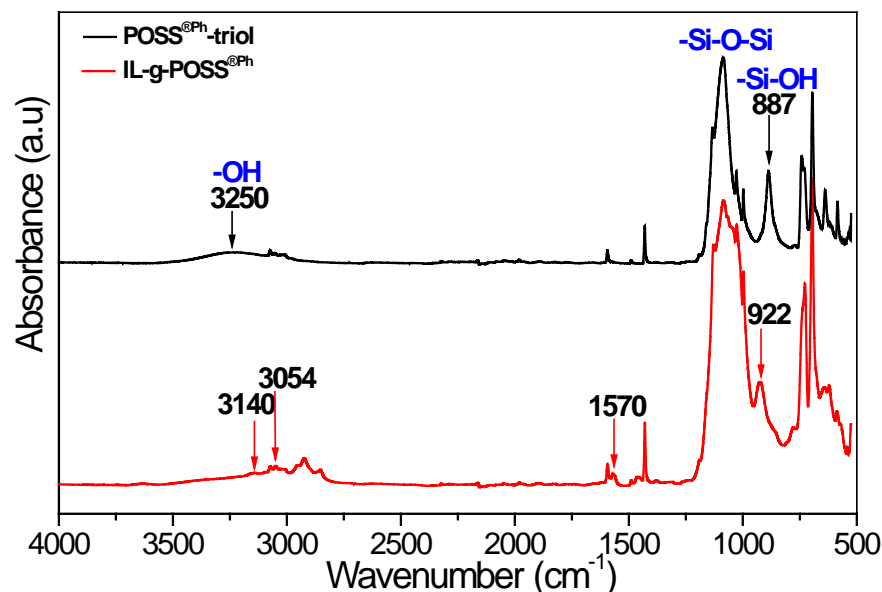


Figure II. 2: IR spectra of POSS^{Ph}-triol (upper curve) and IL-g-POSS^{Ph} (lower curve).

²⁹Si NMR is a powerful technique to determine the molecular structure and to evidence the functionalization of POSS[®] by the silylated-IL from the corner-capping reaction. Thus, ²⁹Si NMR spectra of unmodified- and modified-POSS[®] denoted POSS^{®iB}-triol, POSS^{®Ph}-triol, IL-g-POSS^{®iB}, and IL-g-POSS^{®Ph} are shown in Figure II. 3.

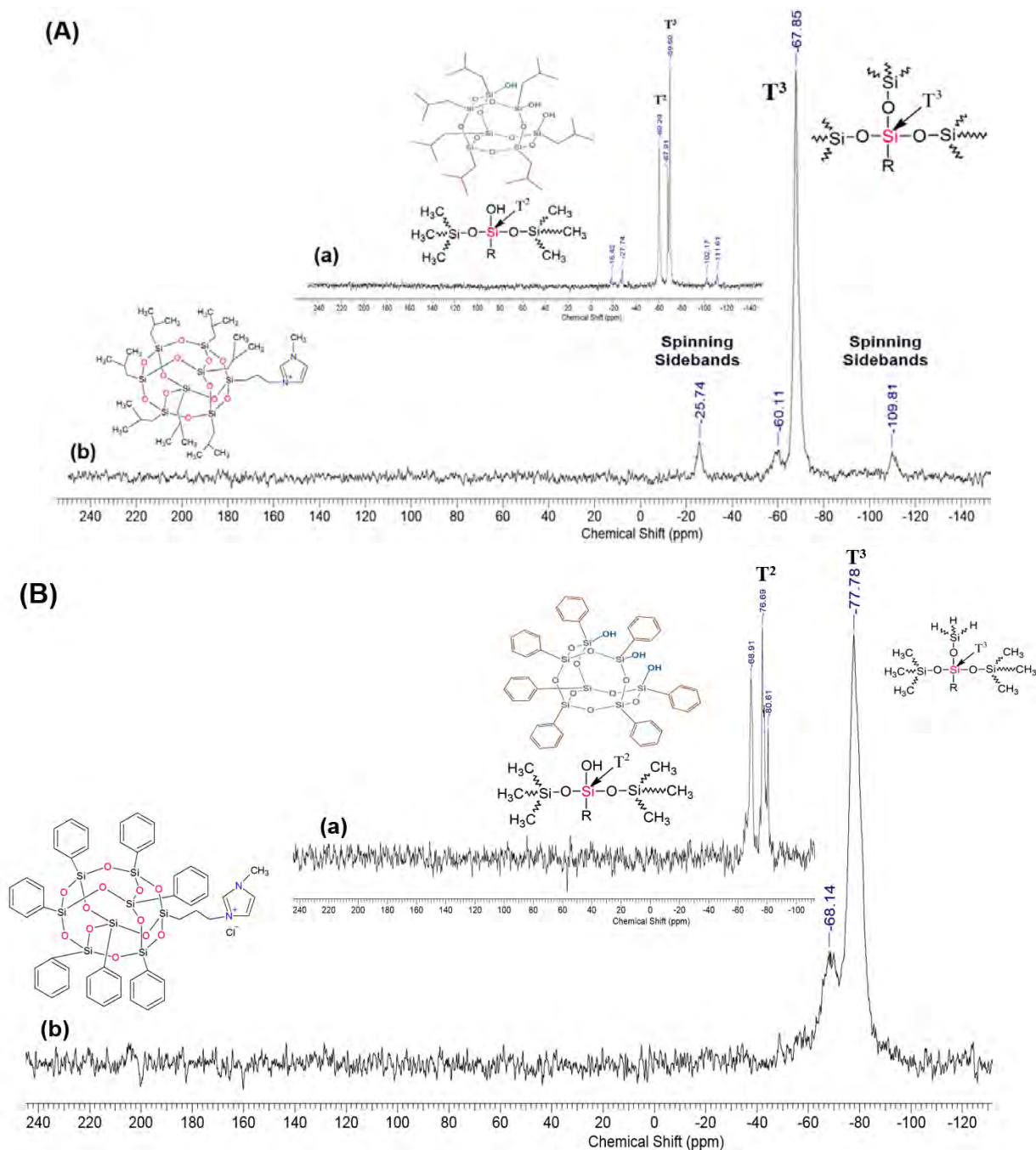


Figure II. 3: (A): ²⁹Si NMR spectra of a) POSS^{®iB}-triol and b) IL-g-POSS^{®iB}, (B): ²⁹Si NMR spectra of a) POSS^{®Ph}-triol, and b) IL-g-POSS^{®Ph} (solid state; 600 MHz).

In the case of unmodified heptaphenyl- and heptaisobutyl-POSS[®], denoted as POSS^{®iB}-triol and POSS^{®Ph}-triol, respectively, similar signals have been highlighted in the ²⁹Si NMR spectra. In fact, two main resonances are evidenced at -69 and at -77 ppm for POSS^{®Ph}-triol while POSS^{®iB}-triol displays also two signals at -60 and at -69 ppm. The first peak with an abundance of 43 % for POSS^{®Ph}-triol (calculated by the peak integration from -62 to -72 ppm) and with an abundance of 42 % for POSS^{®iB}-triol (calculated by the peak integration from -55 to -63 ppm) corresponds to Si atoms from silanol groups. The second peak with an abundance of 57 % (calculated by the peak integration from -74 to -84 ppm) for POSS^{®Ph}-triol and with an abundance of 58 % (calculated by the peak integration from -65 to -74 ppm) for POSS^{®iB}-triol is assigned to Si atoms of the POSS[®] cage (Si-O-Si). These results are in agreement with the literature ⁴⁵. Maven Ye *et al.* ⁴⁵ reported the same assignments for POSS^{®iB}-triol with two distinct signals at -59 and -69 ppm for the POSS^{®Ph}-triol and two Si resonance peaks at -69 and -78 ppm.

After the reaction with ionic liquid-functionalized silane (Si-g-Im-Cl), the resonances at -69 and -60 ppm which are attributed to the silanol species from the partially condensed POSS[®], significantly decrease in intensity (from 43 to 22 % for IL-g-POSS^{®Ph} and from 42 to 8 % for IL-g-POSS^{®iB}). The quantification of the two types of Si atoms for the POSS[®]-triol and IL-g-POSS[®] obtained by ²⁹Si-NMR are summarized in Table S2.1 in the SI of chapter II.

In order to confirm the chemical structure of the obtained IL-g-POSS[®], MALDI-TOF mass spectrometry was used and the different spectra are presented in Figure S2.3 (see the SI of chapter II). For the two synthesized IL-g-POSS[®] with phenyl or isobutyl ligands, two expected peaks are clearly identified on the positive MALDI-TOF mass spectra for both of them. The first peaks detected at m/z 939.2 and m/z 1079.2 were assigned to the cationic species $[R_7T_7(\text{Si-g-Im})]^+$. This value is in agreement with the mass of a monomeric structure in which the Si-g-Im⁺ ion is completely bound to the Si-O- units of the POSS[®] cage. Then, another peaks were observed on the spectrum at m/z 957.5 for IL-g-POSS^{®iB} and at m/z 1097.2 for IL-g-POSS^{®Ph} corresponding to POSS[®]-triol containing one IL function with two free Si-OH groups (open cage) as described in Figure II. 4. This structure of IL-g-POSS[®] obtained can be attributed to the steric hindrance of the isobutyl and phenyl substituents of the cage that limit the complete closure of all the POSS[®]-triol cages. No evidence of dimeric or multimeric species was detected for IL-g-POSS[®].

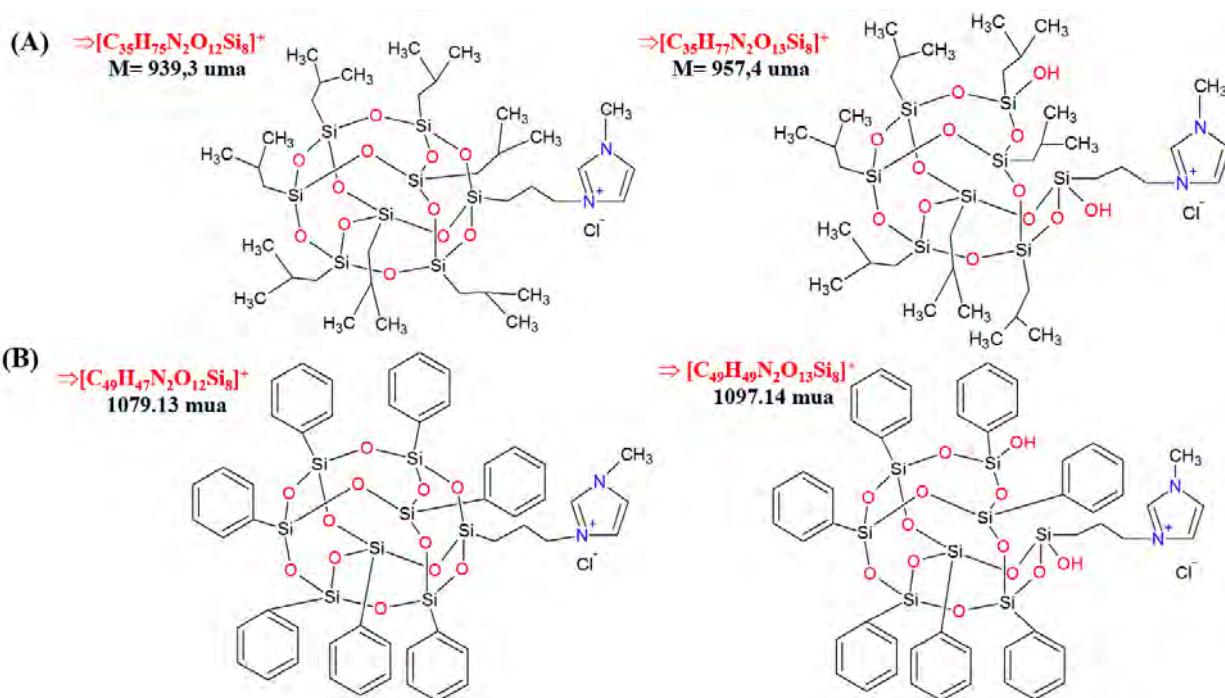


Figure II. 4: Chemical formula of IL-g-POSS[®] obtained by corner-capping reaction from A) POSS^{®iB}-triol with Si-g-Im-Cl and B) POSS^{®Ph}-triol with Si-g-Im-Cl.

¹H-NMR spectrum (Figure II. 5) of the IL-g-POSS^{®iB} provided the important information that dialkylation of imidazole had been conserved. This was inferred from the existence of seven new signals attributed: *i*) to the imidazolium ring protons at $\delta = 10.85$, 7.52, and 7.35 ppm; *ii*) to the double alkylation protons at $\delta = 4.14$ ppm corresponding to the N-CH₃ and *iii*) the chemical shifts at $\delta = 4.33$, 2.01, and 0.95 ppm to the silicopropyl Si-(CH₂)₃ chain. The disappearance of methoxy proton signal at around 3.51 ppm of the IL proves the completion of hydrosilylation reaction. The significant suppression of -OH proton signals at 7.14 ppm indicates the successful coupling of Si-g-Im-Cl to the POSS^{®iB}-triol and confirms the results obtained by ²⁹Si-NMR.

The ¹³C-NMR spectrum of IL-g-POSS^{®iB} in CDCl₃ (Figure II. 6) shows resonance peaks at 25.59, 23.72 - 24.06, and 22.34 ppm ascribed to -CH₃, -CH₂, and -CH carbon of the isobutyl groups bound to the siliceous framework⁴⁵. Additionally, seven major peaks centered at 8.86, 22.92, and 36.61 ppm corresponding to the Si-(CH₂)₃ silicopropyl chain, 51.85 ppm to N-CH₃, and the others at 120.86, 123.52, and 138.42 ppm to the imidazole ring with total disappearance of methoxy carbon peaks at 50.74 ppm of the IL, are evidence of a completed reaction.

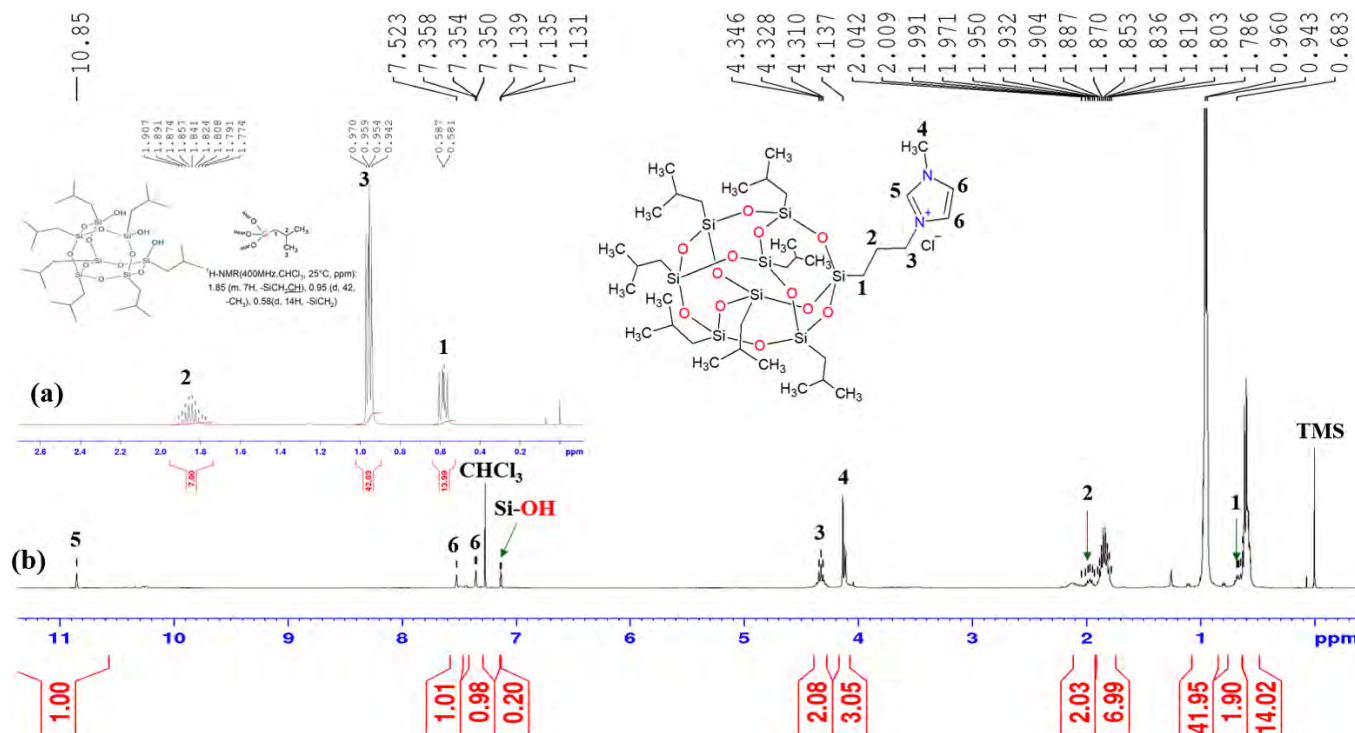


Figure II. 5: ¹H NMR spectra of a) POSS[®]iB-triol and b) IL-g-POSS[®]iB (CDCl₃; 400 MHz).

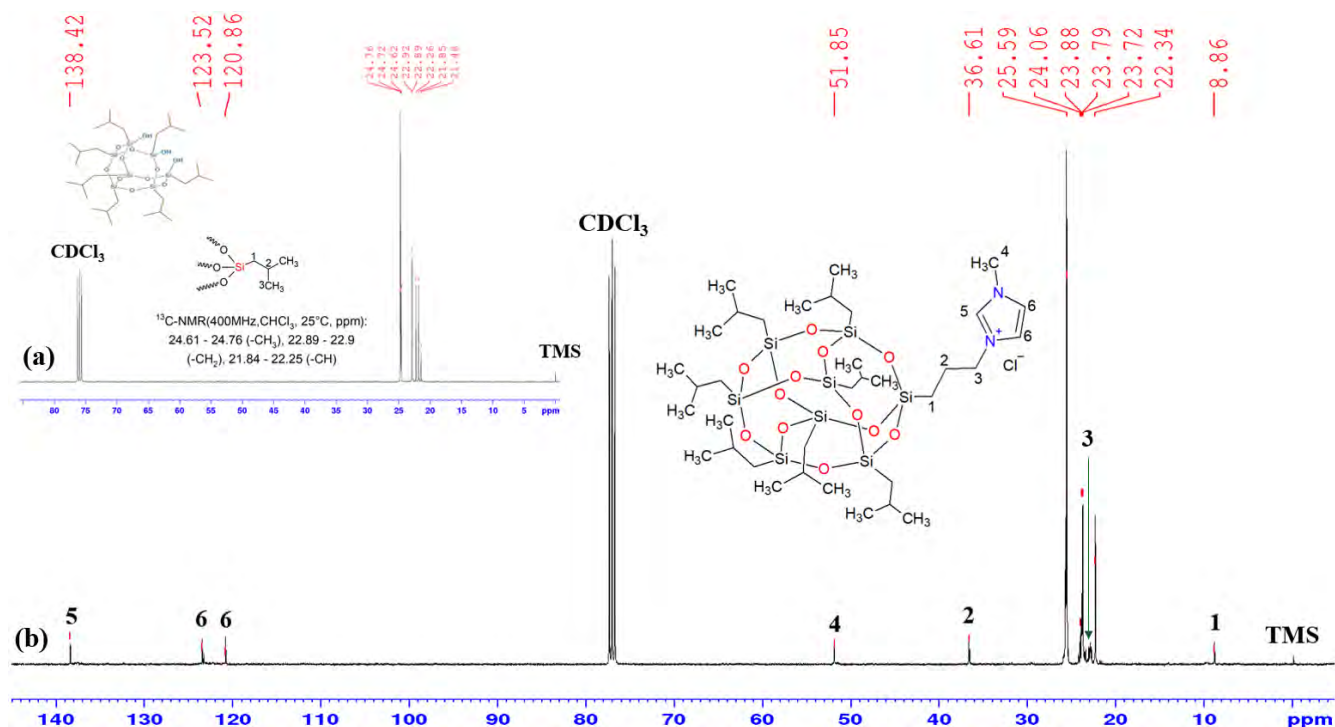


Figure II. 6: ¹³C NMR spectra of a) POSS[®]iB-triol and b) IL-g-POSS[®]iB (CDCl₃; 400 MHz).

On the ¹³C-NMR spectrum of IL-g-POSS^{®Ph} in DMSO-d₆ (Figure II. 7), peaks of the phenyl carbons groups appear at 133.79, 131.22, and 128.22, and six major additional peaks centered at 23.90, 36.22 ppm (corresponding to the Si-(CH₂)₃ silicopropyl chain), 51.1 ppm (corresponding to N-CH₃), and the others at 124.02 and 137.23 ppm (corresponding to the imidazole ring) with a total disappearance of methoxy carbon peaks at 50.74 ppm of the IL, are evidence of a completed reaction.

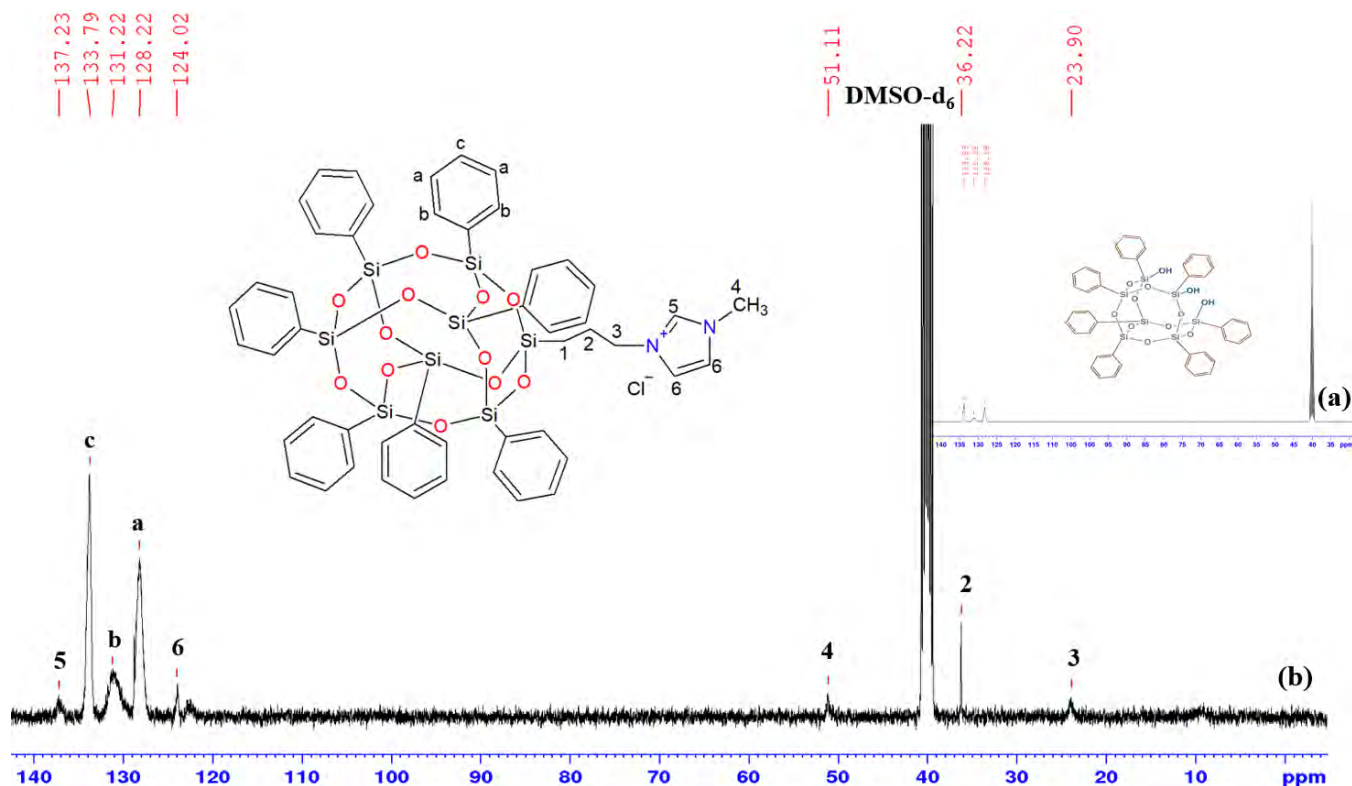


Figure II. 7: ¹³C NMR spectra of a) POSS^{®Ph}-triol and b) IL-g-POSS^{®Ph} (DMSO-d₆; 400 MHz).

b. Thermal characterization of the IL-g-POSS[®]

The DSC traces of POSS[®]-triols and IL-g-POSSs[®] are given in Figures II. 8 and S2.6, respectively. For both types, the DSC thermograms of IL-g-POSS[®] compounds indicate a similar thermal behavior as well as a broad crystallization region. For IL-g-POSS^{®iB}, a glass transition temperature, *T_g*, of 23 °C and a crystallization region centered at 89 °C followed by two smaller melting endotherms at 127 and 167 °C, are observed. In the case of IL-g-POSS^{®Ph}, a *T_g* at 14 °C, a crystallization exotherm centered at 67 °C and two melting endotherms at 134 and 168 °C, are also observed. The two melting points are due to the presence of the two types of crystalline

phases of the IL-g-POSS[®] (Figure II. 4). In the opposite, the POSS[®]-triols compounds display higher melting temperatures: 200 °C for POSS[®]iB-triol and 217, 230 °C for the POSS[®]Ph-triol. In the literature, Tanaka *et al.* have obtained the same behavior for synthesized imidazolium-type ionic liquid-grafted POSS[®] ⁴⁶. This author attributed the decrease of the melting temperature to the presence of large globular POSS[®] entities reducing the packing density and isolating the distal ion pairs. These results demonstrate that the addition of ionic liquid on the POSS[®] cores affects the mobility of chains and the free volume leading to the presence of a glass transition temperature as well as to the formation of regular structures in the liquid phase. In fact, the hydrophobic effects among the ion pair moieties of the IL-g-POSS[®] molecules lead to the formation of well-aligned and high-dimensional structures.

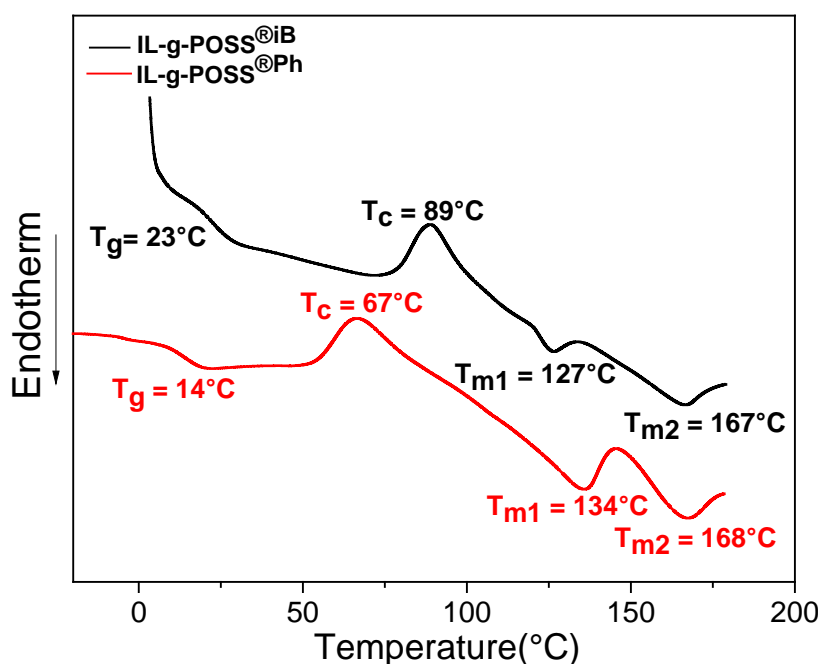


Figure II. 8: DSC traces for IL-g-POSS[®]: IL-g-POSS[®]iB and IL-g-POSS[®]Ph (heating rate: 10 K.min⁻¹).

Thermogravimetric analyses (TGA) were carried out to highlight the impact of ILs on the thermal behavior of the modified POSS[®]. Figure II. 9 show the evolution of the weight loss as a function of the temperature. The initial decomposition temperature, which can be also defined as the temperature corresponding to a mass loss of 5 wt. % (T_{d5%}), the temperature at the first maximum loss rate (T_{dmax1}), the temperature at the second maximum mass loss rate (T_{dmax2}), and the residue yield at 800 °C are reported in Table S2.2 (see SI of chapter II).

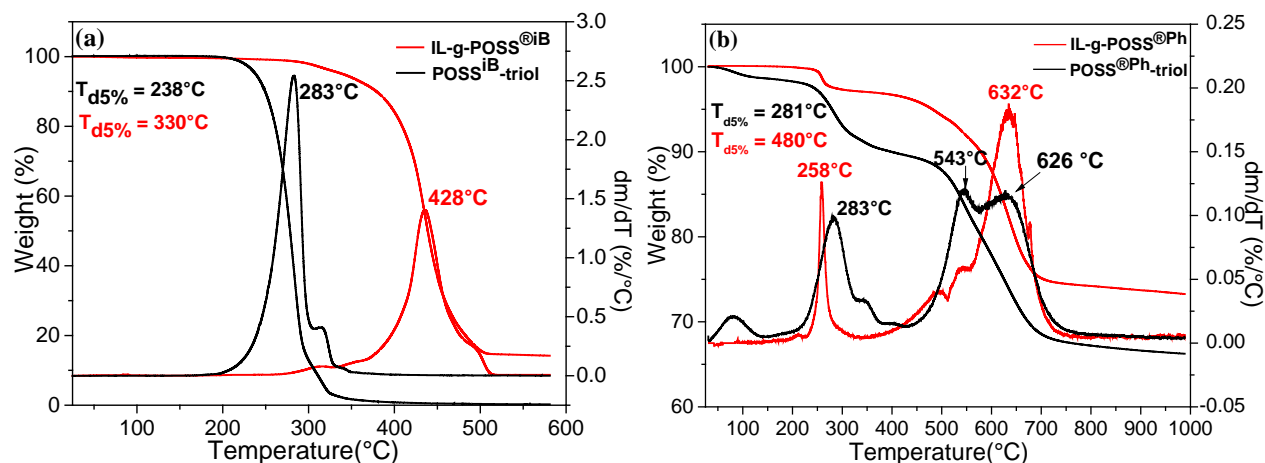


Figure II. 9: TGA traces for: a) IL-g-POSS[®]iB with POSS[®]iB-triol and b) IL-g-POSS[®]Ph with POSS[®]Ph-triol (heating rate: 10 K.min⁻¹; atmosphere: nitrogen flow).

In all cases, an excellent thermal stability was shown for unmodified and IL-modified POSS[®] with a thermal degradation starting at temperatures higher than 200 °C. The presence of the imidazolium IL in the POSS[®]-triol plays a key role on the thermal stability of IL-g-POSS[®]iB and IL-g-POSS[®]Ph. Indeed, a significant increase (100 K) of the decomposition temperatures ($T_{d5\%}$ and T_{dmax}) could be evidenced. These results confirm the stabilizing effect obtained by closing the silica core of the POSS[®]-triols using IL. In both cases, TGA traces of the two IL-g-POSS[®] display a two-step degradation process corresponding to water loss resulting from the hydroxyl crosslinking and the breakage of the POSS[®] structure⁴⁵. Based on the literature, the first decomposition step corresponds to the degradation of the alkyl chain of the imidazolium and to the water loss between 250 and 400 °C. The second degradation that takes place from 400 to 650 °C corresponds to the decomposition of alkyl chain contained in the POSS[®] core⁴⁷⁻⁴⁹. Moreover, the residue yields (73 %) for IL-g-POSS[®]Ph is higher than that of the IL-g-POSS[®]iB (12 %) due to the decomposition of substituted oligomeric silsesquioxane, which depends strongly on the nature of grafted organic groups. In general, POSS[®] with small aliphatic side chains sublime during heating in absence of oxygen and have relatively low residue yield. Larger aliphatic and aromatic substituents prevent sublimation, and polymerization of the POSS[®] cage may occur, that attributed to the entrapment of carbon in the structure, resulting in a larger amount of residue^{49,50}. A similar effect was observed by Jifang *et al.* who obtained increases of 100 to 200 K compared to their unmodified POSS[®]⁵¹. These results indicate that the connection of ILs onto POSS[®]-triol allow to prepare closed structures. These structures may increase the

stability of the system by limiting the thermal motion of the remote alkyl chains⁵². In summary, the supported ionic liquid-polyhedral oligomeric silsesquioxane (IL-g-POSS[®]) are thermally stable and can be used for the design of new advanced nanostructured epoxy-amine networks requiring high processing temperatures and open also new perspectives in the development of polymer materials with improved thermal resistance.

II.3.1.2. Difunctional imidazolium ionic liquid grafted-POSS[®]

a. Synthesis of POSS[®]-N-2IL

The reaction between amino groups of POSS[®]-NH₂ and epoxy groups of ILM can take place under mild conditions as we can see in Scheme II. 4. The FTIR spectra in Figure II. 10 of POSS[®]-NH₂ (black) and POSS[®]-N-2IL (red) show very similar IR features in the region of the stretching and bending modes of the ligands (isobutyl) chains and the ν_{as} (Si-O-Si) of the cage framework (1,500 - 1,100 cm⁻¹).

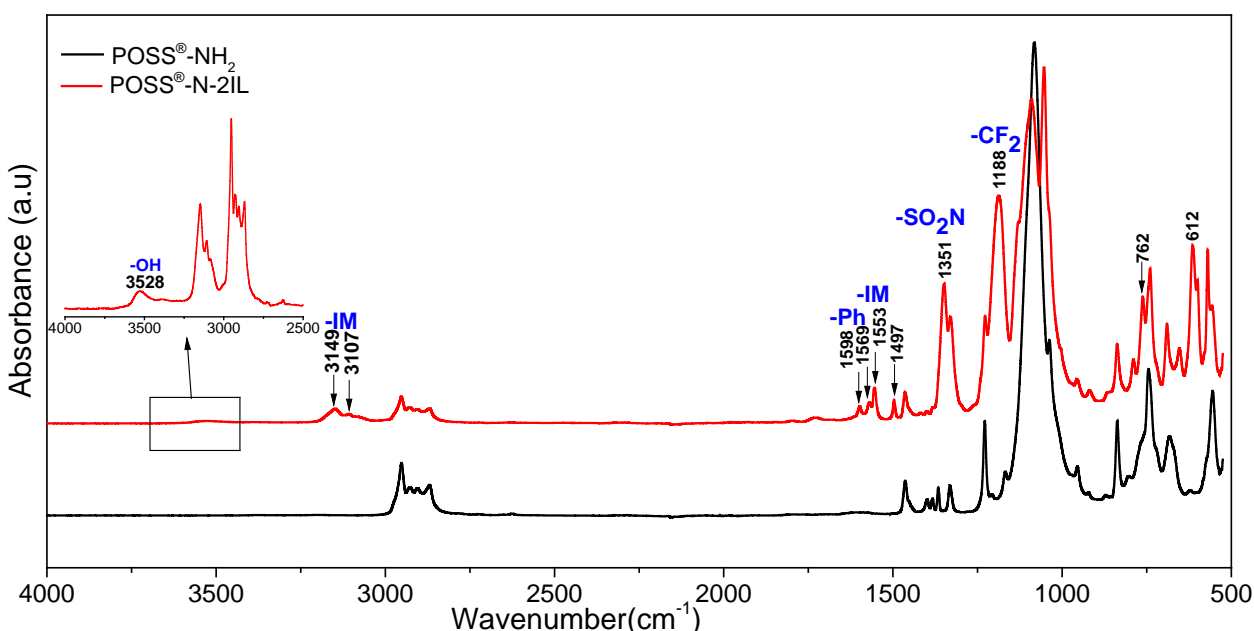


Figure II. 10: IR spectra of POSS[®]-NH₂ (black curve) and POSS[®]-N-2IL (red curve).

It is seen also that after the reaction, some new peaks appear for the POSS[®]-N-2IL. The newly emerged peak at 1,553 cm⁻¹ and the corresponding C-H stretching ring modes at 3,149 and 3,107 cm⁻¹ clearly confirmed the presence of the imidazolium ring⁴⁴. The two peaks between 1,351 and 1,188 cm⁻¹ suggest the presence of both sulfonamide (-SO₂-N) and trifluoromethyl (-CF₃) groups composing the bis(trifluoromethanesulfonyl)imide counter anion (NTf₂⁻)⁴⁴, and

the ones at 1,598 and 1,569 cm⁻¹ show the presence of the phenyl ring ⁴⁵ which is absent in POSS[®]-NH₂ spectra. The wide adsorption band of O-H (about 3,500 cm⁻¹) is obvious in POSS[®]-N-2IL. In addition, we have observed in our experiments that it is difficult for the reaction between the N-H bond in -NH₂ with ILM after the reaction between the first N-H bond and ILM which gave two types of structure (see Scheme II. 4). Probably it is due to the steric hindrance and the lower reactivity of the secondary amine compared with the primary amine. FTIR data have been supported by ¹H and ¹³C-NMR spectroscopy (Figures S2.4 and S2.5 in the SI of chapter II) and MALDI-TOF mass spectrometry (Figure II. 11).

In order to confirm the chemical structure of the POSS[®]-N-2IL obtained, MALDI-TOF mass spectrometry was used and the different spectra are presented in Figure II. 11. For the POSS[®]-N-2IL, the peaks detected at *m/z* 1,088.5 and at *m/z* 1,431.5 were assigned to the cationic species [R₇T₇ (ILM)]⁺ in agreement with the mass of a monomeric structure in which the [ILM]⁺ ion is reacted with N-H of the POSS[®]-NH₂ cage. Then, the peaks observed on the spectrum at *m/z* 1,303.6 and at *m/z* 1,585.5 corresponding to POSS[®]-NH₂ reacted with two ILM as described in Figure II. 11.

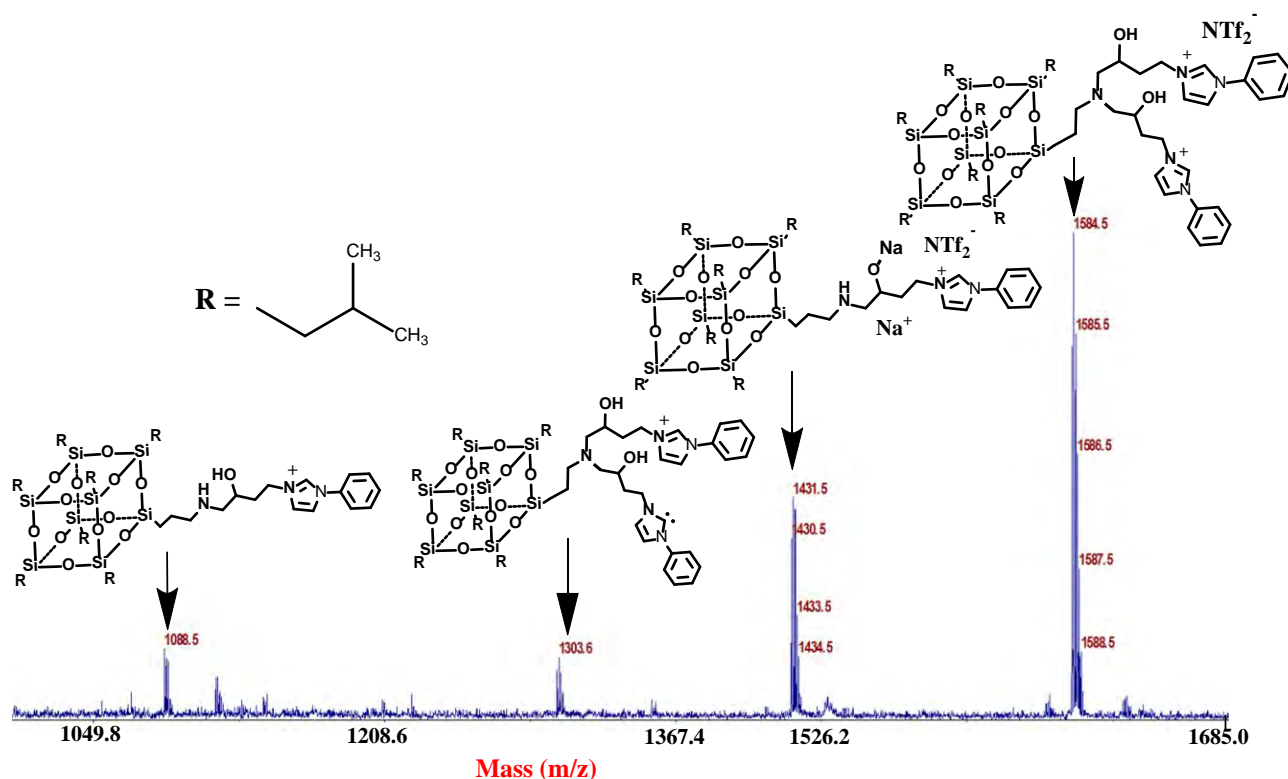


Figure II. 11: Positive MALDI-TOF mass spectra of POSS[®]-N-2IL (Dithranol matrix).

The ¹H and ¹³C-NMR spectrum of the POSS[®]-N-2IL compared with POSS[®]-NH₂ and ILM spectrum in CDCl₃ (see Figures S2.4 and S2.5 in the SI), shows the disappearance of peaks of the oxirane and aminopropylisobutyl groups with appearance of new peaks indicating the successful reaction and confirms the results obtained by FTIR and MALDI-TOF mass spectrometry.

b. Thermal characterization of the POSS[®]-N-2IL

POSS[®] are thermally stable compounds showing degradation above 300 °C^{37,53}. The melting temperature can be lowered or increased by the substitution of flexible or rigid structures attached to the cube corners, which prevents or allows close packing. In general, connecting the IL to POSS[®] can simultaneously lead to a lowering of the melting temperature and an enhancement of the thermal stability^{46,54}.

The DSC thermograms (Figure II. 12) of the as-received POSS[®]-NH₂ show a well-defined melting peak at 58 °C with a melting enthalpy of 21.37 J.g⁻¹ without the presence of glass transition temperature. A crystallization peak at 44 °C was also present on the cooling trace (Figure II. 12a). The functionalization of POSS[®]-NH₂ by ILM changes the thermograms with the appearance of a glass transition temperature at -34 °C combined with a decrease in the melting temperature (at 45 °C with a melting enthalpy of 11.75 J.g⁻¹) and a crystallization region (at 35 °C) (Figure II. 12b). These observations can be explained by the isolation of the side chains inducing by electrostatic repulsion, *i.e.* the POSS[®]-N-2IL does not have the same structure or distribution in the crystals compared to the initial POSS[®]-NH₂, resulting in the decrease of the enthalpy of melting and compensate for the entropy decrease^{46,54}.

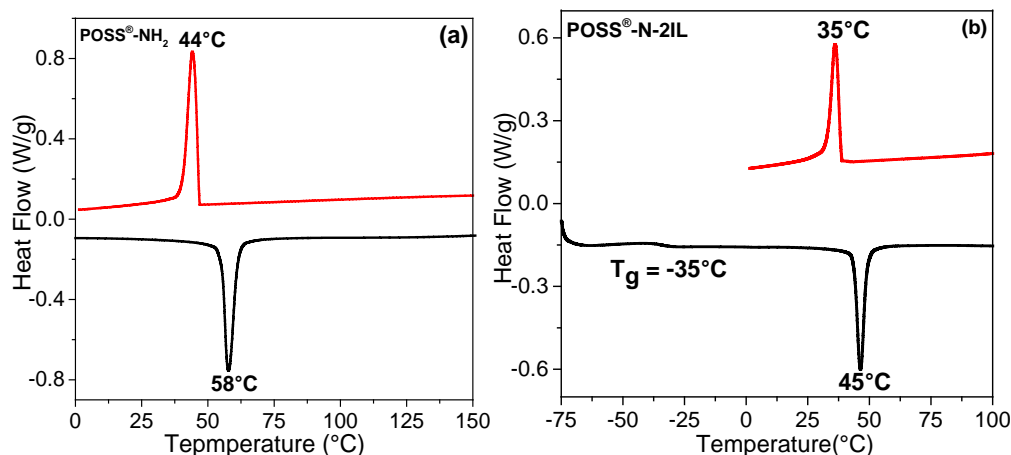


Figure II. 12: DSC traces for a) POSS[®]-NH₂ and b) POSS[®]-N-2IL (heating and cooling rate: 10 K.min⁻¹).

The thermal stability of the synthetic compounds was investigated by thermogravimetric analysis (TGA). Figure II. 13 shows the TGA and DTG profiles of the POSS[®]-N-2IL compared with the initial POSS[®]-NH₂ product. The values of the initial decomposition temperature ($T_{d5\%}$) and the temperature at the maximum rate of decomposition (T_{dmax}) are also reported. Two significant weight losses in the TGA trace of POSS[®]-N-2IL occur indicating two decomposition steps. This can be explained by the decomposition of the secondary and tertiary amines, and then by the intrinsic thermal stability of ILM (see structures in the Scheme II. 4). Indeed, the $T_{d5\%}$ value of POSS[®]-N-2IL was 20 K higher than that of POSS[®]-NH₂. This result clearly indicates that thermal stability is enhanced by the connection of ILM to POSS[®]-NH₂.

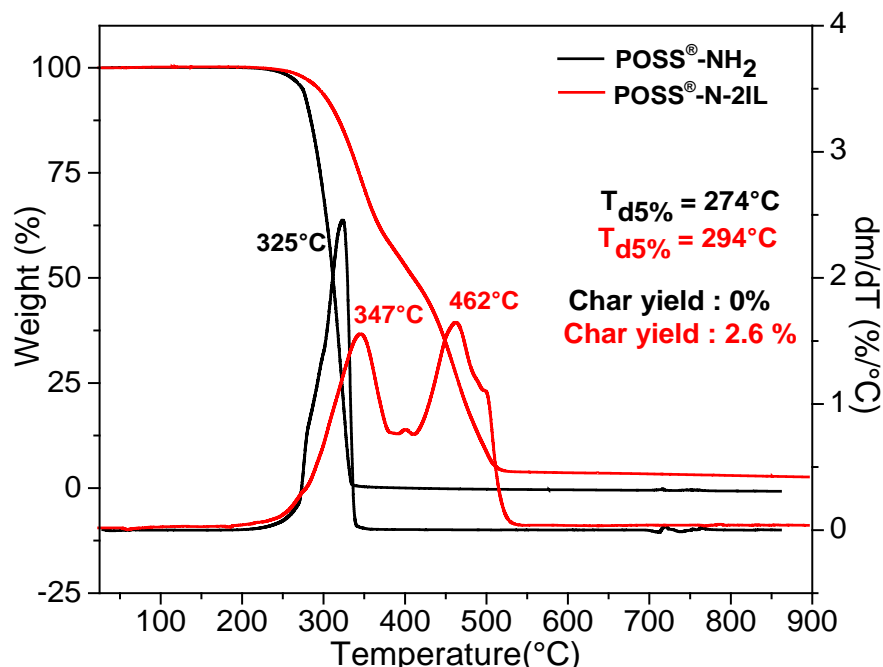


Figure II. 13: TGA and DTG traces for POSS[®]-N-2IL compared to the initial POSS[®]-NH₂ (heating rate: 10 K.min⁻¹; atmosphere: nitrogen flow).

II.3.2. Morphology and glass transition of hybrid O/I networks containing IL-g-POSS[®] or POSS[®]-N-2IL

POSS[®] described in the previous section were employed to obtain epoxy-amine hybrid O/I networks (see section II.2.3). The obtained hybrids were studied by transmission electronic microscopy to highlight the influence of the grafting of imidazolium IL on the dispersion of the POSS[®] nanoclusters. In addition, a preliminary study on the impact of the IL-g-POSS[®] nanoclusters on the glass transition of epoxy networks was conducted.

a. Morphology of hybrid O/I networks containing IL-g-POSS[®]

The morphologies obtained for initial and IL-grafted POSS[®]-modified epoxy-amine networks (cured) are displayed in Figures II. 14 and S2.7 (see SI of chapter II). In addition, size distribution analysis using Image J Software is reported in Figure II. 15.

In all cases, TEM micrographs confirmed a homogeneous distribution of the non-modified POSS[®] clusters in the epoxy matrix whatever the nature of the ligands (isobutyl or phenyl). Nevertheless, the hybrid networks based on POSS[®]-triol display a morphology characterized by a spherical or ellipsoidal shape POSS[®]-rich phase uniformly dispersed in the continuous epoxy matrix. The size of the POSS[®]-rich aggregates is from 100 to 1600 nm and from 30 to 280 nm for POSS[®]_{iB}-triol and POSS[®]_{Ph}-triol, respectively (see Figures II. 14 a and c).

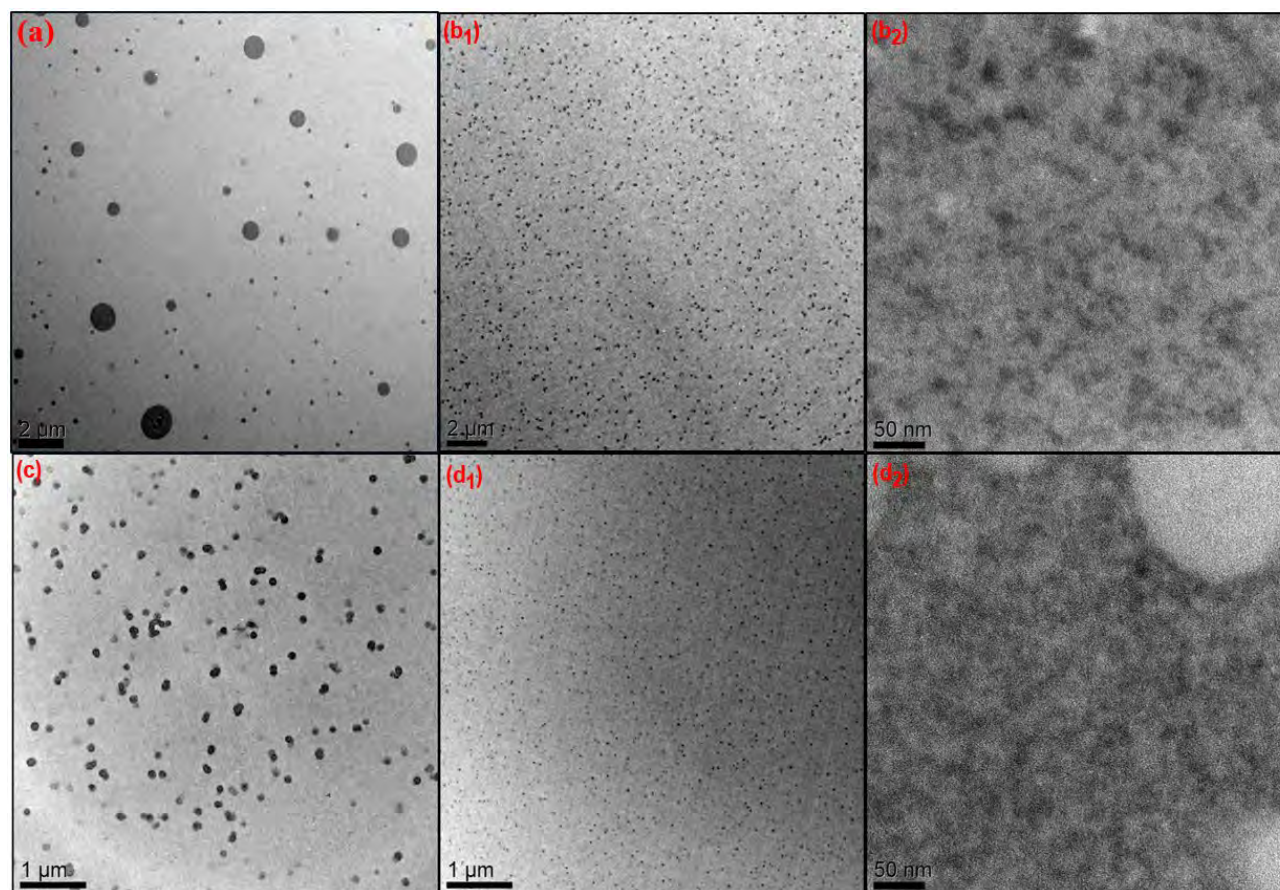


Figure II. 14: TEM image of the epoxy-amine networks with: a) POSS[®]_{iB}-triol, b): IL-g-POSS[®]_{iB} at different magnifications (b₁; b₂), c) POSS[®]_{Ph}-triol, and d): IL-g-POSS[®]_{Ph} at different magnifications (d₁; d₂).

For the epoxy networks containing 5 wt. % of IL-g-POSS[®], the TEM images show that the phase separation between epoxy network and POSS[®] occurred on the nanoscale. A spherical dispersed phase is composed of small assemblies generated from POSS[®]-POSS[®] interactions with an average diameter from 10 to 80 nm and from 20 to 50 nm for IL-g-POSS^{®iB} and IL-g-POSS^{®Ph}, respectively. The imidazolium IL grafted on POSS[®] leads to a better distribution of POSS[®] nanoclusters in the epoxy matrix and acts as an interfacial agent. This observation is in agreement with the results reported in the literature for similar systems based on nanofillers combined with ionic liquids⁵⁵⁻⁵⁷. Recently, similar results were obtained by Donato *et al.* who used ionic liquid-grafted silica (IL-silica) with different anions^{58,59}. Uniform and well-dispersed silica aggregates of about 30 nm were formed when less than 6.8 wt. % of IL-silica were introduced into the epoxy-amine network.

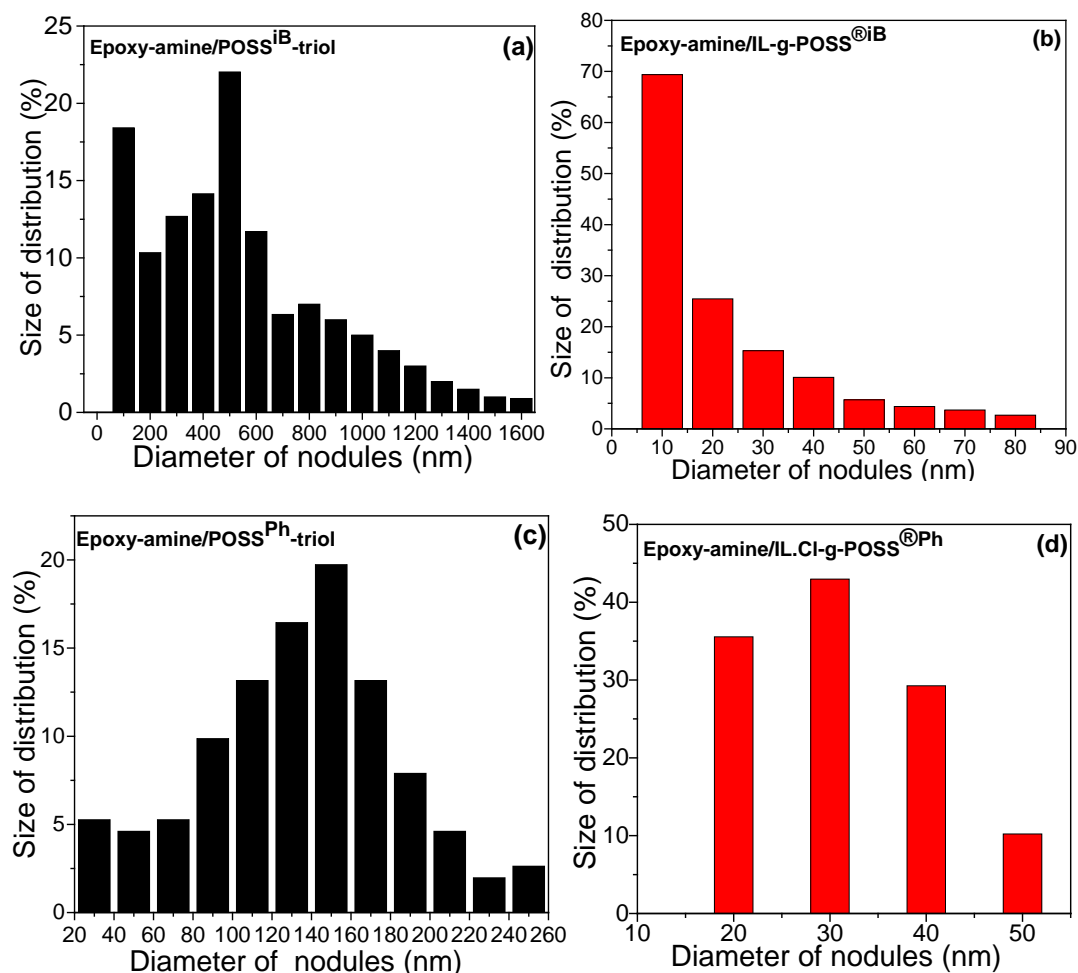


Figure II. 15: Size distribution of POSS[®]-rich dispersed phase in the epoxy matrix containing a) POSS^{®iB}-triol, b) IL-g-POSS^{®iB}, c) POSS^{®Ph}-triol, and d) IL-g-POSS^{®Ph}.

b. Morphology of hybrid O/I networks containing POSS[®]-N-2IL

Figures II. 16 and II. 17 show the TEM micrographs at different magnifications of the hybrid O/I epoxy-amine networks containing POSS[®]-NH₂ and POSS[®]-N-2IL, respectively. In these TEM images, the dark part corresponds to the POSS[®] aggregate and the bright continuous phase corresponds to the epoxy network as a consequence of reaction induced phase separation phenomena⁶⁰⁻⁶². In addition, the structure and size of the POSS[®]-rich phase are strongly influenced by the presence of ILM.

In Figure II. 16, the addition of 5 wt. % of POSS[®]-NH₂ clearly induces the formation of large non-uniform aggregates characterized by the presence of large rods with sizes from 3 to 6 μm. In addition, the topographic view shows some holes meaning that the POSS[®]-NH₂ clusters weakly interact with the epoxy network as shown in Figure II. 16 and could be removed easily. Similar results were obtained by Matějka *et al.*^{5,63} when they prepared DGEBA-D2000-POSS[®]Bu-NH₂ in one or two steps. These authors observed the formation of large clusters randomly dispersed in the matrix with sizes from 2 to 4 μm. The clusters and the auto-aggregation ability of the POSS[®] can be related with the fact that the amines in the chemical structure of POSS[®] are less reactive than the amines of the IPD hardener. This means that the DGEBA-IPD reaction occurs at a much faster rate than the DGEBA/POSS[®] reaction. Therefore, most POSS[®] clusters, are not bonded to the epoxy-amine network architectures but will segregate as POSS[®]-rich domains dispersed in the epoxy matrix, as seen in TEM images (Figure II. 16).

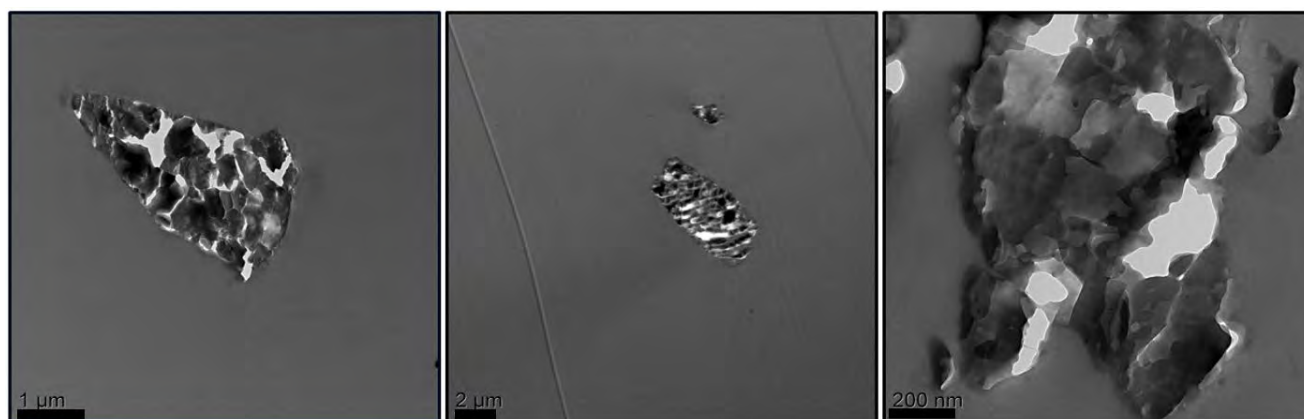


Figure II. 16: TEM images of the epoxy-amine networks containing POSS[®]-NH₂ at different magnifications.

The incorporation of the POSS[®]-N-2IL with the same amount (5 wt. %) in the epoxy networks (Figure II. 17) induces a multi-scale morphology composed of POSS[®]-rich particles and a co-continuous phase. In fact, IL-modified POSS[®] particle size was found to be significantly smaller and particles are apparently inhomogeneously dispersed in the matrix. These have an ellipsoidal or spherical shape with the larger diameters from 40 to 80 nm. Moreover, it can be observed that POSS[®]-N-2IL form non-connected aggregates as an island-in-the-sea. These two types of morphologies can be explained by the mixture of two types of O/I compounds, *i.e.* one with one ionic liquid function presenting one-hydroxyl group and one amino reactive group and the other with two ionic liquids and two hydroxyl reactive groups (Figure II. 4). In fact, two distinct reasons can be responsible for such a morphology. Firstly, ionic liquids can act as interfacial agents preventing the agglomeration of clusters by providing an electrostatic and steric ionic layer around nanoparticles^{64,65} below a given content⁶⁶ and secondly, according to the presence of the hydroxyl groups generated during the reaction of ILM with POSS[®]-NH₂ (Scheme II. 4) which can promote the reaction with residual amino groups⁶⁷.

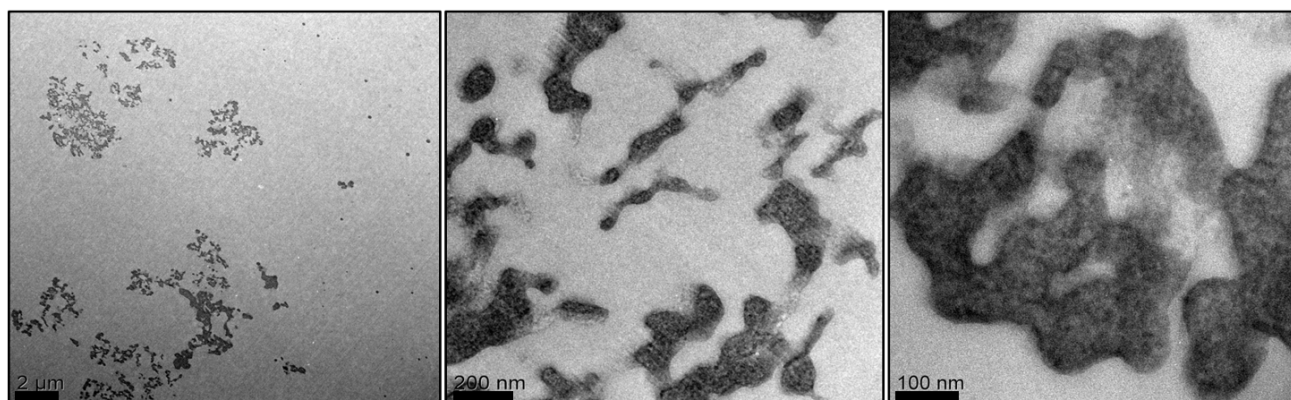


Figure II. 17: TEM images of the epoxy-amine networks containing POSS[®]-N-2IL at different magnifications.

c. Glass transition of hybrid O/I networks containing IL-g-POSS[®] or POSS[®]-N-2IL

The thermal behavior of the epoxy hybrid nanomaterials containing POSS[®] was investigated by DSC in order to determine the glass transition temperatures. The DSC thermograms of the resulting epoxy networks are presented in Figure II. 18. The presence of a single glass transition temperature is attributed to the epoxy matrix since the T_g of POSS[®]-rich phases cannot be detected due to their very poor mobility.

For the neat epoxy-amine network one glass transition temperature of 164 °C was obtained corresponding to the T_g values reported in the literature ^{68,69}. Then, the incorporation of POSS[®]-triols, denoted, POSS^{®iB}-triol, and POSS^{®Ph}-triol or POSS[®]-NH₂, displayed lower T_g s compared to the neat epoxy-amine network. In contrast, the epoxy nanomaterials containing IL-g-POSS[®] or POSS[®]-N-2IL kept a glass transition temperature close to the value of the neat epoxy-amine network. According to the literature, two competitive factors can affect the glass transition temperatures. Firstly, the restriction effect of POSS[®] cages on polymer chain motions must enhance the glass transition temperature. Secondly, the inclusion of the bulky POSS[®] cages could give rise to an increase in free volume of the system due to voluminous POSS[®] molecule, leading to a decrease of the T_g . As a consequence, T_g strongly depends on the nature of the interactions between POSS[®] cages and polymer chains (*e.g.*, functionalities of POSS[®], types of polymer matrices, and organic groups in POSS[®] vertexes, etc.). Thus, POSS[®] could act as a nanofiller or as a plasticizing agent. In fact, the POSS[®]-containing nanocomposites can display increased ⁷⁰⁻⁷² or decreased ^{73,74} T_g in comparison with the neat polymers. The behavior of glass transition of the epoxy nanomaterials based on POSS[®]-triols and IL modified POSSs[®] could be the comprehensive embodiment of the above two factors. These results imply that the presence of the IL ligand of different natures on the POSS[®] cages compensates the plasticizing effect of the POSS[®] cages keeping the glass transition close to the one of the neat system.

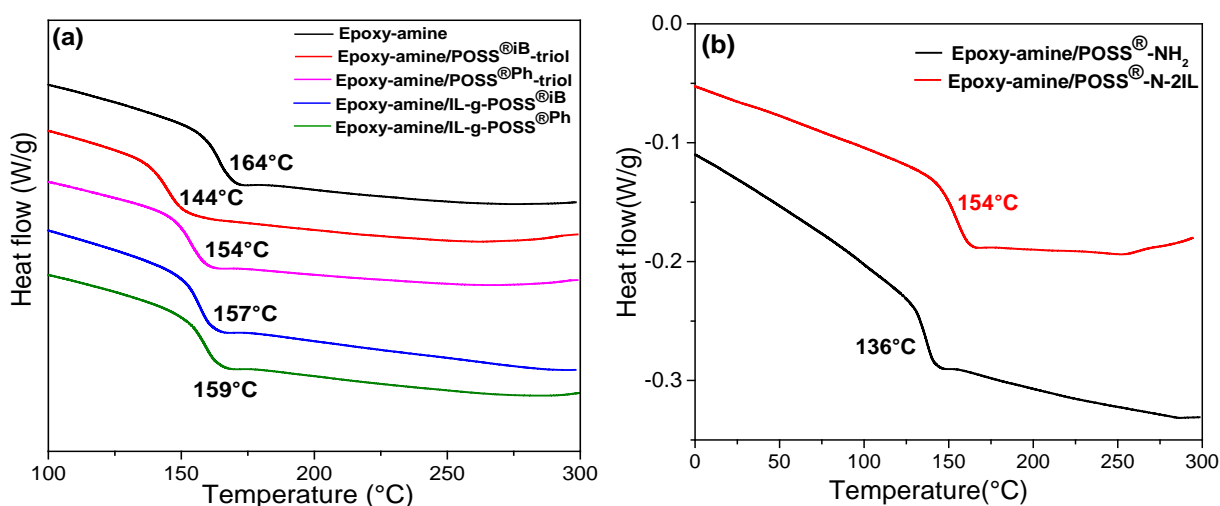


Figure II. 18: DSC curves of the epoxy-amine network and epoxy hybrid O/I nanomaterials containing a) POSS^{®iB}-triol, IL-g-POSS^{®iB}, POSS^{®Ph}-triol, IL-g-POSS^{®Ph}, and b) with POSS[®]-N-2IL and POSS[®]-NH₂ (heating rate: 10 K.min⁻¹).

II.4. Conclusion of chapter II

In this chapter, the molecular design of nanostructured epoxy-amine networks by using IL-grafted POSS[®] as organic-inorganic nano-building blocks was described for the first time. Firstly, two ionic liquids with different functions have been successfully synthesized with high yield and purity. Secondly, the synthesis and characterization of two mono-functionalized imidazolium ionic liquids based POSS[®] (IL-g-POSS^{®iB} and IL-g-POSS^{®Ph}), and a di-functionalized imidazolium ionic liquid (POSS[®]-N-2IL), were performed. IL-g-POSS[®] were obtained from a partially condensed POSS[®]-triol (POSS^{®iB}-triol and POSS^{®Ph}-triol), and POSS[®]-N-2IL was obtained from POSS[®] bearing two amino-hydrogen functions (POSS[®]-NH₂). Their chemical structures were confirmed from investigation by ²⁹Si NMR and MALDI-TOF mass spectrometry. Their thermal properties were also studied by TGA and DSC highlighting an excellent thermal stability (up to 400 °C) of these new compounds. Then, 5 wt. % of IL-modified POSS[®] (IL-g-POSS[®] or POSS[®]-N-2IL) were incorporated into epoxy-amine networks leading to the formation of nanostructured networks or co-continuous morphologies. The IL substituted POSS[®] is miscible with the epoxy system leading to transparent nanomaterials despite limited reaction induced microphase separation and formation of nanosized (< 100 nm) aggregates. Regarding the epoxy networks containing POSS[®]-N-2IL, the multiple IL-substitution gives a mixed morphology composed of nanosized POSS[®]-rich clusters and a co-continuous phase probably due to the presence of two ionic liquid by POSS[®]. In the case of other substituents, the low POSS[®]-polymer compatibility and the strong POSS[®]-POSS[®] interactions lead to larger POSS[®] mainly crystalline-like domains (diameter up to 1 μm) dispersed in the epoxy-amine matrix. In conclusion, these promising results open up new perspectives in the development of nanostructured organic-inorganic epoxy-amine networks and highlight the role of ionic liquids as a dispersion agent for such new organic-inorganic hybrid nanomaterials. Future works will be presented in the next chapter to show the impact of this POSS[®]-based nanostructuration on the functionalities of these nanomaterials.

Supporting Information of Chapter II

The MALDI-TOF mass spectrum of the Si-g-Im-Cl IL (Figure S2.1) and ILM (Figure S2.2) confirmed the expected cationic species of the ILs and reveals that the chemical environment around ILs (Si-g-Im-Cl or ILM) atoms is the same, which confirms that very pure ILs have been obtained without any other side reaction.

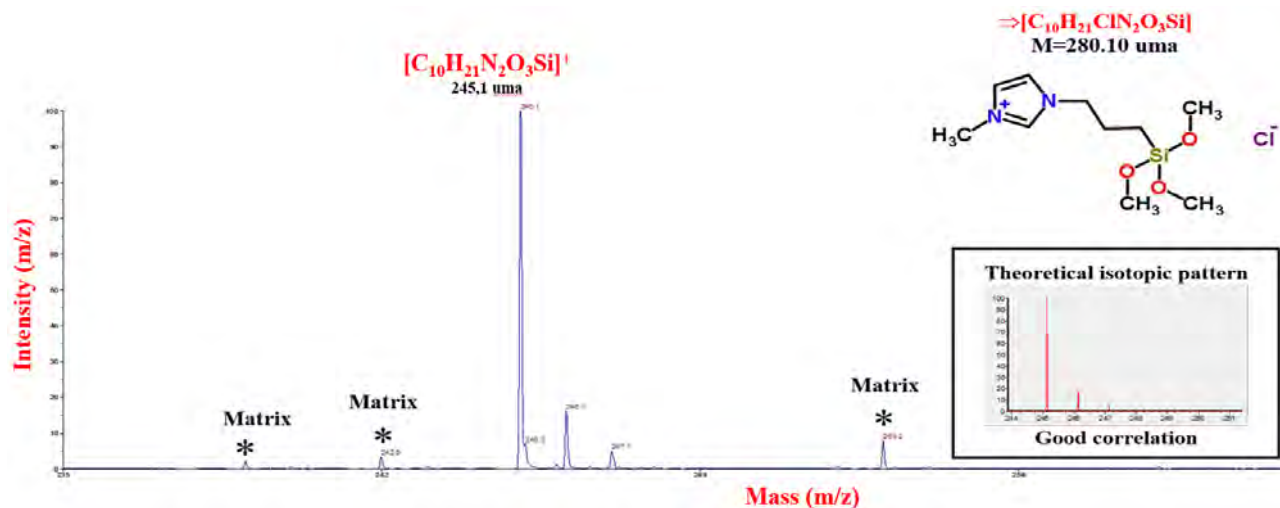


Figure S2.1: Mass spectrum of 1-(3-trimethoxysilylpropyl)-3-methyl imidazolium Chloride (Si-g-Im-Cl) (Dithranol matrix).

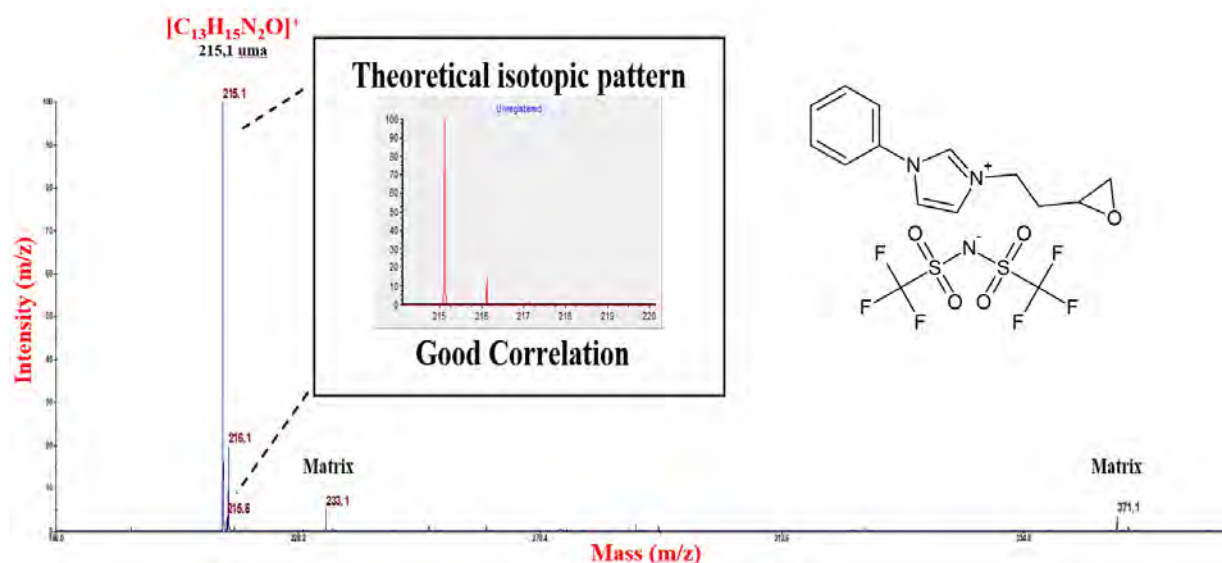


Figure S2.2: Mass spectrum of ILM (Dithranol matrix).

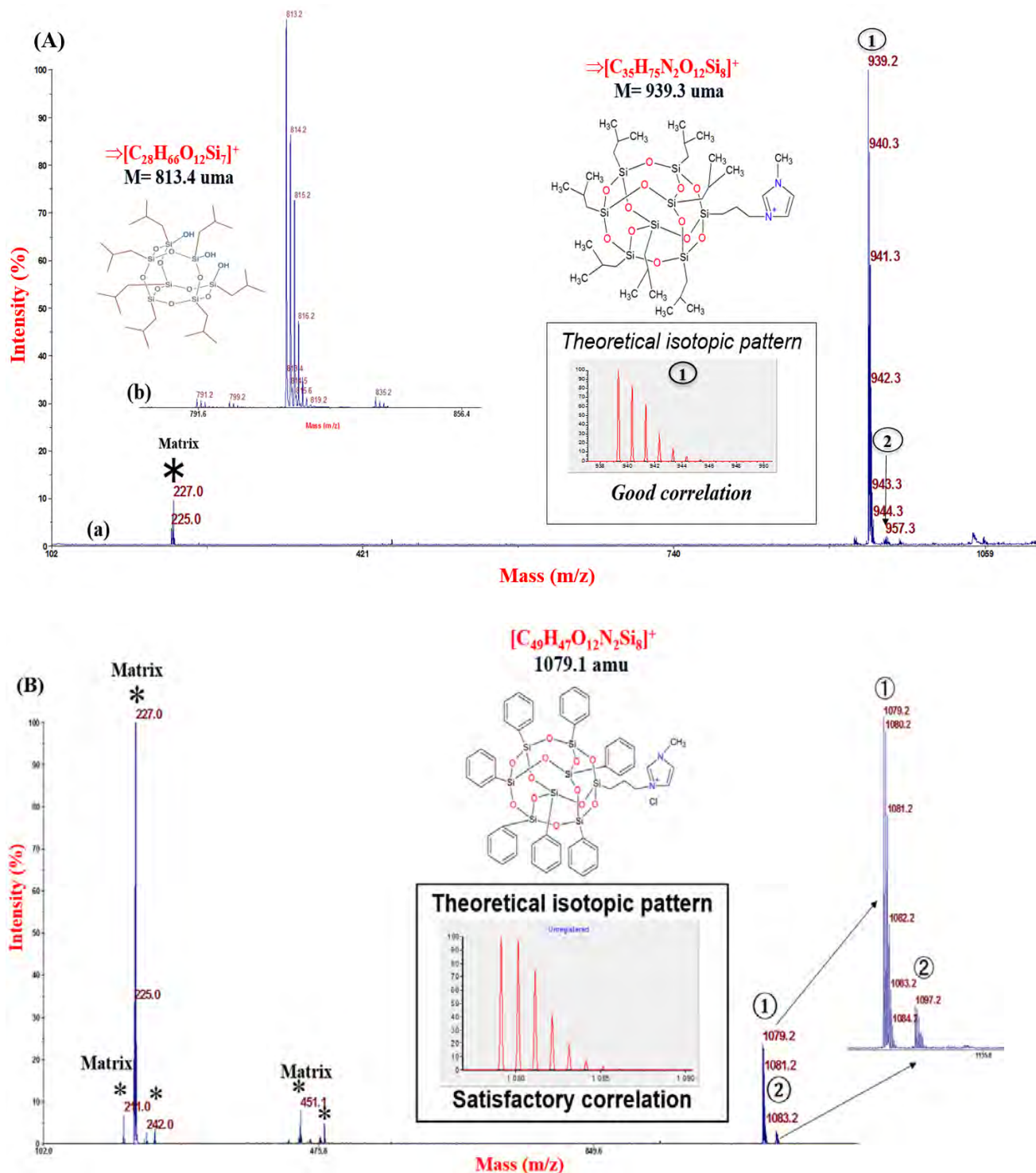


Figure S2.3: Positive MALDI-TOF mass spectra of A) IL-g-POSS^{®iB} and B) IL-g-POSS^{®Ph} (Dithranol matrix).

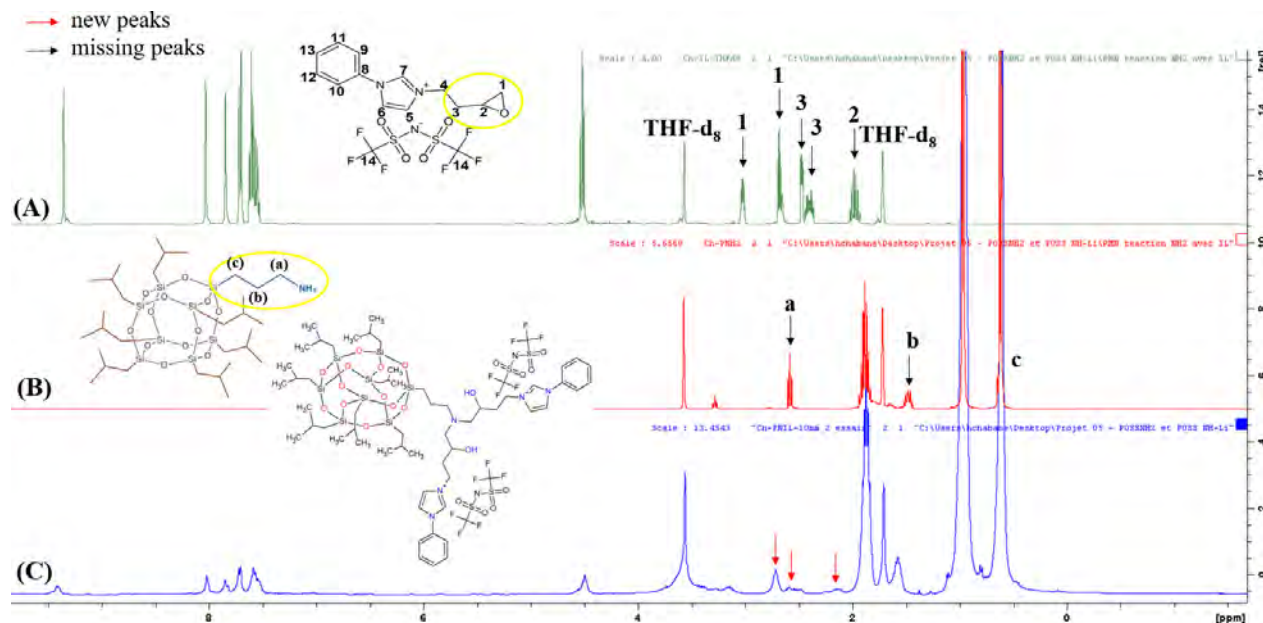


Figure S2.4: ¹H NMR spectra of A) ILM, B) POSS[®]-NH₂ and C) POSS[®]-N-2IL (THF-d₈; 400 MHz).

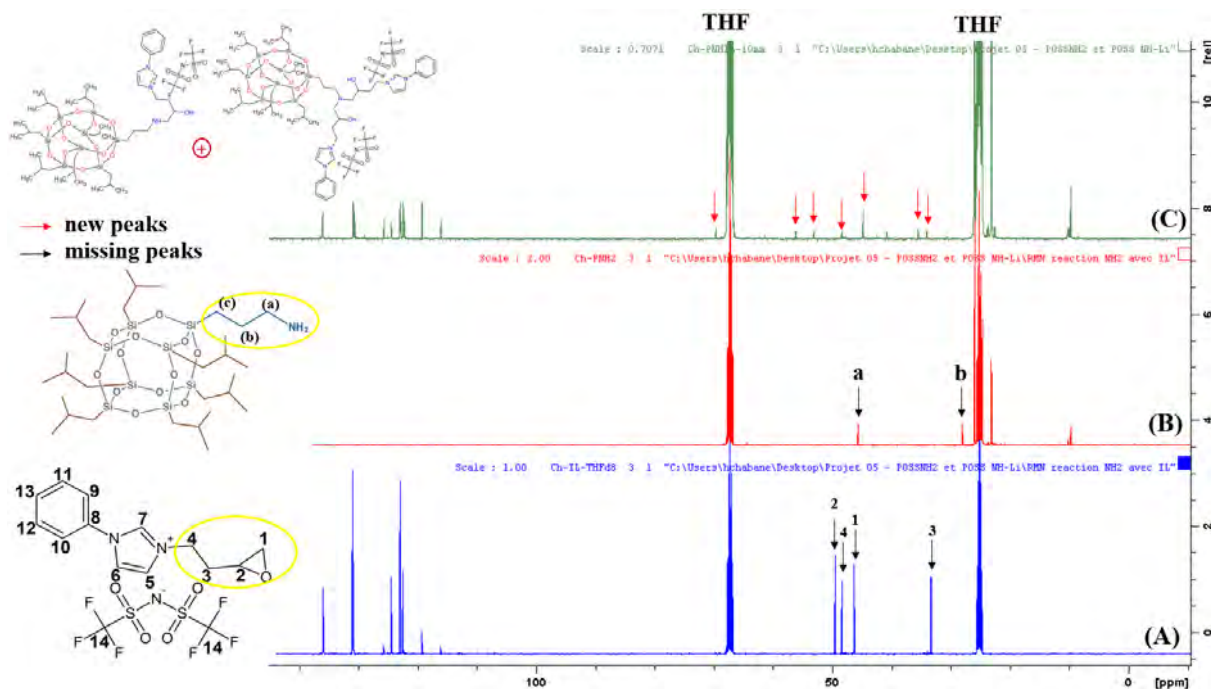


Figure S2.5: ¹³C NMR spectra of A) ILM, B) POSS[®]-NH₂, and C) POSS[®]-N-2IL (THF-d₈; 400 MHz).

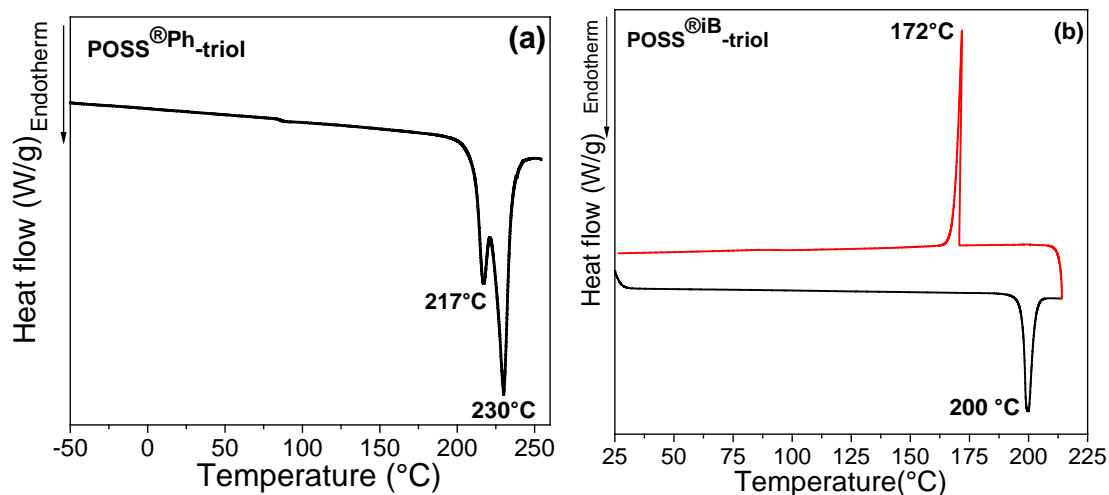


Figure S2.6: DSC traces for POSS[®]-triols: a) POSS[®]Ph-triol, and b) POSS[®]iB-triol (heating and cooling rate: 10 K.min⁻¹).

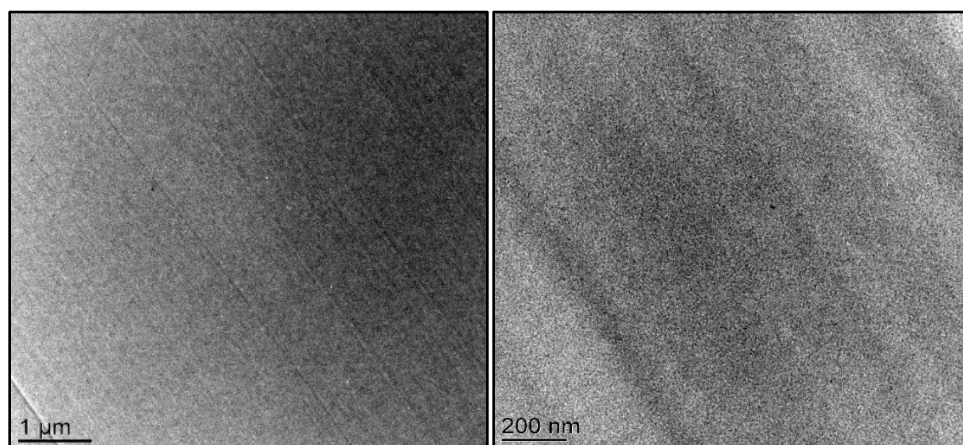


Figure S2.7: TEM images of the epoxy matrix (epoxy-amine) at different magnifications.

Table S2.1: Contents of the two types of Si atoms in the POSS[®] cage.

Compound	Si-OH band (%) ^a	Si-R band (%) ^a
POSS [®] Ph-triol	43	57
IL-g-POSS [®] Ph	22	78
POSS [®] iB-triol	42	58
IL-g-POSS [®] iB	8	92

^a Calculated from ²⁹Si from ²⁹Si NMR results:

An abundance of 43%, calculated by the peak integration from -62 to -72 ppm;

An abundance of 57%, calculated by the peak integration from -74 to -84 ppm;

An abundance of 42%, calculated by the peak integration from -55 to -63 ppm;

An abundance of 58%, calculated by the peak integration from -65 to -74 ppm.

Table S2.2: TGA data of POSS^{®iB}-triol, POSS^{®Ph}-triol, IL-g-POSS^{®iB} and IL-g-POSS^{®Ph} (heating rate: 10 K.min⁻¹, atmosphere: nitrogen flow).

Sample	T _{d5%} (°C) ^a	T _{dmax1} (°C) ^b	T _{dmax2} (°C) ^c	Residue (%) ^d
POSS ^{®iB} -triol	238	-	283	0.25
POSS ^{®Ph} -triol	281	543	626	66
IL-g-POSS ^{®iB}	330	-	428	12
IL-g-POSS ^{®Ph}	490	-	632	73

^a T_{d5%}: Degradation temperature determined at a mass loss of 5 wt. %, ^b T_{dmax1}: Degradation temperature determined at the first maximum of from the first derivative of the weight loss as temperature, ^c T_{dmax2}: Degradation temperature determined at the second maximum of the first derivative of the weight loss as temperature, ^d Residue yield at 800 °C.

Reference of chapter II

- (1) Liu, P.; Cottrill, A. L.; Kozawa, D.; Koman, V. B.; Parviz, D.; Liu, A. T.; Yang, J.; Tran, T. Q.; Wong, M. H.; Wang, S. Emerging trends in 2D nanotechnology that are redefining our understanding of “Nanocomposites”. *Nano Today* **2018**, *21*, 18-40.
- (2) Reddy, B. in *Advances in Nanocomposites: Synthesis, Characterization and Industrial Applications*; Ed by Boreddy Reddy, Copyright © Intech, **2011**.
- (3) Peponi, L.; Puglia, D.; Torre, L.; Valentini, L.; Kenny, J. M. Processing of nanostructured polymers and advanced polymeric based nanocomposites. *Materials Science and Engineering: R: Reports* **2014**, *85*, 1-46.
- (4) Laine, R. M. Nanobuilding blocks based on the $[\text{OSiO}_{1.5}]_x$ ($x = 6, 8, 10$) octasilsesquioxanes. *Journal of Materials Chemistry* **2005**, *15*, 3725-3744.
- (5) Matějka, L.; Murias, P.; Pleštil, J. Effect of POSS[®] on thermomechanical properties of epoxy-POSS[®] nanocomposites. *European Polymer Journal* **2012**, *48*, 260-274.
- (6) Li, G.; Wang, L.; Ni, H.; Pittman, C. U. Polyhedral oligomeric silsesquioxane (POSS[®]) polymers and copolymers: a review. *Journal of Inorganic and Organometallic Polymers* **2001**, *11*, 123-154.
- (7) Cordes, D. B.; Lickiss, P. D.; Rataboul, F. Recent developments in the chemistry of cubic polyhedral oligosilsesquioxanes. *Chemical reviews* **2010**, *110*, 2081-2173.
- (8) Kim, K. M.; Chujo, Y. Liquid-crystalline organic-inorganic hybrid polymers with functionalized silsesquioxanes. *Journal of Polymer Science Part A: Polymer Chemistry* **2001**, *39*, 4035-4043.
- (9) Leu, C. M.; Chang, Y. T.; Wei, K. H. Synthesis and dielectric properties of polyimide-tethered polyhedral oligomeric silsesquioxane (POSS[®]) nanocomposites via POSS[®]-diamine. *Macromolecules* **2003**, *36*, 9122-9127.
- (10) Pescarmona, P. P.; Masters, A. F.; van der Waal, J. C.; Maschmeyer, T. Osmium silsesquioxane as model compound and homogeneous catalyst for the dihydroxylation of alkenes. *Journal of Molecular Catalysis A: Chemical* **2004**, *220*, 37-42.
- (11) Awad, W. H.; Gilman, J. W.; Nyden, M.; Davis, R.; Harris, R. H.; Sutto, T. E.; Callahan, J. H.; DeLong, H. C.; Trulove, P. C. Thermal degradation studies of alkyl-imidazolium salts and their application in nanocomposites. *ECS Proceedings Volumes* **2002**, *19*, 200-211.

- (12) Hapiot, P.; Lagrost, C. Electrochemical reactivity in room-temperature ionic liquids. *Chemical Reviews* **2008**, *108*, 2238-2264.
- (13) Livi, S.; Duchet-Rumeau, J.; Gérard, J. F.; Pham, T. N. Polymers and ionic liquids: A successful wedding. *Macromolecular Chemistry and Physics* **2015**, *216*, 359-368.
- (14) Livi, S.; Silva, A. A.; Thimont, Y.; Nguyen, T. K. L.; Soares, B. G.; Gérard, J. F.; Duchet-Rumeau, J. Nanostructured thermosets from ionic liquid building block-epoxy prepolymer mixtures. *RSC Advances* **2014**, *4*, 28099-28106.
- (15) Sanes, J.; Carrión, F.; Bermúdez, M. Effect of the addition of room temperature ionic liquid and ZnO nanoparticles on the wear and scratch resistance of epoxy resin. *Wear* **2010**, *268*, 1295-1302.
- (16) Soares, B. G.; Livi, S.; Duchet-Rumeau, J.; Gerard, J. F. Synthesis and characterization of epoxy/MCDEA networks modified with imidazolium-based ionic liquids. *Macromolecular Materials and Engineering* **2011**, *296*, 826-834.
- (17) Zheng, Z.; Xu, Q.; Guo, J.; Qin, J.; Mao, H.; Wang, B.; Yan, F. Structure-antibacterial activity relationships of imidazolium-type ionic liquid monomers, poly (ionic liquids) and poly (ionic liquid) membranes: effect of alkyl chain length and cations. *ACS Applied Materials & Interfaces* **2016**, *8*, 12684-12692.
- (18) Adzima, B. J.; Taylor, S. C.; He, H.; Luebke, D. R.; Matyjaszewski, K.; Nulwala, H. B. Vinyl-triazolium monomers: Versatile and new class of radically polymerizable ionic monomers. *Journal of Polymer Science Part A: Polymer Chemistry* **2014**, *52*, 417-423.
- (19) Ly Nguyen, T. K.; Obadia, M. M.; Serghei, A.; Livi, S.; Duchet-Rumeau, J.; Drockenmuller, E. 1, 2, 3-Triazolium-Based Epoxy-Amine Networks: Ion-Conducting Polymer Electrolytes. *Macromolecular Rapid Communications* **2016**, *37*, 1168-1174.
- (20) Radchenko, A. V.; Chabane, H.; Demir, B.; Searles, D. J.; Duchet-Rumeau, J.; Gerard, J. F.; Baudoux, J. r. m.; Livi, S. New Epoxy thermosets derived from a bisimidazolium ionic liquid monomer: An experimental and modeling investigation. *ACS Sustainable Chemistry & Engineering* **2020**, *8*, 12208-12221.
- (21) Radchenko, A. V.; Duchet-Rumeau, J.; Gérard, J. F.; Baudoux, J.; Livi, S. Cycloaliphatic epoxidized ionic liquids as new versatile monomers for the development of shape memory PIL networks by 3D printing. *Polymer Chemistry* **2020**, *11*, 5475-5483.

- (22) Nguyen, T. K. L.; Livi, S.; Pruvost, S.; Soares, B. G.; Duchet-Rumeau, J. Ionic liquids as reactive additives for the preparation and modification of epoxy networks. *Journal of Polymer Science Part A: Polymer Chemistry* **2014**, 52, 3463-3471.
- (23) Sonnier, R.; Dumazert, L.; Livi, S.; Nguyen, T. K. L.; Duchet-Rumeau, J.; Vahabi, H.; Laheurte, P. Flame retardancy of phosphorus-containing ionic liquid based epoxy networks. *Polymer Degradation and Stability* **2016**, 134, 186-193.
- (24) Nguyen, T. K. L.; Livi, S.; Soares, B. G.; Benes, H.; Gérard, J. F.; Duchet-Rumeau, J. Toughening of epoxy/ionic liquid networks with thermoplastics based on poly (2, 6-dimethyl-1, 4-phenylene ether)(PPE). *ACS Sustainable Chemistry & Engineering* **2017**, 5, 1153-1164.
- (25) Nguyen, T. K. L.; Livi, S.; Soares, B. G.; Pruvost, S.; Duchet-Rumeau, J.; Gérard, J. F. Ionic liquids: A new route for the design of epoxy networks. *ACS Sustainable Chemistry & Engineering* **2016**, 4, 481-490.
- (26) Bara, J. E.; Lessmann, S.; Gabriel, C. J.; Hatakeyama, E. S.; Noble, R. D.; Gin, D. L. Synthesis and performance of polymerizable room-temperature ionic liquids as gas separation membranes. *Industrial & Engineering Chemistry Research* **2007**, 46, 5397-5404.
- (27) Druvari, D.; Koromilas, N. D.; Lainioti, G. C.; Bokias, G.; Vasilopoulos, G.; Vantarakis, A.; Baras, I.; Dourala, N.; Kallitsis, J. K. Polymeric quaternary ammonium-containing coatings with potential dual contact-based and release-based antimicrobial activity. *ACS Applied Materials & Interfaces* **2016**, 8, 35593-35605.
- (28) Livi, S.; Lins, L. C.; Capeletti, L. B.; Chardin, C.; Halawani, N.; Baudoux, J.; Cardoso, M. B. Antibacterial surface based on new epoxy-amine networks from ionic liquid monomers. *European Polymer Journal* **2019**, 116, 56-64.
- (29) Cui, J.; Nie, F. M.; Yang, J. X.; Pan, L.; Ma, Z.; Li, Y. S. Novel imidazolium-based poly (ionic liquid) s with different counterions for self-healing. *Journal of Materials Chemistry A* **2017**, 5, 25220-25229.
- (30) Lins, L. C.; Livi, S.; Maréchal, M.; Duchet-Rumeau, J.; Gérard, J. F. Structural dependence of cations and anions to building the polar phase of PVDF. *European Polymer Journal* **2018**, 107, 236-248.
- (31) Livi, S.; Duchet-Rumeau, J.; Gérard, J. F. Nanostructuration of ionic liquids in fluorinated matrix: Influence on the mechanical properties. *Polymer* **2011**, 52, 1523-1531.

- (32) Yang, G.; Oh, H.; Chanthad, C.; Wang, Q. Dumbbell-shaped octasilsesquioxanes functionalized with ionic liquids as hybrid electrolytes for lithium metal batteries. *Chemistry of Materials* **2017**, 29, 9275-9283.
- (33) Yang, J.; Pruvost, S.; Livi, S.; Duchet-Rumeau, J. Understanding of versatile and tunable nanostructuration of ionic liquids on fluorinated copolymer. *Macromolecules* **2015**, 48, 4581-4590.
- (34) Mąka, H.; Szychaj, T.; Zenker, M. High performance epoxy composites cured with ionic liquids. *Journal of Industrial and Engineering Chemistry* **2015**, 31, 192-198.
- (35) Ghanbari, H.; Cousins, B. G.; Seifalian, A. M. A nanocage for nanomedicine: polyhedral oligomeric silsesquioxane (POSS[®]). *Macromolecular Rapid Communications* **2011**, 32, 1032-1046.
- (36) Ullah, A.; Ullah, S.; Khan, G. S.; Shah, S. M.; Hussain, Z.; Muhammad, S.; Siddiq, M.; Hussain, H. Water soluble polyhedral oligomeric silsesquioxane based amphiphilic hybrid polymers: synthesis, self-assembly, and applications. *European Polymer Journal* **2016**, 75, 67-92.
- (37) Zhang, W.; Camino, G.; Yang, R. Polymer/polyhedral oligomeric silsesquioxane (POSS[®]) nanocomposites: An overview of fire retardance. *Progress in Polymer Science* **2017**, 67, 77-125.
- (38) Jovanovski, V.; Orel, B.; Ješe, R.; Šurca Vuk, A.; Mali, G.; Hoc̣evar, S. B.; Grdadolnik, J.; Stathatos, E.; Lianos, P. Novel polysilsesquioxane- Γ/I_3^- ionic electrolyte for dye-sensitized photoelectrochemical cells. *The Journal of Physical Chemistry B* **2005**, 109, 14387-14395.
- (39) Fox, D. M.; Maupin, P. H.; Harris, R. H.; Gilman, J. W.; Eldred, D. V.; Katsoulis, D.; Trulove, P. C.; De Long, H. C. Use of a polyhedral oligomeric silsesquioxane (POSS[®])-imidazolium cation as an organic modifier for montmorillonite. *Langmuir* **2007**, 23, 7707-7714.
- (40) Shang, D.; Fu, J.; Lu, Q.; Chen, L.; Yin, J.; Dong, X.; Xu, Y.; Jia, R.; Yuan, S.; Chen, Y. A novel polyhedral oligomeric silsesquioxane based ionic liquids (POSS[®]-ILs) polymer electrolytes for lithium ion batteries. *Solid State Ionics* **2018**, 319, 247-255.
- (41) Čolović, M.; Jerman, I.; Gaberšček, M.; Orel, B. POSS[®] based ionic liquid as an electrolyte for hybrid electrochromic devices. *Solar Energy Materials and Solar Cells* **2011**, 95, 3472-3481.

- (42) Jerman, I.; Koželj, M.; Orel, B. The effect of polyhedral oligomeric silsesquioxane dispersant and low surface energy additives on spectrally selective paint coatings with self-cleaning properties. *Solar Energy Materials and Solar Cells* **2010**, 94, 232-245.
- (43) Jerman, I.; Jovanovski, V.; Vuk, A. Š.; Hočevár, S.; Gabersček, M.; Jesih, A.; Orel, B. Ionic conductivity, infrared and Raman spectroscopic studies of 1-methyl-3-propylimidazolium iodide ionic liquid with added iodine. *Electrochimica Acta* **2008**, 53, 2281-2288.
- (44) Brun, N.; Hesemann, P.; Laurent, G.; Sanchez, C.; Birot, M.; Deleuze, H.; Backov, R. Macrocellular Pd@ ionic liquid@ organo-Si (HIPE) heterogeneous catalysts and their use for Heck coupling reactions. *New Journal of Chemistry* **2013**, 37, 157-168.
- (45) Ye, M.; Wu, Y.; Zhang, W.; Yang, R. Synthesis of incompletely caged silsesquioxane (T7-POSS[®]) compounds via a versatile three-step approach. *Research on Chemical Intermediates* **2018**, 44, 4277-4294.
- (46) Tanaka, K.; Ishiguro, F.; Chujo, Y. POSS[®] ionic liquid. *Journal of the American Chemical Society* **2010**, 132, 17649-17651.
- (47) Fina, A.; Tabuani, D.; Carniato, F.; Frache, A.; Boccaleri, E.; Camino, G. Polyhedral oligomeric silsesquioxanes (POSS[®]) thermal degradation. *Thermochimica Acta* **2006**, 440, 36-42.
- (48) Ledin, P.; Tkachenko, I.; Xu, W.; Choi, I.; Shevchenko, V.; Tsukruk, V. Star-shaped molecules with POSS[®] core and azobenzene dye arms. *Langmuir* **2014**, 30, 8856-8865.
- (49) Wilkie, C. A. An introduction to the use of fillers and nanocomposites in fire retardancy. Ed by Michel Le Bras; Charles A. Wilkie; Serge Bourbigot. The Royal Society of Chemistry, in *Fire retardancy of polymers: New applications of mineral fillers* **2005**, chapter 1, 1-15.
- (50) Blanco, I.; Abate, L.; Bottino, F.; Bottino, P.; Chiacchio, M. Thermal degradation of differently substituted cyclopentyl polyhedral oligomeric silsesquioxane (CP-POSS[®]) nanoparticles. *Journal of Thermal Analysis and Calorimetry* **2012**, 107, 1083-1091.
- (51) Fu, J.; Lu, Q.; Shang, D.; Chen, L.; Jiang, Y.; Xu, Y.; Yin, J.; Dong, X.; Deng, W.; Yuan, S. A novel room temperature POSS[®] ionic liquid-based solid polymer electrolyte. *Journal of Materials Science* **2018**, 53, 8420-8435.
- (52) Tanaka, K.; Ishiguro, F.; Jeon, J. H.; Hiraoka, T.; Chujo, Y. POSS[®] ionic liquid crystals. *NPG Asia Materials* **2015**, 7, e174-e174.

- (53) Wang, X.; Hu, Y.; Song, L.; Xing, W.; Lu, H. Thermal degradation behaviors of epoxy resin/POSS[®] hybrids and phosphorus-silicon synergism of flame retardancy. *Journal of Polymer Science Part B: Polymer Physics* **2010**, *48*, 693-705.
- (54) Tanaka, K.; Ishiguro, F.; Chujo, Y. Thermodynamic study of POSS[®]-based ionic liquids with various numbers of ion pairs. *Polymer Journal* **2011**, *43*, 708-713.
- (55) Liu, Y. E.; He, C. E.; Peng, R. G.; Tang, W.; Yang, Y. K. Ionic liquid assisted dispersion of reduced graphene oxide in epoxy composites with improved mechanical properties. In *Advanced Materials Research*; Trans Tech Publ, **2013**; Vol. 738, p 56-60.
- (56) Lopes Pereira, E. C.; Soares, B. G. Conducting epoxy networks modified with non-covalently functionalized multi-walled carbon nanotube with imidazolium-based ionic liquid. *Journal of Applied Polymer Science* **2016**, *133*, 43976 (1-9).
- (57) Zhang, C.; Mi, X.; Tian, J.; Zhang, J.; Xu, T. Supported ionic liquid silica as curing agent for epoxy composites with improved mechanical and thermal properties. *Polymers* **2017**, *9*, 478.
- (58) Donato, R. K.; Matějka, L.; Schrekker, H. S.; Pleštil, J.; Jigounov, A.; Brus, J.; Šlouf, M. The multifunctional role of ionic liquids in the formation of epoxy-silica nanocomposites. *Journal of Materials Chemistry* **2011**, *21*, 13801-13810.
- (59) Perchacz, M.; Donato, R. K.; Seixas, L.; Zhigunov, A.; Konefał, R.; Serkis-Rodzeń, M.; Beneš, H. Ionic liquid-silica precursors via solvent-free sol-gel process and their application in epoxy-amine network: A theoretical/experimental study. *ACS Applied Materials & Interfaces* **2017**, *9*, 16474-16487.
- (60) Franchini, E.; Galy, J.; Gérard, J. F.; Tabuani, D.; Medici, A. Influence of POSS[®] structure on the fire retardant properties of epoxy hybrid networks. *Polymer Degradation and Stability* **2009**, *94*, 1728-1736.
- (61) Ni, Y.; Zheng, S.; Nie, K. Morphology and thermal properties of inorganic-organic hybrids involving epoxy resin and polyhedral oligomeric silsesquioxanes. *Polymer* **2004**, *45*, 5557-5568.
- (62) Xu, Y.; Ma, Y.; Deng, Y.; Yang, C.; Chen, J.; Dai, L. Morphology and thermal properties of organic-inorganic hybrid material involving monofunctional-anhydride POSS[®] and epoxy resin. *Materials Chemistry and Physics* **2011**, *125*, 174-183.
- (63) Perchacz, M. Hybrid materials with improved thermomechanical properties. *Thesis in Institute of Macromolecular Chemistry AS CR* **2017**.

- (64) Hu, J.; Yang, Q.; Yang, L.; Zhang, Z.; Su, B.; Bao, Z.; Ren, Q.; Xing, H.; Dai, S. Confining noble metal (Pd, Au, Pt) nanoparticles in surfactant ionic liquids: Active non-mercury catalysts for hydrochlorination of acetylene. *ACS Catalysis* **2015**, 5, 6724-6731.
- (65) Liu, Y.; Qiao, L.; Xiang, Y.; Guo, R. Adsorption behavior of low-concentration imidazolium-based ionic liquid surfactant on silica nanoparticles. *Langmuir* **2016**, 32, 2582-2590.
- (66) He, Z.; Alexandridis, P. Ionic liquid and nanoparticle hybrid systems: Emerging applications. *Advances in Colloid and Interface Science* **2017**, 244, 54-70.
- (67) Pascault, J. P.; Williams, R. J. in *Epoxy polymers: New materials and innovations*; John Wiley & Sons, **2009**.
- (68) Bellenger, V.; Dhaoui, W.; Verdu, J.; Galy, J.; Won, Y.; Pascault, J. Glass transition temperature predictions for non-stoichiometric epoxide-amine networks. *Polymer* **1989**, 30, 2013-2018.
- (69) Garcia, F. G.; Soares, B. G.; Pita, V. J.; Sánchez, R.; Rieumont, J. Mechanical properties of epoxy networks based on DGEBA and aliphatic amines. *Journal of Applied Polymer Science* **2007**, 106, 2047-2055.
- (70) Deng, Y.; Bernard, J.; Alcouffe, P.; Galy, J.; Dai, L.; Gérard, J. F. Nanostructured hybrid polymer networks from in situ self-assembly of RAFT-synthesized POSS[®]-based block copolymers. *Journal of Polymer Science Part A: Polymer Chemistry* **2011**, 49, 4343-4352.
- (71) Ni, Y.; Zheng, S. Epoxy resin containing octamaleimidophenyl polyhedral oligomeric silsesquioxane. *Macromolecular Chemistry and Physics* **2005**, 206, 2075-2083.
- (72) Xu, H.; Kuo, S. W.; Lee, J. S.; Chang, F. C. Preparations, thermal properties, and T_g increase mechanism of inorganic/organic hybrid polymers based on polyhedral oligomeric silsesquioxanes. *Macromolecules* **2002**, 35, 8788-8793.
- (73) Abad, M. J.; Barral, L.; Fasce, D. P.; Williams, R. J. Epoxy networks containing large mass fractions of a monofunctional polyhedral oligomeric silsesquioxane (POSS[®]). *Macromolecules* **2003**, 36, 3128-3135.
- (74) Zucchi, I. A.; Galante, M. J.; Williams, R. J.; Franchini, E.; Galy, J.; Gérard, J. F. Monofunctional epoxy-POSS[®] dispersed in epoxy-amine networks: Effect of a prereaction on the morphology and crystallinity of POSS[®] domains. *Macromolecules* **2007**, 40, 1274-1282.

Chapter III:

Design and Properties of Nanostructured IL-g-POSS^{®Ph}/Epoxy-amine Hybrid Organic-Inorganic Networks

Abstract: Designing innovative multi-functional thermoset polymers represents a major challenge in materials science. In this work, two novel imidazolium ionic liquid supported on oligomeric silsesquioxane nanocages having chloride (Cl⁻) and bis-trifluoromethanesulfonimide (NTf₂⁻) counter anions have been synthesized. These ionic nano-clusters were used to nanostructure a model epoxy network. Hence, networks displaying a homogeneous nanoscale morphology were obtained by introducing 5wt % of such organic-inorganic (O/I) silicon-oxo clusters functionalized with ionic liquids. The obtained ionic hybrid O/I epoxy-amine networks display an excellent thermal stability (> 400 °C) compared to their neat counterparts, as well as a pronounced hydrophobic character (23 mJ.m⁻²) and enhanced mechanical performances. Moreover, these O/I nanostructured networks display an improved fire resistance according to pyrolysis-combustion flow calorimetry (PCFC) and cone calorimetry analyses. In fact, the use of low amounts of imidazolium ionic liquid-modified polyhedral oligomeric silsesquioxanes induces a significant decrease of heat release rate (about 55 %) as well as a delay of the ignition (close to 29 %) compared to the neat epoxy-amine network.

Graphical abstract of the chapter

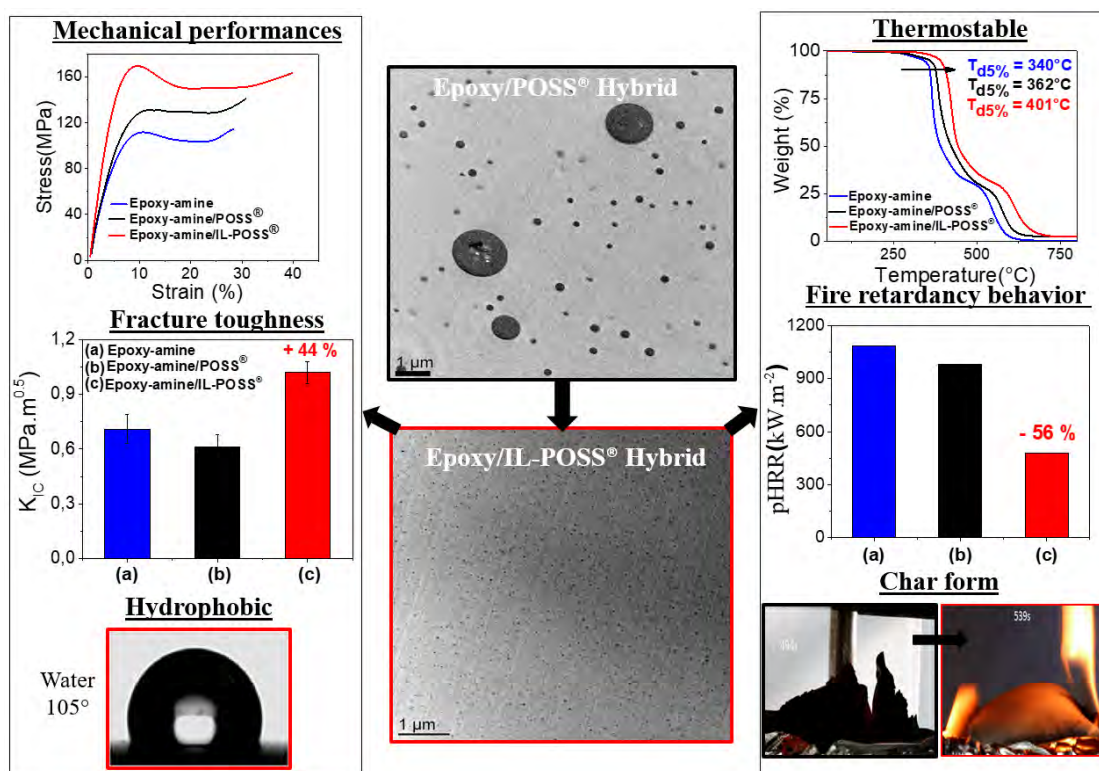


Table of contents

III.1. Introduction	134
III.2. Materials and characterization methods	138
III.2.1. Materials	138
III.2.2. Anionic exchange procedure of polyhedral oligomeric silsesquioxane (POSS ^{®Ph}) (Chloride Cl ⁻ versus bis(trifluoromethanesulfonyl)imide NTf ₂ ⁻)	139
III.2.3. Epoxy network synthesis	139
III.2.4. Determination of the soluble fraction extractable from hybrid O/I networks	140
III.2.5. Characterization.....	140
III.3. Results and Discussion	143
III.3.1. Curing of epoxy-amine and hybrid O/I networks.....	143
III.3.2. Morphology of hybrid O/I networks	146
III.3.3. Thermomechanical properties of the resulting networks	148
III.3.4. Mechanical properties.....	149
III.3.4.1. Elastic and large strain mechanical properties.....	149
III.3.4.2. Fracture properties.....	150
III.3.5. Surface properties	152
III.3.6. Thermal-oxidative stability.....	153
III.3.7. Fire resistance	155
III.3.7.1. Flammability.....	155
III.3.7.2. Fire behavior.....	156
III.4. Conclusion of chapter III	163
Supporting Information of chapter III.....	165
References of chapter III	169

III.1. Introduction

Due to their excellent physical properties including optical transparency, high electrical resistance, and thermal insulation capabilities in parallel with good thermo-mechanical properties and dimensional stability, epoxy networks represent an important class of thermoset polymers, widely used in applications going from adhesives, paints and coatings, insulating layers in electronics to matrices for composites used in automotive and aerospace industries ^{1,2}. However, the highly crosslinked nature of such thermoset polymers leads to a brittle behavior, *i.e.* materials have a poor resistance to crack propagation when subjected to mechanical loading as well as thermal changes ^{3,4}. More particularly, the fire resistance of epoxy polymers based on diglycidyl ether of bisphenol A (DGEBA) is a major drawback restricting their use for applications requiring high-standard fire safety ^{5,6}. In order to overcome these limitations, several routes have been investigated over the years. Regarding improvement of toughness, the most common approach consists of introducing a dispersed ductile phase within the epoxy network using thermally stable and high-T_g thermoplastic polymers (TPs) such as polyetherimide (PEI), polyethersulfone (PES), and polyphenylene ether (PPE). Reactive elastomers such as functionalized poly(butadiene-co-acrylonitrile) rubbers (CTBN, ETBN) may also be used. Reaction-induced phase separation occurs during curing giving rise to different morphologies and toughening mechanisms ⁷⁻⁹. Nevertheless, the incorporation of such compounds usually results in a significant reduction of stiffness (*i.e.* Young modulus) and in some cases to a lower glass transition temperature due to non-perfect microphase separation but significant increase of the flammability properties.

Regarding fire resistance, two main approaches have been investigated to obtain fire resistant (FR) epoxy polymers: the first one consists of introducing halogenated fire-retardant compounds in a conventional epoxy polymer and the second involves modifying the chemical structure of the epoxy prepolymer (*e.g.* brominated epoxy resins). Nowadays, such compounds tend to be subjected to drastic regulations in terms of quantity and field of use, due to environmental and health concerns regulated by new European directives such as REACH ¹⁰. Thus, research groups have been looking for alternatives among which phosphorus-based compounds. As a consequence, phosphorus-modified resin backbones and/or hardeners have attracted great interest ¹¹. In many cases, these compounds require to be used in high concentration. This addition may affect other material properties such as mechanical performances ¹². More recently, other

pathways have been reported in the literature towards the introduction of nanoparticles, such as layered silicates or carbon nanotubes in order to combine the effects of nano-reinforcement and the fire resistance brought by the nanoparticles^{13,14}. Nonetheless, such synergetic effect can only be obtained if the nanoparticles are well dispersed. Obtaining a good dispersion at nanoscale remains challenging and rather difficult for most polymers. Referring to recent studies, a promising route seems to be the introduction of polyhedral oligomeric silsesquioxane (POSS[®]) which are known for their fire-retardant effects into epoxy networks^{13,15,16}.

Polyhedral Oligomeric Silsesquioxanes, now called POSS[®], refer to all the molecular structures with the empirical formula (RSiO_{1.5})_n, where R is a hydrogen atom or an organofunctional derivative of alkyl, alkylene aryl, or arylene groups. The term “silesqui” refers to the ratio of the silicon to oxygen atoms, *i.e.* Si:O = 1:1.5¹⁷. POSS[®] are incompletely oxidized silicate compound compared to SiO₂ with a cage structure having different numbers of silicon atoms. The sizes of these molecular objects range from 1 to 3 nm¹⁷. The most common POSS[®] have cubic T₈ cages with a general formula R₈Si₈O₁₂¹⁷. Numerous papers reported studies on hybrid organic-inorganic (O/I) nanomaterials based on epoxy matrices modified by POSS[®]. For example, Laine *et al.*¹⁸⁻²² and Matejka *et al.*²³ described the effect of a series of functionalized and non-functionalized POSS[®] with various R groups such as aminophenyl, dimethylsiloxypolyglycidyl ether, epoxy, or alkyl groups (isobutyl, methyl, and ethyl) on the dynamic mechanical properties, fracture toughness, and thermal stability of the resulting O/I epoxy nanomaterials. The incorporation of POSS[®] in epoxy networks can result in either an increase²⁴⁻²⁶ or decrease^{27,28} of mechanical properties, *i.e.* stiffness and toughness. In fact, POSS[®] nanoclusters usually tend to easily aggregate, leading to the formation of inorganic-rich domains within the epoxy networks²³. Therefore, tailoring the balance of interactions between the polymer medium, the O/I nano-objects and the POSS[®]-POSS[®] interactions (leading to the formation of microsize aggregates) is a key issue for designing proper inorganic-rich nanostructures required for enhancements of mechanical properties²⁹⁻³⁶ in addition to fire resistance. Recently, several groups reported significant advantages of using ionic liquids (ILs) as dispersing agents for epoxy matrices reinforced with silica nanoparticles^{37,38}. These authors have shown that the introduction of ILs based on imidazolium-based cations is a promising strategy for tailoring nanocomposite morphology at the nanoscale^{37,38}.

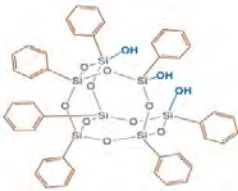
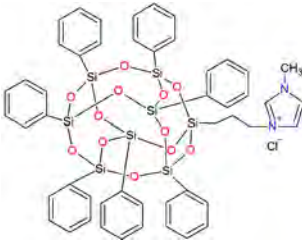
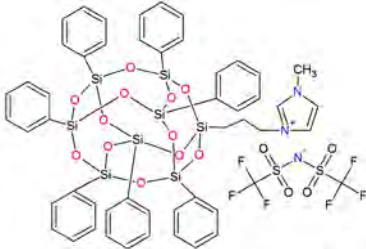
ILs are organic salts with a melting temperature lower than 100 °C that were recently proposed to be combined with epoxy curing chemistry to prepare novel functional materials³⁹⁻⁴¹. These ionic compounds have interesting properties such as high thermal and chemical stabilities, a low saturation vapor pressure, non-flammability, dispersant capabilities, catalytic activity, and a high ionic conductivity which makes them very attractive not only for the present purpose but for the whole of polymer science⁴²⁻⁵¹. Hence, ILs have now emerged in many polymer-based applications. For instance, in epoxy chemistry, ILs can act as catalysts and/or “catalytic” curing agents promoting an anionic polymerization of the epoxy prepolymer leading to significant improvements of the final properties of the resulting networks compared to conventional epoxy networks⁵²⁻⁵⁴. POSS[®] and ionic liquids have also been recently combined to prepare new hybrid compounds by synthesizing IL-grafted POSS[®]. The corresponding ionic O/I nanoclusters have been used as electrolytes for electrochemical devices⁵⁵ or to enhance the proton conductivity of membranes⁵⁶ but to the best of our knowledge, no authors have proposed to introduce such nanoclusters in epoxy network. In the previous chapter, we reported that the connection of ion pairs to POSS[®] nanoclusters, *i.e.* from grafting an ionic liquid of POSS[®] bearing different organic ligands (isobutyl or phenyl), can significantly improve the POSS[®]/epoxy matrix interactions and promote the formation of well-dispersed POSS[®] nanodomains⁵⁷. From these first promising results, we investigate here ionic liquid grafted on phenyl POSS[®], denoted as IL-g-POSS^{®Ph} with two different anions (Cl⁻ and NTf₂⁻) considered as hybrid O/I nanoclusters for designing nanostructured and multifunctional epoxy-amine networks. The anionic exchange of Cl⁻ to NTf₂⁻ was considered in our study because the later one is known to give materials with better thermal stability and higher T_g^{54,58}. The present study unfolds as following: first, the influence of non-modified POSS^{®Ph} (POSS^{®Ph}-triol) and ionic liquid modified POSS^{®Ph} (IL-g-POSS^{®Ph}) on the polymerization of the epoxy prepolymer is described. Then, the morphologies of the two types of POSS^{®Ph} modified-epoxy networks are compared as well as their physical and mechanical properties. Moreover, the potential for fire retardancy of IL-grafted POSS^{®Ph} modified epoxies is more specifically investigated.

III.2. Materials and characterization methods

III.2.1. Materials

1-methylimidazole (99 %), 3-chloropropyltrimethoxysilane (97 %), isophoronediamine (IPD), and lithium bistrifluoromethanesulfonimide (LiNTf₂) considered for anionic exchange procedure, 1-butyl-3-methylimidazolium chloride denoted IL.Cl, 1-butyl-3-methylimidazolium bis(trifluoromethanesulfonyl)imide, denoted IL.NTf₂, and the solvents (diethyl ether, ethanol, chloroform, and dichloromethane) were purchased from Sigma Aldrich and used as received. Epoxy prepolymer based on diglycidyl ether of bisphenol A (DGEBA) (Epon 828 from Hexion) and heptaphenyl-trisilanol POSS[®], denoted POSS^{®Ph}-triol, from Hybrid Plastics were used as received. All the chemical structures of non-grafted and IL-grafted POSS[®] used and synthesized are summarized in Table III. 1.

Table III. 1: Chemical structures of non-grafted and IL-grafted POSS[®].

Name	Chemical formula	Characteristics
Heptaphenyl-trisilanol POSS [®] (POSS ^{®Ph} -triol)		M = 931.34 g mol ⁻¹ , T _{m1} = 217 °C ^a , T _{m2} = 230 °C ^a , T _d = 617 °C ^b CAS No. 444315-26-8
1-methyl-3-propyl heptaphenyl octasilesquioxane imidazolium chloride (IL.Cl-g-POSS ^{®Ph})		M = 1116.04 g mol ⁻¹ , T _{m1} = 134 °C ^a , T _{m2} = 168 °C ^a , T _d = 543 °C ^b
1-methyl-3-propyl heptaphenyl octasilesquioxane imidazolium bis(trifluoromethanesulfonyl)imi date (IL.NTf ₂ -g-POSS ^{®Ph})		M = 1360.73 g mol ⁻¹ , T _{m1} = 135 °C ^a , T _{m2} = 158 °C ^a , T _d = 534 °C ^b

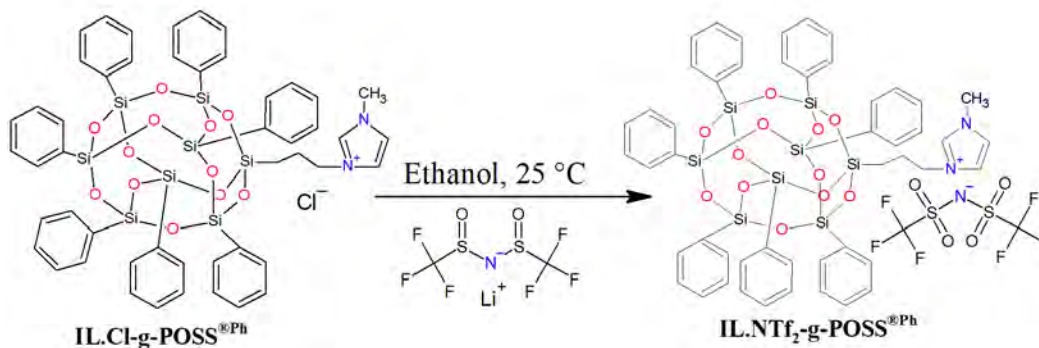
^a T_m: Melting temperature, ^b T_d: Degradation temperature determined at the maximum of the first derivative of the weight loss as function of the temperature (see Figure S3.1 in the SI of chapter III).

III.2.2. Anionic exchange procedure of polyhedral oligomeric silsesquioxane (POSS^{®Ph}) (Chloride Cl⁻ versus bis(trifluoromethanesulfonyl)imide NTf₂⁻)

The anion exchange reaction of Cl⁻ by NTf₂⁻ (Scheme III. 1) following the same procedure as described in Ref. ^{59,60} was performed. An equimolar amount (2.83 g, 9.86 mmol) of LiNTf₂ was added to a solution of IL.Cl-g-POSS^{®Ph} (10 g, 8.96 mmol) in dried ethanol (150 mL) and the mixture was left under stirring at room temperature for 24 hours. The resulting white powder was solubilized in dichloromethane (CH₂Cl₂), dried, filtered, and washed several times with water. The obtained product, *i.e.* IL.NTf₂-g-POSS^{®Ph} was then dried at 80 °C for 48 h. The anionic exchange was checked by complexometric chloride titration considering silver nitrate (AgNO₃). The structure of the resulting salts was confirmed by ¹³C-NMR and FT-IR spectroscopies as illustrated in Figures S3.2 and S3.3 of the supporting information (SI).

FT-IR (KBr, 25 °C): The two absorbance peaks located from 1356 to 1133 cm⁻¹ suggest the presence of both sulfonamide (-SO₂-N) and trifluoromethyl (-CF₃) groups of bis(trifluoromethanesulfonyl)imide counter anion (NTf₂⁻) (see Figure S3.2 of SI) ⁶¹.

¹³C-NMR (100 MHz, acetone-d₆, 25 °C, ppm): 36.65 (CH₂N), 116.28, 119.77, 122.67, 125.86 (q, J_{CF} = 320.8 Hz -CF₃), 128.82, 131.53, 134.79 (Ph) (see Figure S3.3 in the SI of chapter III) ^{60,62}.



Scheme III. 1: Synthesis of imidazolium ionic liquid-modified polyhedral oligomeric silsesquioxane (IL.NTf₂-g-POSS^{®Ph}).

III.2.3. Epoxy network synthesis

Epoxy prepolymer (DGEBA) and isophoronediamine (IPD) were used as comonomers considering a stoichiometric ratio, *i.e.* amino hydrogen-to-epoxy group equal to one. Then, 5 wt.

% of POSS^{®Ph}-triol or IL-g-POSS^{®Ph}, either with chloride (Cl⁻) or bis(trifluoromethanesulfonyl)imide (NTf₂⁻) as counter anions, were incorporated in the epoxy reactive systems. DGEBA and POSS^{®Ph}-triol or IL-g-POSS^{®Ph} were mixed at 120 °C in order to obtain a homogeneous and transparent solution before adding the isophorone diamine used as hardener. Next, the mixture was degassed and then poured into a mold. As a last step, the reactive systems were polymerized for 1 h at 140 °C and post-cured 8 h at 190 °C⁶³⁻⁶⁵ while the epoxy-amine networks with IL-g-POSS^{®Ph} were post-cured a second time at 230 °C for an additional 3 h in order to ensure a complete polymerization.

III.2.4. Determination of the soluble fraction extractable from hybrid O/I networks

A complete characterization of the POSS[®]-modified networks is required to determine the amount of POSS[®] nanocages bonded to the epoxy network. Thus, the POSS[®]-modified networks were submitted to THF extraction at 60 °C for 24 h to determine a fraction of the soluble fraction containing unbounded POSS[®]. The soluble fraction, denoted as w_s , was evaluated from the weight of the dried specimen, m_{dry} , and the one of the specimen after extraction, $m_{dry-ext}$ using the following equation (1):

$$w_s = 1 - (m_{dry-ext}/m_{dry}) \quad (1)$$

III.2.5. Characterization

Fourier Transform Infrared Spectroscopy (FTIR): FT-IR spectra were recorded using a Thermo-Scientific Nicolet iS10 Spectrometer operating from 4,000 to 500 cm⁻¹.

¹³C-NMR spectra were recorded using a Bruker Avance II 400 MHz spectrometer at room temperature with appropriate deuterated solvent (acetone-d₆).

Transmission electron microscopy (TEM) was carried out at the Technical Center of Micro-Structures (University of Lyon) using a Phillips CM 120 microscope operating at 80 kV. 60 nm-thick ultrathin sections of samples obtained by ultramicrotomy.

Differential Scanning Calorimetry (DSC) measurements were performed using a DSC Q10 (TA Instruments) in a dynamic mode, *i.e.* with a heating rate of 10 K min⁻¹ under nitrogen flow (50 mL min⁻¹) from -70 to 300 °C.

Dynamic mechanical analyses (DMA) were performed using parallelepipedic specimens (30 x 6 x 3 mm³) in an ARES-G2 rheometer under torsion mode as a function of temperature under a

heating rate of 3 K min⁻¹. Storage modulus, G', loss modulus, G'', and loss factor, tan δ, were measured from -120 to 250 °C.

Uniaxial compression tests were performed using a MTS 2/M electromechanical testing system at 22 ± 1 °C and 50 ± 5 °C relative humidity for a crosshead speed of 1 mm min⁻¹ on conventional specimens (5 x 5 x 16 mm³). ASTM D695 standard test recommendations were followed. Young's modulus, E, was determined as the slope of the stress-strain curve in the linear domain, *i.e.* at low strain values. Yield strength, σ_y, was taken, as the maximum stress value on stress-strain curve, the strain and stress at break were also determined.

Fracture toughness (K_{IC}, G_{IC})

Fracture properties of neat epoxy-amine and epoxy hybrid O/I networks were determined using compact tension (CT) specimens following the ISO 13586 standard (Scheme III. 2). The primary V notch was machined with a milling machine and the final sharp crack was created by razor tapping at the edge of the main notch. The ratio of the crack length to width, *i.e.* a/w, must be maintained between 0.2 and 0.8. K_{IC} was calculated using the following equation (2):

$$K_{IC} = f(a/w) F_Q / h \sqrt{w} \quad (2)$$

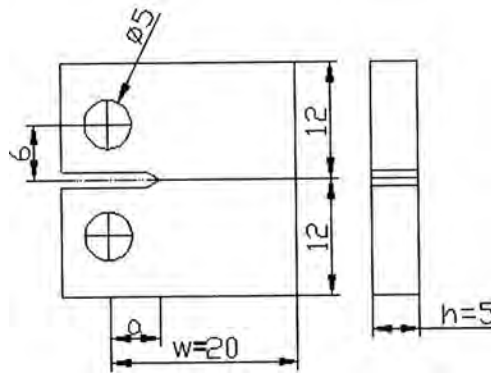
where F_Q (N) is the load for crack propagation, a (m) the crack length, w (m) the width, h (m) the thickness of the specimen, and f(a/w) a geometrical constant (Equation 3) :

$$f(a/w) = ((2 + a)/(1 - a)^2)^3 (0.886 + 4.64a - 13.32a^2 + 14.72a^3 - 5.6a^4) \quad (3)$$

The critical stress intensity factor, K_{IC}, is obtained following the standard procedure while the fracture energy, G_{IC}, in plane stress conditions, was calculated using the following equation (4):

$$G_{IC} = \frac{K_{IC}^2}{E} (1 - \nu^2) \quad (4)$$

where ν is the Poisson's ratio (taken to be 0.35) and E the Young's modulus.



Scheme III. 2: Compact Tension specimen configuration.

Surface energy of resulting epoxy networks was determined from the sessile drop method using a GBX goniometer. From contact angle measurements measured with water and diiodomethane as probe liquids. Polar and dispersive components of surface energy were determined using Owens-Wendt theory ⁶⁶.

Thermogravimetric analyses (TGA) were performed using a Q500 thermogravimetric analyzer (TA instruments). The samples were heated from 30 to 900 °C at 20 K min⁻¹ under air.

Flammability was investigated using a pyrolysis combustion flow calorimeter (PCFC from Fire Testing Technology, UK) initially developed by Lyon and Walters ⁶⁷. The sample (3 ± 0.5 mg) was heated up to 750 °C at 1 K.s⁻¹ in a pyrolyzer under nitrogen flow (anaerobic pyrolysis). The pyrolysis gases were sent to a combustor and mixed with oxygen in excess at 900 °C. In such conditions, these gases were fully oxidized. Heat Release Rate (HRR) was then calculated by oxygen depletion according to Huggett's relation (1 kg of consumed oxygen corresponds to 13.1 MJ of released energy) ⁶⁸.

Cone calorimeter experiments were performed using a fire Testing Technology equipment, according to the standard ISO 5660 ⁶⁹. Square samples of 100 x 100 x 30 mm³ were cut out of larger sheets and their edges polished and wrapped in an aluminum foil leaving only the upper surface apparent to the heater and the lower surface insulated by rock wool. The sample holder was left to cool to room temperature between each test. Every specimen was exposed horizontally under an external heat flow (irradiation) of 35 Kw.m⁻². Two specimens were tested for each material and the reported data are the average of the two measurements.

Some tests were recorded using an infrared camera (Optris) placed in an inclined position above the specimen in order to record the temperatures of the top surface. The measured temperature depends not only on the surface temperature but also on the tilt of the apparatus relatively to the surface and the emissivity of the materials. Emissivity was chosen equal to 1 (close to conventional values for polymer materials). In these tests, the distance between the radiant cone and the sample was set to 60 mm. Thereby; the tilt of the infrared camera is only of few degrees relative to the perpendicular position, which limits the error of measurements. The uncontrolled expansion of the specimen during burning can also modify this tilt during the test. Finally, the flame can slightly change the measured temperatures. Further description of such device can be found elsewhere ⁷⁰.

Scanning electron microscopy (SEM) (performed using FEI Quanta 200 ESEM) at an acceleration voltage of 12.5 kV was used to characterize the microstructure of the residual char of samples after the fire test as well as the fracture surface of broken K_{IC} specimens.

Energy Dispersive X-ray spectroscopy (EDX) using Oxford INCA Energy 300 system and a detector of 133 eV was used to determine elemental compositions of residues from the cone calorimeter tests.

III.3. Results and Discussion

III.3.1. Curing of epoxy-amine and hybrid O/I networks

First, the curing behavior of the epoxy-amine and the different hybrid O/I networks were evaluated with DSC measurements in order to highlight the impact of IL-g-POSS^{®Ph} and POSS^{®Ph}-triol on the reactivity of the polymerization reaction (Figure III. 1). As shown in Figure III. 1, all the reactive systems, *i.e.* DGEBA/IPD without and with unmodified or modified POSS[®], display an exotherm with a shoulder. According to the literature, such behavior can be attributed to the adduct formation followed by a step-growth polymerization^{2,40}. Nevertheless, two different behaviors were observed. DGEBA/IPD system with and without POSS^{®Ph}-triol displays the same behavior with an exothermic peak located at 115 °C while DGEBA/IPD containing IL-modified POSS^{®Ph} shows a significant decrease of the temperature of the exotherm. This shift of the exothermic peak to lower temperatures can be explained by the presence of imidazolium-based ionic liquid well-known to act as catalytic agent in epoxy-amine systems^{54,71,72}, *i.e.* favoring an early initiation of the polymerization. In addition, a slight increase of the total enthalpy value, ΔH , was observed in presence of IL.Cl-g-POSS^{®Ph} (482.1 J g⁻¹) and IL.NTf₂-g-POSS^{®Ph} (496.5 J g⁻¹) compared to neat epoxy-amine system (460.4 J g⁻¹). Furthermore, the thermograms of hybrid O/I networks containing IL-g-POSS^{®Ph} with different anions show a small additional exothermic peak at higher temperatures (200 - 250 °C) that can be attributed to the reaction of the imidazolium ionic liquid with epoxy groups^{37,54,72-74}. To confirm this hypothesis, the remaining soluble fraction after curing of the different systems was determined and characterized by FT-IR and ¹³C-NMR in order to check their compositions (see Figures S3.4, S3.5 and S3.6). In the case of epoxy networks containing 5 wt. % of POSS^{®Ph}-triol, the soluble fraction was determined to be 4.8 % which means that POSS^{®Ph}-triol clusters are not chemically attached to the epoxy network. For the same amount of IL-grafted POSS^{®Ph}, the

soluble fraction was found to be 3.4 and 3.6 % for IL.Cl-g-POSS^{®Ph} and IL.NTf₂-g-POSS^{®Ph}, respectively. Hence, a covalent grafting of these IL-modified POSS^{®Ph} with the epoxy network is ensured for about 30 % of the nano-clusters, while the rest of POSS^{®Ph} remained unbound. In summary, all these results suggest that the use of imidazolium ionic liquid grafted to the POSS^{®Ph}-triol with both anions (Cl⁻, NTf₂⁻) acts as an initiator for the ring-opening reaction of the epoxy and a co-curing agent of DGEBA, in agreement with previous studies^{37,72}.

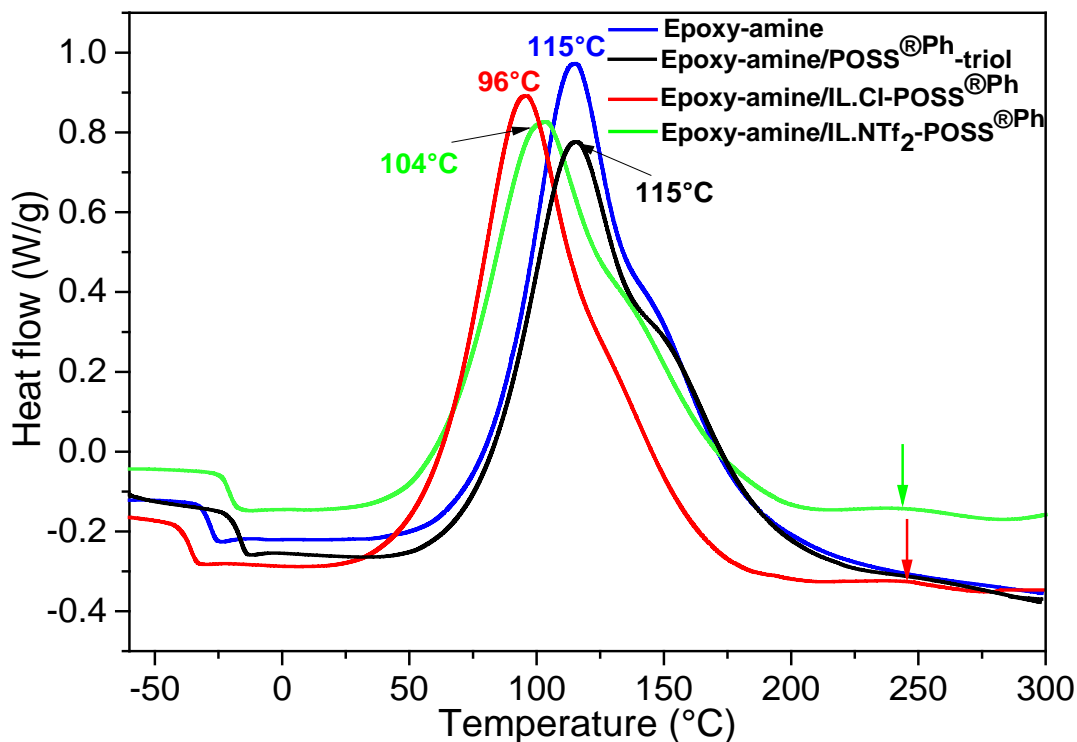


Figure III. 1: DSC traces of the neat epoxy-amine and the epoxy hybrid O/I reactive systems containing 5 wt. % POSS^{®Ph}-triol or IL-g-POSS^{®Ph} functionalized with Cl⁻ and NTf₂⁻ (heating rate: 10 K min⁻¹).

In addition, the reaction kinetics, *i.e.* the quantification of the epoxide groups conversion, for all the reactive systems were investigated by FT-IR spectroscopy following the curing conditions. All the reactive systems were analyzed in the wavelength region of 800 - 1,300 cm⁻¹ in order to follow the changes of the adsorption bands at 914 and 1,184 cm⁻¹ corresponding to the epoxy groups and the ether linkage, respectively⁵². The conversion of epoxy groups was calculated using equation (5)^{40,52,58,75}:

$$X\% = ((A_0 - A_t) / A_0) 100\% \quad (5)$$

where A_0 and A_t are the ratios between the area of two absorption bands at 914 and 1,184 cm^{-1} (A_{914}/A_{1184}) of the reactive system at the beginning of the reaction ($t = 0$) and at a given reaction time t , respectively. Thus, the epoxy conversion versus the polymerization time, is presented in Figure III. 2 for the neat epoxy-amine and the various epoxy hybrid O/I systems.

In all cases, a final epoxy conversion higher than 90 % was obtained confirming the reactivity of DGEBA with IPD and with or without the presence of unmodified or modified POSS^{®Ph}. During the step at 140 °C, a fast consumption of epoxy functions was observed for epoxy containing IL-g-POSS^{®Ph} (see inset in Figure III. 2) whatever the chemical nature of the anion. At 190 and 230 °C, a progressive consumption of epoxy groups was evidenced confirming the DSC results and highlighting a competition between two polymerization mechanisms, *i.e.* the epoxy-amine reaction and the reaction between IL-g-POSS^{®Ph} and epoxy prepolymer³⁷.

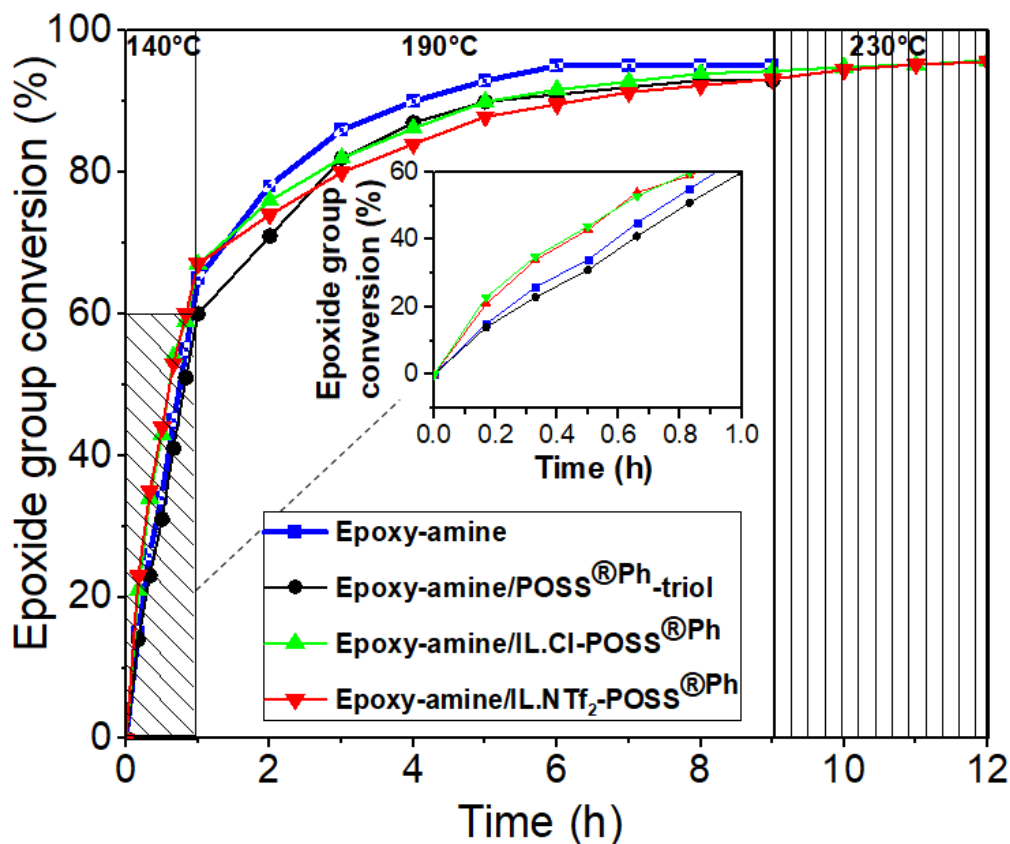


Figure III. 2: Conversion of epoxide groups versus reaction time during the curing process of the neat epoxy-amine and the epoxy hybrid O/I networks containing POSS^{®Ph}-triol and IL-g-POSS^{®Ph} with different anions (Cl⁻ and NTf₂⁻).

It can be concluded, one can conclude that whatever the anion nature, the reactivity of the imidazolium ionic liquid grafted onto the POSS^{®Ph}-triol nanoclusters towards the epoxy prepolymer (DGEBA) compared to the reactivity of the diamine co-monomer (IPD) plays a key role in the kinetics of polymerization and consequently on the architecture of the formed hybrid O/I epoxy networks.

III.3.2. Morphology of hybrid O/I networks

Transmission electronic microscopy is a powerful tool to highlight the effect of IL-g-POSS^{®Ph} combined with Cl⁻ or NTf₂⁻ on the dispersion of the POSS[®] nanoclusters into epoxy networks. The morphologies obtained for the different epoxy hybrid O/I networks are displayed in Figure III. 3 and the distributions of the POSS[®]-rich dispersed phase sizes (using Image J Software) are reported in Figure III. 4. In all TEM micrographs, the dark zones correspond to the silicon-rich phases and the bright continuous phase corresponds to the epoxy-amine network.

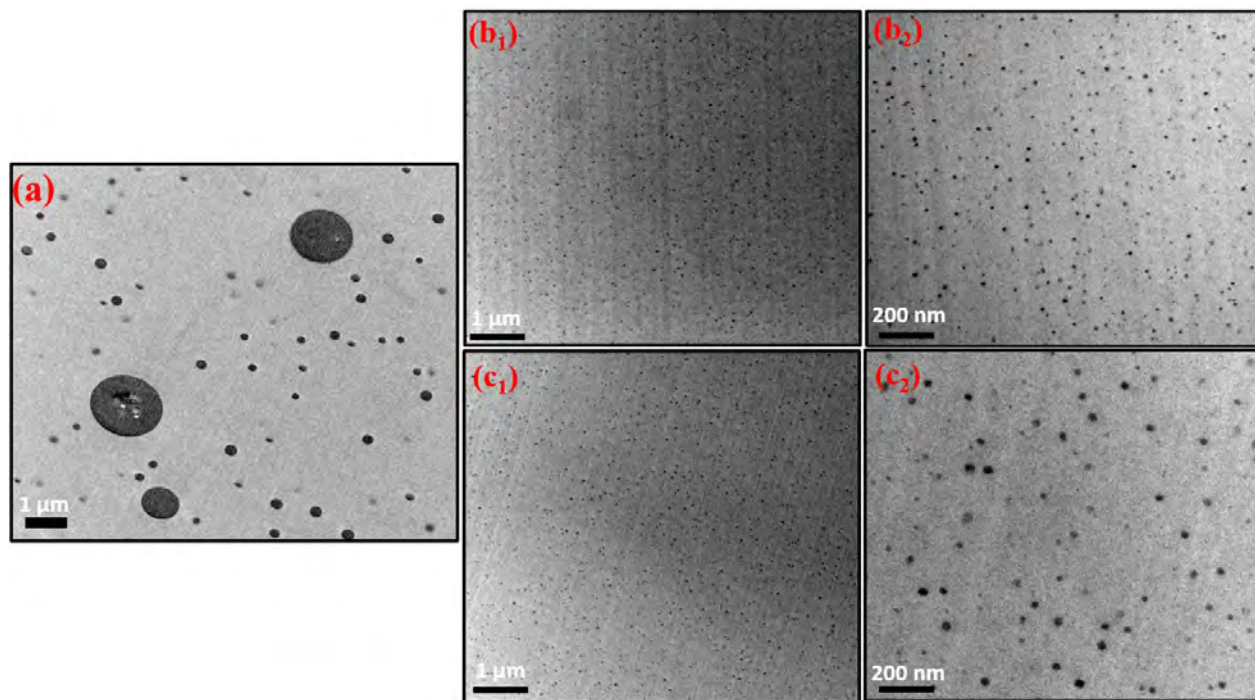


Figure III. 3: TEM micrographs of the epoxy hybrid O/I networks containing a) POSS^{®Ph}-triol; b) IL.Cl-g-POSS^{®Ph} at different magnification (b₁; b₂) and c) IL.NTf₂-g-POSS^{®Ph} at different magnification (c₁; c₂).

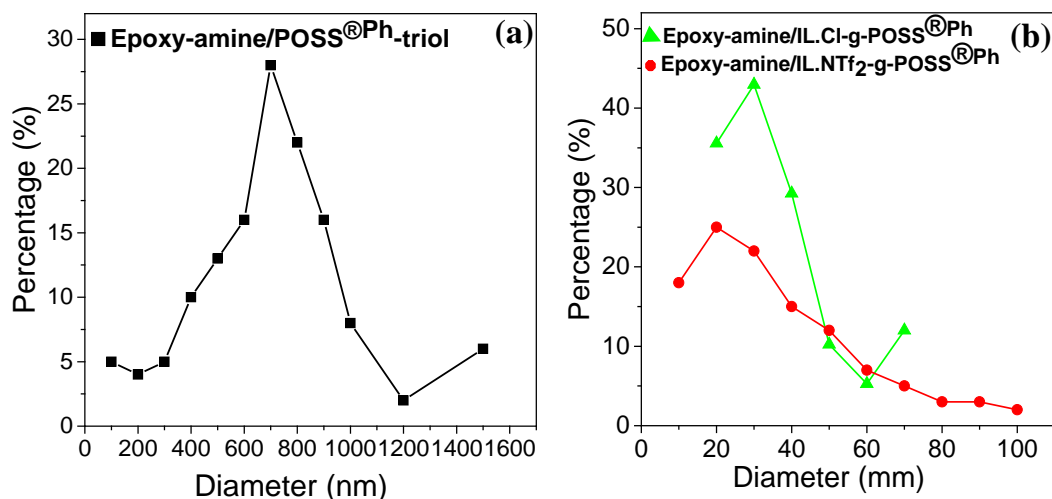


Figure III. 4: Size distribution of POSS[®]-rich dispersed phases in the epoxy hybrid O/I networks containing a) POSS^{®Ph}-triol and b) IL-g-POSS^{®Ph} with different types of anion (Cl⁻ and NTf₂⁻).

In all cases, a homogeneous distribution in the epoxy matrix was observed. The POSS^{®Ph}-rich dispersed phase has spherical or ellipsoidal shapes in the different systems with a large diameter distribution ranging from 0.1 to 1.5 μm for the epoxy hybrid networks containing POSS^{®Ph}-triol. Regarding the literature there is no difference on the TEM images between any closed inert POSS^{®Ph} and open POSS^{®Ph}-triol, generally inert POSS[®] remains undispersed or non-homogeneously dispersed and even tends to agglomerate in the mixing system due to the poor interfacial adhesion^{76,77}. The POSS^{®Ph}-triol can also form hybrids with large aggregates due to the hydroxyl groups of the open cage (POSS[®]-triol) that are well hidden because of hydrogen bonds between POSS[®]-triol particles^{78,79}. For this reason, several authors have tried to use some modifiers (metal complex) for better dispersion^{78,79}. The epoxy networks containing IL-g-POSS^{®Ph} have a narrower diameter distribution ranging only from 10 to 100 nm whatever the chemical nature of the counter anions (Cl⁻ or NTf₂⁻). According to the literature, various authors demonstrated that IL-functionalized silica nanoparticles having different counter anions (Cl⁻ and MeSO₃⁻) led to well dispersed silica aggregates having a size of few tens of nanometers^{37,38,80}. Thus, as for nanocomposites based on silica nanoparticles, the imidazolium ILs act as efficient interfacial agents for inorganic-rich nano-objects in epoxy-amine networks.

III.3.3. Thermomechanical properties of the resulting networks

The influence of the unmodified and modified POSS^{®Ph} on the thermomechanical properties of the epoxy-amine networks was investigated by Dynamic Mechanical Analysis (DMA) (Figure III. 5a).

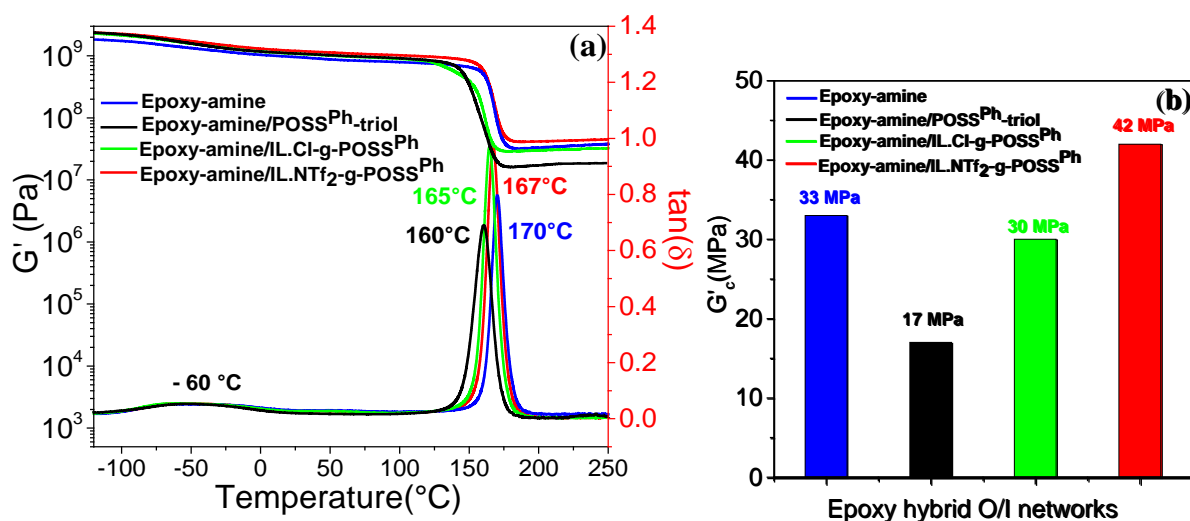


Figure III. 5: a) Dynamic mechanical spectra and b) shear storage moduli in the rubbery state, G'_c (at 200 °C) of the epoxy-amine and the epoxy hybrid O/I networks containing POSS^{®Ph}-triol and IL-g-POSS^{®Ph} (5 wt.%) with different anions (Cl⁻ and NTf₂⁻) at 1 Hz.

The DMA spectra of the different epoxy networks allow to determine the storage and loss moduli, as well as the temperature positions of the tan δ relaxation peaks (T_β, T_α) over the investigated temperature range (from -100 to 250 °C) at a given frequency. For all the epoxy networks, the narrowness of the main relaxation peak (T_α - associated to the glass transition) in the 160 - 170 °C temperature range suggests that the epoxy-amine networks display a homogeneous structure^{19,81}. Moreover, all the epoxy networks exhibit a secondary transition at -60 °C corresponding to the β-relaxation which is attributed to the local motions of hydroxyether [-CH₂-CH(OH)-CH₂-O-] and bisphenol-A units of the epoxy-amine network⁸². The hybrid O/I epoxy network containing POSS^{®Ph}-triol displays the lowest temperature of the α-transition (160 °C) as well as the lowest shear modulus in the rubbery state, G'_c. This observation suggests that POSS^{®Ph}-triol displays poor interactions at the epoxy-amine network/POSS[®]-rich dispersed phase interface in agreement with the previously observed morphologies. Indeed, the reaction between the hydroxyl groups from POSS^{®Ph}-triol and epoxy functions from the DGEBA prepolymer

requires specific conditions to occur, like those reported by Hongzhi *et al.*⁷⁹ who obtained epoxy/POSS^{®Ph}-triol networks only through the introduction of a metal complex such as aluminum triacetylacetonate (Al), used as catalyst.

The DMA results are also in good agreement with the DSC measurements as only one glass transition temperature could be evidenced (see Figure S3.7 in the SI of chapter III). The shear storage moduli, G'_c (Figure III. 5b) in the rubbery state of the hybrid O/I epoxy networks containing IL-g-POSS^{®Ph} with different anions are slightly higher than the one of the neat epoxy possibly due to a nanoreinforcement effect and a slightly increased crosslink density. Such behavior is a direct consequence of both chemical bonding and physical interactions generated at the O/I interface, *i.e.* between the ionic liquid-grafted POSS^{®Ph} nano-objects and the epoxy network as well as between POSS[®] cages via their phenyl ligands²³.

III.3.4. Mechanical properties

III.3.4.1. Elastic and large strain mechanical properties

The influence of the presence of non-modified and IL-grafted POSS^{®Ph} on the uniaxial compression response of the different epoxy networks was studied. The values of Young's modulus, yield stress, strain and stress at break are summarized in Table III. 2. In addition, the stress-strain curves are given in Figure III. 6.

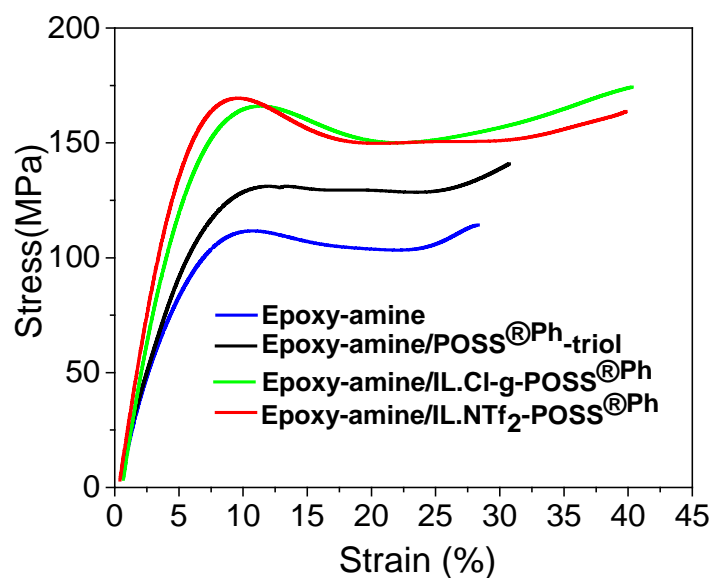


Figure III. 6: Stress-strain curves recorded under compression of the neat epoxy-amine and the epoxy hybrid O/I networks at room temperature (1 mm.min⁻¹).

The addition of POSS^{®Ph}-triol improves all the mechanical components. However, the presence of IL-g-POSS^{®Ph} nanoclusters with both anions (Cl⁻ or NTf₂⁻) induces a significant reinforcement effect. Increasing both stiffness, yield strength, and the ability to sustain larger deformation and stress at break is not a common feature for highly crosslinked networks even less when they are filled with inorganic nano-objects^{83,84}. For example, Donato *et al.*⁸⁰ considering epoxy-silica nanocomposites and using different imidazolium ILs only as free additive catalysts, reported lower improvements for higher silica contents (7.5 wt %), *i.e.* an increase in the Young's modulus and strain at break up to 2 and 41 %, respectively. The same group also reported significant improvements of mechanical properties (Young's modulus increased only of 7 % and strain at break increased of 47 %) by grafting imidazolium IL combined with different anions (Cl⁻ and MeSO₃⁻) onto silica particles and with less content of each IL-silica (< 6.8 wt %) ³⁸. We attributed the improved properties to the very fine dispersion of the IL-grafted POSS^{®Ph} nanoclusters into the epoxy-amine network as well as to the strong interactions formed at their interface. In fact, the grafted imidazolium-based ILs reduce the POSS^{®Ph} aggregation and generate a strong and reversible interaction between nanoclusters and the epoxy-amine matrix. The mutual dipole-ion interactions between IL-g-POSS^{®Ph} nanostructures and the network chains enable a higher cohesion and can sustain larger stresses and strains before break.

Table III. 2: Mechanical properties of the neat epoxy-amine and the epoxy hybrid O/I networks measured under uniaxial compression (1 mm.min⁻¹; 25 °C).

Material	Young's modulus (GPa)	Yield stress (MPa)	Stress at break (MPa)	Strain at break (%)
Epoxy-amine	2.3 ± 0.1	114 ± 9	114 ± 4	28 ± 2
Epoxy-amine/POSS ^{®Ph} -triol	2.9 ± 0.1	131 ± 9	141 ± 6	31 ± 2
Epoxy-amine/IL.Cl-g-POSS ^{®Ph}	3.0 ± 0.1	166 ± 11	174 ± 3	40 ± 3
Epoxy-amine/IL.NTf ₂ -g-POSS ^{®Ph}	3.1 ± 0.1	170 ± 10	164 ± 5	40 ± 2

III.3.4.2. Fracture properties

The influence of the non-modified and IL-grafted POSS^{®Ph} on the stress intensity factor, K_{IC}, and fracture toughness, G_{IC}, of epoxy-based networks was investigated using compact-tension

fracture test (CT). The values of the critical stress intensity factor, K_{IC} , of neat epoxy-amine and epoxy hybrid O/I networks are summarized in Table III. 3.

Table III. 3: Fracture properties of the neat epoxy-amine and the epoxy hybrid O/I networks.

Material	K_{IC} (MPa m ^{1/2})	G_{IC} (J m ⁻²)
Epoxy-amine	0.71 ± 0.08	192 ± 40
Epoxy-amine/POSS ^{®Ph} -triol	0.61 ± 0.08	113 ± 40
Epoxy-amine/IL.Cl-g-POSS ^{®Ph}	1.02 ± 0.06	305 ± 30
Epoxy-amine/IL.NTf ₂ -g-POSS ^{®Ph}	0.98 ± 0.06	271 ± 30

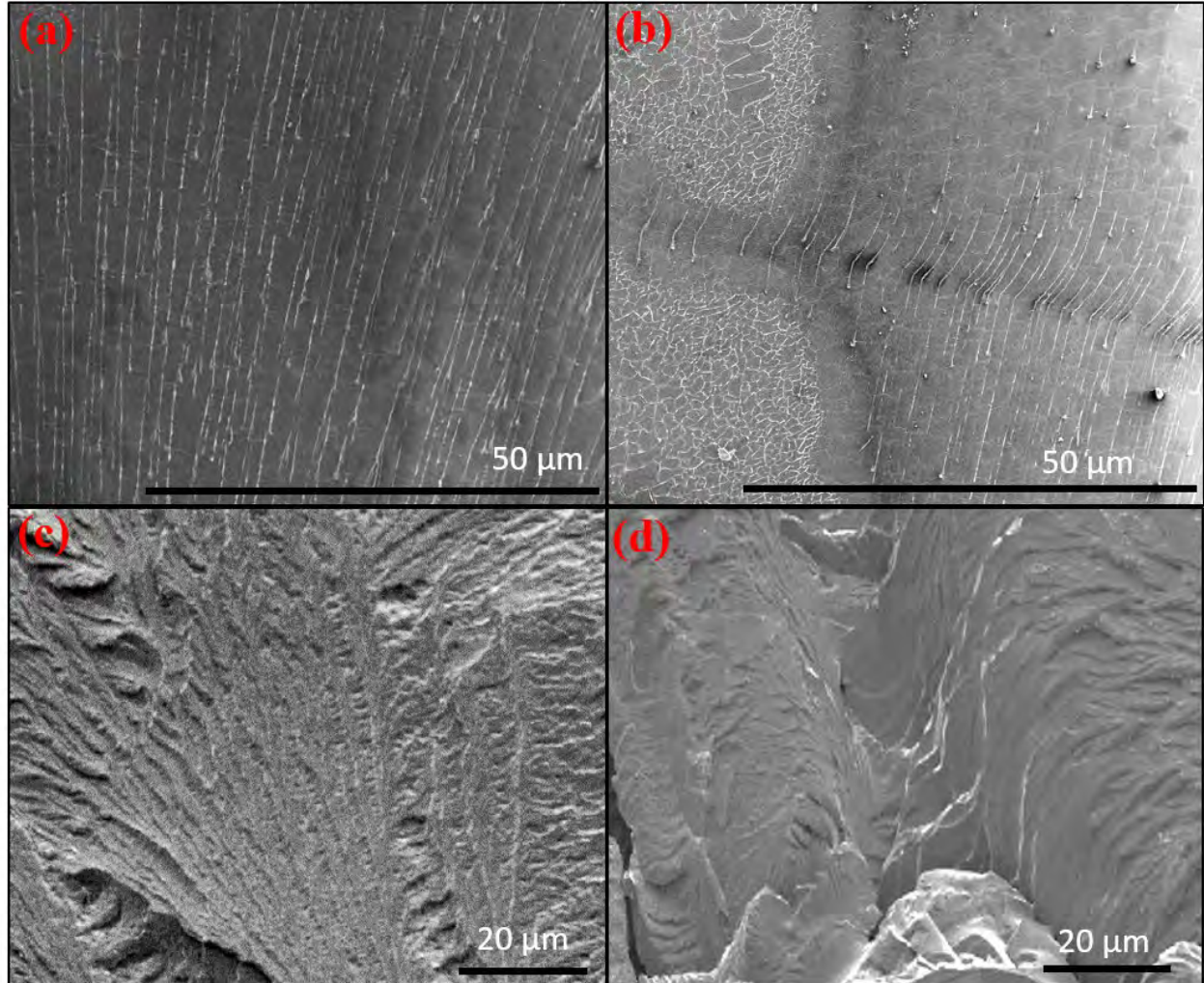


Figure III. 7: SEM images of fractured surfaces of a) the neat epoxy-amine and the epoxy hybrid O/I networks containing b) POSS^{®Ph}-triol, c) IL.Cl-g-POSS^{®Ph}, and d) IL.NTf₂-g-POSS^{®Ph}.

The fracture properties of the neat epoxy-amine network are in agreement with the literature^{65,85,86}. In the case of the hybrid O/I epoxy networks based on the different types of POSS[®], two different behaviors are observed. The hybrid network containing the POSS^{®Ph}-triol displays lower fracture properties compared to the neat epoxy-amine network whereas the hybrid O/I epoxy networks containing IL-g-POSS^{®Ph} exhibit higher K_{IC} and G_{IC} . As shown in Figure III. 3, this difference can be attributed to the smaller (10 - 100 nm) and more uniform and well-dispersed POSS[®] aggregates for IL-g-POSS^{®Ph} hybrids whatever the nature of the anion (Cl^- or NTf_2^-) as well as to their improved interfacial interactions. While, the non-grafted POSS[®], which are assembled in larger (up to micron-size) and less cohesive aggregates, act as local defects leading to a lower crack propagation resistance. According to the literature, ILs can act as dispersing agents for high- T_g thermoplastics⁸⁷, core-shell particles^{88,89}, or nanoparticles added to epoxy networks and have a significant influence on the fracture toughness of the modified networks^{80,87,90-92}. Also, as K_{IC} is known to be strongly affected by the nanocomposites morphology and interfacial characteristics, a fine dispersion of such stiffer fillers ensures the promotion of efficient toughening mechanisms: increase of the process zone size, crack pinning and branching leading to a deviation of the crack propagation^{38,80,93}.

SEM micrographs of fractured surface after crack initiation and catastrophic failure are presented in Figure III. 7. Two types of fracture behaviors are evidenced depending on the presence or not of imidazolium IL. The smooth and featureless surface, as shown in Figures III. 7a and 7b for the neat epoxy-amine and the epoxy hybrid containing POSS^{®Ph}-triol, gives evidence of its brittle failure and low fracture toughness, which can be denoted as mirror-like fracture surface. On the opposite, the epoxy hybrid O/I networks by the addition of IL-g-POSS^{®Ph} with different anions (NTf_2^- , Cl^-) show a very rough and irregular fracture surface with ridges, river and cracks marks (Figures III. 7c and 7d). According to the literature, such features are representative of a higher energy for the crack propagation, *i.e.* a higher fracture toughness⁹⁴⁻⁹⁶.

III.3.5. Surface properties

Surface energies of the neat epoxy-amine and the hybrid O/I epoxy networks were determined by the sessile drop method using Owen-Wendt theory⁶⁶. Therefore, the non-dispersive and dispersive components were calculated from the water and methylene diiodide contact angles (Table III. 4).

In all cases, the addition of 5 wt % of unmodified (POSS^{®Ph}-triol) or IL-grafted modified POSS[®] (IL-g-POSS^{®Ph}) leads to a decrease of the surface energy which results from the combined reductions of the dispersive and non-dispersive components. These results can be explained by the hydrophobic character of the POSS[®] molecules composed of phenyl ligands ⁹⁷. However, the grafting of POSS^{®Ph} with imidazolium ionic liquids also plays a key role in the hydrophobicity of the epoxy network as shown by the significantly decreased surface energy for IL-modified POSS^{®Ph} systems (Table III. 4). Indeed, the values obtained here are similar to the ones measured for different fluorinated polymers such as PTFE ⁹⁸. This surface behavior can be clearly attributed to the presence of the imidazolium IL which is well-known to have low surface tension ⁹⁹. According to the literature, the incorporation of various amounts of phosphonium or imidazolium ILs into epoxy networks leads to the formation of highly hydrophobic networks opening many perspectives in the field of paints and coatings used as protective layers for corrosion. These results are also lower than those of epoxy modified by fillers with 3.5 phr of silica ¹⁰⁰ or 10 phr of an amphiphilic triblock copolymer bearing a poly(butadiene-g-POSS[®] block) ¹⁰¹. Similar results were also found in the literature when using high amount (10 wt %) of POSS[®]-capped poly(ethylene oxide) ^{102,103}.

Table III. 4: Determination of dispersive and non-dispersive components of the surface energy of the neat epoxy-amine and the epoxy hybrid O/I networks from contact angles with water and methylene diiodide (at 25 °C).

Samples	Θ_{Water} (°)	$\Theta_{\text{CH}_2\text{I}_2}$ (°)	$\gamma_{\text{non-dispersive}}$ (mJ.m ⁻²)	$\gamma_{\text{dispersive}}$ (mJ.m ⁻²)	γ_{total} (mJ.m ⁻²)
Epoxy-amine	79	49	4.8	34.8	39.6
Epoxy-amine/POSS ^{®Ph} -triol	96	51	0.7	33.4	34.1
Epoxy-amine/IL.Cl-g-POSS ^{®Ph}	99	64	0.4	26.2	26.6
Epoxy-amine/IL.NTf ₂ -g-POSS ^{®Ph}	105	67	0.5	22.7	23.2

III.3.6. Thermal-oxidative stability

The weight loss as a function of temperature under air atmosphere as well as the initial decomposition temperature ($T_{d5\%}$) and the maximal degradation temperature ($T_{d\text{max}}$) of the hybrid O/I epoxy networks were measured by TGA and are presented in Figures III. 8a and 8b.

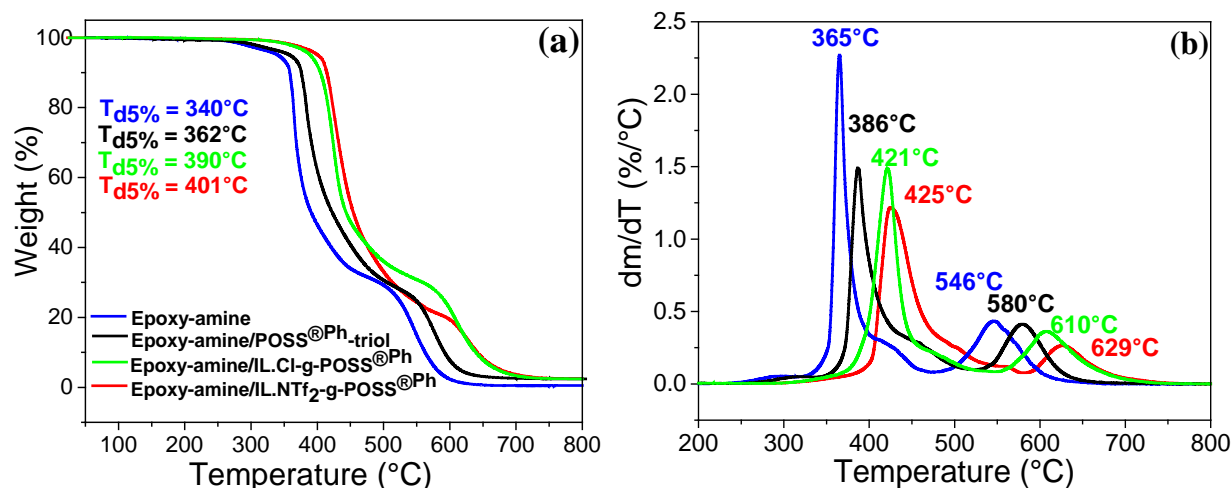


Figure III. 8: a) Weight loss (TGA) and b) derivative of TGA as a function of temperature (DTG) of the neat epoxy-amine and the epoxy hybrid O/I networks under air atmosphere (10 K.min⁻¹; atmosphere: air flow).

The TGA traces of the epoxy-amine hybrid O/I networks display the same decomposition behavior as the neat system which is characterized by two decomposition steps. The first and more pronounced weight loss occurs from 350 to 500 °C and corresponds to the simultaneous decomposition of the organic matrix, IL, and phenyl ligands of the POSS^{®Ph} cages as well as the formation of carbonaceous compounds. During the second step of thermal degradation occurring from 500 to 650 °C, these carbonaceous compounds are oxidized and volatilized¹⁰⁴. An increase of thermal stability of epoxy networks containing POSS^{®Ph} nanoclusters compared to the neat epoxy-amine network is clearly observed. It is worth noting that the epoxy/IL-g-POSS^{®Ph} hybrid containing the different types of anion exhibit a higher stability compared to the epoxy/POSS^{®Ph}-triol hybrid. In addition, the presence of the NTf₂⁻ anion improves better the thermal stability, especially the resistance to oxidation during the second step (see Figure III. 8b). This phenomena can be explained from the existence of improved interfacial interactions between the epoxy matrix and the IL-grafted POSS^{®Ph}^{105,106} and the nanoscale dispersion of the later nano-objects acting as a more efficient barrier against heat and oxygen transport²². In fact, well-dispersed POSS[®] nanoclusters at the molecular level can suppress mass loss from segmental decomposition via gaseous fragments. Such a behavior is very similar to that reported in the literature for fully exfoliated clay-polymer nanocomposites³³. In summary, a real synergistic effect between

POSS^{®Ph} and ionic liquids takes place leading to a significant increase of the thermal stability of the resulting networks.

III.3.7. Fire resistance

III.3.7.1. Flammability

Flammability data from PCFC tests are listed in Table III. 5 and HRR curves are plotted versus temperature in Figure III. 9 for all the different epoxy networks. In addition, epoxy-amine without POSS[®] but with both IL, *i.e.* IL.Cl or IL.NTf₂ have also been considered as extra references.

Peak of heat release rate (pHRR) and Total heat release (THR) are respectively 559 W g⁻¹ and 29.4 kJ g⁻¹ for the neat epoxy-amine network and are in a good agreement with previously published data ¹⁰⁷. The epoxy hybrid O/I network containing POSS^{®Ph}-triol does not exhibit much better flammability properties. In fact, pHRR is just slightly lower and appears at the same temperature while THR is reduced to 26.9 kJ g⁻¹. Nevertheless, the residue content is slightly increased (from 6 to 15 wt %). The epoxy-amine networks containing only ILs without POSS[®] exhibit a lower pHRR (400 - 450 W g⁻¹) while their THR is still in the range 26 - 28 kJ g⁻¹, and their residue content is still relatively low (< 10 wt %). The main difference between the two systems concerns their thermal stability. While IL.NTf₂ does not modify the temperature at pHRR in comparison to the neat epoxy-amine network, IL.Cl leads to a significant increase of the temperature of pHRR up to 450 °C. Both hybrid O/I epoxy networks containing IL.Cl-g-POSS^{®Ph} and IL.NTf₂-g-POSS^{®Ph} also show better performances than the neat epoxy-amine network and the network containing POSS^{®Ph}-triol. Epoxy hybrid O/I network containing IL.Cl-g-POSS^{®Ph} exhibits similar performances to the epoxy-amine network containing IL.Cl. Nonetheless, a significant change was observed when IL.NTf₂ is grafted to a POSS^{®Ph}-triol in comparison to the network containing only IL.NTf₂. Indeed, the temperature at pHRR is shifted to a higher value of 442 °C while the residue content increases to 14 wt % and THR decreases to 21.9 kJ g⁻¹, making it the best flammability-resistant performer. Even if the temperature at peak is similar for both hybrids, epoxy-amine/IL.NTf₂-g-POSS^{®Ph} also appears to be slightly more thermally stable at low temperatures (in the range from 350 to 450 °C). Heat of complete combustion, Δh, is in the range 29 - 32 kJ g⁻¹, except for epoxy-amine/IL.NTf₂-g-POSS^{®Ph} (25.5 kJ g⁻¹) confirming once again its best flammability-resistance. One can notice that no additional peak is evidenced at high

temperatures (above 500 °C) as observed in TGA. In fact, the second TGA peak is attributed to the thermo-oxidation of residues while pyrolysis in PCFC is performed under anaerobic conditions thus inhibiting this second step.

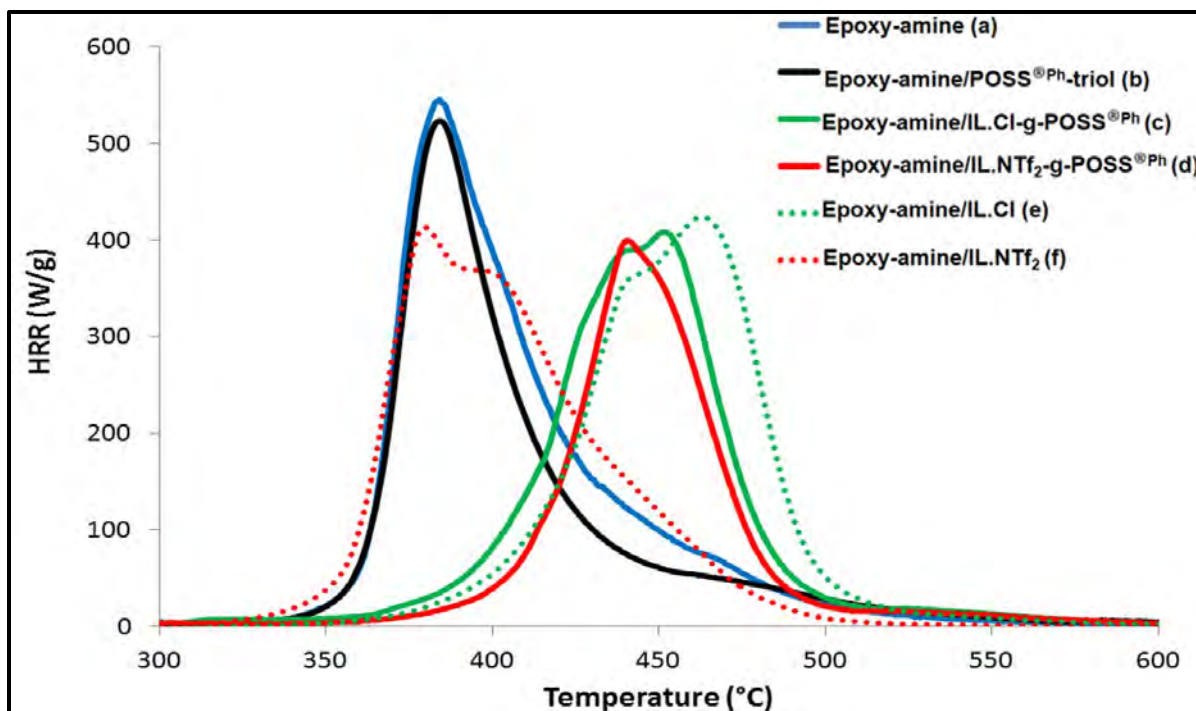


Figure III. 9: PCFC HRR traces of the neat epoxy-amine, the epoxy hybrid O/I networks, and the epoxy-amine networks containing IL.

Table III. 5: PCFC data of the neat epoxy-amine and the epoxy hybrid O/I networks.

Materials	pHRR (W.g ⁻¹)	TpHRR (°C)	THR (kJ.g ⁻¹)	Residue (wt. %)	Δh (kJ.g ⁻¹)
Epoxy-amine	559	382	29.4	6	31.1
Epoxy-amine/POSS ^{®Ph} -triol	498	379	26.9	15	31.6
Epoxy-amine/IL.Cl-g-POSS ^{®Ph}	418	447	26.5	9	29.2
Epoxy-amine/IL.NTf ₂ -g-POSS ^{®Ph}	409	449	21.9	14	25.5
Epoxy-amine/IL.Cl	433	450	26.2	8	28.5
Epoxy-amine/IL.NTf ₂	442	384	28.2	3	29.2

III.3.7.2. Fire behavior

Fire behavior of the neat epoxy-amine, the hybrid O/I epoxy networks, and the epoxy-amine networks containing only ILs was evaluated with cone calorimeter experiments, closer to real-world fire conditions. Indeed, PCFC cannot assess some phenomena as barrier effect. The HRR

curves, displayed in Figure III. 10, come as a support for Table III. 6 that lists the following data extracted from the cone calorimeter tests: time to ignition (TTI, in second), total heat released (THR, in kJ g⁻¹), peak of heat release rate (pHRR, in kW m⁻²), residual weight (RW in %), effective heat of combustion (EHC, in kJ g⁻¹), and total smoke released (TSR in m⁻²). Inspection of the char residues morphology was also carried out.

TTI is used to determine the influence of a flame-retardant on ignitability. Epoxy network containing only IL.NTf₂ exhibits a low time-to-ignition, *i.e.* 53 s. For other materials, TTI is much higher, close to 90 s. For the epoxy hybrid O/I networks, TTI does not decrease in comparison to neat epoxy-amine network. Such a stability of TTI is very valuable for enhancement of the flame-retardancy properties of epoxy resins³⁰. Indeed, phosphorus compounds are efficient fire-retardant additives promoting charring and reducing heat release rate in epoxy resins; unfortunately, most of them also enable an earlier ignition due to the deterioration of epoxy thermal stability by phosphoric acids while the present materials avoid this drawback.

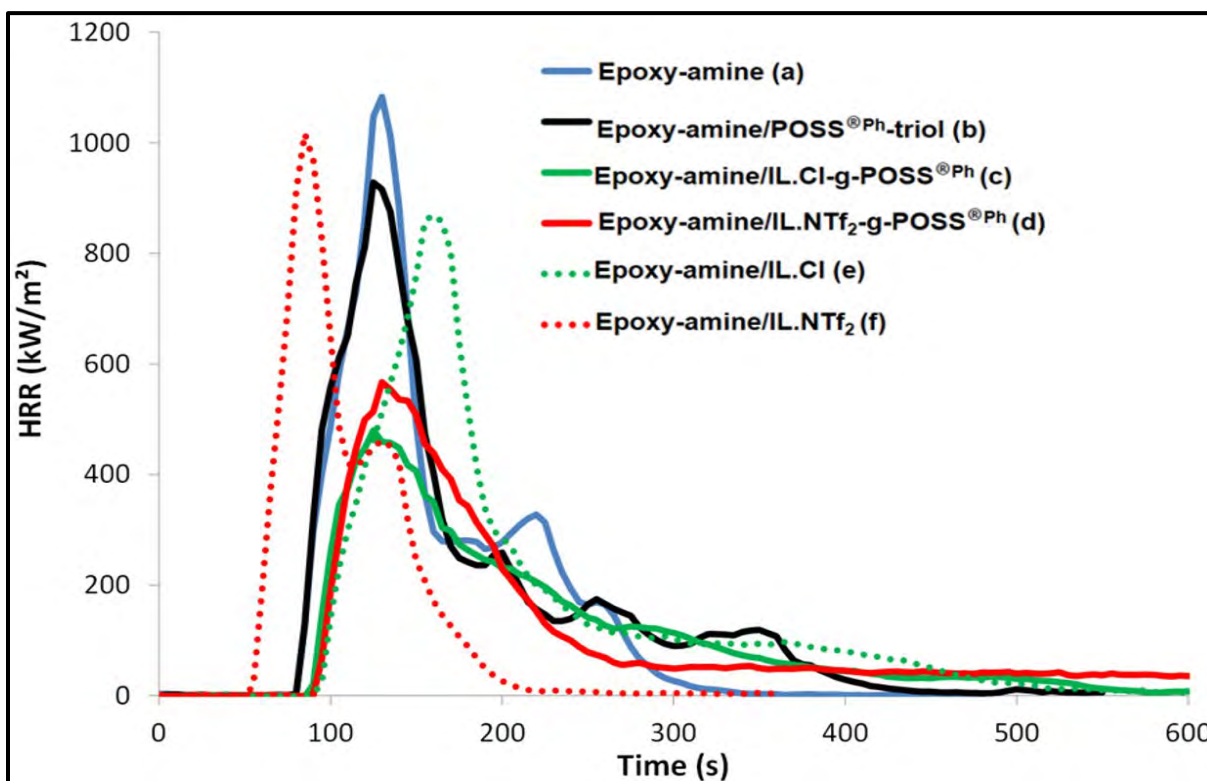


Figure III. 10: Cone calorimeter HRR curves of the neat epoxy-amine, the epoxy hybrid O/I networks, and the epoxy-amine networks containing IL.

Table III. 6: Cone calorimeter data of the neat epoxy-amine, the epoxy hybrid O/I networks, and the epoxy-amine networks containing IL.

Materials	TTI (s)	THR (kJ.g ⁻¹)	pHRR (kW.m ⁻²)	RW (%)	EHC (kJ.g ⁻¹)	TSR (m ²)
Epoxy-amine	82	22.2	1084	11.5	25.1	25.0
Epoxy-amine/POSS ^{®Ph} -triol	92	22.2	983	11.7	25.1	25.1
Epoxy-amine/IL.Cl-g-POSS ^{®Ph}	94	20.7	480	6.3	22.2	24.1
Epoxy-amine/IL.NTf ₂ -g-POSS ^{®Ph}	106	20.8	508	9.8	23.2	23.1
Epoxy-amine/IL.Cl	92	23.1	870	5.5	24.5	32.3
Epoxy-amine/IL.NTf ₂	53	25.0	1017	6.9	26.9	17.5

HRR curves for a, b, e, and f (Figure III. 10) show a sharp pHRR followed by a fast decrease to flame out. Such curves are indicative of a fast and uncontrolled burning. The neat epoxy-amine network is highly flammable and the HRR shows a sharp peak heat release rate (pHRR) of 1084 kW m⁻². When the POSS^{®Ph}-triol or ILs alone are added, the pHRR remains close to 1000 kW m⁻² while the two IL-g-POSS^{®Ph} modified epoxy networks exhibit a significant decrease. In several cases, a second peak is observed at the end of the test. pHRR for c and d are much lower (480 and 508 kW m⁻²) and a progressive decrease of HRR is observed from 250 s to flame out due to slow thermo-oxidation of the residue (flame is reduced and does not cover the whole sample, therefore thermo-oxidation can occur). These curves show that these samples highlight a so-called thick-charring behavior, *i.e.* the accumulation of a stable residue limiting the heat transfer from the flame to the outer part of the material slowing down its pyrolysis¹⁰⁸. The lack of additional peak at the end of burning may be ascribed to a quite good protective effect of the residue.

All the epoxy networks have a limited RW (5 - 12 %), similar THR (20 - 25 kJ g⁻¹) and TSR (21 - 26 m²) except the epoxy networks containing only ILs. Indeed, TSR is significantly higher for the network containing IL.Cl (maybe due to the presence of chlorine atoms) and lower for networks with IL.NTf₂. EHC is only slightly lower for the epoxy hybrid O/I networks containing IL.Cl-g-POSS^{®Ph} and IL.NTf₂-g-POSS^{®Ph} (22 - 23 kJ g⁻¹ versus 24.5 - 27 kJ g⁻¹). The combustion efficiency, *i.e.* the ratio between the effective heat of combustion and the heat of complete combustion measured in PCFC, is in the range of 0.76 - 0.90 for polymeric materials. It is not significantly lower for epoxy-amine containing IL.Cl or IL.Cl-g-POSS^{®Ph} despite the release of chlorine-containing gases. Chlorine is not detected in the residue from EDX analyses.

Nevertheless, this halogen is well known to act as flame poisoner but is probably in too low content to be effective here.

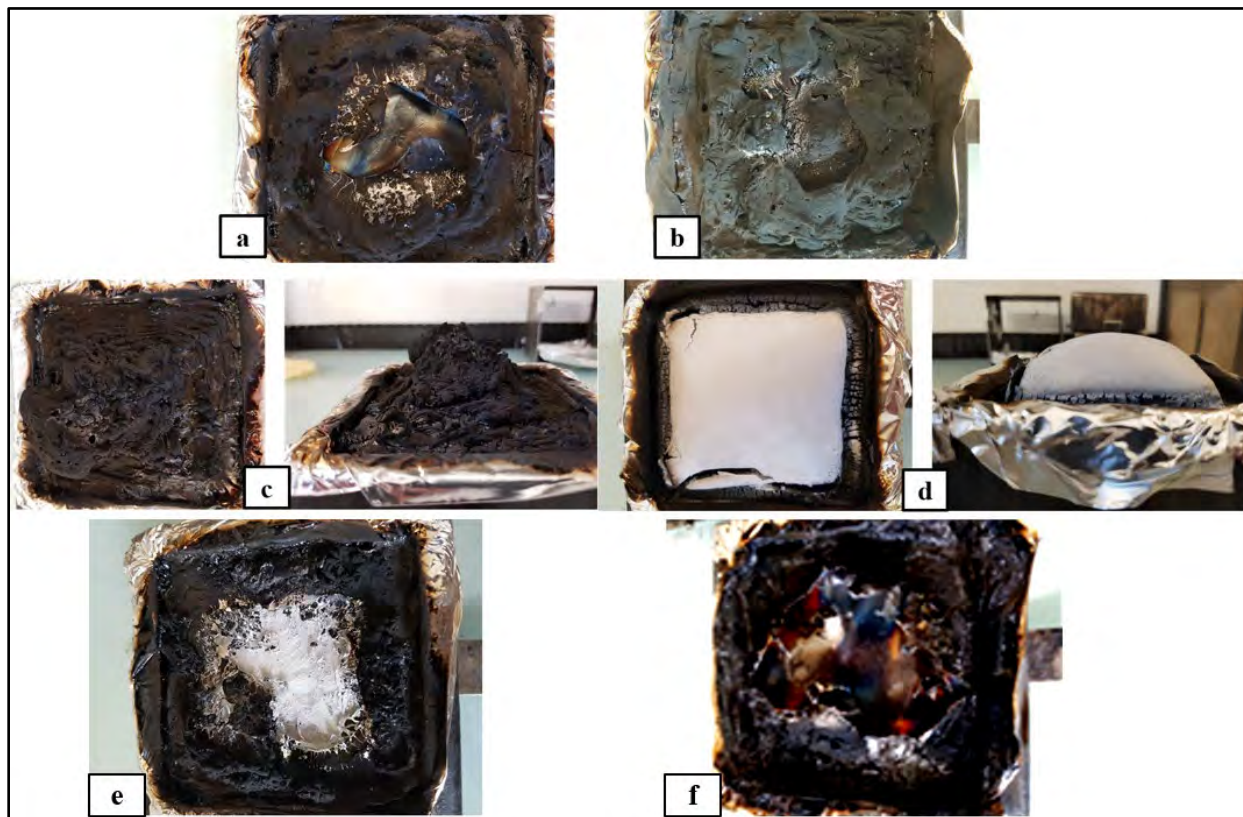


Figure III. 11: Cone calorimeter residue of a) the neat epoxy-amine and the epoxy hybrid O/I networks containing b) POSS^{®Ph}-triol, c) IL.Cl-g-POSS^{®Ph}, and d) IL.NTf₂-g-POSS^{®Ph}. Epoxy networks containing e) IL.Cl and f) IL.NTf₂.

Photographs of post-fire residues obtained after the cone calorimeter experiments are shown in Figure III. 11. As can be seen, the neat epoxy-amine, the epoxy networks containing just ILs and the epoxy hybrid O/I containing POSS^{®Ph}-triol and IL.Cl-g-POSS^{®Ph} networks left a small and poorly cohesive dome-like char whose top part has collapsed. On the contrary, for the epoxy hybrid O/I containing the IL-g-POSS^{®Ph} with NTf₂⁻ anion (Figure III. 11d), the residue has swollen distinctly, and the top layer is white and still seems protective. EDX and SEM analysis were carried out on the upper and lower layers of the residue for the epoxy-amine/IL.NTf₂-g-POSS^{®Ph} network (Figure S3.8 in the SI of chapter III). On one hand, the top layer appears as a dense porous homogeneous network. More surprisingly, it does not contain carbon and the proportions of oxygen and silicon are very close to the theoretical ones for silica. We can thus

assume this upper surface is pure silica. Such layer is not observed for the other hybrids for which the silicon content in residue remains close to 10 wt %. On the other hand, the bottom surface of epoxy-amine/IL.NTf₂-g-POSS^{®Ph} is completely different and exhibits a composition closer to the original network. Such a top layer may be mechanically stable enough to enhance the fire resistance of the composite material, but this assumption needs further investigation.

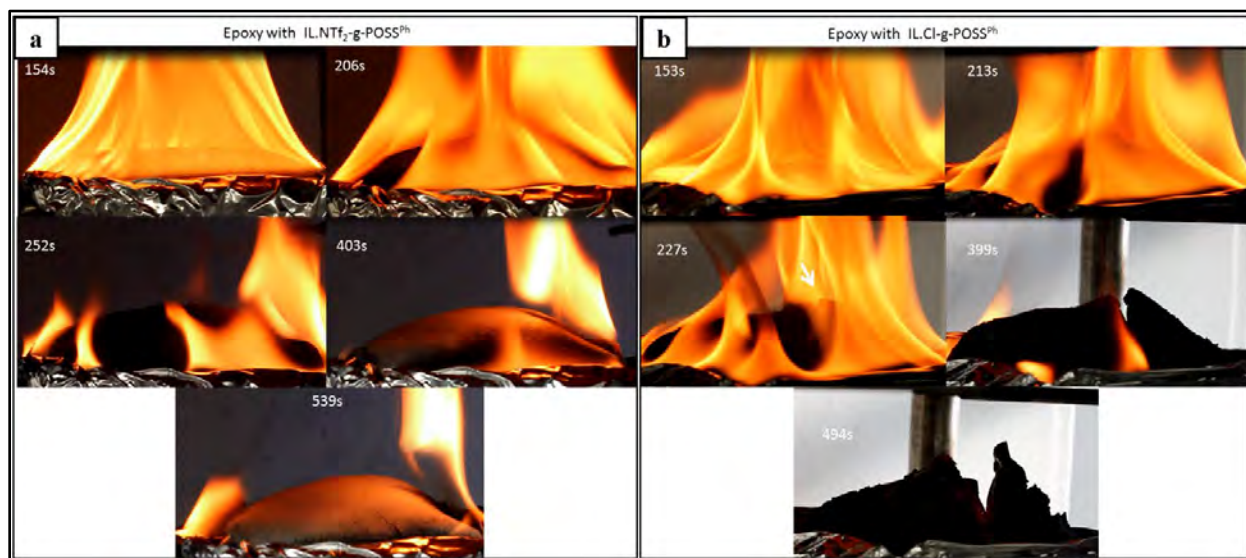


Figure III. 12: Pictures from cone calorimeter test of the epoxy hybrid O/I networks containing a) IL.NTf₂-g-POSS^{®Ph} and b) IL.Cl-g-POSS^{®Ph}.

The whole burning process was recorded using both an optical camera and a thermal camera to get new insights on the decomposition kinetics of the epoxy containing IL-g-POSS^{®Ph} (note that the pictures and the temperature curves do not correspond exactly to the HRR curves in Figure III. 9 because the distance between radiant cone and samples was increased from 25 to 60 mm). The optical pictures in Figure III. 12 follow the combustion of the epoxy hybrid O/I networks containing IL.NTf₂-g-POSS^{®Ph} and IL.Cl-g-POSS^{®Ph} respectively. It can be seen that the expansion of both char layers occurs slowly and only around 200 s, *i.e.* well after the peak of heat release rate, when the HRR is decreased at a lower level. It means that the expansion is not responsible for the better fire performances of these materials. For epoxy-amine/IL.NTf₂-g-POSS^{®Ph}, the flames are observed shortly after and only on the edges of the sample. Therefore, thermo-oxidation can occur and char is progressively removed from the surface, which becomes white (*i.e.* corresponding to the silica layer, as discussed above). Nevertheless, the surface remains cohesive without any cracks. In contrast, for epoxy-amine/IL.Cl-g-POSS^{®Ph}, cracks are

observed very quickly (after 200 s - white arrow) but the cracks develop slowly and the char residue fully breaks only at the end of the test.

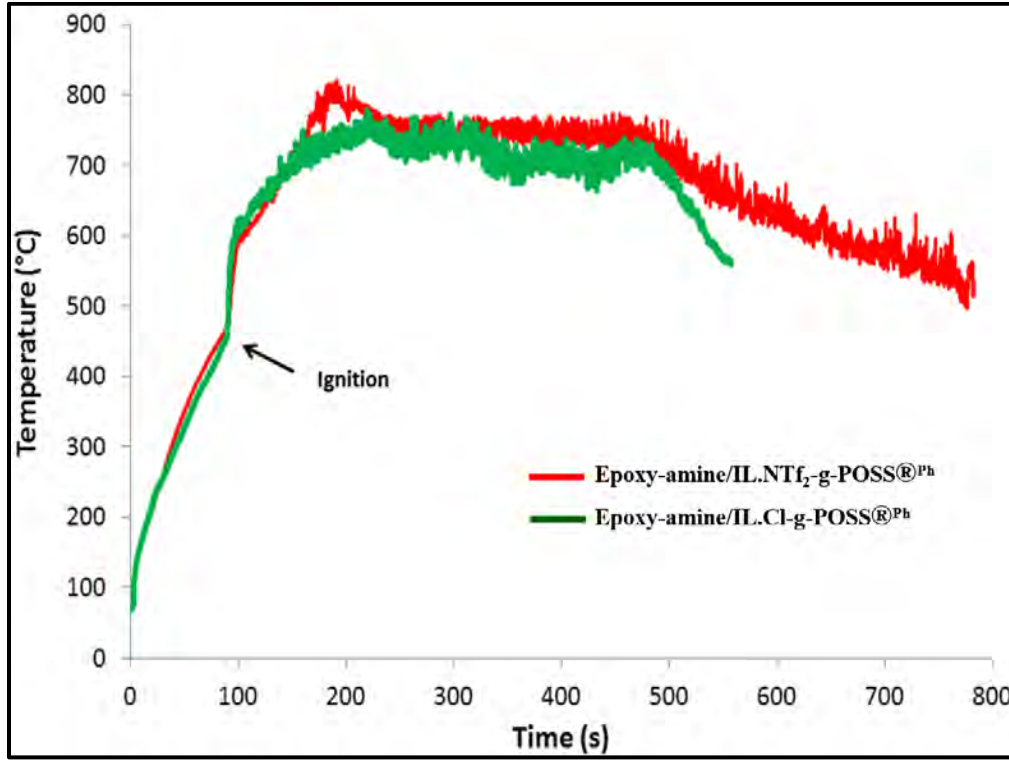


Figure III. 13: Temperature curves of the top surface during cone calorimeter tests for epoxy hybrid O/I networks containing IL.Cl-g-POSS^{®Ph} and IL.NTf₂-g-POSS^{®Ph}.

The top surface temperatures measured using a thermal camera are shown in Figure III. 13. The temperature measured is the mean temperature of a small zone located on the top surface center. The temperature was also measured for a larger zone (corresponding to more than 50 % of the surface). The temperature values for this larger zone were slightly lower than the first ones but the change versus time was similar in both cases. The heating of the surface is the same for both epoxy networks containing IL-g-POSS^{®Ph} up to ignition occurring at a surface temperature of 440 - 450 °C which is in reasonable agreement with the temperatures of peak of mass loss rate and heat release rate measured with TGA and PCFC. After ignition, the temperature increases up to 700 - 800 °C, well above the pyrolysis temperature of neat epoxy. This allows the sample to re-radiate a fraction of heat flux. The re-radiation of a hot surface is given in the following equation (6):

$$q'_{reradiation} = \sigma \varepsilon T^4 \quad (6)$$

with σ the Stefan-Boltzmann constant ($\text{W.m}^{-2}.\text{K}^{-4}$), ε the emissivity, and T the surface temperature (K).

Considering an emissivity of 0.9, the corresponding re-radiated heat flux ranges between 45 and 68 kW.m^{-2} for a surface temperature between 700 and 800 °C. This re-radiation thus significantly contributes to reducing the burning rate of the materials. This phenomenon is slightly more important for epoxy-amine/IL.NTf₂-g-POSS^{®Ph} whose surface temperature is 25 - 40 °C higher than for epoxy-amine/IL.Cl-g-POSS^{®Ph}.

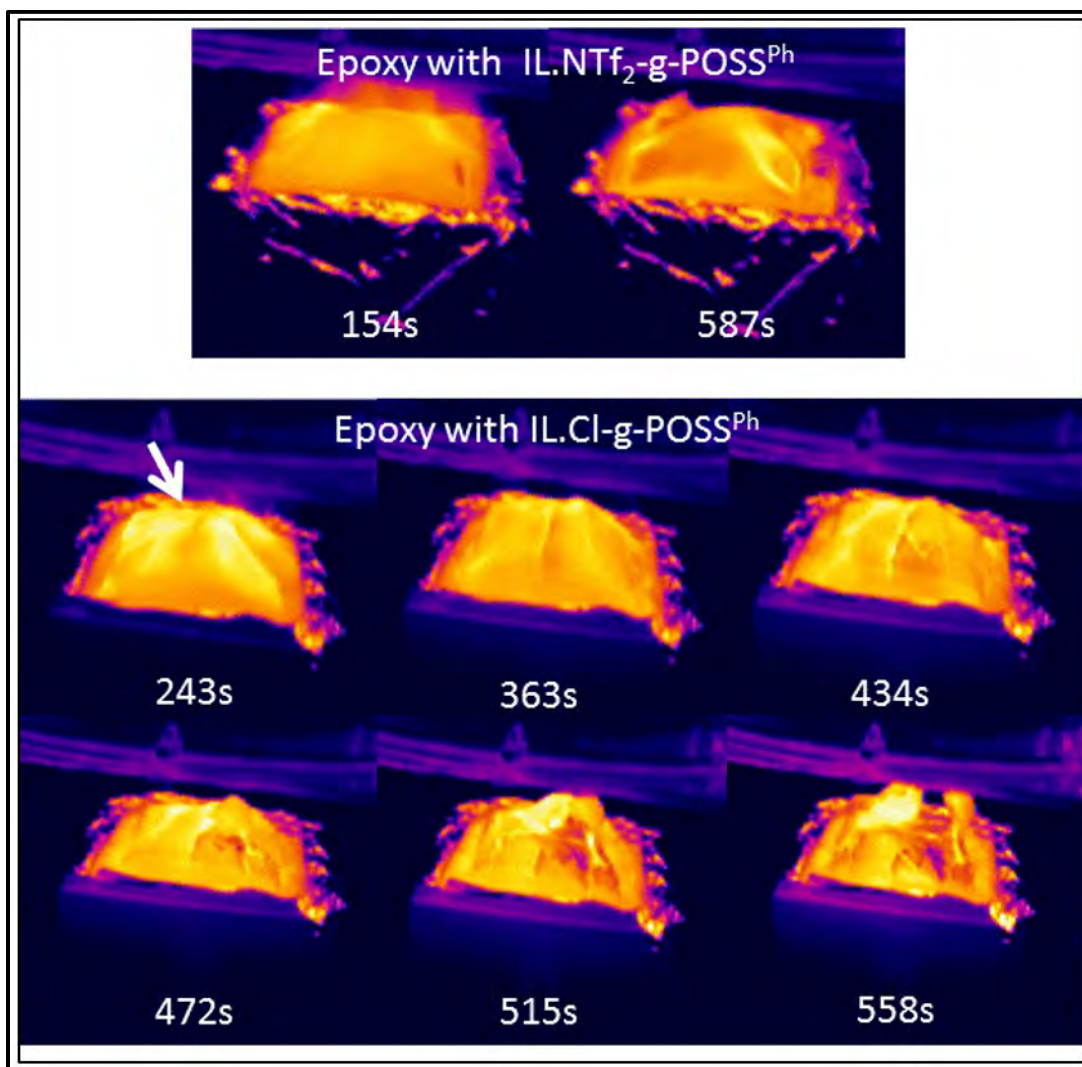


Figure III. 14: Pictures obtained using thermal camera from cone calorimeter test of the epoxy hybrid O/I networks containing IL.NTf₂-g-POSS^{®Ph} and IL.Cl-g-POSS^{®Ph}.

Figure III. 14 shows the pictures of both networks recorded from the thermal camera. While the surface appears unchanged during the whole test for epoxy-amine/IL.NTf₂-g-POSS^{®Ph}, the formation of cracks (indicated by a white arrow) and the final breaking of the residue layer is clearly shown for epoxy-amine/IL.Cl-g-POSS^{®Ph} confirming the observations from Figure III. 12b.

As a conclusion, the use of ionic liquid grafted onto the POSS^{®Ph} cages whatever the chemical nature of the anion (Cl⁻ or NTf₂⁻) highlighted a significant enhancement on the pHRR compared to the neat epoxy network. These results are better than those of epoxy-amine/POSS^{®Ph}-triol modified with the aluminum triacetylacetonate (Al) ^{5,104} or with 9,10-dihydro-9-oxa-10-phosphaphenanthrene-10-oxide (DOPO) ^{30,109}. A similar effect was also found in fully layered silicate-epoxy nanocomposites but with higher ignitability ^{110,111}. This enhancement of fire behavior can be explained not only by the nanodispersion of POSS[®] moieties but also by the nature of the IL (cation/anion) associated to the POSS[®] cage, which affects the thermal stability and the combustion process ³⁰. Even if pHRR is in the same range for both epoxy networks containing IL.Cl-g-POSS^{®Ph} and IL.NTf₂-g-POSS^{®Ph}, it can be assumed that IL-g-POSS^{®Ph} with NTf₂⁻ anion allows creating a well-organized and compact residue on the top surface of the epoxy composite, limiting more efficiently the heat diffusion in the condensed phase in other fire conditions.

III.4. Conclusion of chapter III

In this work, IL-grafted polyhedral oligomeric silsesquioxanes (IL-g-POSS^{®Ph}) were successfully designed and used as modifiers of a standard epoxy-amine network (DGEBA/IPD). The incorporation of a low amount (5 wt %) of such organic-inorganic and ionic hybrid nanoclusters leads to a fine nanostructuration of epoxy-based thermosets. We demonstrated that the chemical nature of the counter anion, *i.e.* chloride (Cl⁻) versus bis(trifluoromethanesulfonyl)imide (NTf₂⁻), has no influence on the polymerization kinetics. However, due to the catalytic effect of the IL, it plays a key role in the final properties of the resulting networks thanks to the formation of strong interactions between the epoxy network and the IL-grafted POSS^{®Ph}. As a consequence, the introduction of IL-g-POSS^{®Ph} contributed to significant improvements of the mechanical properties of the resulting networks, *i.e.* both stiffness and toughness were increased without any decrease of the glass transition temperature. Moreover, the fire retardancy behavior of the hybrid O/I epoxy networks was also deeply

evaluated from pyrolysis-combustion flow calorimetry (PCFC) and cone calorimeter analyses. These first results clearly highlighted the promising synergistic effect of POSS^{®Ph} nanoclusters combined to imidazolium ILs inducing impressive reductions of the pHRR (55 %) and an important retardancy effect by significantly increasing the ignition time. Hence, IL modified POSS[®] can be envisioned as a novel alternative for FR additive that not only shows efficient fire resistance capabilities but also improves the mechanical properties of the designed epoxy nanomaterials. Finally, the grafting of POSS^{®Ph} by ILs definitely opens new interesting perspectives in the fine-tuning of the interfacial interactions in such polymer nanomaterials.

Supporting Information of Chapter III

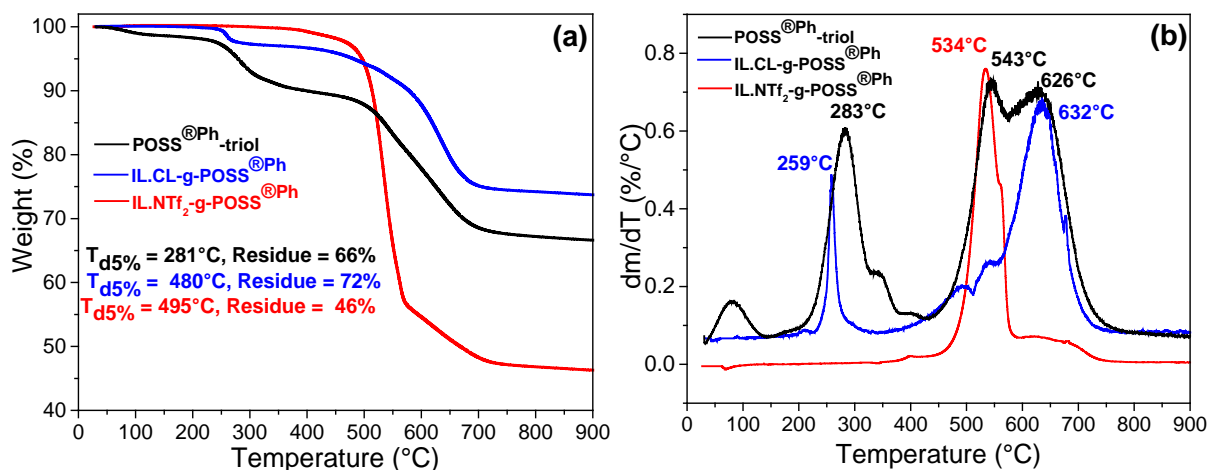


Figure S3.1: a) Evolution of weight loss as a function of temperature (TGA) and b) derivative of TGA traces (DTG) (10 K.min⁻¹; atmosphere: nitrogen flow).

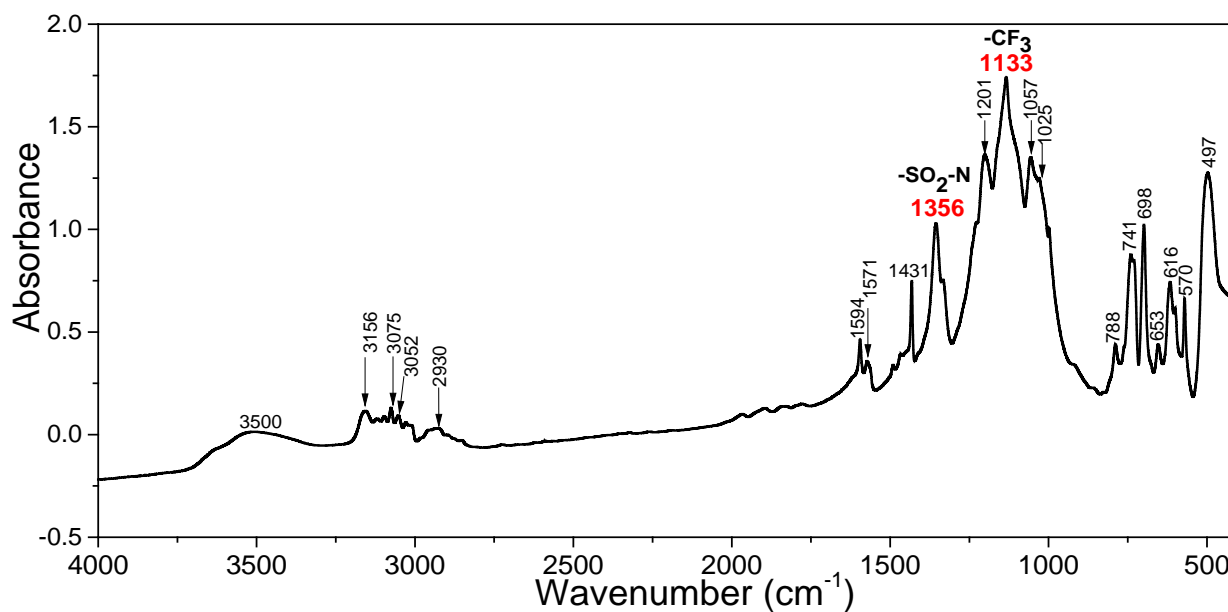


Figure S3.2: IR spectra of IL-NTf₂-g-POSS^{®Ph}.

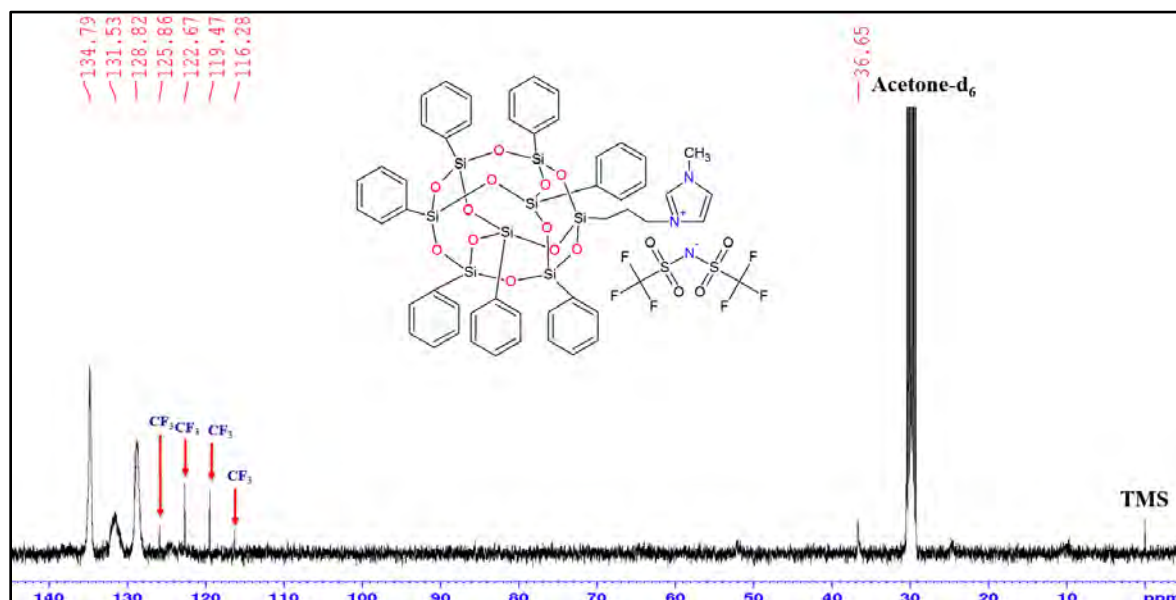


Figure S3.3: ^{13}C -NMR spectrum of IL.NTf₂-g-POSS^{®Ph} (Acetone-d₆; 400 MHz).

The analyses of the sol fraction of the residue obtained were characterized by FT-IR spectroscopy and ^{13}C -NMR spectrum. The IR and ^{13}C -NMR spectra of the sol fraction obtained for each system after evaporation of the solvent were compared with the spectral profile of the reactants before reaction (POSS^{®Ph}-triol or IL-g-POSS^{®Ph}). The spectra compared show the same IR features and very similar ^{13}C -NMR bands, which prove the identity of the expected sol fraction obtained.

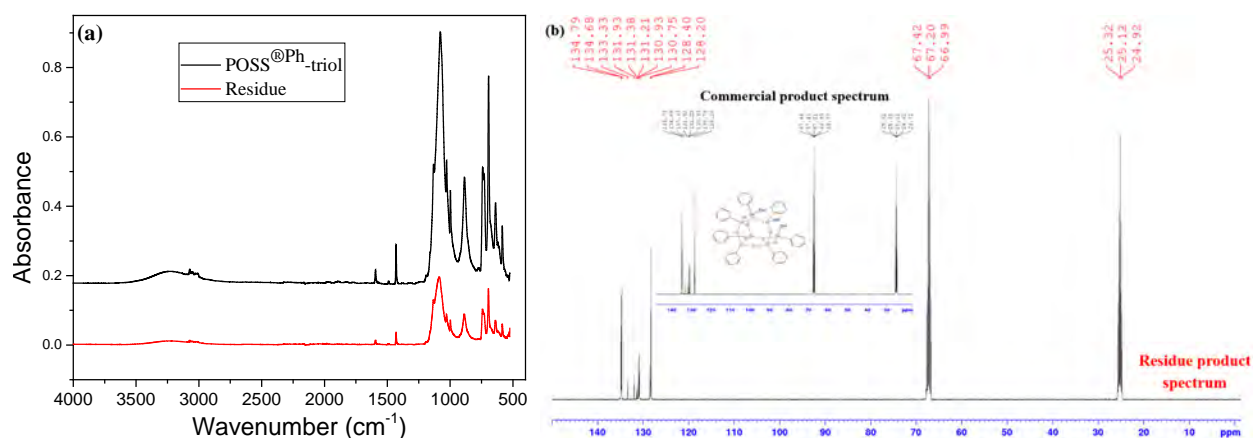


Figure S3.4: a) IR spectra and b) ^{13}C -NMR spectrum (CDCl₃; 400 MHz) of the POSS^{®Ph}-triol residue compared to the spectra of the initial product.

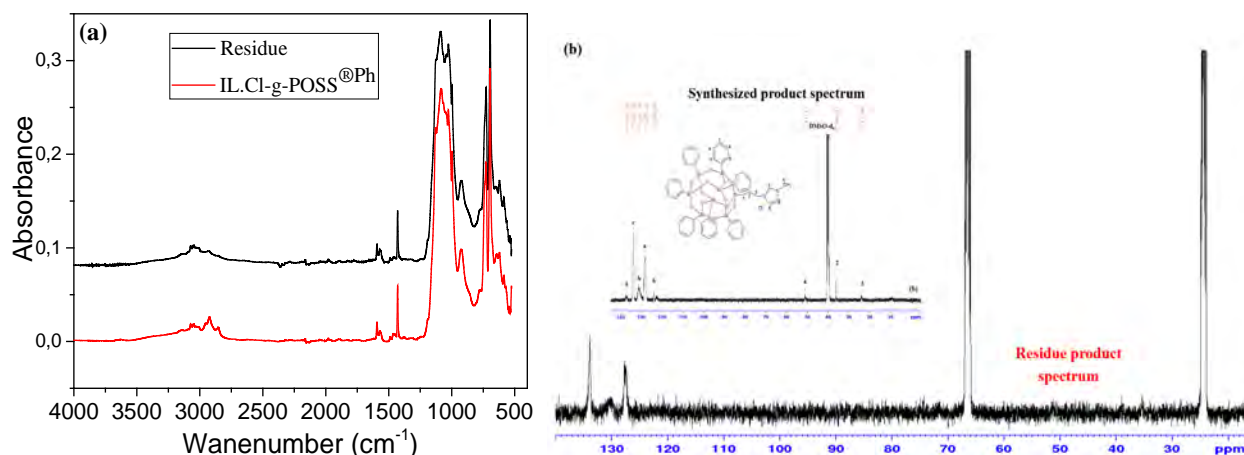


Figure S3.5: a) IR spectra and b) ¹³C-NMR spectrum (CDCl₃; 400 MHz) of the IL.Cl-g-POSS^{®Ph} residue compared to the spectra of the synthesized product.

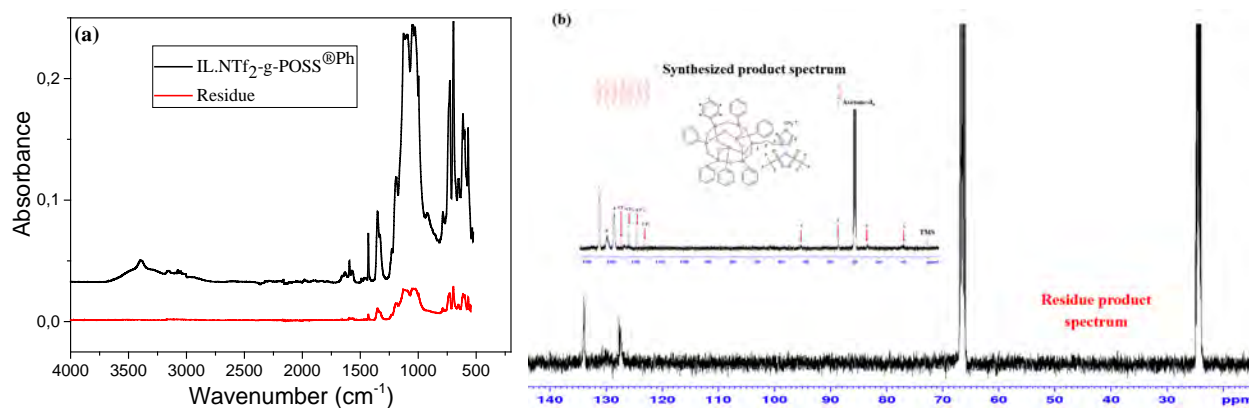


Figure S3.6: a) IR spectra and b) ¹³C-NMR spectrum (CDCl₃; 400 MHz) of the IL.NTf₂-g-POSS^{®Ph} residue compared to the spectra of the synthesized product.

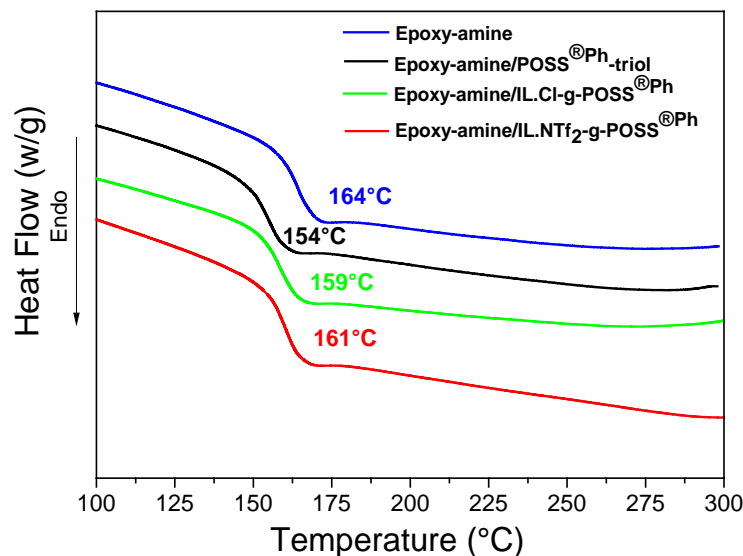


Figure S3.7: DSC curves of the neat epoxy-amine and the corresponding epoxy hybrid O/I networks containing POSS^{®Ph}-triol and IL-g-POSS^{®Ph} with different anions (Cl⁻ and NTf₂⁻) (heating rate: 10 K.min⁻¹).

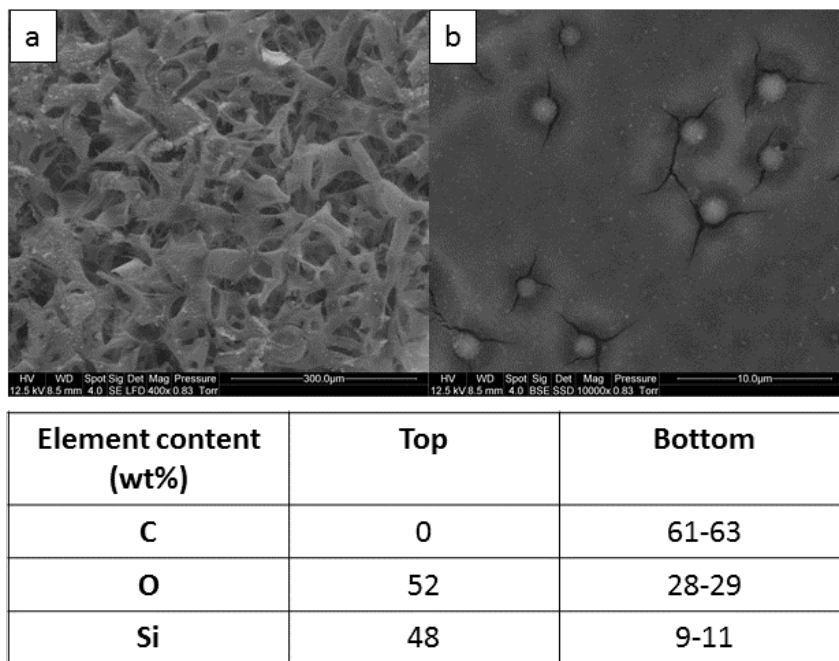


Figure S3.8: SEM images of a) the top layer and b) the bottom layer of residue of the epoxy hybrid O/I network containing IL.NTf₂-g-POSS^{®Ph} and corresponding element composition measured by EDX.

References of chapter III

- (1) Petrie, E. in *Epoxy Adhesive Formulations (McGraw-Hill Chemical Engineering)*; McGraw-Hill Professional New York, NY, **2005**.
- (2) Pascault, J. P.; Williams, R. J. in *Epoxy polymers: new materials and innovations*; John Wiley & Sons, **2009**.
- (3) Vidil, T.; Tournilhac, F.; Musso, S.; Robisson, A.; Leibler, L. Control of reactions and network structures of epoxy thermosets. *Progress in Polymer Science* **2016**, 62, 126-179.
- (4) Rohde, B. J.; Le, K. M.; Krishnamoorti, R.; Robertson, M. L. Thermoset blends of an epoxy resin and polydicyclopentadiene. *Macromolecules* **2016**, 49, 8960-8970.
- (5) Laik, S.; Galy, J.; Gérard, J. F.; Monti, M.; Camino, G. Fire behaviour and morphology of epoxy matrices designed for composite materials processed by infusion. *Polymer Degradation and Stability* **2016**, 127, 44-55.
- (6) Saba, N.; Jawaid, M.; Paridah, M.; Al-Othman, O. A review on flammability of epoxy polymer, cellulosic and non-cellulosic fiber reinforced epoxy composites. *Polymers for Advanced Technologies* **2016**, 27, 577-590.
- (7) Hodgkin, J.; Simon, G.; Varley, R. J. Thermoplastic toughening of epoxy resins: a critical review. *Polymers for Advanced Technologies* **1998**, 9, 3-10.
- (8) Frigione, M.; Mascia, L.; Acierno, D. Oligomeric and polymeric modifiers for toughening of epoxy resins. *European Polymer Journal* **1995**, 31, 1021-1029.
- (9) Bagheri, R.; Marouf, B.; Pearson, R. Rubber-toughened epoxies: a critical review. *Journal of Macromolecular Science®, Part C: Polymer Reviews* **2009**, 49, 201-225.
- (10) Kemmlein, S.; Herzke, D.; Law, R. J. Brominated flame retardants in the European chemicals policy of REACH-Regulation and determination in materials. *Journal of Chromatography A* **2009**, 1216, 320-333.
- (11) Ren, H.; Sun, J.; Wu, B.; Zhou, Q. Synthesis and properties of a phosphorus-containing flame retardant epoxy resin based on bis-phenoxy (3-hydroxy) phenyl phosphine oxide. *Polymer Degradation and Stability* **2007**, 92, 956-961.
- (12) Toldy, A.; Szolnoki, B.; Marosi, G. Flame retardancy of fibre-reinforced epoxy resin composites for aerospace applications. *Polymer Degradation and Stability* **2011**, 96, 371-376.

- (13) Buchman, A.; Dodiuk-Kenig, H.; Dotan, A.; Tenne, R.; Kenig, S. Toughening of epoxy adhesives by nanoparticles. *Journal of Adhesion Science and Technology* **2009**, *23*, 753-768.
- (14) Ababsa, H. S.; Safidine, Z.; Mekki, A.; Grohens, Y.; Ouadah, A.; Chabane, H. Fire behavior of flame-retardant polyurethane semi-rigid foam in presence of nickel (II) oxide and graphene nanoplatelets additives. *Journal of Polymer Research* **2021**, *28*, 1-14.
- (15) Yari, H.; Mohseni, M.; Messori, M. Toughened acrylic/melamine thermosetting clear coats using POSS[®] molecules: mechanical and morphological studies. *Polymer* **2015**, *63*, 19-29.
- (16) Mishra, K.; Singh, R. P. Quantitative evaluation of the effect of dispersion techniques on the mechanical properties of polyhedral oligomeric silsesquioxane (POSS[®])-epoxy nanocomposites. *Polymer Composites* **2018**, 1-9.
- (17) Cordes, D. B.; Lickiss, P. D.; Rataboul, F. Recent developments in the chemistry of cubic polyhedral oligosilsesquioxanes. *Chemical Reviews* **2010**, *110*, 2081-2173.
- (18) Laine, R. M.; Choi, J.; Lee, I. Organic-inorganic nanocomposites with completely defined interfacial interactions. *Advanced Materials* **2001**, *13*, 800-803.
- (19) Choi, J.; Yee, A. F.; Laine, R. M. Toughening of Cubic Silsesquioxane Epoxy Nanocomposites Using Core-Shell Rubber Particles: A Three-Component Hybrid System. *Macromolecules* **2004**, *37*, 3267-3276.
- (20) Choi, J.; Yee, A. F.; Laine, R. M. Organic/inorganic hybrid composites from cubic silsesquioxanes. Epoxy resins of octa (dimethylsiloxyethylcyclohexylepoxy) silsesquioxane. *Macromolecules* **2003**, *36*, 5666-5682.
- (21) Choi, J.; Tamaki, R.; Kim, S. G.; Laine, R. M. Organic/inorganic imide nanocomposites from aminophenylsilsesquioxanes. *Chemistry of Materials* **2003**, *15*, 3365-3375.
- (22) Choi, J.; Kim, S. G.; Laine, R. M. Organic/inorganic hybrid epoxy nanocomposites from aminophenylsilsesquioxanes. *Macromolecules* **2004**, *37*, 99-109.
- (23) Matějka, L.; Murias, P.; Pleštil, J. Effect of POSS[®] on thermomechanical properties of epoxy-POSS[®] nanocomposites. *European Polymer Journal* **2012**, *48*, 260-274.
- (24) Zhang, C.; Li, T.; Song, H.; Han, Y.; Su, H.; Wang, Y.; Wang, Q. Epoxy Resin/POSS[®] Nanocomposites with Toughness and Thermal Stability. *Journal of Photopolymer Science and Technology* **2017**, *30*, 25-31.
- (25) Fu, J.; Shi, L.; Chen, Y.; Yuan, S.; Wu, J.; Liang, X.; Zhong, Q. Epoxy nanocomposites containing mercaptopropyl polyhedral oligomeric silsesquioxane: Morphology, thermal

- properties, and toughening mechanism. *Journal of Applied Polymer Science* **2008**, *109*, 340-349.
- (26) Abdelwahab, M. A.; Misra, M.; Mohanty, A. K. Epoxidized pine oil-siloxane: Crosslinking kinetic study and thermomechanical properties. *Journal of Applied Polymer Science* **2015**, *132*, 42451.
- (27) Constable, G. S.; Lesser, A. J.; Coughlin, E. B. Morphological and mechanical evaluation of hybrid organic-inorganic thermoset copolymers of dicyclopentadiene and mono-or tris (norbornenyl)-substituted polyhedral oligomeric silsesquioxanes. *Macromolecules* **2004**, *37*, 1276-1282.
- (28) Chen, G. X.; Si, L.; Lu, P.; Li, Q. Epoxy hybrid composites cured with octaaminophenyl polyhedral oligomeric silsesquioxane. *Journal of Applied Polymer Science* **2012**, *125*, 3929-3935.
- (29) Zhao, B.; Xu, S.; Adeel, M.; Zheng, S. Formation of POSS[®]-POSS[®] interactions in polyurethanes: From synthesis, morphologies to shape memory properties of materials. *Polymer* **2019**, *160*, 82-92.
- (30) Zhang, W.; Camino, G.; Yang, R. Polymer/polyhedral oligomeric silsesquioxane (POSS[®]) nanocomposites: An overview of fire retardance. *Progress in Polymer Science* **2017**, *67*, 77-125.
- (31) Turgut, G.; Dogan, M.; Tayfun, U.; Ozkoc, G. The effects of POSS[®] particles on the flame retardancy of intumescent polypropylene composites and the structure-property relationship. *Polymer Degradation and Stability* **2018**, *149*, 96-111.
- (32) Su, X.; Xu, H.; Deng, Y.; Li, J.; Zhang, W.; Wang, P. Preparation and optical limiting properties of a POSS[®]-containing organic-inorganic hybrid nanocomposite. *Materials Letters* **2008**, *62*, 3818-3820.
- (33) Ray, S. S.; Okamoto, M. Polymer/layered silicate nanocomposites: a review from preparation to processing. *Progress in Polymer Science* **2003**, *28*, 1539-1641.
- (34) Paul, D.; Robeson, L. M. Polymer nanotechnology: Nanocomposites. *Polymer* **2008**, *49*, 3187-3204.
- (35) Dintcheva, N. T.; Morici, E.; Arrigo, R.; La Mantia, F.; Malatesta, V.; Schwab, J. Structure-properties relationships of polyhedral oligomeric silsesquioxane (POSS[®]) filled PS nanocomposites. *Express Polymer Letters* **2012**, *6*, 561-571.

- (36) Dantas, A.; Beatrice, C. A. G. Polymer nanocomposites with different types of nanofiller. in *Nanocomposites-Recent Evolution's*; IntechOpen, **2018**.
- (37) Zhang, C.; Mi, X.; Tian, J.; Zhang, J.; Xu, T. Supported ionic liquid silica as curing agent for epoxy composites with improved mechanical and thermal properties. *Polymers* **2017**, *9*, 478.
- (38) Perchacz, M.; Donato, R. K.; Seixas, L.; Zhigunov, A.; Konefał, R.; Serkis-Rodzeń, M.; Beneš, H. Ionic liquid-silica precursors via solvent-free sol-gel process and their application in epoxy-amine network: A theoretical/experimental study. *ACS Applied Materials & Interfaces* **2017**, *9*, 16474-16487.
- (39) Ly Nguyen, T. K.; Obadia, M. M.; Serghei, A.; Livi, S.; Duchet-Rumeau, J.; Drockenmuller, E. 1, 2, 3-triazolium-based epoxy-amine networks: Ion-conducting polymer electrolytes. *Macromolecular Rapid Communications* **2016**, *37*, 1168-1174.
- (40) Livi, S.; Chardin, C.; Lins, L. C.; Halawani, N.; Pruvost, S.; Duchet-Rumeau, J.; Gérard, J. F.; Baudoux, J. From ionic liquid epoxy monomer to tunable epoxy-amine network: Reaction mechanism and final properties. *ACS Sustainable Chemistry & Engineering* **2019**, *7*, 3602-3613.
- (41) Livi, S.; Lins, L. C.; Capeletti, L. B.; Chardin, C.; Halawani, N.; Baudoux, J.; Cardoso, M. B. Antibacterial surface based on new epoxy-amine networks from ionic liquid monomers. *European Polymer Journal* **2019**, *116*, 56-64.
- (42) Wasserscheid, P.; Welton, T. Ionic liquids in synthesis, second, completely revised and enlarged edition. Weinheim, Wiley-WCH Verlag GmbH & Co. KGaA, **2008**.
- (43) Somers, A. E.; Howlett, P. C.; MacFarlane, D. R.; Forsyth, M. A review of ionic liquid lubricants. *Lubricants* **2013**, *1*, 3-21.
- (44) Ranu, B. C.; Banerjee, S. in Ionic liquid as catalyst and reaction medium. The dramatic influence of a task-specific ionic liquid, [bmIm] OH, in michael addition of active methylene compounds to conjugated ketones, carboxylic esters, and nitriles. *Organic Letters* **2005**, *7*, 3049-3052.
- (45) Radchenko, A. V.; Duchet-Rumeau, J.; Gérard, J. F.; Baudoux, J.; Livi, S. Cycloaliphatic epoxidized ionic liquids as new versatile monomers for the development of shape memory PIL networks by 3D printing. *Polymer Chemistry* **2020**, *11*, 5475-5483.
- (46) Plechkova, N. V.; Seddon, K. R. Applications of ionic liquids in the chemical industry. *Chemical Society Reviews* **2008**, *37*, 123-150.

- (47) Leclère, M.; Livi, S.; Maréchal, M.; Picard, L.; Duchet-Rumeau, J. The properties of new epoxy networks swollen with ionic liquids. *RSC Advances* **2016**, *6*, 56193-56204.
- (48) Le Bideau, J.; Viau, L.; Vioux, A. Ionogels, ionic liquid based hybrid materials. *Chemical Society Reviews* **2011**, *40*, 907-925.
- (49) Dupont, J.; de Souza, R. F.; Suarez, P. A. Ionic liquid (molten salt) phase organometallic catalysis. *Chemical Reviews* **2002**, *102*, 3667-3692.
- (50) Xing, C.; Li, J.; Yang, C.; Li, Y. Local grafting of ionic liquid in poly (vinylidene fluoride) amorphous region and the subsequent microphase separation behavior in melt. *Macromolecular Rapid Communications* **2016**, *37*, 1559-1565.
- (51) Xing, C.; You, J.; Li, Y.; Li, J. Nanostructured poly (vinylidene fluoride)/ionic liquid composites: formation of organic conductive nanodomains in polymer matrix. *The Journal of Physical Chemistry C* **2015**, *119*, 21155-21164.
- (52) Silva, A. A.; Livi, S.; Netto, D. B.; Soares, B. G.; Duchet, J.; Gérard, J. F. New epoxy systems based on ionic liquid. *Polymer* **2013**, *54*, 2123-2129.
- (53) Shi, T.; Livi, S.; Duchet, J.; Gérard, J. F. Ionic Liquids-Containing Silica Microcapsules: A Potential Tunable Platform for Shaping-Up Epoxy-Based Composite Materials? *Nanomaterials* **2020**, *10*, 881.
- (54) Maka, H.; Spychaj, T.; Pilawka, R. Epoxy resin/ionic liquid systems: the influence of imidazolium cation size and anion type on reactivity and thermomechanical properties. *Industrial & Engineering Chemistry Research* **2012**, *51*, 5197-5206.
- (55) Shang, D.; Fu, J.; Lu, Q.; Chen, L.; Yin, J.; Dong, X.; Xu, Y.; Jia, R.; Yuan, S.; Chen, Y. A novel polyhedral oligomeric silsesquioxane based ionic liquids (POSS[®]-ILs) polymer electrolytes for lithium ion batteries. *Solid State Ionics* **2018**, *319*, 247-255.
- (56) Zhang, F.; Bao, X.; Liu, Q.; Huang, M. High-temperature polymer electrolyte membranes based on poly (2, 5-benzimidazole)(ABPBI) and POSS[®] incorporated ionic liquid. *Journal of Materials Chemistry Engineering* **2014**, *2*, 86-93.
- (57) Chabane, H.; Livi, S.; Benes, H.; Ladavière, C.; Ecorchard, P.; Duchet-Rumeau, J.; Gérard, J. F. Polyhedral oligomeric silsesquioxane-supported ionic liquid for designing nanostructured hybrid organic-inorganic networks. *European Polymer Journal* **2019**, *114*, 332-337.

- (58)Radchenko, A. V.; Chabane, H.; Demir, B.; Searles, D. J.; Duchet-Rumeau, J.; Gerard, J. F.; Baudoux, J.; Livi, S. New epoxy thermosets derived from bisimidazolium ionic liquid monomer: An experimental and modelling investigation. *ACS Sustainable Chemistry & Engineering* **2020**, 8, 12208-12221.
- (59)Lesniewski, A.; Niedziolka, J.; Palys, B.; Rizzi, C.; Gaillon, L.; Opallo, M. Electrode modified with ionic liquid covalently bonded to silicate matrix for accumulation of electroactive anions. *Electrochemistry Communications* **2007**, 9, 2580-2584.
- (60)Chardin, C.; Rouden, J.; Livi, S.; Baudoux, J. 3-[2-(Oxiran-2-yl) ethyl]-1-{4-[(2-oxiran-2-yl) ethoxy] benzyl} imidazolium bis (Trifluoromethane) sulfonimide. *Molbank* **2018**, 2018, M974.
- (61)Brun, N.; Hesemann, P.; Laurent, G.; Sanchez, C.; Birot, M.; Deleuze, H.; Backov, R. Macrocellular Pd@ ionic liquid@ organo-Si (HIPE) heterogeneous catalysts and their use for Heck coupling reactions. *New Journal of Chemistry* **2013**, 37, 157-168.
- (62)Ye, M.; Wu, Y.; Zhang, W.; Yang, R. Synthesis of incompletely caged silsesquioxane (T7-POSS[®]) compounds via a versatile three-step approach. *Research on Chemical Intermediates* **2018**, 44, 4277-4294.
- (63)Won, Y. g.; Galy, J.; Gérard, J. F.; Pascault, J. P.; Bellenger, V.; Verdu, J. Internal antiplasticization in copolymer and terpolymer networks based on diepoxides, diamines and monoamines. *Polymer* **1990**, 31, 1787-1792.
- (64)Mounif, E.; Bellenger, V.; Mazabraud, P.; Nony, F.; Tcharkhtchi, A. Chemorheological study of DGEBA/IPD system for reactive rotational molding (RRM). *Journal of Applied Polymer Science* **2010**, 116, 969-976.
- (65)Garcia, F. G.; Soares, B. G.; Pita, V. J.; Sánchez, R.; Rieumont, J. Mechanical properties of epoxy networks based on DGEBA and aliphatic amines. *Journal of Applied Polymer Science* **2007**, 106, 2047-2055.
- (66)Owens, D. K.; Wendt, R. Estimation of the surface free energy of polymers. *Journal of Applied Polymer Science* **1969**, 13, 1741-1747.
- (67)Lyon, R. E.; Walters, R. N. Pyrolysis combustion flow calorimetry. *Journal of Analytical and Applied Pyrolysis* **2004**, 71, 27-46.
- (68)Huggett, C. Estimation of rate of heat release by means of oxygen consumption measurements. *Fire and Materials* **1980**, 4, 61-65.

- (69) Callister Jr, W. D.; Rethwisch, D. G. in *Fundamentals of materials science and engineering: an integrated approach*; John Wiley & Sons, **2012**.
- (70) Sonnier, R.; Caro-Bretelle, A. S.; Dumazert, L.; Longerey, M.; Otazaghine, B. Influence of radiation-crosslinking on flame retarded polymer materials-How crosslinking disrupts the barrier effect. *Radiation Physics and Chemistry* **2015**, *106*, 278-288.
- (71) Ham, Y. R.; Kim, S. H.; Shin, Y. J.; Lee, D. H.; Yang, M.; Min, J. H.; Shin, J. S. A comparison of some imidazoles in the curing of epoxy resin. *Journal of Industrial and Engineering Chemistry* **2010**, *16*, 556-559.
- (72) Soares, B. G.; Livi, S.; Duchet-Rumeau, J.; Gerard, J. F. Synthesis and characterization of epoxy/MCDEA networks modified with imidazolium-based ionic liquids. *Macromolecular Materials and Engineering* **2011**, *296*, 826-834.
- (73) Soares, B. G.; Livi, S.; Duchet-Rumeau, J.; Gérard, J. F. Preparation of epoxy/MCDEA networks modified with ionic liquids. *Polymer* **2012**, *53*, 60-66.
- (74) Rahmathullah, M. A. M.; Jeyarajasingam, A.; Merritt, B.; VanLandingham, M.; McKnight, S. H.; Palmese, G. R. Room temperature ionic liquids as thermally latent initiators for polymerization of epoxy resins. *Macromolecules* **2009**, *42*, 3219-3221.
- (75) Livi, S.; Silva, A. A.; Thimont, Y.; Nguyen, T. K. L.; Soares, B. G.; Gérard, J. F.; Duchet-Rumeau, J. Nanostructured thermosets from ionic liquid building block-epoxy prepolymer mixtures. *RSC Advances* **2014**, *4*, 28099-28106.
- (76) Weickmann, H.; Delto, R.; Thomann, R.; Brenn, R.; Döll, W.; Mülhaupt, R. PMMA nanocomposites and gradient materials prepared by means of polysilsesquioxane (POSS[®]) self-assembly. *Journal of Materials Science* **2007**, *42*, 87-92.
- (77) Ni, Y.; Zheng, S.; Nie, K. Morphology and thermal properties of inorganic-organic hybrids involving epoxy resin and polyhedral oligomeric silsesquioxanes. *Polymer* **2004**, *45*, 5557-5568.
- (78) Wu, Q.; Zhang, C.; Liang, R.; Wang, B. Combustion and thermal properties of epoxy/phenyltrisilanol polyhedral oligomeric silsesquioxane nanocomposites. *Journal of Thermal Analysis and Calorimetry* **2010**, *100*, 1009-1015.
- (79) Liu, H.; Zheng, S.; Nie, K. Morphology and thermomechanical properties of organic-inorganic hybrid composites involving epoxy resin and an incompletely condensed polyhedral oligomeric silsesquioxane. *Macromolecules* **2005**, *38*, 5088-5097.

- (80) Donato, R.; Perchacz, M.; Ponyrko, S.; Donato, K.; Schrekker, H.; Beneš, H.; Matějka, L. Epoxy-silica nanocomposite interphase control using task-specific ionic liquids via hydrolytic and non-hydrolytic sol-gel processes. *RSC Advances* **2015**, 5, 91330-91339.
- (81) Deng, Y.; Bernard, J.; Alcouffe, P.; Galy, J.; Dai, L.; Gérard, J. F. Nanostructured hybrid polymer networks from in situ self-assembly of RAFT-synthesized POSS[®]-based block copolymers. *Journal of Polymer Science Part A: Polymer Chemistry* **2011**, 49, 4343-4352.
- (82) Mangion, M.; Johari, G. Relaxations of thermosets. III. Sub-T_g dielectric relaxations of bisphenol-A-based epoxide cured with different cross-linking agents. *Journal of Polymer Science Part B: Polymer Physics* **1990**, 28, 71-83.
- (83) Yang, B. X.; Pramoda, K. P.; Xu, G. Q.; Goh, S. H. Mechanical reinforcement of polyethylene using polyethylene-grafted multiwalled carbon nanotubes. *Advanced Functional Materials* **2007**, 17, 2062-2069.
- (84) Tseng, C. H.; Wang, C. C.; Chen, C. Y. Functionalizing carbon nanotubes by plasma modification for the preparation of covalent-integrated epoxy composites. *Chemistry of Materials* **2007**, 19, 308-315.
- (85) Silva, B. L.; Bello, R. H.; Ferreira Coelho, L. A. The role of the ratio (PEG: PPG) of a triblock copolymer (PPG-b-PEG-b-PPG) in the cure kinetics, miscibility and thermal and mechanical properties in an epoxy matrix. *Polymer International* **2018**, 67, 1248-1255.
- (86) Abdollahi, H.; Salimi, A.; Barikani, M.; Samadi, A.; Hosseini Rad, S.; Zanjanijam, A. Systematic investigation of mechanical properties and fracture toughness of epoxy networks: Role of the polyetheramine structural parameters. *Journal of Applied Polymer Science* **2019**, 136, 47121.
- (87) Nguyen, T. K. L.; Livi, S.; Soares, B. G.; Benes, H.; Gérard, J. F.; Duchet-Rumeau, J. Toughening of epoxy/ionic liquid networks with thermoplastics based on poly (2, 6-dimethyl-1, 4-phenylene ether)(PPE). *ACS Sustainable Chemistry & Engineering* **2017**, 5, 1153-1164.
- (88) Nguyen, T. K. L.; Soares, B. G.; Duchet-Rumeau, J.; Livi, S. Dual functions of ILs in the core-shell particle reinforced epoxy networks: Curing agent vs dispersion aids. *Composites Science and Technology* **2017**, 140, 30-38.

- (89) Haldorai, Y.; Lyoo, W. S.; Noh, S. K.; Shim, J. J. Ionic liquid mediated synthesis of silica/polystyrene core-shell composite nanospheres by radical dispersion polymerization. *Reactive and Functional Polymers* **2010**, 70, 393-399.
- (90) Kinloch, A.; Mohammed, R.; Taylor, A.; Eger, C.; Sprenger, S.; Egan, D. The effect of silica nano particles and rubber particles on the toughness of multiphase thermosetting epoxy polymers. *Journal Materials Science* **2005**, 40, 5083-5086.
- (91) Johnsen, B.; Kinloch, A.; Mohammed, R.; Taylor, A.; Sprenger, S. Toughening mechanisms of nanoparticle-modified epoxy polymers. *Polymer* **2007**, 48, 530-541.
- (92) AJ, K.; YOUNG, R. in Fracture Behavior of Polymers. *App. Sci. Publishers, London* **1983**.
- (93) Nguyen, T. K. L.; Livi, S.; Soares, B. G.; Pruvost, S.; Duchet-Rumeau, J.; Gérard, J. F. Ionic liquids: A new route for the design of epoxy networks. *ACS Sustainable Chemistry & Engineering* **2016**, 4, 481-490.
- (94) Yang, G.; Fu, S. Y.; Yang, J. P. Preparation and mechanical properties of modified epoxy resins with flexible diamines. *Polymer* **2007**, 48, 302-310.
- (95) Mishra, K. Study on developing of epoxy/POSS[®] nanocomposite and to investigate their thermomechanical behavior. Oklahoma State University. *Thesis* **2011**.
- (96) Jin, H.; Yang, B.; Jin, F. L.; Park, S. J. Fracture toughness and surface morphology of polysulfone-modified epoxy resin. *Journal of Industrial and Engineering Chemistry* **2015**, 25, 9-11.
- (97) Kim, K.; Lichtenhan, J. D.; Otaigbe, J. U. Facile route to nature inspired hydrophobic surface modification of phosphate glass using polyhedral oligomeric silsesquioxane with improved properties. *Applied Surface Science* **2019**, 470, 733-743.
- (98) Włoch, J.; Terzyk, A. P.; Wiśniewski, M.; Kowalczyk, P. Nanoscale water contact angle on Polytetrafluoroethylene surfaces characterized by molecular Dynamics-Atomic force microscopy imaging. *Langmuir* **2018**, 34, 4526-4534.
- (99) Kaur, M.; Singh, G.; Kumar, S.; Kang, T. S. Thermally stable microemulsions comprising imidazolium based surface active ionic liquids, non-polar ionic liquid and ethylene glycol as polar phase. *Journal of Colloid and Interface Science* **2018**, 511, 344-354.
- (100) Livi, S.; Silva, A. A.; Pereira, J.; Nguyen, T. K. L.; Soares, B. G.; Cardoso, M. B.; Gérard, J. F.; Duchet-Rumeau, J. Supercritical CO₂-organosilane mixtures for modification of silica:

- Applications to epoxy prepolymer matrix. *Chemical Engineering Journal* **2014**, 241, 103-111.
- (101) Peng, W.; Xu, S.; Li, L.; Zhang, C.; Zheng, S. Organic-inorganic nanocomposites via self-assembly of an amphiphilic triblock copolymer bearing a Poly (butadiene-g-POSS[®]) subchain in epoxy thermosets: morphologies, surface hydrophobicity, and dielectric properties. *The Journal of Physical Chemistry B* **2016**, 120, 12003-12014.
- (102) Zeng, K.; Zheng, S. Nanostructures and surface dewettability of epoxy thermosets containing hepta (3, 3, 3-trifluoropropyl) polyhedral oligomeric silsesquioxane-capped poly (ethylene oxide). *The Journal of Physical Chemistry B* **2007**, 111, 13919-13928.
- (103) Wang, L.; Zheng, S. Surface morphology and dewettability of self-organized thermosets involving epoxy and POSS[®]-capped poly(ethylene oxide) telechelics. *Materials Chemistry and Physics* **2012**, 136, 744-754.
- (104) Wu, Q.; Zhang, C.; Liang, R.; Wang, B. Combustion and thermal properties of epoxy/phenyltrisilanol polyhedral oligomeric silsesquioxane nanocomposites. *Journal of Thermal Analysis and Calorimetry* **2009**, 100, 1009-1015.
- (105) Sanes, J.; Saurin, N.; Carrion, F.; Ojados, G.; Bermudez, M. Synergy between single-walled carbon nanotubes and ionic liquid in epoxy resin nanocomposites. *Composites Part B: Engineering* **2016**, 105, 149-159.
- (106) Gu, J.; Yang, X.; Lv, Z.; Li, N.; Liang, C.; Zhang, Q. Functionalized graphite nanoplatelets/epoxy resin nanocomposites with high thermal conductivity. *International Journal of Heat and Mass Transfer* **2016**, 92, 15-22.
- (107) Sonnier, R.; Otazaghine, B.; Dumazert, L.; Ménard, R.; Viretto, A.; Dumas, L.; Bonnaud, L.; Dubois, P.; Safronava, N.; Walters, R. Prediction of thermosets flammability using a model based on group contributions. *Polymer* **2017**, 127, 203-213.
- (108) Schartel, B.; Hull, T. R. Development of fire-retarded materials-interpretation of cone calorimeter data. *Fire and Materials: An International Journal* **2007**, 31, 327-354.
- (109) Zhang, W.; Li, X.; Fan, H.; Yang, R. Study on mechanism of phosphorus-silicon synergistic flame retardancy on epoxy resins. *Polymer Degradation and Stability* **2012**, 97, 2241-2248.
- (110) Wu, G. M.; Schartel, B.; Kleemeier, M.; Hartwig, A. Flammability of layered silicate epoxy nanocomposites combined with low-melting inorganic ceepree glass. *Polymer Engineering & Science* **2012**, 52, 507-517.
- (111) Camino, G.; Tartaglione, G.; Frache, A.; Manfredi, C.; Costa, G. Thermal and combustion behaviour of layered silicate-epoxy nanocomposites. *Polymer Degradation and Stability* **2005**, 90, 354-362.

Chapter IV:

New Epoxy Thermosets Organic-Inorganic Hybrid Nanomaterials Derived from Imidazolium Ionic Liquid Monomers and POSS^{®Ph}

Abstract: Novel polymerizable ionic liquid monomers (ILMs) based on an imidazolium salt were synthesized in order to substitute bisphenol A diglycidyl ether (DGEBA) as starting material, and then copolymerized with isophorone diamine (IPD). Then, these networks were modified by three types of POSS^{®Ph}: trisilanol phenyl POSS[®] (POSS^{®Ph}-triol) and two IL-modified POSS^{®Ph} having Cl⁻ and NTf₂⁻ counter anions, respectively. POSS^{®Ph} have been incorporated into the epoxy/ILM networks with the content of 5 wt. % and also copolymerized with the isophorone diamine in order to design nanostructured epoxy PILs networks. In the first part, the substitution of DGEBA by these ILMs led to a thermosetting polymer with high thermal stability (up to 450 °C), hydrophobic behavior (21 mJ.m⁻²), and promising mechanical performance including shape memory behavior. Then, in the second part, the organic-inorganic hybrid nanomaterials were prepared via *in situ* polymerization of epoxy/ILM monomers in the presence of POSS^{®Ph} which started homogeneous solutions. Phase separation induced by polymerization occurred, and the fine phase-separated structures were obtained in which the spherical POSS^{®Ph} aggregates are dispersed homogeneously on the nanoscale (80 to 400 nm) in the continuous epoxy matrices. As a consequence, the effect of IL-g-POSS^{®Ph} into ILM/IPD networks are a high decrease on the glass transition temperature (45 vs 71 °C) and an important enhancement of thermal stability (> 380 °C) combined with high oxidation resistance. Interestingly, a significant improvement of the hydrophobicity with very low surface energy and high oil repellency was obtained by incorporating IL.NTf₂-g-POSS^{®Ph} in the ILM2/IPD network. Such results are important for designing highly hydrophobic paint coatings with self-cleaning ability. Moreover, all the nanostructured epoxy PILs exhibit outstanding high ionic conductivities (from 3.4 x 10⁻⁸ to 6.84 x 10⁻² S.m⁻¹).

Graphical abstract of the chapter

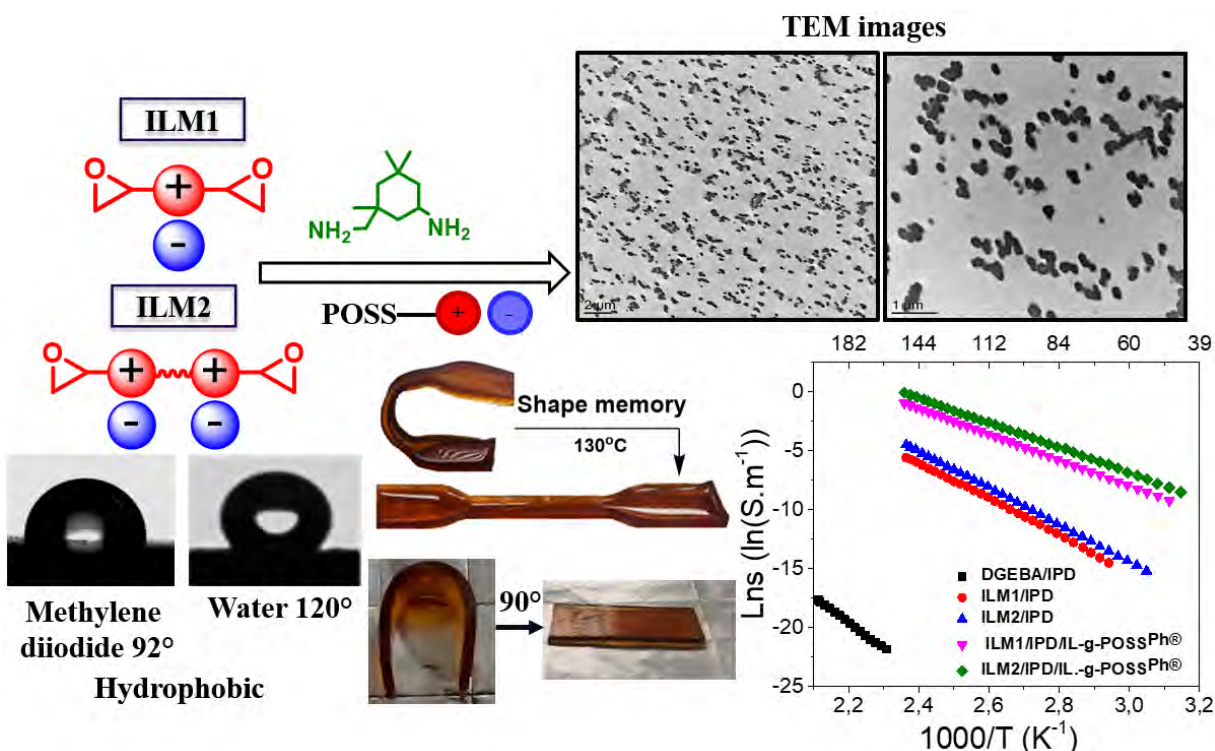


Table of contents

IV.1. Introduction	181
IV.2. Experimental	183
IV.2.1. Materials	183
IV.2.2. Synthesis of materials.....	184
IV.2.2.1. Synthesis of difunctional ionic liquid monomer (ILM1).....	184
IV.2.2.2. Synthesis of difunctional ionic liquid monomer (ILM2).....	186
IV.2.3. Epoxy network preparation	187
IV.2.4. Determination of the soluble fraction extractable from hybrid O/I networks	187
IV.2.5. Characterization.....	188
IV.3. Results and discussion	190
IV.3.1. Curing Behavior of Epoxy ILM/IPD: Reactivity study (DSC) and determination of the epoxy conversion (FTIR).....	190
IV.3.2. Thermomechanical properties of ILM/IPD networks	194
IV.3.3. Morphology investigation of ILM/IPD networks	198
IV.3.4. Thermal stability of ILM/IPD networks.....	199
IV.3.5. Surface energy of DGEBA/IPD and ILM/IPD networks	201
IV.3.6. Mechanical properties	201
IV.3.7. Shape memory	202
IV.3.8. Conclusion.....	205
IV.4. Epoxy hybrid ILM/IPD containing POSS^{®Ph}-triol or IL-g-POSS^{®Ph}	205
IV.4.1. Morphology of hybrid O/I networks	205
IV.4.2. Glass transition behavior and epoxy conversion	208
IV.4.3. Thermal-oxidative stability	210
IV.4.4. Surface properties.....	213
IV.4.5. Ionic conductivity.....	215
IV.4.6. Conclusion.....	223
Supporting information of chapter IV	224
References of chapter IV	228
Chapter V: Conclusions and Perspectives	241

IV.1. Introduction

In the field of thermosetting polymers, ionic liquid monomers (ILMs) represent a real opportunity to design new smart and (multi)functional-dedicated polymer materials with enhanced properties such as thermal stability ¹⁻⁴, mechanical performance ^{5,6}, gas or water barrier properties ⁷, anti-bacterial ^{8,9}, and self-healing properties ¹⁰. According to the literature, the main relevant studies focused on the design of ILMs based on ammonium ^{11,12}, triazolium ¹³, or imidazolium ^{14,15} backbones containing polymerizable groups such as alkene, alkyne, or amine mainly due to their availability ¹⁶. However, the ammonium and triazolium-based ILs are not suitable for polymerization conditions at high temperatures due to the Hofmann elimination, *i.e.* an elimination reaction of alkylammonium salts leading to the formation of C-C double bonds ¹⁷. As imidazolium are thermally more stable, very few studies were dedicated to the syntheses of versatile sequences in order to design imidazolium monomers bearing aromatic rings and epoxy functions ^{18,19}. Usually, these imidazolium monomers were obtained by the alkylation of the imidazole ring using the highly toxic and carcinogenic epichlorohydrin ¹⁸⁻²⁰.

In 2014, Gin & Noble *et al.* developed ion-gel membranes based on diepoxy-functionalized ILM copolymerized with a triamine, *i.e.* tris (2-aminoethyl)amine in order to investigate their CO₂ sorption as well as their gas separation performance ²¹. In addition, the authors have studied the effect of the stoichiometric ratio on the epoxy conversion with and without the presence of different amounts of conventional ILs, especially imidazolium ILs. They have highlighted that the stoichiometric reaction between amine hardener and epoxy functions plays a key role in the CO₂ adsorption efficiency ²¹. In fact, the addition of high amount of an IL into the epoxy-amine network resulted in both high CO₂ permeability and selectivity ²¹. Similar networks were subsequently prepared by the same authors from three new imidazolium and pyrrolidinium ILs functionalized with two epoxy functions and various multifunctional amines (primary and secondary amines). Their study has highlighted that the chemical nature of the ILs (*i.e.* imidazolium versus pyrrolidinium cation) had no impact on the CO₂ selectivity. However, the permeability as well as the diffusion were strongly dependent on the epoxy-amine network architectures ²².

More recently, Drockenmuller *et al.* have synthesized a new class of epoxy-amine network based on the 1,2,3-triazolium structure and polyoxypropylene diamine comonomers and have investigated the final properties of these networks including the thermo-mechanical properties as

well as the ionic conductivity ²³. Such an approach suggested the preparation of ion-conducting epoxy-amine networks with ionic conductivity of $2 \times 10^{-7} \text{ S.cm}^{-1}$ at 30 °C combined with a low glass transition (-52 °C). Despite a high epoxy conversion of approximately 90 %, these low T_g networks displayed poor thermal stability (< 250 °C) due to the early degradation of triazolium salts ²³ and the polymerization kinetics of these reactive systems are extremely slow, significantly limiting their applications for the development of new structural epoxy networks. However, these networks may be a good alternative as solid polymer electrolytes for Li-ion batteries. Very recently, our groups have investigated the synthesis of polyfunctional imidazolium ILs bearing two epoxide functions ^{24,25}. The synthesis of these novel ILMs was a real challenge for the development of new epoxy networks. In these studies, several architectures have been considered in order to highlight the influence of the backbone on the properties of the resulting networks by adding one or two aromatic groups, by incorporating ether or ester groups, and by inserting the spacer arms between the imidazolium core and the epoxide functions or aromatic groups ^{24,26}. The influence of several oxidizing agents on the synthesis of polyfunctional imidazoliums was also investigated. It was clearly demonstrated that dimethyldioxirane (DMDO) or *meta*-chloroperoxybenzoic acid (mCPBA) are efficient oxidizing agents to prepare mono- or di-epoxide ILMs with high yields and purities ²⁴. Thus, a totally new generation of imidazolium ILMs has been synthesized at multi-grams scale (from 10 to 200 g) by using a new powerful and flexible methodology in order to oxidize terminal alkenes directly and quantitatively on an imidazolium backbone by avoiding the use of highly toxic epichlorohydrin ²⁴. More recently, various authors have developed supramolecular ionic networks based on dicationic ionic liquids combined with various counter anions ²⁷⁻²⁹. In these works, the authors have highlighted a thermoreversibility phenomenon for the resulting supramolecular ionic networks. This thermoreversibility could be an asset for the development of an epoxy network with a shape memory behavior.

In the present work, we report the synthesis of two ionic liquid monomers (ILM1 and ILM2) based on imidazolium salt composed of two epoxy functions in order to substitute the use of highly toxic and carcinogenic bisphenol A and epichlorohydrin products. In the first section, the synthesis of these new epoxy-functionalized imidazolium ionic liquid monomers and their copolymerization with the isophorone diamine (IPD) are described. In order to confirm the interest of this type of ILMs, a comparative study with the DGEBA-type prepolymer has been

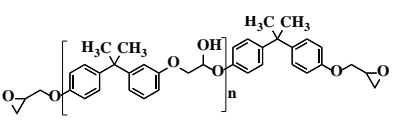
studied in order to investigate the relationships between the networks architecture and the final properties of these networks such as thermo-mecanical behavior (DMA), thermal properties (TGA, DSC), mechanical and surface performances, and shape memory behavior. In the second section, the behavior of these epoxy ionic liquids monomers on the structure and dispersion morphology of an non-fully condensed polyhedral oligomeric silsesquioxane, denoted POSS^{®Ph}-triol, and IL-modified POSS^{®Ph} with two different anions chloride and bis(trifluoromethanesulfonyl)imide (NTf₂⁻) denoted, IL.Cl-g-POSS^{®Ph} and IL.NTf₂-g-POSS^{®Ph} respectively, was investigated (see Table IV.1). The influence of these nanoclusters on the final properties of the resulting networks was also investigated in terms of thermal behavior (DSC), thermal stability and thermo-oxidative resistance (TGA), surface hydrophobicity, and ionic conductivity properties (DEA).

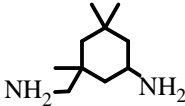
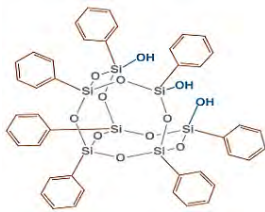
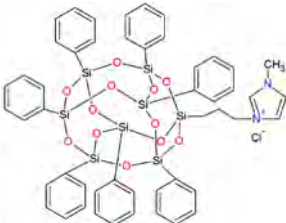
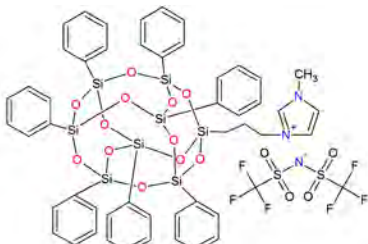
IV.2. Experimental

IV.2.1. Materials

All reagents were purchased from Sigma Aldrich, Alfa Aesar or TCI, and were used as received. Solvents were used in RPE grade without further purification. Anhydrous solvents were obtained from a Puresolv SPS400 apparatus developed by Innovative Technology Inc. Epoxy prepolymer based on diglycidyl ether of bisphenol A (DGEBA) Epon 828 was provided by Hexion. The diamine hardener named isophorone diamine (IPD) from Aldrich was used as co-monomer of the synthesized epoxy ionic liquid monomers ILMs, the commercial epoxy prepolymer DGEBA, and the heptaphenyl-trisilanol POSS^{®Ph}, denoted POSS^{®Ph}-triol, from Hybrid Plastics were used as received. All the chemical structures of non-modified and modified POSS[®] used and synthesized are summarized in Table IV. 1.

Table IV. 1: Chemical formula of chemicals.

Name	Chemical formula	Characteristics
Diglycidyl ether of bisphenol A (DGEBA)	 <p style="text-align: center;">n = 0.15</p>	$M_n = 377 \text{ g.mol}^{-1}$, EEW : (185-192 g/eq) ^a , $T_g = -13 \text{ }^{\circ}\text{C}^b$, $T_d = 330 \text{ }^{\circ}\text{C}^d$ CAS No. 1675-54-3

Isophoronediamine (IPD)		M = 170.3 g.mol ⁻¹ CAS No. 2855-13-2
Heptaphenyl-trisilanol POSS [®] (POSS ^{®Ph} -triol)		M = 931.34 g mol ⁻¹ , T _{m1} = 217 °C ^a , T _{m2} = 230 °C ^a , T _d = 626 °C ^b CAS No. 444315-26-8
1-methyl-3-propyl heptaphenyl octasilesquioxane imidazolium chloride (IL.Cl-g-POSS ^{®Ph})		M = 1116.04 g mol ⁻¹ , T _{m1} = 127 °C ^a , T _{m2} = 168 °C ^a , T _d = 632 °C ^b
1-methyl-3-propyl heptaphenyl octasilesquioxane imidazolium bis(trifluoromethanesulfonyl)imide (IL.NTf ₂ -g-POSS ^{®Ph})		M = 1360.73 g mol ⁻¹ , T _{m1} = 135 °C ^a , T _{m2} = 158 °C ^a , T _d = 534 °C ^b

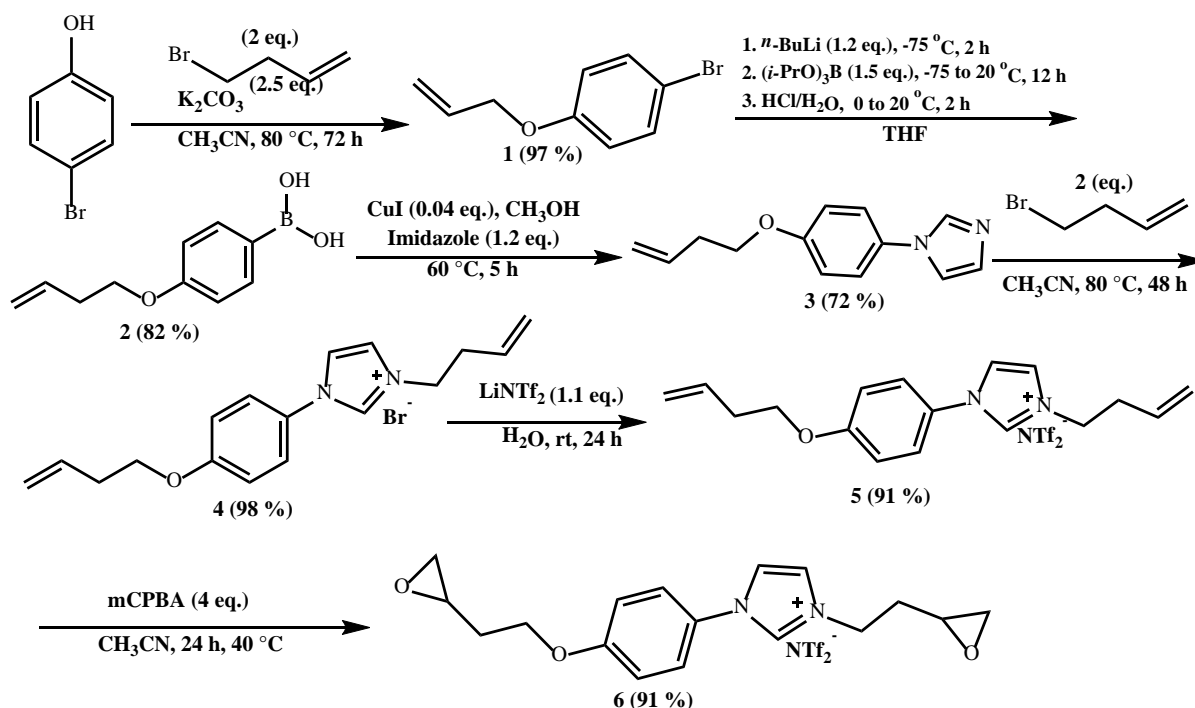
^a T_m: Melting temperature, ^b T_d: Degradation temperature determined at the maximum of the first derivative of the weight loss as temperature. (All TGA and DSC thermograms of the starting materials are presented in the chapter II).

IV.2.2. Synthesis of materials

IV.2.2.1. Synthesis of difunctional ionic liquid monomer (ILM1)

According to a previous study ²⁶, the imidazolium salt **6** (see scheme IV. 1) was synthesized in 6 steps from 4-bromophenol (Scheme IV. 1). In a first step, the etherification reaction between the alcohol 4-bromophenol (1.0 equiv) and 4-bromo-1-butene (2 equiv.) in CH₃CN (140 ml) was carried out in the presence of potassium carbonate (2.5 equiv.) at 80 °C for 72 h to generate the compound **1** with excellent yield (97 %). The aryl-imidazolium backbone was prepared by a copper-catalyzed arylation to create carbon nitrogen bond in methanol. To achieve this Chan-Lam coupling, the imidazole was added to the boronic acid **2** previously prepared by adding n-

butyl lithium, aryl bromide **1**, and triisopropylborate in THF. This Cu-catalyzed reaction is perfectly reproducible on several grams of reagents. After purification, 4-bromo-1-butene was added to imidazole **3** in presence of CH₃CN to afford imidazolium bromide **4** in quantitative yield as a yellow oil. The anionic metathesis of this salt was carried out in H₂O (250 mL) with bis(trifluoromethanesulfonyl)imide lithium salt. Finally, the diepoxide **6** was obtained quantitatively by the Prilezhaev reaction with *m*-chloroperbenzoic acid (4 eq.) and compound **5** in CH₃CN at 40 °C. All products were characterized by FT-IR, ¹H/¹⁹F/³¹C-NMR, HR-MS, and DSC analysis (the assignment of resonance peaks of **ILM1** are reported below):



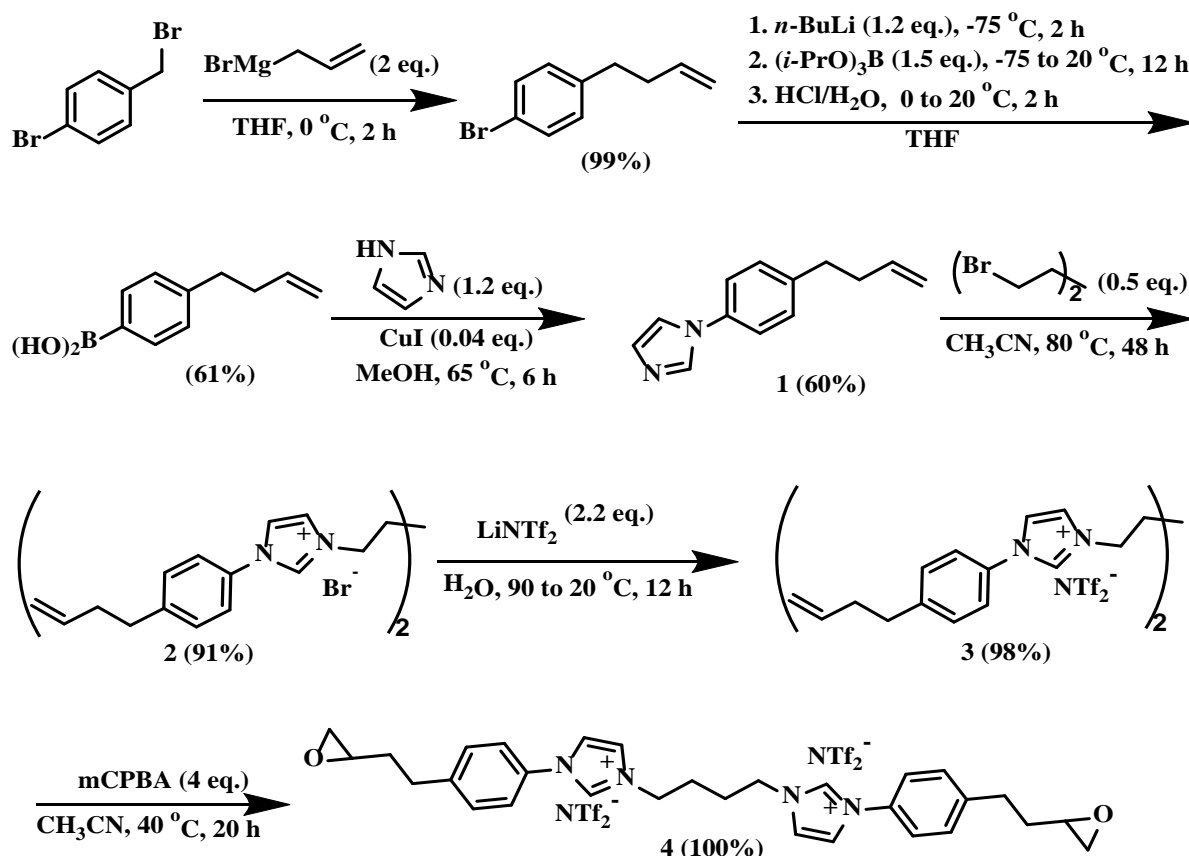
Scheme IV. 1: Synthesis of the ILM1.

¹H NMR (400 MHz, CDCl₃, 25°C, ppm): 8.97 (s, 1H), 7.46-7.59 (m, 4H), 7.05 (d, J = 9.0 Hz, 2H), 4.50 (t, J = 6.7 Hz, 2H), 4.11-4.19 (m, 2H), 3.03-3.16 (m, 2H), 2.75-2.83 (m, 2H), 2.39-2.58 (m, 3H), 2.11-2.19 (m, 1H), 1.87-1.97 (m, 2H). ¹³C NMR (100 MHz, CDCl₃, 25°C, ppm): 160.2, 134.2, 127.4, 123.8, 123.5, 121.9, 116.0, 115.0 (q, JCF = 322.4 Hz), 65.4, 49.5, 49.2, 47.8, 47.1, 46.3, 32.5, 32.2. ¹⁹F NMR (376 MHz, CDCl₃, 25°C, ppm): -78.9. IR (neat, cm⁻¹): 3146, 2933, 1555, 1513, 1348, 1254, 1178, 1132, 1052, 908, 831, 788, and 739. HR-MS m/z (ESI): calcd. for C₁₇H₂₁N₂O₃ [M]⁺: 301.1550, found: 301.1547 and Calcd. for C₂F₆NO₄S₂ [M]⁻: 279.9188, found:

279.9178. $M = 581 \text{ g.mol}^{-1}$. T_g : -39°C (see Figure S4.1 in the SI of chapter IV). $T_{d5\%}$: 345°C ; and T_{dmax} : 482°C (see Figure S4.2 in the SI of chapter IV).

IV.2.2.2. Synthesis of difunctional ionic liquid monomer (ILM2)

The bisimidazolium ionic liquid monomer **4** was synthesized in 6 steps from 4-bromobenzyl bromide (Scheme IV. 2). The first three steps to obtain compound **1** were already described in the first synthesis (Scheme IV. 1). Imidazole **1** was employed for coupling reaction with 1,4-dibromobutane (0.5 equiv.) in CH_3CN at 80°C for 48 h to synthesize diene **2**. The anionic metathesis of salt **2** with LiNTf_2 in H_2O gave bis-imidazolium **3** in 98 % yield. This reaction required heating up to 90°C before addition of LiNTf_2 (2.2 equiv.) for better solubility of **2** in water. Finally, the diepoxide **4** was obtained quantitatively by the Prilezhaev reaction with *m*-chloroperbenzoic acid (4 equiv.) in CH_3CN at 40°C for 24 h as a white solid. All products were characterized by FT-IR, $^1\text{H}/^{19}\text{F}/^{31}\text{C}$ -NMR, HR-MS and DSC analysis (the assignment of resonance peaks of **ILM2** are reported below):



Scheme IV. 2: Synthesis of the ILM2.

¹H NMR (500 MHz, CDCl₃, ppm): 8.99 (s, 2H), 7.64-7.69 (m, 2H), 7.55-7.59 (m, 2H), 7.45 (d, $J = 8.3$ Hz, 4H), 7.37 (d, $J = 8.3$ Hz, 4H), 4.33-4.44 (m, 4H), 2.76-2.96 (m, 6H), 2.71-2.76 (m, 2H), 2.43-2.49 (m, 2H), 2.06-2.16 (m, 4H), 1.85-1.94 (m, 2H), 1.72-1.83 (m, 2H). **¹³C NMR** (126 MHz, CDCl₃, ppm): 144.6, 133.9, 132.5, 130.5, 123.7, 122.3, 121.8, 119.8 (q, $J_{CF} = 322.4$ Hz), 51.6, 49.7, 47.3, 34.0, 31.9, 26.8. **¹⁹F NMR** (471 MHz, CDCl₃, ppm): -78.7. **IR (neat, cm⁻¹)**: 3146, 2939, 1554, 1515, 1347, 1329, 1178, 1132, 1051, 833. **HRMS m/z (ESI)**: calcd. for C₃₀H₃₆N₄O₂ [M]²⁺: 242.1419, found: 242.1413 and Calcd. for C₂F₆NO₄S₂ [M]⁻: 279.9188, found: 279.9178. **M_p**: 68 °C (see Figure S4.1 in the SI of chapter IV). **M** = 802 g.mol⁻¹. **T_{d5%}**: 295 °C; and **T_{dmax}**: 460 °C (see Figure S4.2 in the SI of chapter IV).

IV.2.3. Epoxy network preparation

To prepare epoxy-amine networks, epoxy prepolymer (DGEBA) or the epoxy ionic liquid monomers (ILM1 and ILM2) (see schemes IV. 1 and IV. 2) were mixed with the isophoronediamine (IPD) used as co-monomer under mechanical stirring with a stoichiometric ratio amino hydrogen-to-epoxy equal to one. For the POSS^{®Ph}-modified epoxy networks, the desired amount of 5 wt. % of POSS^{®Ph}-triol or IL-g-POSS^{®Ph} were premixed in the DGEBA or the epoxy ionic liquid monomers (ILM1 or ILM2) at 100 °C for 45 min in order to obtain a homogeneous and transparent solution before adding the isophoronediamine (IPD). Then, the mixture was degassed and poured into molds. Finally, the different systems were polymerized under different conditions: The neat epoxy-amine and the POSS^{®Ph}-modified epoxy based on ILM2 networks were cured for 1 h at 140 °C and post-cured 8 h at 190 °C whereas the other system based on ILM1 was cured for 3 h at 80 °C and 6 h at 120 °C, followed by a post-curing process at 200 °C for 1 h in order to ensure a complete crosslinking of the resulting networks.

IV.2.4. Determination of the soluble fraction extractable from hybrid O/I networks

The solubilization was considered to determine the fraction of POSS^{®Ph} bonded to the architecture of the networks. The extraction was done with THF at 60 °C for 24 h to determine a fraction of the soluble part containing non-bonded POSS^{®Ph}. The soluble fraction, w_s , was evaluated from the weight of the dry sample before (m_{dry}) and after extraction ($m_{dry-ext}$).

IV.2.5. Characterization

Fourier Transform infrared absorption spectra (FTIR) were recorded on a Thermo Scientific Nicolet iS10 spectrometer in transmission mode from 4,000 to 500 cm⁻¹ (32 scans, resolution 4 cm⁻¹).

¹³C HR-MAS NMR spectroscopy analysis was done using a Bruker Advance II spectrometer (400 MHz), equipped with a 4 mm diameter rotor ¹H/¹³C HR-MAS probe with z-gradient coil at 5 kHz rotation speed operating at 298 K.

Thermogravimetric analyses (TGA) of the neat ILMs and the resulting epoxy/POSS^{®Ph} networks were performed on a Q500 thermogravimetric analyzer (TA instruments). The samples were heated from 30 to 900 °C at a heating rate of 20 K.min⁻¹ under nitrogen flow.

Differential scanning calorimetry analyses (DSC) of ILMs reactive system and thermosetting networks were performed on a Q10 (TA instruments) in a dynamic mode at a heating rate of 10 K.min⁻¹ under nitrogen flow of 50 mL.min⁻¹ from -70 to 300 °C.

Dynamic mechanical analysis (DMA) were performed on rectangular samples with dimensions of 30 x 6 x 3 mm³ using an ARES-G2 rheometer with torsional fixture (TA Instruments). The material response was measured with a heating rate of 3 K.min⁻¹. All tests were performed within the linear viscoelastic region of each material at a frequency of 1 Hz. Storage modulus G', loss modulus G'', and loss factor tan δ were measured during temperature ramps from -120 to 250 °C.

Transmission electron microscopy (TEM) was performed at the Technical Center of Microstructures (University of Lyon) using a Phillips CM 120 microscope operating at 80 kV to characterize the resulting epoxy networks. The 60 nm-thick ultrathin sections were obtained using an ultramicrotome equipped with a diamond knife and were then set on copper grids.

Surface energy of epoxy networks was determined according to the sessile drop method using a GBX goniometer. From contact angle measurements performed with water and methylene diiodide as probe liquids, non-dispersive and dispersive components of surface energy were determined according to the Owens-Wendt theory³⁰.

Tensile tests were performed on a MTS 2/M electromechanical testing system at 22 ± 1 °C and 50 ± 5 °C relative humidity at a crosshead speed of 1 mm.min⁻¹. ASTM D695 standard test recommendation was followed. Tensile modulus, E, *i.e.* Young's modulus, was taken as the slope of the stress-strain curve in the linear domain, *i.e.* at low strain values (usually lower than 0.05).

Yield strength, σ_y , was taken, as the maximum stress value on the stress-strain curve. The strain and the stress at break were also determined.

Shape memory tests were performed similarly to a previously reported procedure³¹. A dog bone shaped samples was placed in the oven at a given temperature for 30 min. In a second step, the sample was bent to a U-shape and cooled down to room temperature. The sample was fixed in a clamp and placed in the oven in a such way to avoid gravity influence on the shape recovery. The process was filmed and remaining deformation at different times was determined by formula (1):

$$D_t = \left(\frac{180 - \alpha_t}{180} \right) \times 100\% \quad (1)$$

where D_t is remaining deformation and α_t is the angle between sample ends at time t .

The shape memory behavior was evaluated by shape fix ratio (R_f) and shape recovery ratio (R_r) calculated as follows:

$$R_f = \left(\frac{180 - \alpha_f}{180} \right) \times 100\% \quad (2)$$

$$R_r = 1 - \left(\frac{180 - \alpha_r}{180} \right) \times 100\% \quad (3)$$

where α_f and α_r the angle between the straight ends of the bent specimen after shape fixation and shape recovery respectively.

Dielectric measurements were performed using an AMETEK Solatron analytical (Modulab XM MTS) dielectric spectrometer, equipped with a LakeShore 335 Temperature controller in two steps. Initially, all the formulations were assessed at room temperature (20 - 22 °C) than the measurements were carried out from - 80 to 200 °C under helium atmosphere. The temperature was controlled by the use of liquid nitrogen circulating around the measurement chamber containing the sample. The samples used circular with a 3 cm diameter and a thickness of 0.6 up to 1.25 mm. Two gold electrodes, 25 mm in diameter, were sputtered on both sides using a Quorum Q300TD Sputter Coater. Dielectric measurements were done under isothermal conditions (temperature steps of 3 K) with a frequency range of 10^{-1} - 10^6 Hz (10 points per decade) applying $V_{rms} = 5$ V. The complex conductivity, σ^* , is calculated from the equation (4):

$$\sigma^* (\omega) = \omega \epsilon_0 \epsilon^* (\omega) \quad (4)$$

where the angular frequency $\omega = 2\pi f$ (f being the frequency), ϵ_0 the vacuum permittivity (8.85×10^{-12} F.m⁻¹) and ϵ^* the complex permittivity. The DC conductivity, σ_{DC} , was extrapolated from the real part of the conductivity $\sigma' (\omega) = \omega \epsilon_0 \epsilon'' (\omega)$ for $\omega \rightarrow 0$, where a plateau is observed.

IV.3. Results and discussion

IV.3.1. Curing behavior of epoxy ILM/IPD: Reactivity study (DSC) and determination of the epoxy conversion (FTIR)

The copolymerization between ILM1 or ILM2 and IPD was studied by differential scanning calorimetry (DSC) (Figure IV. 1a and b) in order to evaluate the ability of the imidazolium ionic liquids to be used as a substitute for conventional diglycidyl ether of bisphenol A prepolymers (DGEBA).

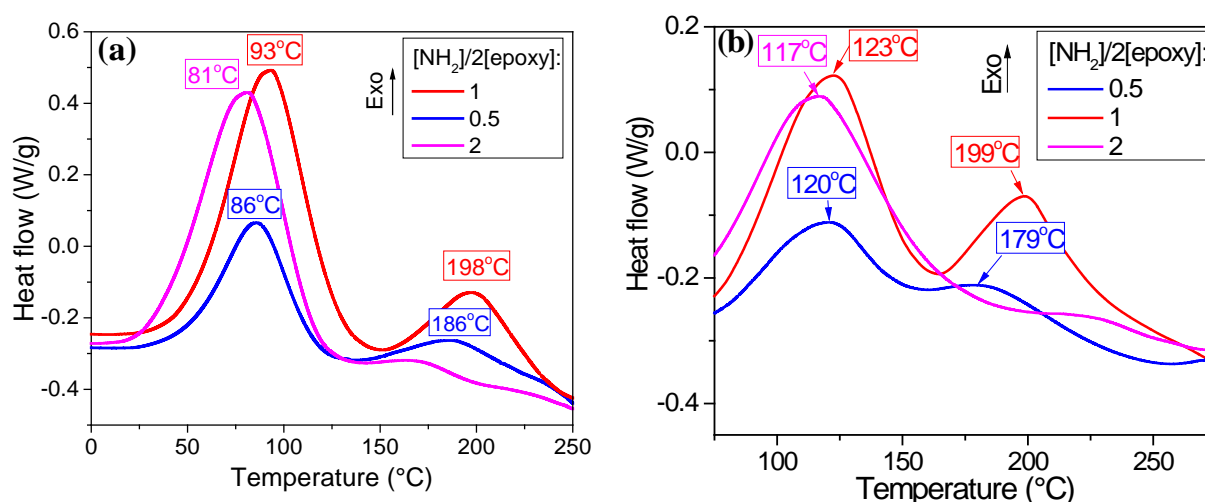
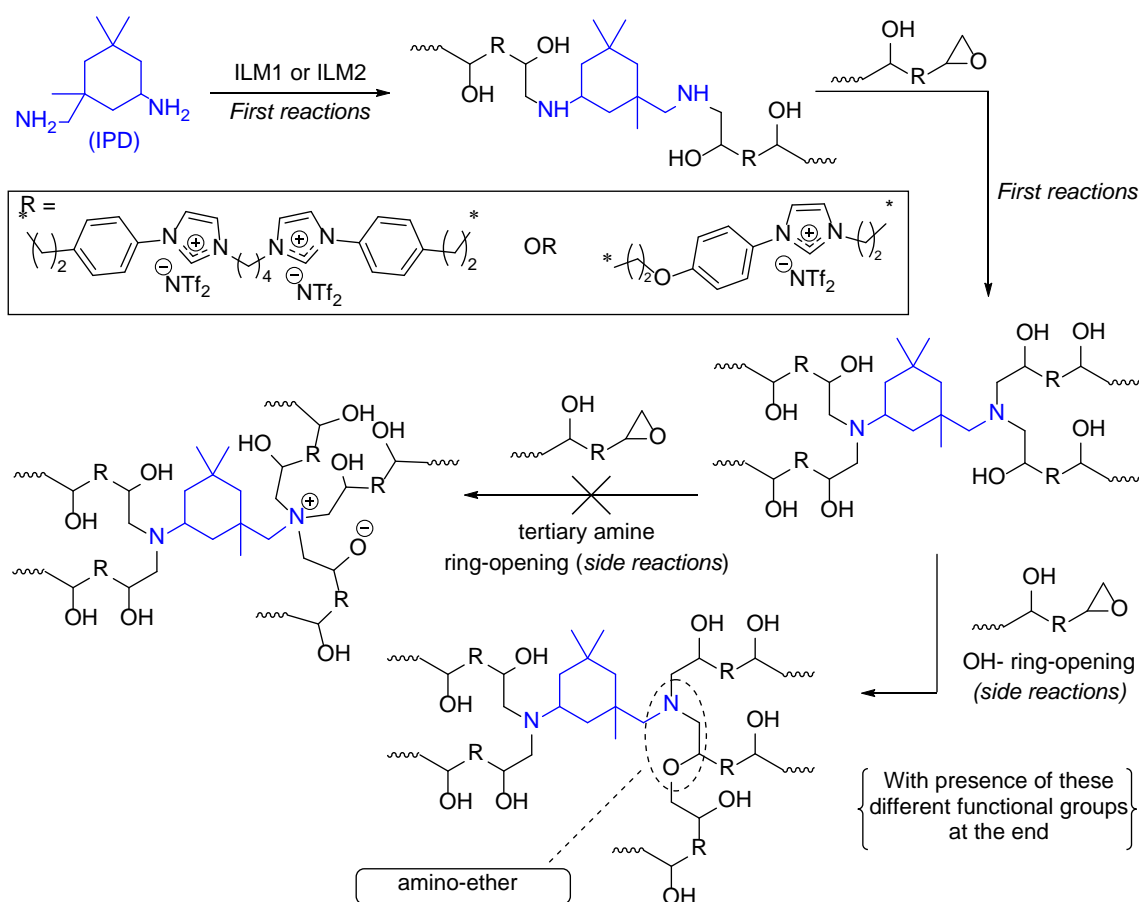


Figure IV. 1: DSC traces for a first heating run a) ILM1/IPD and b) ILM2/IPD reactive mixtures considering different amino hydrogen-to-epoxy stoichiometric ratios (heating rate : 10 K.min⁻¹).

As can be seen in Figure IV. 1a and b (red line), the use of stoichiometric quantity of IPD as a curing agent of the ionic liquid monomers leads to two exothermic peaks at 93 °C and 198 °C for ILM1/IPD and at 123 and 199 °C for ILM2/IPD with a lower total enthalpy value (around 250 J.g⁻¹) compared to the one of the first peak (550 - 600 J.g⁻¹) which is usually encountered for epoxy-amine systems³²⁻³⁷. This value is close to those reported in various studies on the use of ionic liquid as an initiator/curing agent of anionic polymerizations^{2,38,39} and also when imidazolium ionic liquid was used as a co-monomer^{14,40-43}. The lower value of enthalpy per gram as ILMs are used as diepoxy co-monomers can be explained by its higher molar mass, *i.e.* the lower concentration of epoxy-reactive groups. In fact, the enthalpy calculated for one mole of epoxy groups is slightly higher between ILMs (close to 270 kJ.mol⁻¹) and the DGEBA (from 191.25 to 212.5 kJ.mol⁻¹) co-monomers. According to the literature, the presence of two

exothermic peaks corresponds to a bimodal character, *i.e.* a two-step mechanism or two different reaction mechanisms as previously suggested by Maka *et al.*⁴⁰ It can be suggested that the first peak mainly corresponds to the primary and the secondary amine-epoxy addition reactions (Scheme IV. 3) as it is well-known that this reaction for similar epoxy-ILs is rather fast and can occur even from 40 °C²³. While at the later stage of crosslinking, when the concentration of remaining amines (primary and secondary) is already low, viscosity and crosslinked medium prevent free diffusion of unreacted components, side reactions corresponding to the peak at about 199 °C (Figure IV. 1) become more preferable. Hydroxy groups linked to a tertiary amine by two carbon atoms are known to be stronger nucleophiles than other aliphatic alcohols due to hydrogen bonding with nitrogen atom^{44,45}. That is why it can be suggested that OH-groups formed at the first stage of reaction (hydroxyl ether) may react with remaining epoxy groups (Scheme VI. 3, OH- ring opening). The previous tertiary amine is also a nucleophile which can participate in epoxide ring-opening forming an ammonium salt²³.



Scheme IV. 3: Possible reaction paths of epoxy-functionalized IL with IPD.

However, based on a previous reported system ²⁶, the absence of endothermic peaks on the DSC thermograms (Figure IV. 1) showed that the reaction did not take place in this case (Scheme IV. 3). Such an interpretation of the occurrence of two reaction enthalpy peaks on the DSC traces are not in opposition to the ones reported by Galy *et al.* who observed a double exothermic peak for DGEBA-IPD systems at the same heating rate which was associated with the reactivity difference between the primary and secondary amines of the diisophorone diamine ⁴⁶. In fact, as the first exotherm occurred at about the same range of temperature (119 °C) as the one reported here, the second one was evidenced at 150 °C, *i.e.* very far from the second exotherm of these epoxy-IL/IPD reactive systems. To confirm the presence of this side reaction, DSC analysis of ILM1/IPD and ILM2/IPD mixtures with different ratio was performed (Figure IV.1a and 1b, blue and pink lines). An excess of IPD (pink line, Figure IV. 1a and 1b) led to a faster reaction at slightly lower temperature and to almost complete disappearance of the second exotherm, indicating that almost all epoxides were consumed by the reaction with primary and secondary amines. The lower concentration of IPD (blue line, Figure IV. 1a and 1b) results in lower intensity of both peaks. Obviously, the first reaction is limited by the introduced quantity of IPD, while the second one is limited by the amino alcohols formed at the first step, which confirms presence of the suggested side reactions leading to coexistence of tertiary amines with ethers at the end of the reaction. (Scheme IV. 3).

The curing behavior of ILMs with IPD system was also investigated by FTIR in the following reaction conditions: 3 h at 80 °C, 6 h at 120 °C, and 1h at 200 °C for ILM1/IPD and 1 h at 140 °C followed by 8 h at 190 °C for ILM2/IPD. The conversion of epoxide group was calculated from the changes of the adsorption bands at 914 cm⁻¹ (epoxide groups) with reference as the absorption band at 1,132 cm⁻¹ (trifluoromethyl (-CF₃) of bis(trifluoromethanesulfonyl)imide counterions (NTf₂⁻) ⁴⁷ by using equation (5) ^{2,26,38,42,43}:

$$X\% = \frac{A_0 - A_t}{A_t} \times 100\% \quad (5)$$

where A₀ and A_t are the ratio between the area of two absorption peaks (914 cm⁻¹ and 1,132 cm⁻¹) at t = 0 as well as the reaction time t. Thus, the epoxy conversion versus the polymerization time is presented in Figure IV.2b and 2c.

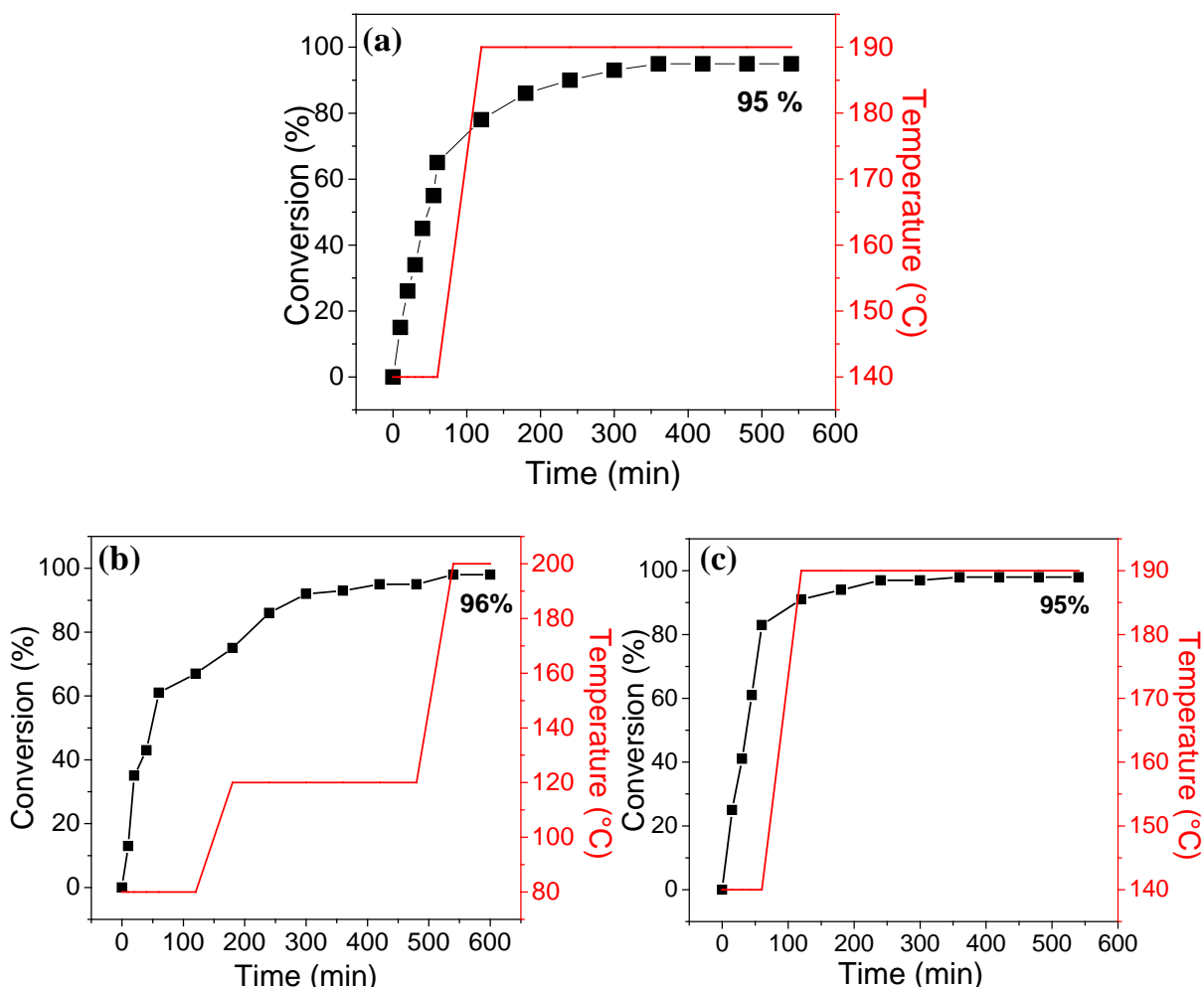


Figure IV. 2: Epoxy group conversion as a function of the reaction time and during temperature steps from FT-IR for a) DGEBA/IPD, b) ILM1/IPD, and c) ILM2/IPD reactive systems.

As expected, the FTIR spectra of the ILM1/IPD and ILM2/IPD systems along the reaction show a decrease of the absorption peak at 914 cm^{-1} corresponding to epoxide group, indicating the efficient ring opening of epoxides during curing process.^{38,48} At the end of the copolymerization reaction, this absorption peak nearly disappears suggesting a high conversion of epoxy-groups ($> 95\%$). To compare the reactivity of ILM1 (or ILM2) with DGEBA, the same experiment was carried out for DGEBA/IPD system (Figure IV.2a). The reaction kinetics being almost similar to both epoxy monomers, indicating that the ILM1 or ILM2 monomers architecture and their ionic character do not influence their reactivity compared to a conventional bisphenol-A-based diepoxy monomer.

In addition, ¹³C HR-MAS NMR spectroscopy was also used on ILM1/IPD and ILM2/IPD networks and compared to the spectrum of ILM1 and ILM2 (Figure IV. 3a and 3b) confirming the disappearance of the epoxy functions (signals at 34, 47, and 52 ppm) after the curing protocol.

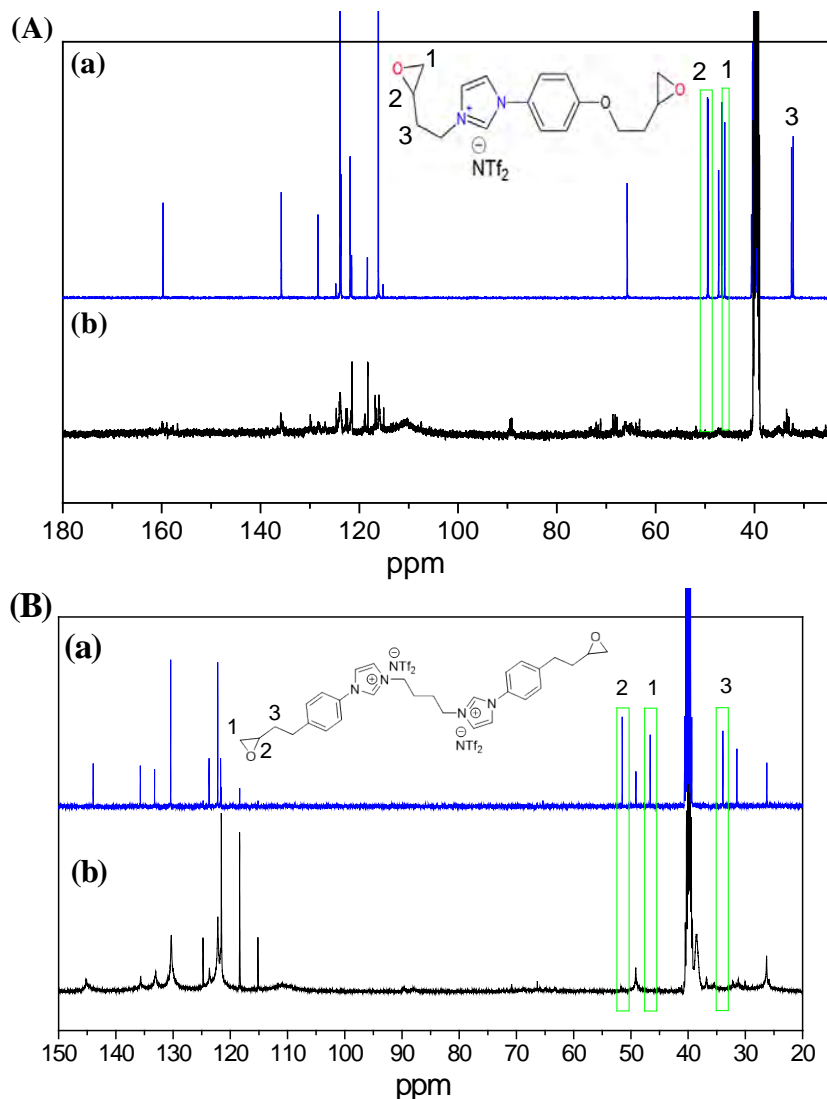


Figure IV. 3: (A): ¹³C NMR spectrum of a) ILM1 and HR-MAS ¹³C NMR spectrum of b) ILM1/IPD network; (B): ¹³C NMR spectrum of a) ILM2 and HR-MAS ¹³C NMR spectrum of b) ILM2/IPD network (DMSO-d₆; 400MHz).

IV.3.2. Thermomechanical properties of ILM/IPD networks

As presented in Figure IV. 4, the dynamic mechanical spectra of ILM/IPD and DGEBA/IPD networks evidence changes of the storage moduli G' and the main relaxation peaks as function of

the temperature. In addition, the viscoelastic characteristics of the different systems are summarized in Table IV. 2.

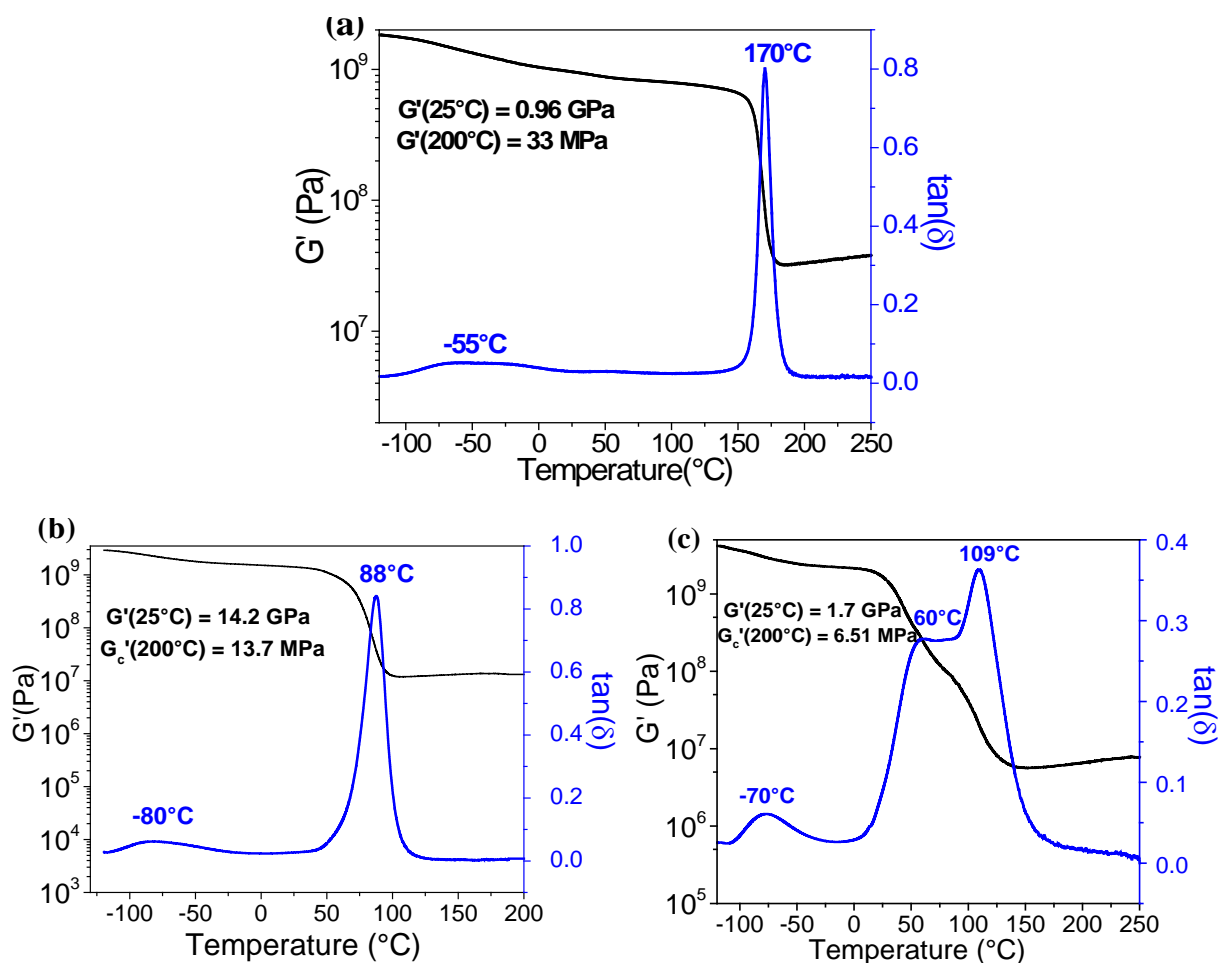


Figure IV. 4: Shear storage modulus, G' (black), and loss factor, $\tan \delta$, (blue) as a function of temperature at 1 Hz for a) DGEBA/IPD, b) ILM1/IPD, and c) ILM2/IPD networks.

In all cases, a noticeable reduction of G_c' in the high temperature range corresponding to the main relaxation phenomenon, α , associated to the glass transition was observed. However, notable differences are observed for the two epoxy ILM/IPD networks compared to DGEBA/IPD network. For ILM1/IPD and DGEBA/IPD networks, DMA spectrum indicated the formation of a homogenous network (in terms of relaxation times) characterized by one narrow well-defined relaxation peak located at 88 and 170°C , respectively. For DGEBA/IPD, the T_α value corresponds to the obtained reported in the literature ^{49,26}. In contrast, the same relaxation for ILM2/IPD network is a quite broad peak (109°C , α_1) with a shoulder at 60°C (α_2). Such a double relaxation peak (α_1 and α_2) could be associated to two populations of chains having

different mobility distributions. In other words, the network has a heterogeneous crosslink density with clearly distinguishable types of chain mobilities. This phenomenon is in good agreement with our hypotheses on the occurrence of side reactions (Scheme IV. 3). These side-reactions lead to a new type of crosslinks which could contribute to increase the crosslink density and generate less mobile chain segments. But also the side reactions result in the presence of unreacted secondary amines. The secondary amines act as chain extenders leading to longer chain lengths between crosslinks displaying an easier segmental mobility signed by the occurrence of the α_2 relaxation peak⁵⁰. Thus, two networks have been formed independently and simultaneously during the thermal cycle. Regarding the ILM1/IPD network, the difference is related to the epoxy monomer structure having single aromatic and imidazolium rings which is not influenced by the side-reaction showed in Scheme IV. 3. Moreover, we can also observe in both cases a secondary relaxation peak at lower temperatures, denoted β that is associated to the motions of hydroxyethers⁵¹⁻⁵³. For DGEBA/IPD, ILM1/IPD, and ILM2/IPD networks, T_β values of -55 °C, -80 °C, and -77 °C were obtained, respectively. The higher intensity of the β relaxation peak explained the large difference of modulus at room temperature between ILM1/IPD and ILM2/IPD as G' change is associated to this relaxation (below T_β the moduli are the same for these two networks).

Table IV. 2: Thermomechanical data of the epoxy DGEBA/IPD and ILM/IPD networks (at 1 Hz).

Network	T_{a1} (°C)	T_{a2} (°C)	$G'_c(200\text{ °C})$ (MPa)	M_c (g.mol ⁻¹)	$M_c\text{ ther}$ (g.mol ⁻¹)
ILM1/IPD	88	-	13.7	≈ 1102	≈ 430
ILM2/IPD	109	60	6.5	≈ 774	≈ 320
DGEBA/IPD	170	-	33.2	≈ 395	≈ 218

The lower values of T_g and the storage modulus for ILM/IPD compared to DGEBA/IPD networks (Table IV. 2) can be explained by the chemical structure and the molar masses of the epoxy monomers. All molecules epoxy co-monomers contain rigid aromatic rings, but in the case of DGEBA, there is only one carbon atom between the rings, that makes whole molecule rather rigid, while ILM1 or ILM2 contains the rather flexible tetramethylene linkage. It is also well-

known that addition of acyclic aliphatic fragments in amino-epoxy networks leads to a decrease of T_g ⁵⁰. Thus, this longer distance between two reactive ends of ILM1 or ILM2 in the ILM/IPD networks provided a higher mobility and flexibility to the resulting matrix compared to the DGEBA/IPD network.

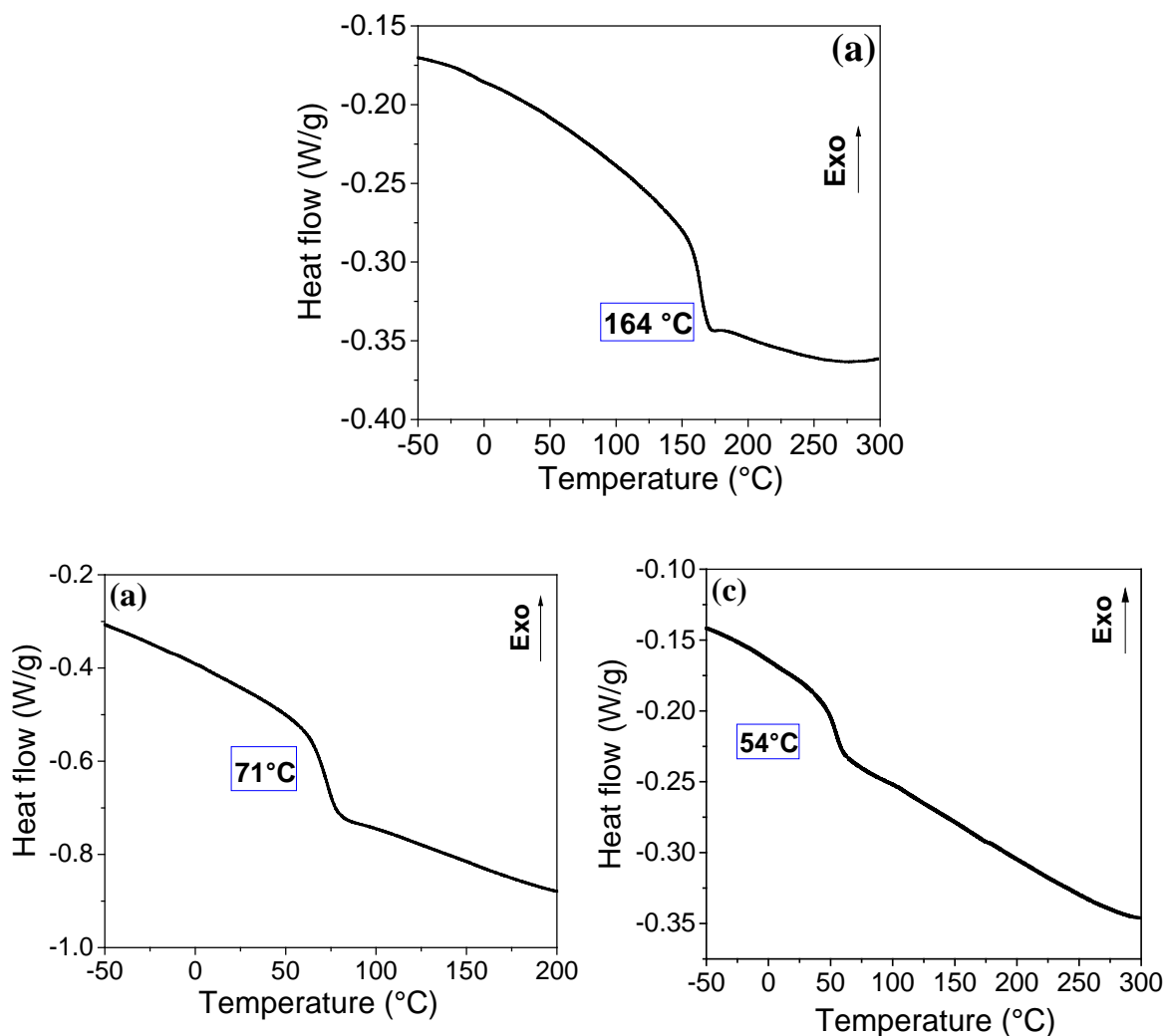


Figure IV. 5: DSC thermograms after curing of a) DGEBA/IPD, b) ILM1/IPD, and c) ILM2/IPD.

The G'_c moduli in the rubbery state could be considered to calculate the molar mass, M_c , between crosslinks according to the rubber elasticity theory:

$$G'_c = \rho_0 RT / M_c \quad (6)$$

where ρ is the density, R is the gas constant ($8.314 \text{ J.K}^{-1}.\text{mol}^{-1}$), and T the temperature at which G'_c is measured. The calculated M_c values and theoretical ones (from the molar mass of the epoxy monomers) are reported in Table IV. 2. Except for the DGEBA-based network, the calculated molar masses between crosslinks are 2 to 3 times higher than the expected ones. This indicates clearly that the architecture of ILM-based networks are non-ideal and cannot be modelled according to simple amino hydrogen/epoxy additions. These conclusions are in agreement with complex reaction pathways for such monomers. In addition, according to these features on rubbery modulus, the lower T_g of ILM/IPD based networks cannot be explained only by the higher flexibility of chains (ILMs) between crosslinks.

Interestingly DSC analysis of obtained networks showed T_g at 71°C for ILM1/IPD and 54°C for ILM2/IPD (Figure IV. 5), that is close to the $T_{\alpha 1}$ and $T_{\alpha 2}$ determined by DMA, respectively (Table IV. 2). However, for ILM2/IPD, the α_2 -transition was not visible on DSC thermograms probably due to the temperature interval of the transition and not sufficient sensitivity for DSC.

As a conclusion, one can observe that a lower T_g is obtained on ILMs based networks in comparison with that of DGEBA/IPD networks but could be attractive for potential shape memory applications (see *Shape memory test* section for more details). In addition, the dynamic mechanical spectroscopy (DMA) clearly shows that ILM2/IPD network is characterized by the presence of two heterogenous crosslinked densities, *i.e.* ILM2/IPD network architecture is strongly heterogenous.

IV.3.3. Morphology investigation of ILM/IPD networks

To reveal the presence or not of a potential phase separation during polymerization of reaction systems on the ionic liquid monomers, transmission electronic microscopy (TEM) was performed (Figure IV. 6).

ILM1 and ILM2 form initially the homogeneous and transparent mixtures with IPD indicating a good miscibility due to the formation of intermolecular specific interactions (*e.g.*, hydrogen bonding) between ILMs and IPD. The homogeneous and transparent mixtures were cured at the elevated temperatures to prepare *in situ* the networks. It was observed that the resulting networks were homogeneous and transparent; *i.e.*, no discernible phase separation occurred on the scale exceeding the wavelength of visible light (see Figure IV. 6a and 6b).

As can be seen in Figure IV. 6, no clear and distinct phase separation was observed confirming a good miscibility between imidazolium ILM1 or ILM2 and amine hardener. However, some dark spots are appearing across the epoxy network in the contrast mode due to impurities introduced during the preparation.

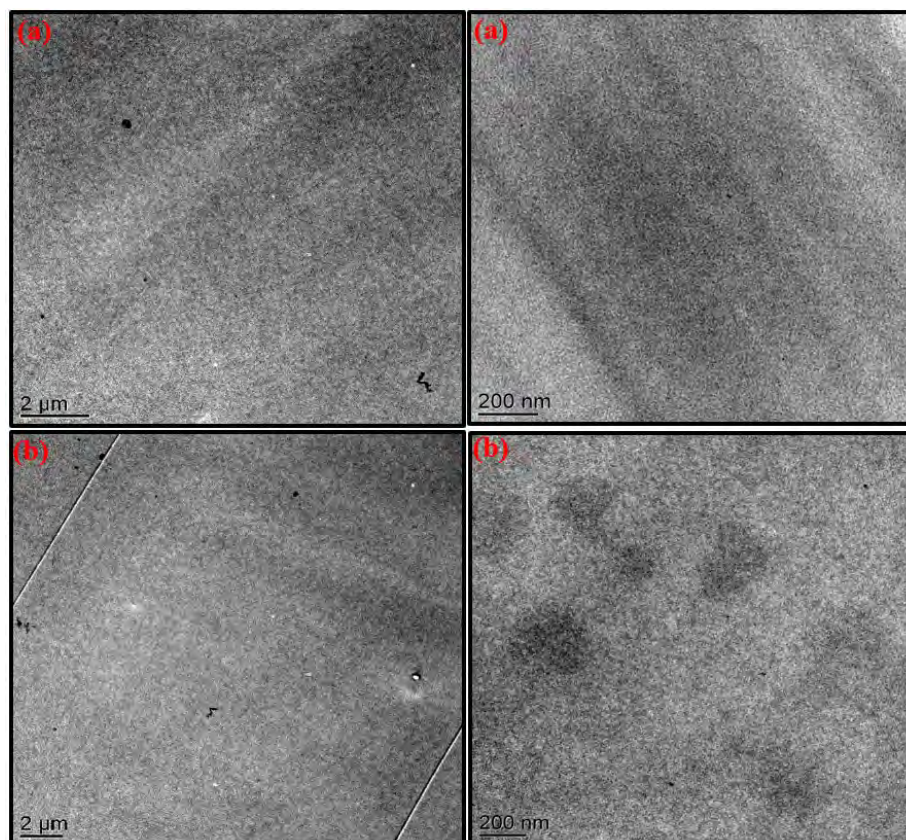


Figure IV. 6: TEM images of a) ILM1/IPD and b) ILM2/IPD (at different magnifications).

IV.3.4. Thermal stability of ILM/IPD networks

Thermogravimetric analysis (TGA) was used to determine the thermal behavior of the ILM/IPD networks. The evolution of the weight loss as a function of the temperature for ILM1/IPD, ILM2/IPD, and DGEBA/IPD networks are shown in Figure IV. 7 and for ILM1 and ILM2 monomers in Figure S4.2 (see SI of chapter IV).

In all cases, an excellent thermal stability of mono and dicationic IL, *i.e.* imidazolium ionic liquids salt ILM1 or ILM2 and their corresponding crosslinked networks with IPD is clearly evidenced. It is widely reported that the majority of ILs are thermally stables^{54,55}. However, many parameters can play a role on their intrinsic stability such as the chemical nature of the

anion (halogens or fluorinated), the cationic backbone (ammonium, imidazolium or phosphonium), the influence of C- and N-substituents, and the type of linker between the two cations as well as the alkyl chain length ⁵⁶⁻⁶¹. It is also well-known that dicationic ILs have a greater thermal stability than conventional ILs thanks to their higher molar masses as well as to their high charge and intermolecular interactions ⁶². As can be seen in Figure S4.2 of the SI in chapter IV, two decomposition peaks at 333 and 489 °C for ILM1 and at 307 and 460 °C as well as a very low loss of mass (close to 1.4 wt. %) between 100 to 160 °C corresponding to the water desorption are observed for ILM2. According to the literature, the first peaks (333 and 307 °C for ILM1, ILM2, respectively) can be attributed to the decomposition of the alkyl substituents on the imidazolium core of the IL ^{62,63}. In fact, various authors have demonstrated that monocationic ILs based on imidazolium cation have a first thermal decomposition at about 300 - 340 °C ^{62,63}. More recently, Patil *et al.* have investigated the thermal decomposition of various dicationic imidazolium ILs combined with bis(trifluoromethanesulfonyl)imide counter anion by using electrospray ionization mass spectra ⁶⁴. In this work, they have shown that at 310 - 340 °C, the C-O bonds are broken whereas at 460 °C, C-N bond rupture is obtained. In conclusion, the ILM1 or ILM2 with IPD crosslinked networks have excellent thermal stability (> 460 °C) with high char residue (16 - 22 %) compared to conventional DGEBA/IPD network ^{34,65} which has a maximal degradation temperature at 369 °C and almost no residue ($\approx 3\%$).

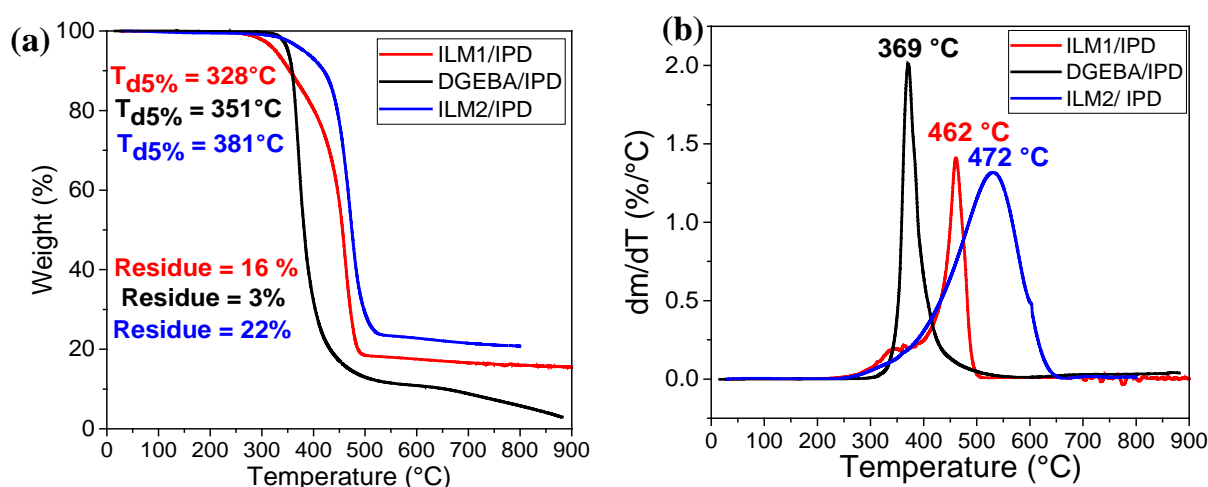


Figure IV. 7: a) Weight loss as a function of temperature (TGA) and b) derivative of TGA curves (DTG) of the epoxy-IL networks ILM1 (or ILM2)/IPD and the epoxy-amine DGEBA/IPD (heating rate: 10 K.min⁻¹; atmosphere: nitrogen flow).

IV.3.5. Surface energy of DGEBA/IPD and ILM/IPD networks

Surface energy of the DGEBA/IPD and the ILM/IPD networks were studied by sessile drop method in order to determine the influence of the epoxy prepolymer. By using Owens-Wendt theory based ³⁰ on two probe liquids which are methylene diiodide and water, the surface energy, the non-dispersive and dispersive components are presented in Table IV. 3.

Compared to the DGEBA/IPD network, the use of ILM1 or ILM2 led to a significant reduction in total surface energy including both non-dispersive and dispersive components (Table IV. 3). These results can be explained by the hydrophobic character of the ionic liquid epoxy monomers incorporating imidazolium cores associated with fluorinated counterions (NTf₂⁻) ^{66,67} which are well-known to have a low surface tension ⁶⁸. In fact, the contact angle values obtained are very similar to the values reported in the literature for polytetrafluoroethylene (PTFE), *i.e.* 110 - 115° for water and 82 - 83° for methylene diiodide ^{69,70} confirming the formation of non wettable and low surface tension polymeric networks. Moreover, we can over pass the limitations of PTFE like its low oil repellency, its semicrystalline surface structure as well as the difficulty of its processing. In summary, this hydrophobicity opens new promising perspectives in the preparation of hydrophobic surface coatings for various applications such as automotive, aerospace, or electronic fields.

Table IV. 3: Contact angle and surface energy of ILM1 (or ILM2)/IPD networks measured by sessile drop method at 25 °C.

Network	Θ_{Water} (°)	$\Theta_{\text{CH}_2\text{I}_2}$ (°)	$\gamma_{\text{non-dispersive}}$ (mJ.m ⁻²)	$\gamma_{\text{dispersive}}$ (mJ.m ⁻²)	γ_{total} (mJ.m ⁻²)
ILM1/IPD	102	62	0.8	24.6	25.4
ILM2/IPD	106	72	0.6	21.0	21.6
DGEBA/IPD	79	49	4.8	34.8	39.6

IV.3.6. Mechanical properties

The mechanical properties of ILM1/IPD and ILM2/IPD epoxy networks determined under uniaxial tensile mode are presented in Figure IV. 8.

According to the literature, the conventional DGEBA/IPD network having a high T_g (160 - 170 °C) is well-known to have also high Young's modulus $\approx 2.6 - 2.7$ GPa combined with low strain at break $\approx 4 - 5$ %^{31,33-36,71}. In the case of ILM1 (or ILM2)/IPD networks, the resulting systems have a relatively high Young's modulus (close to 1.60 GPa) despite relatively low T_g compared to DGEBA/IPD system as well as significant elongation at break (close to 28 %) (see Figure IV. 8a and 8b). This result can be explained by the lower crosslinking density of the ILM1 or ILM2 cured with IPD networks as well as the molecular architecture of the epoxy prepolymers allowing a higher ability to deform. Thus, we can infer the relationships between the mechanical properties and the chemical structure of the monomers that changes the structure of the networks and gives unexpected properties, *i.e.* a lower T_g combined a high Young's modulus and tensile strength.

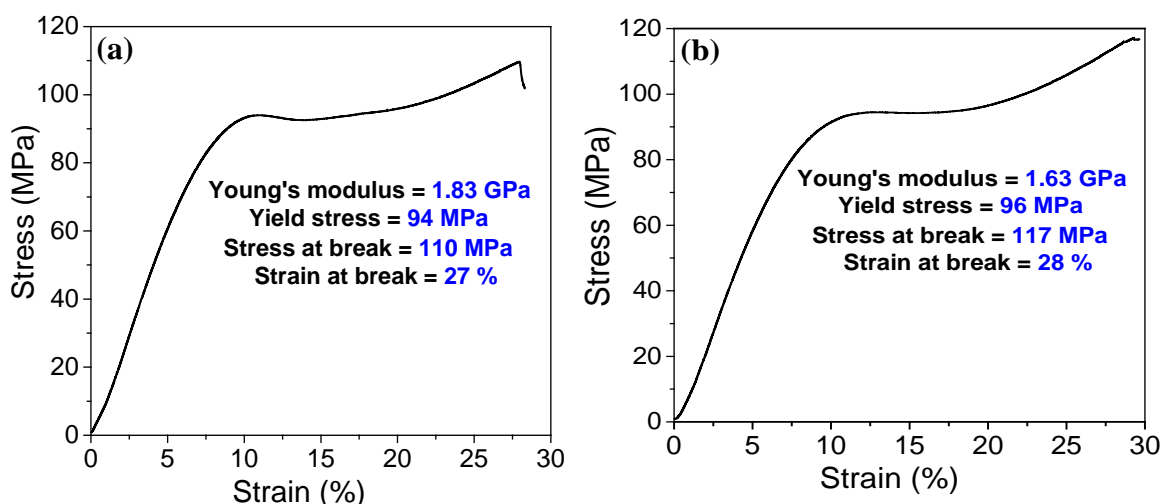


Figure IV. 8: Stress-strain curves of a) ILM1/IPD and b) ILM2/IPD networks (uniaxial tension mode; 1 mm.min⁻¹).

IV.3.7. Shape memory

Shape memory polymers (SMPs) are a very interesting and promising class of smart materials⁷². They can be deformed under certain conditions, *i.e.* fix a temporary shape and recover original permanent shape upon exposure to an external stimulus (most often heat). Such materials have already found application in many areas such as outer space, automotive, and medical applications⁷³. To possess the shape memory behavior, a polymer must be a 3D network with two types of crosslinks: the first one will be responsible for temporary shape fixity and can be removed by applied stimulus whereas the second type of crosslinks induces recovery of the

original shape and must not be influenced by the external stimulus (usually covalent bonds)⁷⁴. Epoxy networks have been already reported to be effective SMPs⁷². Thus, epoxy resins cured by anhydrides⁷⁵⁻⁷⁷, amines^{31,78,79}, or cationic initiators^{80,81} were reported to have shape memory behaviors as to be used as matrices in a fiber-based composite. Moreover, their low curing shrinkage, versatile chemistry of curing, and easy tuned thermomechanical properties make the epoxy-based thermosets good candidates for SMP materials as they display excellent shape fixity and recovery, reaching 95 - 100 %⁸². However, despite their beneficial properties, not too many teams deal with the epoxy based SMPs due to a low deformability and high T_g of the corresponding systems⁸³⁻⁸⁵. Although, an IL was employed to improve shape memory performance of epoxy-silica nanocomposite⁸⁶, but no works have been reported about epoxy-networks having shape memory capability of imidazolium ionic liquid monomers (ILMs). Only two publications can be found describing shape memory polymerizable ionic liquids (PILs)^{86,87}. For example Yan *et al.* obtained shape memory gels by radical copolymerization of ILM with a crosslinker under different conditions⁸⁷. These gels were able to recover the initial form by swelling in β -cyclodextrin solution. Du *et al.* reported PIL-poly(vinyl alcohol) dual network synthesis and applied microwaves as shape recovery stimulus for such materials⁸⁸.

As it was determined by DMA (Figure IV. 3a and 3b), ILM/IPD networks possess an α -relaxation region extending over a temperature range from 0 to 200 °C with two relaxation regions (α_1 and α_2) for ILM2/IPD and one for ILM1/IPD. A parameter which is commonly used to estimate shape memory efficiency is the ratio of storage moduli in glassy and rubbery states^{78,86,89,90}, *i.e.* $G'(25\text{ °C})/G'(200\text{ °C})$ equal to 1,036 and 261 for ILM1/IPD and ILM2/IPD networks, respectively (Figure IV. 3a and 3b). These values are very high compared to the previously described DGEBA/IPD network which displays a ratio of 28 (Figure S4.4 in the SI of chapter IV). These large elastic ratios are beneficial for showing a good shape memory capability since it gives larger shape fixity upon cooling and gives a larger strain at a smaller stress at high temperatures^{78,86,89,90}. Experimentally, the samples were placed at 90 and 130 °C, *i.e.* above the T_α relaxation in order to reach the rubbery state, for 30 min. The hot sample was bent at 130 °C and cooled down to 25 °C with a fixed shape. At room temperature, the sample kept its modified shape (Figure IV. 9a and 9b) ($R_f = 99\%$) confirming that ionic interaction and/or changes conformations in the glassy state can fix the temporary form. Then, the sample stood in the oven at 90 and at 130 °C for ILM1/IPD and ILM2/IPD, respectively (in such a way to avoid gravity

influences on the shape recovery). Figure IV. 10a and 10b show the disappearance of the deformation with time at different temperatures. A period of 6 minutes was required for the sample to recover its initial shape for ILM1/IPD at 90 °C and 5.5 minutes at 130 °C for ILM2/IPD. This time can be reduced to only 3 minutes at 130 °C for ILM1/IPD and at 170 °C for ILM2/IPD (see Figure IV. 10a and 10b). At the end of the tests, the two samples were completely flat ($R_r = 100\%$) (see Figure IV. 9a and 9b) indicating excellent shape recovery.

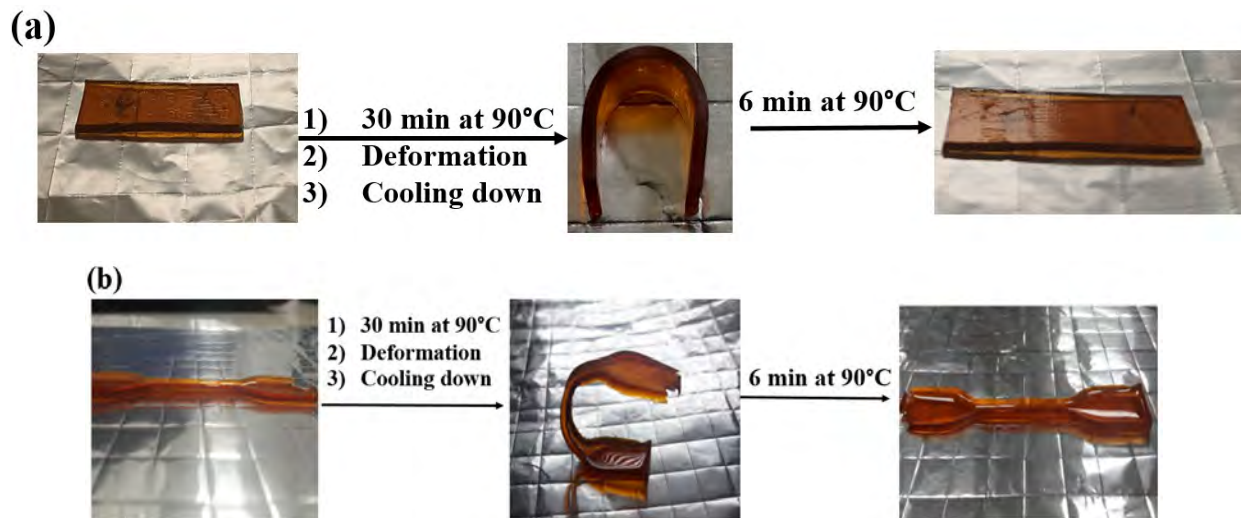


Figure IV. 9: Shape memory test of a) ILM1/IPD and b) ILM2/IPD networks.

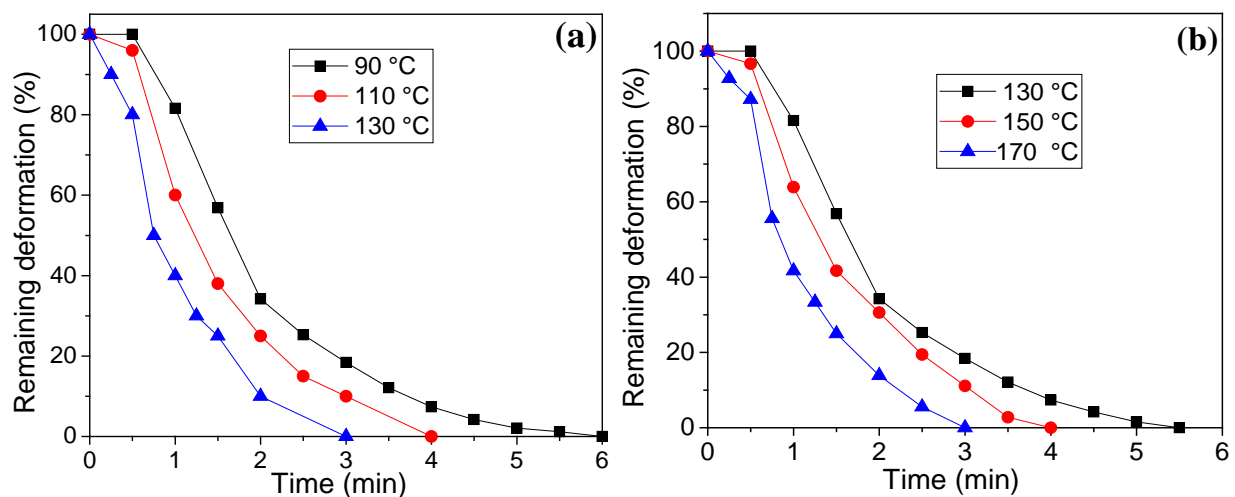


Figure IV. 10: Remaining deformation vs. time dependence for a) ILM1/IPD and b) ILM2/IPD networks at different temperatures.

Such a behavior could be reproduced several times by applying similar temperature-deformation cycles. Of course, the DGEBA/IPD did not behave similarly as this network does not display a shape memory capacity at relatively low temperature. To the best of our knowledge, this is the first example of epoxy-PIL networks displaying a shape memory at relatively low temperature according to their important deformability. This behavior could be explained by the heterogeneous crosslink, *i.e.* leading to a double α relaxation, density and the presence of (reversible) ionic interactions in the ionic ILM/IPD networks.

IV.3.8. Conclusion

Imidazolium salts bearing two epoxy groups (ILM1 or ILM2) were successfully synthesized with the objective to substitute the usual DGEBA prepolymer which is prepared using toxic and carcinogenic compounds (such as bisphenol A synthesized from epichlorohydrin). Novel ionic epoxy-amine thermosets resulting from the copolymerization of ionic epoxy monomers and isophorone diamine were developed. For such ionic monomers, we have identified a polymerization mechanism based on two crosslinking reactions, *i.e.* epoxy-amine reaction and amino-ether formation. The architecture morphology-properties relationships of ILM/IPD networks were investigated. It was demonstrated that the copolymerization of the ILMs and IPD led to homogeneous epoxy network without any phase separation. Such ionic networks combine good thermomechanical properties, high hydrophobic character, and high thermal stability. The mechanical performances of these new epoxy-IL/amine networks were founded to be similar to the reference network but such ionic networks have a shape memory behavior with a 100 % recovery in a few minutes at moderate temperatures. These results open new perspectives in the development of a new generation of (multi)functional-dedicated polymer materials for various types of applications such as the ones requiring fire retardancy and mechanical performances as well as shape memory behavior. Moreover, these novel polymers could be investigated for their ionic conductivities as well as gas barrier properties to be used as solid polymer electrolytes.

IV.4. Epoxy hybrid ILM/IPD containing POSS^{®Ph}-triol or IL-g-POSS^{®Ph}

IV.4.1. Morphology of hybrid O/I networks

When using phenyltrisilanol POSS[®] (POSS^{®Ph}-triol) or IL-g-POSS^{®Ph} with the various counter anions, *i.e.* chloride (Cl⁻) versus bis(trifluoromethanesulfonyl)imide (NTf₂⁻), it can

form a homogeneous and transparent mixture with DGEBA or ILMs and IPD. This is a proof of the solubility of all the monomers at the initial stage, *i.e.* before polymerization. The miscibility could be due to the formation of intermolecular interactions (*e.g.*, including Van der Waals, electrostatic, solvophobic, steric, and hydrogen bonding interactions) between POSS^{®Ph} and ILMs or DGEBA (and/or IPD). However, each type of interaction with nanoclusters contributes to get good dispersions. The homogeneous and transparent mixtures with the contents of 5 wt. % of non-modified (POSS^{®Ph}-triol) or IL-modified POSS^{®Ph} (IL-g-POSS^{®Ph}) were cured at elevated temperatures to prepare *in situ* the organic-inorganic hybrid networks. It was observed that with DGEBA prepolymer during the curing reaction, the initially transparent solutions gradually became cloudy evidencing the occurrence of a phase separation induced by polymerization, denoted RIPS (Reaction Induced Phase Separation). However, with ILMs monomers, the resulting networks were homogeneous and transparent; *i.e.*, no discernible phase separation occurred at macroscale.

Transmission electronic microscopy was used to highlight the effect of the ionic liquid monomers ILMs on the dispersion of the POSS^{®Ph}-triol and IL-g-POSS^{®Ph} nanoclusters into epoxy networks as well as the formation of a possible interphase between the ILM-based networks and POSS^{®Ph}-POSS^{®Ph} aggregates. The morphologies obtained of the epoxy hybrid O/I networks are displayed in Figure IV. 11. In all TEM micrographs, the dark part corresponds to the POSS^{®Ph}-rich phases whereas the brightest continuous phase corresponds to the epoxy ILM/IPD matrix.

In all cases, *i.e.* the epoxy networks based on ILM1 or ILM2 containing POSS^{®Ph}-triol or IL-g-POSS^{®Ph}, a homogeneous distribution of nanoclusters aggregates in the epoxy matrix was revealed by TEM. The difference between the epoxy DGEBA/POSS^{®Ph} (see Figure III. 3 in the chapter III) and ILM/POSS^{®Ph} (Figure IV. 11) hybrid O/I networks is the size of the POSS^{®Ph} aggregates. The POSS^{®Ph}-rich dispersed phases have a spherical or ellipsoidal shape in the different systems, with a diameter range from 0.1 to 1.5 μm for the epoxy based on DGEBA/IPD (see Figure III. 4 in the chapter III) hybrid networks containing POSS^{®Ph}-triol and from 60 to 900 nm for the epoxy networks using ILM1 or ILM2 as epoxy monomers. Such features are usually encountered for a conventional morphologies generated from a phase separation induced during polymerization^{92,93}. In both epoxy networks (ILM1 or ILM2) containing POSS^{®Ph}-triol, the formation of an interphase is observed around some POSS^{®Ph} nodules as shown in Figures IV.

11a and 11d. This interphase has an average thickness of 10 to 30 nm. The interconnected nanophase-separated morphology with uniform domain size is characteristic of self-assembly structures generated as result of a balance of different intermolecular interactions^{94,95}. For the epoxy networks containing IL-g-POSS^{®Ph} with chloride (Cl⁻) or bis(trifluoromethanesulfonyl)imide (NTf₂⁻) counter anions, the TEM images based on DGEBA/IPD matrix show that the phase separation between epoxy network and IL-g-POSS^{®Ph} occurred at nanoscale. In fact, a dispersed phase having spherical shapes based on small assemblies of POSS^{®Ph}, POSS^{®Ph}-POSS^{®Ph} interactions could be observed with an average diameter from 40 to 240 nm (see Figure III. 4 in the chapter III). On the opposite, the use of ILM1 and ILM2 induced smaller assemblies of POSS^{®Ph} (from 80 to 400 nm) for the POSS^{®Ph} cages nanostructuration. The dispersion of the IL-g-POSS^{®Ph} having a chloride anion in the ILM1 or ILM2 epoxy prepolymer is always better compared to IL-g-POSS^{®Ph} having a NTf₂⁻ anion (uniformity of dispersion and aggregate sizes). These differences can be explained by the higher nucleophilicity and the smaller molar masses of the chloride anion compared to the NTf₂⁻ anion⁴⁰. Cl⁻ provides a higher mobility avoiding extra collision force and leading to a high reactivity with the ILMs monomers. According to literature, various authors have explored the ability of imidazolium ionic liquid to be used as dispersing agents or dispersion media⁹⁶. In fact, these one could facilitate the dispersion of metallic⁹⁷, or inorganic nanostructured particles⁹⁸ as well as carbon nanotubes⁹⁹. The average size and size distribution of nanoparticles are managed from the physico-chemical properties of ionic liquids. For example, stabilization of bare silica nanoparticles by imidazolium-based ionic liquids were found to be tuned by the affinity between the ions and particle surface according to careful selection of the ions of ILs and/or the nanoparticle surface modification. Such a management could optimize the ionic liquid-based steric stabilization provided by the non-polar alkyl chains as a protecting group⁶⁰. Donato *et al.* have obtained well dispersed silica aggregates (of about 30 nm diameter) for 6.8 wt. % of IL-functionalized silica particles having different counter anions (Cl⁻ and MeSO₃⁻)^{100,101}. These obtained dispersions are finer than those achieved by using a metal complex catalyst, *i.e.* aluminum triacetylacetonate ([Al]) which is used to reduce the size of POSS^{®Ph}-triol aggregation¹⁰² or by substitution of DGEBA with TGDDM epoxy prepolymer¹⁰³. As a conclusion, one can concluded about the use of imidazolium ILMs as new monomers as a promising route to achieve a nanoscale filler structuration in thermosets (epoxy) networks and to design nanomaterials

combining properties from both ionic liquid and nanoclusters. Such nanomaterials could be useful as novel hybrid materials for electrochemistry applications.

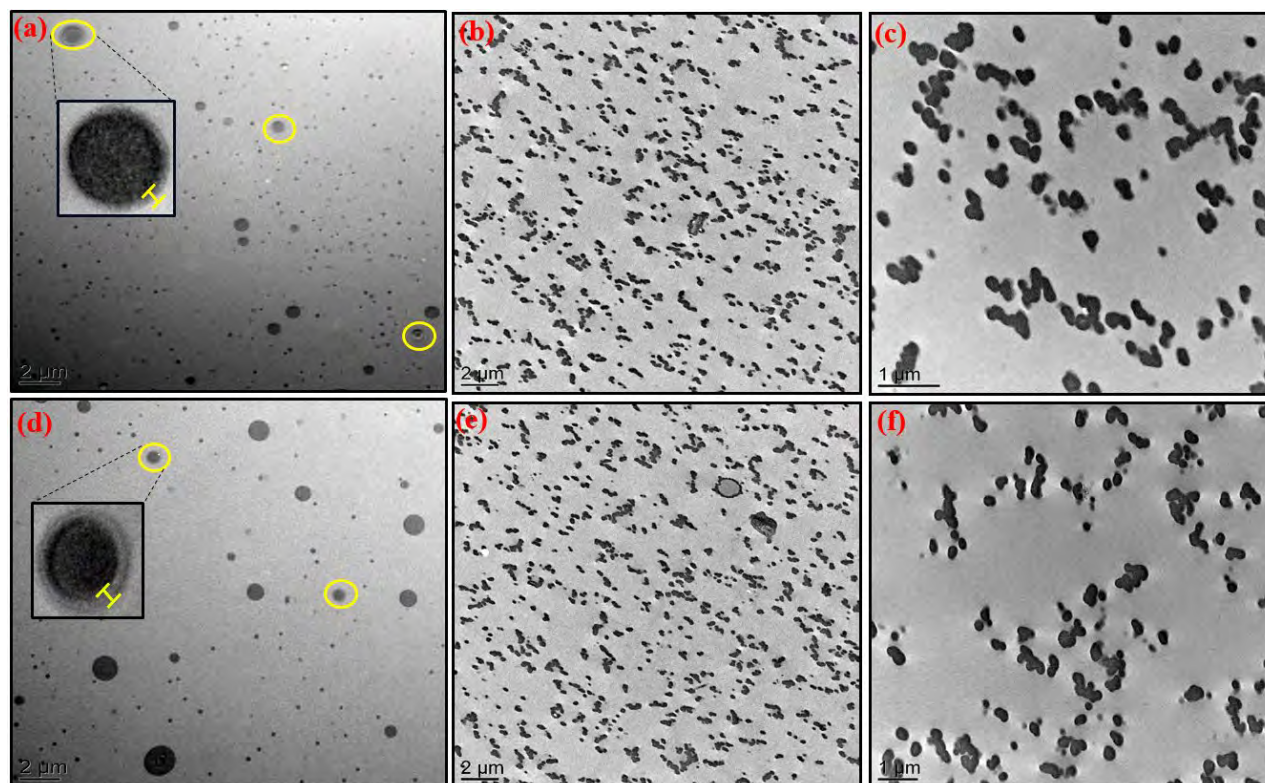


Figure IV. 11: TEM images of the different epoxy ILMs hybrid O/I networks containing (5 wt. %) POSS^{®Ph}-triol, IL.Cl-g-POSS^{®Ph} and IL.NTf₂-g-POSS^{®Ph} respectively, prepared with ILM1 epoxy monomer (a, b, c), and with ILM2 (d, e, f).

IV.4.2. Epoxy conversion and glass transition

It has been observed that the presence of POSS[®] cages on glass transition temperature of the hybrids is dependent on the nature of corner R groups on silsesquioxane cages and epoxy matrix. The DSC thermograms of POSS^{®Ph}-based hybrid O/I networks display a single glass transition temperature, *i.e.* the hybrids are homogenous⁹³. The glass transition of the neat epoxy ILM/IPD networks occurred at 71 and at 54 °C for ILM1/IPD and ILM2/IPD, respectively (Figure IV. 4). It can be noticed that all the hybrids O/I containing POSS^{®Ph}-triol or IL-g-POSS^{®Ph} (whatever the chemical nature of the anion, *i.e.* chloride or bis(trifluoromethanesulfonyl)imide (NTf₂⁻)) show a decrease of their glass transition temperature (close to 60 and 45 °C for ILM1/IPD and ILM2/IPD networks, respectively) (Figure IV. 12a and 12b). Nevertheless, ILM2/IPD epoxy

network containing POSS^{®Ph}-triol displayed higher T_g (74 °C) compared to the neat epoxy ILM2/IPD and the O/I hybrids containing IL-g-POSS^{®Ph} networks (Figure IV. 12b).

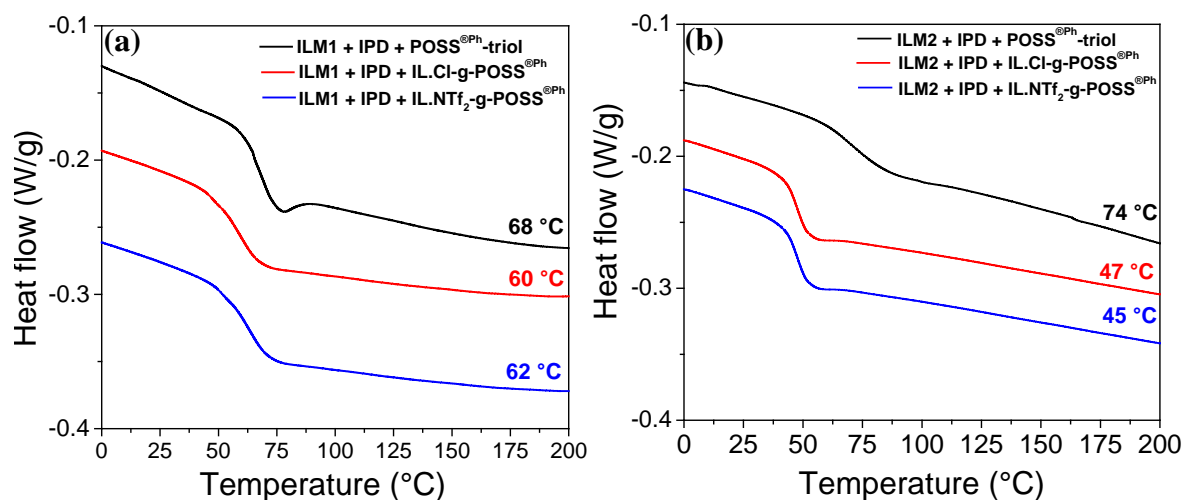


Figure IV. 12: DSC traces of the epoxy hybrid O/I networks containing (5 wt. %) POSS^{®Ph}-triol, IL.Cl-g-POSS^{®Ph} and IL.NTf₂-g-POSS^{®Ph} respectively, prepared based on epoxy IL monomers a) ILM1, and b) ILM2 (heating rate: 10 K.min⁻¹).

It can be proposed that the decrease of the glass transition temperature results from the incomplete curing reaction of the ILMs monomers due to the presence of POSS^{®Ph} nanoclusters¹⁰⁴. To confirm such an assumption, the epoxy conversion was determined. As shown in Figures S4.3 and S4.4 (see SI in chapter IV), FTIR and the ¹³C HR-MAS NMR spectra of the different hybrid O/I networks confirm the high conversion rate of epoxy-groups (> 90 %) and the total disappearance of the epoxy peaks (at 34, 47, and 52 ppm in the ¹³C-NMR spectra) after the curing procedure, suggesting that the curing reactions are completed. Therefore, the decrease of the glass transition temperatures will not be associated with a non-fully completed curing reaction due to the incorporation of POSS^{®Ph}-triol or IL-g-POSS^{®Ph}. The T_g decrease could be attributed to non-completed phase separation; *i.e.*, a low fraction of POSS^{®Ph}-triol or IL-g-POSS^{®Ph} remains dissolved in the ILM-based epoxy matrix and to the possible secondary reactions between IL-g-POSS^{®Ph} and the epoxy ILMs monomers generated by the anion (Cl⁻ or NTf₂⁻)⁴⁰, or from the reaction between the hydroxyl silanol of the POSS^{®Ph} cages and the epoxy groups¹⁰⁵ (see chapter II). To confirm these hypotheses, the remaining soluble fractions after curing schedule of the different systems were determined. In the case of epoxy ILM/IPD networks containing POSS^{®Ph}-triol, the soluble fraction was determined to be 4.2 % with ILM1/IPD and 4.0 % with ILM2/IPD

which means that some POSS^{®Ph}-triol clusters (about 16 to 20 %) are chemically attached to the epoxy networks. For the IL-grafted POSS^{®Ph}, the soluble fraction was found for both epoxy ILM/IPD networks to be about 3.8 and 3.6 % for IL.Cl-g-POSS^{®Ph} and for IL.NTf₂-g-POSS^{®Ph}, respectively. In addition, a covalent grafting of these IL-modified POSS^{®Ph} with the epoxy networks is ensured for about 24 to 28 % of the nanoclusters, while the rest of POSS^{®Ph} remain non-bounded to the epoxy network.

It has been reported for octa-aminophenyl POSS[®] and octa-nitrophenyl POSS[®]-modified epoxies ⁹³ that with a low content of POSS^{®Ph}, a T_g decrease is observed, which can be ascribed to the increase of free volume of the system due to the insertion of bulky POSS^{®Ph} cages between chains. According to the literature, two competitive factors can affect the glass transition temperatures. First, the steric hindrance effect of POSS[®] cages on polymer chain motions will contribute to increase of the glass transition temperature via reduction of local chain motions. Secondly, the inclusion of bulky POSS[®] cages could give rise to the increase of free volume leading to a decrease of the T_g. Nevertheless, the T_g depends on the nature of the interactions between POSS[®] cages and polymer matrix controlled by functionalities of POSS[®], nature of polymer matrix, and organic groups in POSS[®] vertexes, etc. Thus, POSS[®] could act as nanofiller or plasticizer. In fact, POSS^{®Ph}-containing nanomaterials can display increased ^{92,106} or decreased ^{107,108} T_g compared to neat polymers. The introduction of POSS^{®Ph}-triol or IL-g-POSS^{®Ph} in ILM1/IPD or ILM2/IPD networks leads to an increase of free volume due to the occurrence of the phase separation induced by polymerization. The increased T_g for the hybrid O/I network containing POSS^{®Ph}-triol based on ILM2/IPD matrix could be associated to the reactions between POSS^{®Ph}-triol and epoxy groups.

IV.4.3. Thermo-oxidative stability

Epoxies display a lower flame retardancy. Thus, to obtain a higher thermostability of such polymer materials, multicomponent fire retardants are used. It was found that compounds containing Si, N, P, and halogen, compounds are good candidates ^{109,110}. As described in a previous chapter, POSS^{®Ph} tends to create silica which could lead to the generation of ceramic-like coating during combustion protect the inside matrix far away from oxidation. Such an inorganic surface layer could act to stop the attack from the oxygen radical and the thermodegraded active radicals, *i.e.* contributing to improve the resistance to oxidation.

Moreover, the Cl⁻ and NTf₂⁻ anions introduced via the ionic liquids can quench the active radical and limit the probability of chain reaction ¹¹¹. For such a behavior, the effects of the functionalized POSS[®] on the thermal stability of the networks based on ILMs have been investigated.

Thermal stability and the thermo-oxidative resistance of the epoxy hybrid O/I networks were investigated with thermogravimetric analysis (TGA) under air (to favor oxidation reaction) and inert atmosphere (intrinsic degradation) in order to examine the influence of the POSS^{®Ph}-triol and the IL-g-POSS^{®Ph} nanoclusters on the pyrolysis-oxidation resistance of the epoxy ILM/IPD networks. Thus, this evaluation was done from the weight change under air atmosphere as a function of the temperature, the initial decomposition temperature (T_{d5%}), and maximal degradation temperature (T_{dmax}) (Figures IV. 13a and 13b and as well as Figures S4.5a and S4.5b under inert atmosphere).

The thermal degradation (Figures S4.5a and S4.5b in SI of the chapter IV) proceeds from two decomposition steps for the different epoxy hybrid O/I networks under nitrogen atmosphere. These steps occur between 250 – 400 °C and 400 - 550 °C defined from the vertex group degradation and dehydration-vaporization mechanism ¹¹² at higher temperature (900 °C) producing a stable black residue (6 to 18 wt. %). Under air, a similar behavior is obtained. The epoxy hybrid O/I networks display the same decomposition profiles with a low degradation temperature (T_{d5%}) similar to other POSS[®]-modified systems ¹¹³. The thermograms also show a third decomposition step at higher temperature (from 550 to 750 °C) related to the maximum rate of evaporation and full oxidation combustion reactions (Figures IV. 13a and 13b) leading to almost no residue varied (from 0.3 to 2.3 %). Residue production yield decreases for all epoxy hybrid O/I networks under air atmosphere compared to the one obtained under nitrogen atmosphere. The ILM/IPD networks based on IL.NTf₂-g-POSS^{®Ph} leads to more residue than the networks containing IL.Cl-g-POSS^{®Ph} or POSS^{®Ph}-triol. The difference on the residue content could be explained by the competition between the sublimation and/or evaporation and the full oxidation reactions at high temperature in relation with the POSS^{®Ph} content which are grafted onto the epoxy networks. Thermal stability, degradation kinetics and residue content of the epoxy hybrid O/I networks depend mainly on the nature of the organic groups surrounding the POSS^{®Ph} inorganic cage but also that the chemical nature of the co-monomers considered to build the epoxy networks (ILM1 or ILM2).

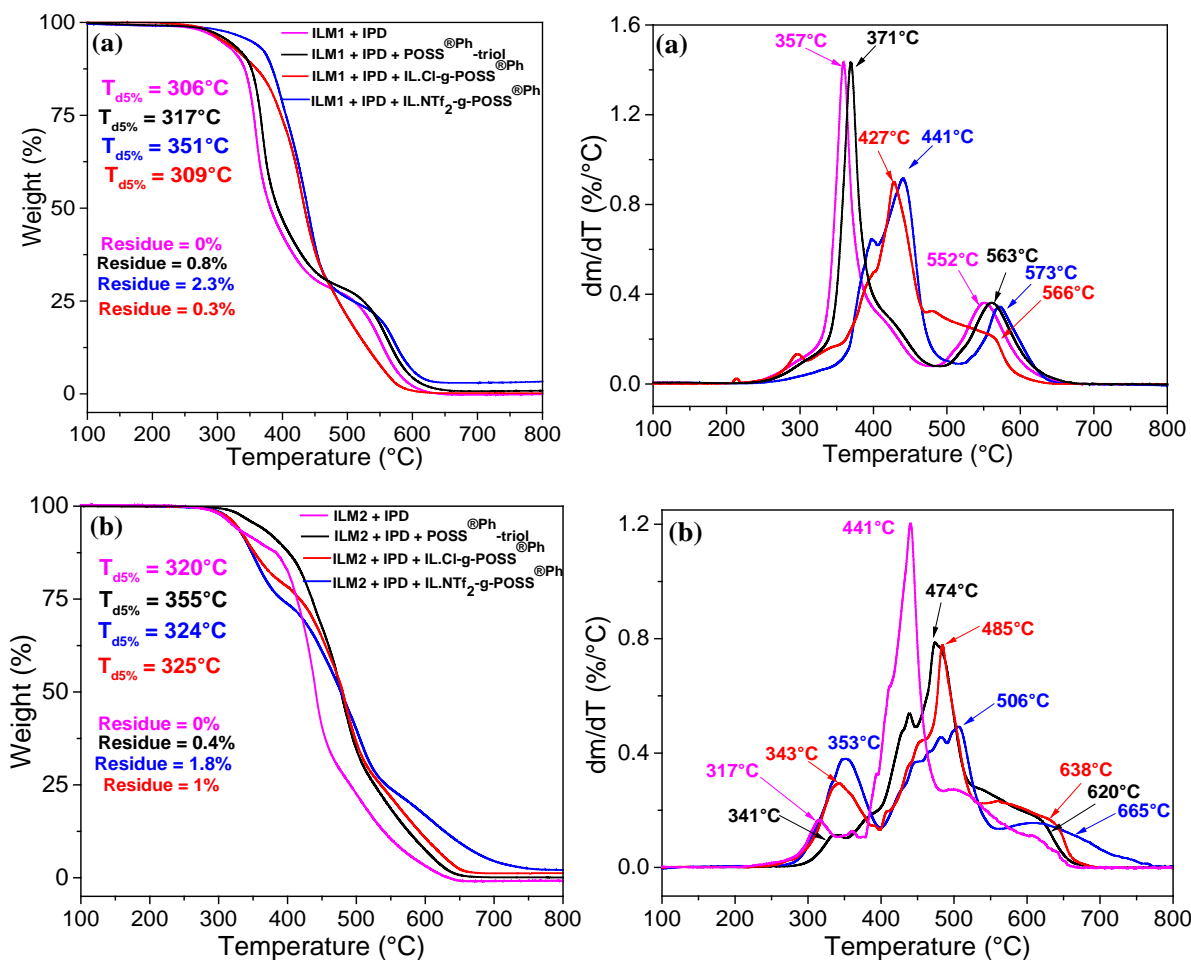


Figure IV. 13: Change of weight loss as a function of the temperature (TGA) and derivative of TGA curves (DTG) for the epoxy hybrid O/I networks containing POSS^{®Ph}-triol, IL.Cl-g-POSS^{®Ph} and IL.NTf₂-g-POSS^{®Ph} respectively, prepared based on epoxy monomer a) ILM1, and on b) ILM2. (10 K.min⁻¹, atmosphere: air flow).

As can be seen in Figures IV. 13a and 13b, the epoxy hybrid O/I networks containing POSS^{®Ph}-triol or IL-g-POSS^{®Ph} nanoclusters with Cl⁻ or NTf₂⁻ as counter anions have a higher thermal stability ($T_{d5\%}$, T_{dmax}) and a higher oxidation resistance than the neat epoxy networks (ILM/IPD). Such behavior could be associated with the nanoscale dispersion of POSS^{®Ph}-triol or IL-g-POSS^{®Ph} clusters in the epoxy matrices as well as to the improved interactions between the ILM monomers and POSS^{®Ph}-POSS^{®Ph} aggregates. In addition, the increased T_d for epoxy hybrids containing POSS^{®Ph} could result from the increased chain spacing which modify also the thermal conductivity of POSS^{®Ph}-modified networks. POSS[®] ceramisation is another important effect, which certainly contributes to improve the thermostability. In general, POSS[®] cage as a

ceramic ¹¹⁴ precursor forms a silica layer after complete oxidation. After the emission of organic groups in POSS^{®Ph} cages, a silica layer seals the polymer, and retards the oxidation of the bulk polymer. On the other hand, POSS[®] is a surface-active moiety, tending to migrate to the surface as a tenside ¹¹⁵. It is worthy of notice that the epoxy hybrid O/I networks based on ILM2 exhibit the highest thermal stability ($T_{d5\%}$) and resistance towards oxidation (DTG peak concerning the network contained IL.NTf₂-g-POSS^{®Ph}, 665 °C with ILM2/IPD against 573 °C with ILM1/IPD matrix) compared to the epoxy hybrid O/I networks based on ILM1.

IV.4.4. Surface properties

Total surface energies of the epoxy hybrid O/I networks containing POSS^{®Ph}-triol, IL.Cl-g-POSS^{®Ph}, and IL.NTf₂-g-POSS^{®Ph} prepared from copolymerization of ILM1 or ILM2 with IPD epoxy monomers were determined by the sessile drop method using Owen-Wendt theory ³⁰. Non-dispersive and dispersive components were determined from water and methylene diiodide contact angles and are summarized in Table IV. 4.

Table IV. 4: Determination of dispersive and non-dispersive components of the surface energy on the neat epoxy ILM/IPD and the corresponding hybrid O/I networks from contact angle with water and methylene diiodide at room temperature.

Samples	Θ_{Water} (°)	$\Theta_{\text{CH}_2\text{I}_2}$ (°)	$\gamma_{\text{non-dispersive}}$ (mJ.m ⁻²)	$\gamma_{\text{dispersive}}$ (mJ.m ⁻²)	γ_{total} (mJ.m ⁻²)
ILM1-IPD/POSS ^{®Ph} -triol	108	75	0.3	20.4	20.7
ILM1-IPD/IL.Cl-g-POSS ^{®Ph}	110	78	0.3	19.9	20.2
ILM1-IPD/IL.NTf ₂ -g-POSS ^{®Ph}	112	82	0.2	19.6	19.8
ILM2-IPD/POSS ^{®Ph} -triol	115	86	0.2	19.4	19.6
ILM2-IPD/IL.Cl-g-POSS ^{®Ph}	116	88	0.2	18.8	19.0
ILM2-IPD/IL.NTf ₂ -g-POSS ^{®Ph}	120	92	0.2	18.0	18.2

First, the results revealed that the substitution of DGEBA with the ILMs and the introduction of 5 wt. % of POSS^{®Ph}-triol or IL-g-POSS^{®Ph} (with Cl⁻ or NTf₂⁻ anion) considerably increased the contact angles formed by the probe liquids at the surface of the epoxy networks (ILM/IPD). For example, a water contact angle of 79° is formed on the surface of the DGEBA/IPD network (see Table III. 4 in the chapter III). On the other hand, a water contact angle greater than 100° is

observed for ILM1 or ILM2 cured with IPD and modified with POSS^{®Ph} (POSS^{®Ph}-triol or IL-g-POSS^{®Ph}) (Table IV. 4). The increase of the contact angle with methylene diiodide with the addition of the POSS^{®Ph} is even more significant. We noticed a large difference (nearly 42°) between the contact angle on the DGEBA/IPD surface (49°) (see Table III. 4 in the chapter III), and the one on the ILM2-IPD/IL.NTf₂-g-POSS^{®Ph} surface (92°). Taking into account the increase of the contact angles of these two probe liquids on ILM-IPD/POSS^{®Ph} surfaces, one can concluded that the introduction of the POSS^{®Ph} and the substitution of DGEBA by ILMs monomers increase the hydrophobic and oleophobic characteristics of the surface.

The calculation of the total surface energy shows a significant decrease of that of the epoxy resin ILM/IPD when modified with the POSS^{®Ph} compared to the DGEBA/IPD network (see Table III. 4 in chapter III). A factor of two separates the two values (**DGEBA/IPD**: $\gamma_{\text{total}} = 39.6 \text{ mJ.m}^{-2}$; **ILM2/IPD/IL.NTf₂-g-POSS^{®Ph}**: $\gamma_{\text{total}} = 18.2 \text{ mJ.m}^{-2}$). A more detailed analysis, taking into account the polar components and dispersive of the surface energy of the epoxy hybrid O/I networks shows that the dispersive component makes the major contribution to the surface energy (98 %). Consequently, the interactions initiated by this type of surface are mainly London dispersive interactions. As DGEBA monomer is replaced by ILMs and modified by the incorporation of the POSS^{®Ph} nanoclusters, a significant decrease of the dispersive component is observed (from 35 mJ.m⁻² for DGEBA/IPD (compare to Table III. 4 in the chapter III) to 18 mJ.m⁻² for ILM2-IPD/IL.NTf₂-g-POSS^{®Ph}). At the same time, the polar component of the initially low surface energy is also diminished (compare Table III. 4 and Table IV. 4). The London dispersive interactions are still predominant but reduced by the addition of the POSS^{®Ph} leading to a decrease of the total surface energy. These results can be explained by the hydrophobic character of POSS^{®Ph} molecules having phenyl ligands ¹¹⁶ and to the epoxy ionic liquid monomers containing imidazolium units with NTf₂⁻ anions ^{66,67} well-known to give a low surface tension ⁶⁸. In addition, the ILM/IPD containing POSS^{®Ph}-triol or IL-g-POSS^{®Ph} networks display a more pronounced hydrophobic than of the DGEBA/IPD modified by POSS^{®Ph} network (see chapter III). Therefore, wetting of the epoxy surface is easier. These new results combined with the high thermal stability open new promising routes in the preparation of surface coating with self-cleaning properties for automotive, aerospace, or electronics applications.

IV.4.5. Ionic conductivity

Many studies were done to propose alternatives to liquid electrolytes considering organic solvents in order to ensure the safety of the installations avoiding liquids and related explosions¹¹⁷⁻¹²⁰. Among those, two strategies focused on the development of polymer electrolytes including solid polymer electrolytes (SPEs) and gel polymer electrolytes (GPEs)^{120,121}. Solid polymer electrolyte (SPEs) are considered as the optimal electrolytes to solve these safety issues and the key to further improvement of the mechanical strength and capability of holding liquid electrolytes as well as to get high ionic conductivity and good electrochemical stability. Recently, polymer ionic liquids (PILs) obtained by incorporating a chemically crosslinking structure connecting the host polymer are preferred to prepare SPEs as they combine both properties of ILs (good electrochemical properties, mechanical stability, processing, and tunable molecular design) and polymers (avoiding liquid leakage, no separator needed). Various poly(ionic liquid)s (PILs) have been considered in the literature. The majority of these studies involve mono-cationic PIL-based electrolytes displaying significant ionic conductivities by using large contents of ionic liquids (from 10 to 90 wt. %) for temperatures ranging from 50 to 100 °C¹²²⁻¹²⁵. For example, Obadia *et al.* have prepared a series of anionic poly(ionic liquid)s with 1,2,3-triazolium counter cations by cation exchange between tailor-made 1,3,4-trialkylated-1,2,3-triazolium iodides and a polystyrene derivative having pendant potassium bis(trifluoromethanesulfonyl)imide groups. The resulting PILs networks showed a great potential for applications that require solid electrolytes with ionic conductivities from 7.8×10^{-8} to $8.4 \times 10^{-7} \text{ S.m}^{-1}$ at 30 °C^{122,123}. Other authors proposed a material having an ionic conductivity of $8.6 \times 10^{-9} \text{ S.m}^{-1}$ at 30 °C by blending 10 wt. % of IL electrolyte with poly(diallyldimethylammonium) bis(trifluoromethanesulfonyl)imide (PDADMA TFSI). Ionic conductivity higher than 10^{-5} S.m^{-1} at the same temperature was obtained by increasing the IL content up to 40 wt.%¹²⁵. Recently, Porcarelli *et al.* synthesized different types of methacrylic ILMs monomers copolymerized with poly(ethylene glycol) methyl ether methacrylate (PEGM) via conventional free radical reaction. The resulting solid polymer electrolytes showed high ionic conductivities (up to 1.9×10^{-6} and $2 \times 10^{-5} \text{ S.m}^{-1}$ at 25 and 70 °C, respectively) combined with a low T_g (from -61 to -27 °C) depending on the copolymer composition and the ILM/PEGM ratio¹²⁴. Solid polymer electrolytes having a T_g close to room temperature showed a very low conductivity (lower than $10^{-11} \text{ S.m}^{-1}$)¹²⁴. Livi *et al.*²⁶ obtained (multi)functional epoxy ionic

liquid networks from the co-polymerization between an imidazolium ionic liquid monomer and conventional polyether-amine (Jeffamine D230) which has a high ionic conductivity of about 7.39×10^{-8} and $4 \times 10^{-4} \text{ S.m}^{-1}$ at 30 and 70 °C, respectively. On the other hand, POSS[®]-based materials can enhance the thermal and electrochemical stability of SPEs due to their unique structures and their inner inorganic silicon oxygen core facilitates ions conduction^{126,127}. Gyu *et al.*¹²⁶ described nanomaterial prepared from polyethylene oxide (PEO)/polyethylene glycol-polyhedraoligomeric silsesquioxane (PEG-POSS[®]) combination which exhibit enhanced ionic conductivity (from 1.19×10^{-5} to $1.27 \times 10^{-4} \text{ S.cm}^{-1}$). Lu *et al.*¹²⁷ also obtained crosslinked polymer membranes (3D-PEs) with star-shaped structures having ionic conductivity up to $2.35 \times 10^{-3} \text{ S.cm}^{-1}$ at room temperature with the introduction of a multifunctional epoxy POSS[®]. These authors also observed that the majority of POSS[®]-epoxy networks have higher real and imaginary parts of the complex permittivity compared to the ones of the neat epoxy network.

In order to characterize this epoxy ILM/IPD networks and the corresponding hybrid networks for potential solid polymer electrolytes applications, dielectric measurements under AC voltage were carried out to analyses the influence of IL-g-POSS^{®Ph} nanoclusters. The real, ϵ'_r , and the imaginary, ϵ''_r , parts of the complex relative permittivity were extracted from measurements done under 5 V sinusoidal applied voltage (Figure IV. 14a and 14b). In order to evaluate the DC conductivity (quasi-steady state) at high temperatures, it is necessary to start by evaluating the changes taking place in the AC conductivity domain. Figure IV. 15 presents the evolution of AC conductivity with respect to frequency for the epoxy DGEBA and ILM1 or ILM2 cured with IPD as well as the different hybrid O/I networks obtained from the addition of IL-g-POSS^{®Ph} with two different anions: chloride (Cl⁻) or bis(trifluoromethanesulfonyl)imide (NTf₂⁻). Taking into account the glass transition temperatures of the ILM/IPD and their corresponding O/I hybrid networks which vary from 45 to 71 °C (Figures IV. 5 and IV.12), the conductivity was measured from - 80 and 200 °C for the DGEBA/IPD and up to 150 °C for ILM/IPD (same for their hybrid O/I networks).

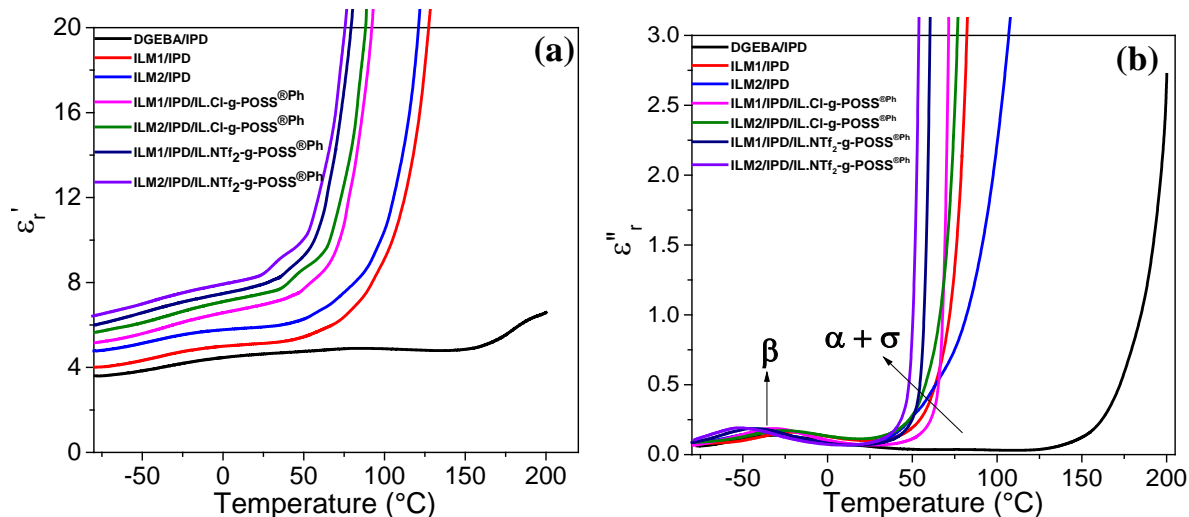
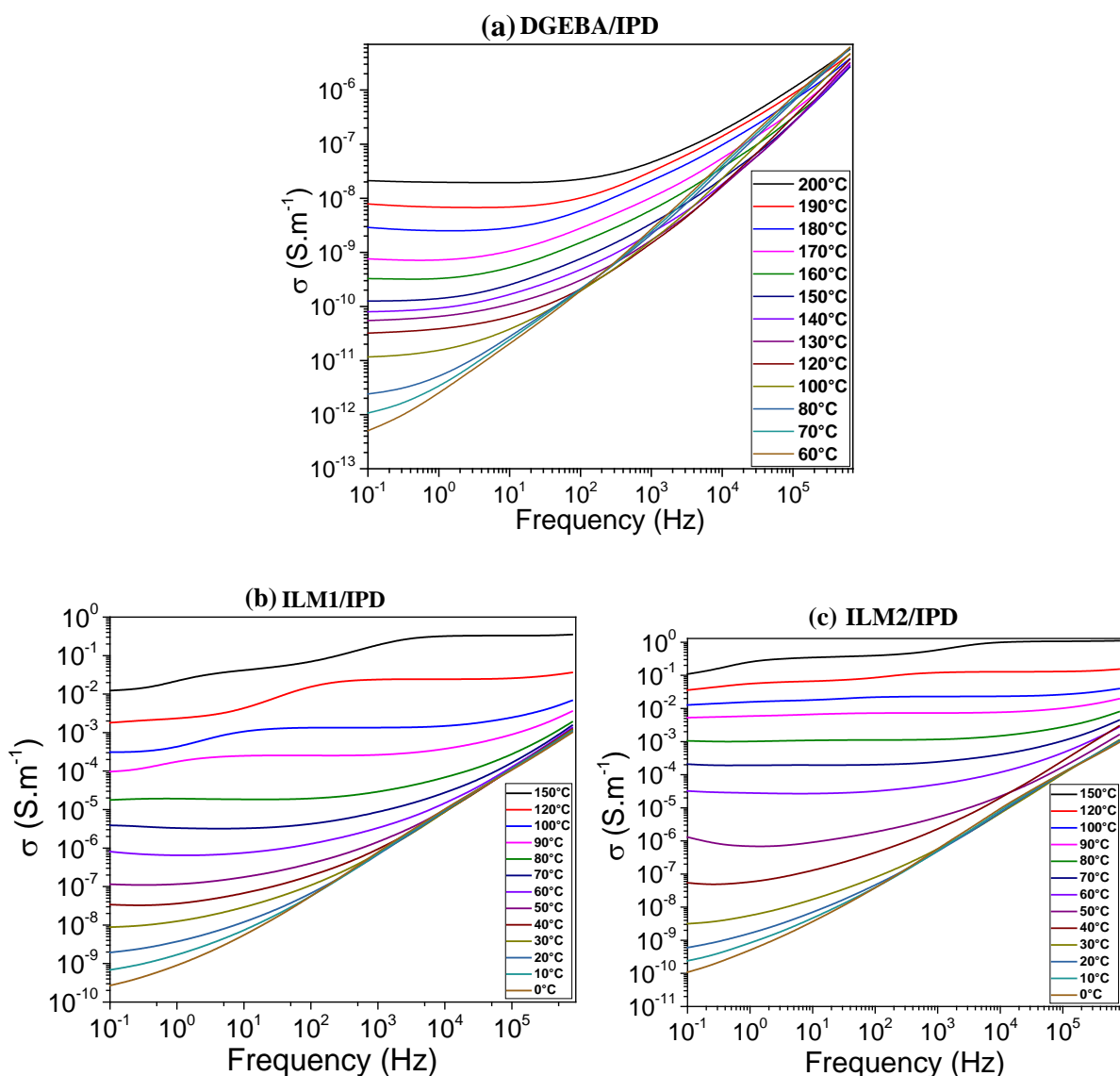


Figure IV. 14: a) Relative permittivity: a) ϵ'_r and b) ϵ''_r for DGEBA/IPD, ILM/IPD, and their corresponding epoxy hybrid O/I networks as a function of temperature, at 100 Hz.

The neat epoxy network (DGEBA/IPD) showed relative permittivity, ϵ'_r , starting from 3.5 at low temperature and up to 6 at temperatures higher than room temperature. A slight increase with a maximum value close to 170 °C corresponds to the α relaxation of the epoxy system. The ILM/IPD and their corresponding O/I hybrids obtained by the introduction of 5 wt. % of IL-g-POSS^{®Ph} nanoclusters with the chloride or bis(trifluoromethanesulfonyl)imide (NTf₂⁻) anions have relative permittivity, ϵ'_r , much higher (from 30 to 50 %) at room temperature and also shows an exponential increase after the glass transition temperature (between 50 to 80 °C depending on the epoxy system) to achieve high values at higher temperatures. The shape of the curves is not influenced by the addition of IL-g-POSS^{®Ph} but only shifted to higher values (Figure IV. 14). The imaginary part of the relative permittivity values, ϵ''_r , show similar behavior variation at room temperature and above glass transition temperature. Figure IV. 14b shows just one broad transition with peaks located close to - 50 °C corresponding to β relaxation associated to the motion of the hydroxyethyl units generated from the crosslinking reaction¹²⁸. The starting of the increase from 30 to 50 °C depending on the system is generally due to the relaxation processes of the main chains of the crosslinked epoxy network (α relaxation). This relaxation is not well visible on the plots (Figure IV. 14b) due to the important conduction phenomenon that gives an exponential variation towards higher values at the same temperature range. This relaxation arises from the fact that free charges are immobilized in the network and at sufficiently high temperatures, *i.e.* above T_g of the polymer, the charges can migrate in the presence of an applied

electric field. As the temperature increases above the glass transition temperature, the conductivity of the system increases giving rise to the increase of the concentration of charge carriers ¹²⁹. This increase of the dielectric constant can be explained by *i*) the nanoscale dispersion of IL-g-POSS^{®Ph} nanoclusters inside the epoxy matrix leading to limited free volume, and *ii*) the increased polarizability of the resulting hybrid nanomaterials as it has the highest ionic liquid content (cation/anion). This allows the formation of conductive interfacial layers around aggregated POSS^{®Ph}, *i.e.* a potential conductive path. Hence, the development of ILM-IPD/IL-g-POSS^{®Ph} nanomaterials with high dielectric constant is expected to find application as suitable electrolyte material.



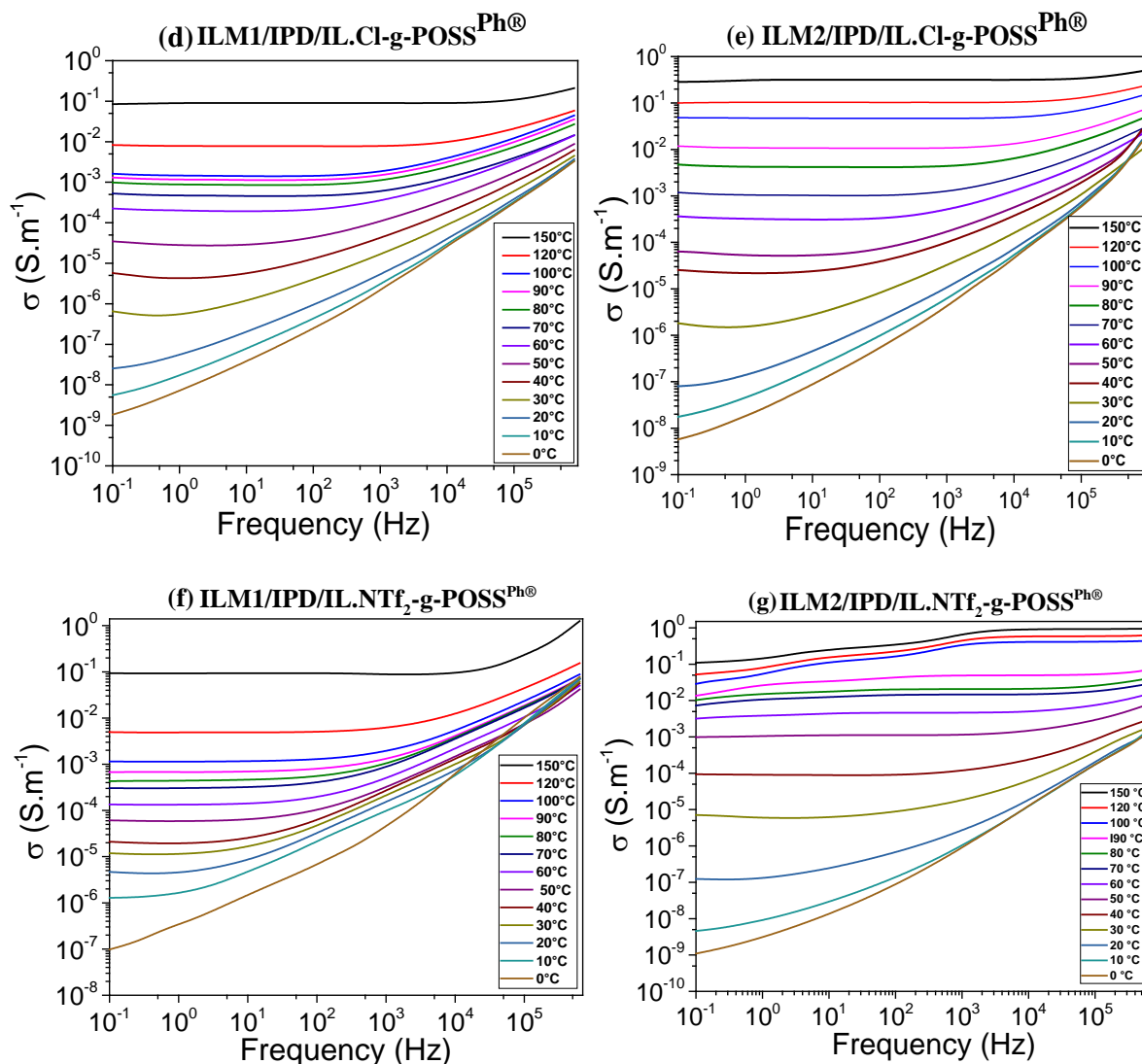


Figure IV. 15: Evolution of AC conductivity as a function of frequency for a) DGEBA/IPD, b) ILM1/IPD, c) ILM2/IPD, d) ILM1/IPD/IL.Cl-g-POSS^{®Ph}, e) ILM2/IPD/IL.Cl-g-POSS^{®Ph}, f) ILM1/IPD/IL. NTf₂-g-POSS^{®Ph}, and g) ILM2/IPD/IL.NTf₂-g-POSS^{®Ph}.

The σ_{AC} conductivity of the networks showed a linear increase with respect to frequency with a dependence equal to 1 at high frequencies. Frequency dependency follows the law:

$$\sigma_{AC}(\omega) = \omega^s \quad (7)$$

with $0 \leq s \leq 1$ characterizing hopping conduction ^{130,131}. As the temperature increases, the conductivity becomes independent on the frequency and increases by 2 to 3 orders of magnitude for all the epoxy networks. A horizontal plateau appears progressively expressing the thermal activation of the DC conductivity. The amplitude of this plateau corresponds to the DC

conductivity at a given temperature. As the temperature increases, the mobility of the electrons increases shifting the plateau to higher frequencies and higher value of conductivity. The plateau appearing for different epoxy ILM/IPD and the corresponding hybrid O/I networks seem to have the same influence with respect to frequency and temperature. A decrease of the conductivity values is observed at high temperatures and low frequencies, such as for ILM1/IPD, ILM2/IPD, and ILM2/IL.NTf₂-g-POSS^{®Ph} over 120 °C and 10² Hz. This can be attributed to the electrode polarization phenomenon leading to blocking electrodes ¹³². Conductivity DC values are extrapolated before this decrease. As a result, the ionic conductivity for all investigated epoxy ionic liquid networks from the plateau region of each dielectric spectrum at room or high temperature follow the following order: ILM2-IPD/IL.NTf₂-g-POSS^{®Ph} > ILM2-IPD/IL.Cl-g-POSS^{®Ph} > ILM1-IPD/IL.NTf₂-g-POSS^{®Ph} > ILM1-IPD/IL.Cl-g-POSS^{®Ph} > ILM2-IPD > ILM1-IPD > DGEBA-IPD, which is the reverse order of T_g shown in Figure IV. 12. These results suggest that polymer chain relaxation plays a dominant role in ion transportation. Specifically, the ILM-IPD/IL-g-POSS^{®Ph} with NTf₂⁻ anions networks shows significantly a higher ionic conductivity compared to the ILM-IPD/IL-g-POSS^{®Ph} with Cl⁻ anion networks, indicating also a strong dependence of the conductivity on the identity of the counterion which coincides with the significantly lower T_g. This can be attributed to the difference in symmetry and size of the anions and to the dissociation energy of the ion pairs when the effects of T_g are removed. Chen *et al.* ¹³³ observed similar effect on ionic conductivity in a PILs when they exchanged chloride (Cl⁻) anion with the bis(trifluoromethanesulfonyl)imide (NTf₂⁻) anion. In addition to that, with increasing temperature, the difference of ionic conductivity between the ILM/IPD and their hybrid O/I networks with different anions decrease, suggesting that at high temperatures the importance of T_g becomes less pronounced. Therefore, ionic conductivity values of about 3.40 x 10⁻⁸ and 9.35 x 10⁻⁵ S.m⁻¹ at 40 °C were obtained depending on the system (see Table IV. 5). Moreover, for high temperatures above the T_g, ionic conductivity increased significantly to reach much higher values (see Table IV. 5 and Figure IV. 15).

Table IV. 5: Ionic conductivity for the different epoxy ionic liquids networks at different temperatures.

Samples	σ_{AC} (S.m ⁻¹) @ 40 °C	σ_{AC} (S.m ⁻¹) @ 50 °C	σ_{AC} (S.m ⁻¹) @ 70 °C	σ_{AC} (S.m ⁻¹) @ 100 °C
ILM1-IPD	3.40 x 10 ⁻⁸	1.15 x 10 ⁻⁷	3.91 x 10 ⁻⁶	3.12 x 10 ⁻⁴
ILM1-IPD/IL.Cl-g-POSS ^{®Ph}	5.74 x 10 ⁻⁶	3.46 x 10 ⁻⁵	3.05 x 10 ⁻⁴	1.63 x 10 ⁻²
ILM1-IPD/IL.NTf ₂ -g-POSS ^{®Ph}	2.11 x 10 ⁻⁵	6.12 x 10 ⁻⁵	6.28 x 10 ⁻⁴	2.15 x 10 ⁻²
ILM2-IPD	5.42 x 10 ⁻⁸	3.80 x 10 ⁻⁶	2.08 x 10 ⁻⁴	1.28 x 10 ⁻³
ILM2-IPD/IL.Cl-g-POSS ^{®Ph}	2.54 x 10 ⁻⁵	8.39 x 10 ⁻⁵	1.19 x 10 ⁻³	4.38 x 10 ⁻²
ILM2-IPD / IL.NTf ₂ -g-POSS ^{®Ph}	9.37 x 10 ⁻⁵	9.81 x 10 ⁻⁴	7.27 x 10 ⁻³	6.84 x 10 ⁻²

Figure IV. 16a presents the evolution of the DC conductivity of all the epoxy ionic liquid networks as a function of temperature extrapolated from dielectric spectroscopy measurements at 0.1 Hz. The measured DC conductivity by dielectric spectroscopy has a linear slope above the glass transition temperature of epoxy for DGEBA/IPD (Figure S4.6 of SI in chapter IV), ILM/IPD and their hybrid O/I networks (Figure IV. 16a). All the slopes are well fitted with the Arrhenius law (equation 5) by exhibiting linear dependence, where the obtained Arrhenius 2-parameters, *i.e.* activation energies, E_a , and infinite conductivity, σ_0 , are presented in Table IV. 6 calculated from the slope of the fitted curves in Figure IV. 16b.

$$\sigma_{DC}(T) = \sigma_0 \exp\left(-\frac{E_a}{k_B T}\right) \quad (8)$$

where k_B is the Boltzmann's constant ($k_B = 8.617 \times 10^{-5} \text{ eV.K}^{-1}$).

The R-square value confirms that the temperature dependence of ionic conductivity is very good in accordance with the Arrhenius equation. Conductivity increases with increasing temperature and follows Arrhenius dependence for all nanomaterials, resulting in an accelerated motion of polymer chains and promoting faster migration of ions at higher temperatures^{134,135}. Thus, the mechanism of ionic conductivity can be understood from activation energy (E_a).

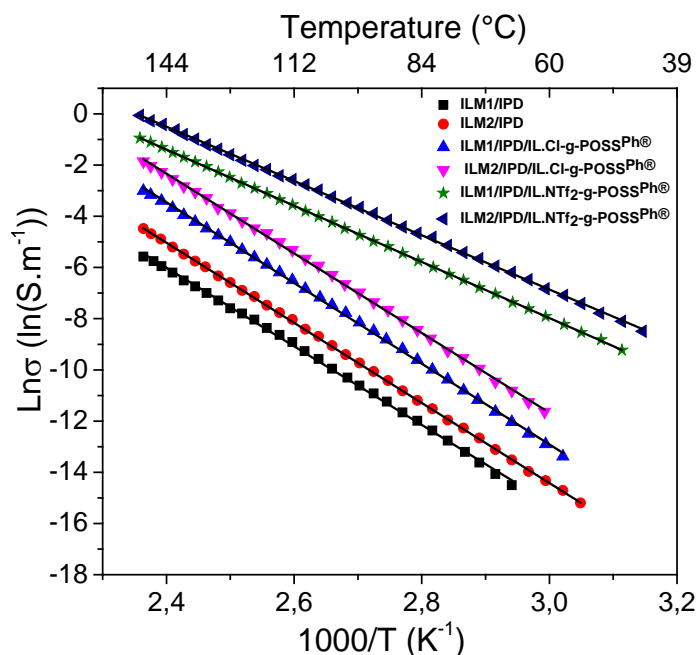


Figure IV. 16: Dependence of DC conductivity with temperature (extrapolated from AC conductivity values at 0.1 Hz). Solid black lines represent a regression to the Arrhenius equation.

Table IV. 6: Arrhenius law applied to ionic conductivity data at room temperature.

Samples	σ_0 (S.m ⁻¹)	E _a (eV)	R-square
ILM1-IPD	4.87 x 10 ¹³	1.36	0.99856
ILM1-IPD/IL.Cl-g-POSS ^{®Ph}	2.71 x 10 ¹⁵	1.14	0.99612
ILM1-IPD/IL.NTf ₂ -g-POSS ^{®Ph}	1.14 x 10 ¹⁵	1.06	0.99712
ILM2-IPD	6.15 x 10 ¹³	1.35	0.99875
ILM2-IPD/IL.Cl-g-POSS ^{®Ph}	7.72 x 10 ¹⁰	0.92	0.99436
ILM2-IPD / IL.NTf ₂ -g-POSS ^{®Ph}	3.28 x 10 ¹⁰	0.86	0.99236

A lower activation energy, E_a, means a better transmission conductor for DGEBA/IPD, ILM/IPD, and their hybrid O/I networks presented in Table IV. 6. The activation energies are in the same range for the ILM1/IPD and ILM2/IPD networks and decrease for both with the addition of IL-g-POSS^{®Ph} whatever the anion nature. This signifies that the substitution of ILM1 with ILM2 did affect neither the DC conductivity values nor the activation energy of the system. The lowest value of E_a is for ILM-IPD/IL-g-POSS^{®Ph} networks as is observed in Table IV. 6, and the highest ionic conductivities are also observed for the same networks as presented in Table IV.

5. Thus, these behaviors indicate that the introduction of IL-g-POSS^{®Ph} is beneficial in improving ions transportation. This is due to decrease in T_g of the ILM/IPD networks by addition of IL-g-POSS^{®Ph} and the presence of high amount of ionic liquid facilitating ionic movement in the matrix. As a result, all investigated epoxy ionic liquids materials displayed a very good ion transmission performance with the maximum ionic conductivity in the temperature range, from 40 to 80 °C.

IV.4.6. Conclusion

In this work, various epoxy hybrid organic/inorganic nanomaterials based on ILMs were synthesized considering 5 wt. % of non-fully condensed polyhedral oligomeric silsesquioxane (POSS^{®Ph}-triol) or IL-modified POSS^{®Ph} combined with two different anions chloride (Cl⁻) or bis(trifluoromethanesulfonyl)imide (NTf₂⁻). POSS^{®Ph}-triol or IL-g-POSS^{®Ph} could generate crosslinks from a pre-reaction with the epoxy prepolymers, ILM1 or ILM2. The analysis of morphologies of hybrid nanomaterials was performed by transmission electron microscopy which evidenced well dispersed POSS[®]-aggregates-based nanostructured networks with nanometer scale particle size of POSS^{®Ph} aggregates in an epoxy ILM/IPD matrix. However, some POSS^{®Ph}-triol rich domains reach sizes close to 1 μm due to a phase separation mechanism induced by polymerization. As a consequence, the nanostructured epoxy hybrid O/I networks display a decrease of the glass transition as compared to the neat ILM/IPD networks. Nevertheless, changing the chemical architecture of ILMs monomers, the introduction of POSS^{®Ph}-triol (ILM2/IPD) compensate the T_g decrease (74 vs 58 °C). The epoxy hybrid O/I networks displayed higher thermal stability and resistance to oxidation, especially with ILM2/IPD matrix. Moreover, these nanostructured materials display low surface energy (18.2 - 20.7 $\text{mJ}\cdot\text{m}^{-2}$), high hydrophobicity (H_2O contact angle from 108 to 120°) and oleophobicity (methylene diiodide contact angle from 75 to 92 °) which make them promising materials for coating applications. Finally, the study of the electrical properties of the epoxy ILM/IPD and their hybrid O/I networks demonstrate the high ionic conductivities values, in particular those of ILM2/IPD/IL.NTf₂-g-POSS^{®Ph} network for which the ionic conductivity of $9.37 \times 10^{-5} \text{ S}\cdot\text{m}^{-1}$ at 40 °C could reach $6.84 \times 10^{-2} \text{ S}\cdot\text{m}^{-1}$ at 100 °C. These results are promising for new solid polymer electrolytes.

Supporting information of Chapter IV

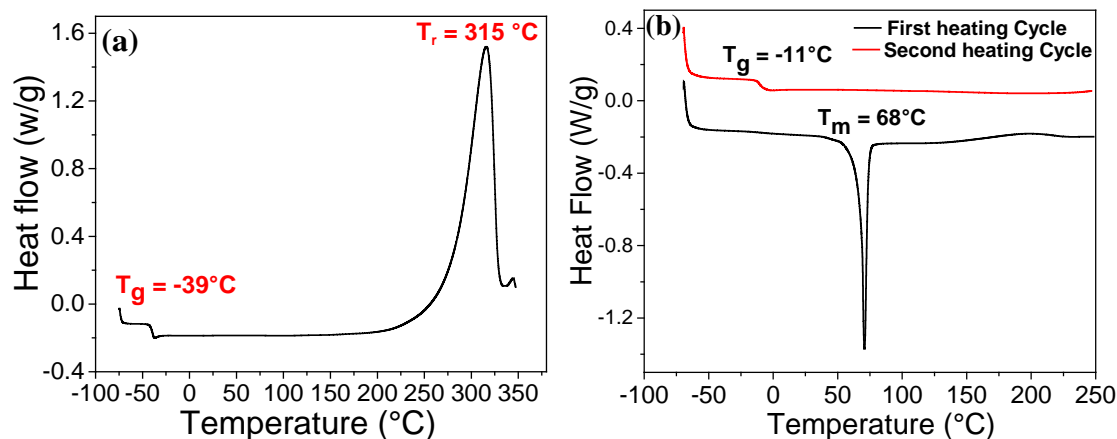


Figure S4.1: DSC thermograms of a) ILM1 and b) ILM2 epoxy monomers (heating rate: $10\text{ K}\cdot\text{min}^{-1}$).

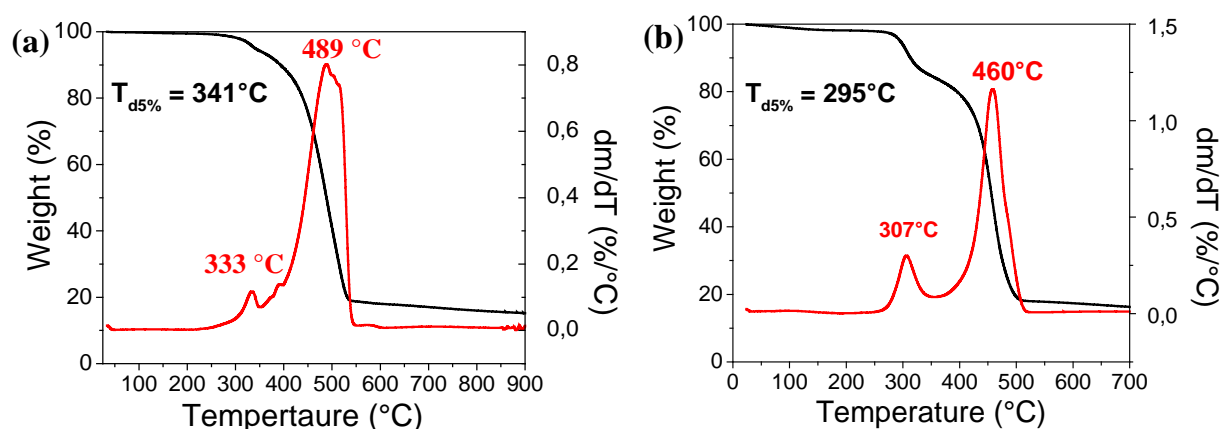


Figure S4.2: Weight loss as a function of temperature (TGA) and derivative of TGA curves (DTG) of a) ILM1 and b) ILM2 epoxy monomers (heating rate: $10\text{ K}\cdot\text{min}^{-1}$; atmosphere: nitrogen flow).

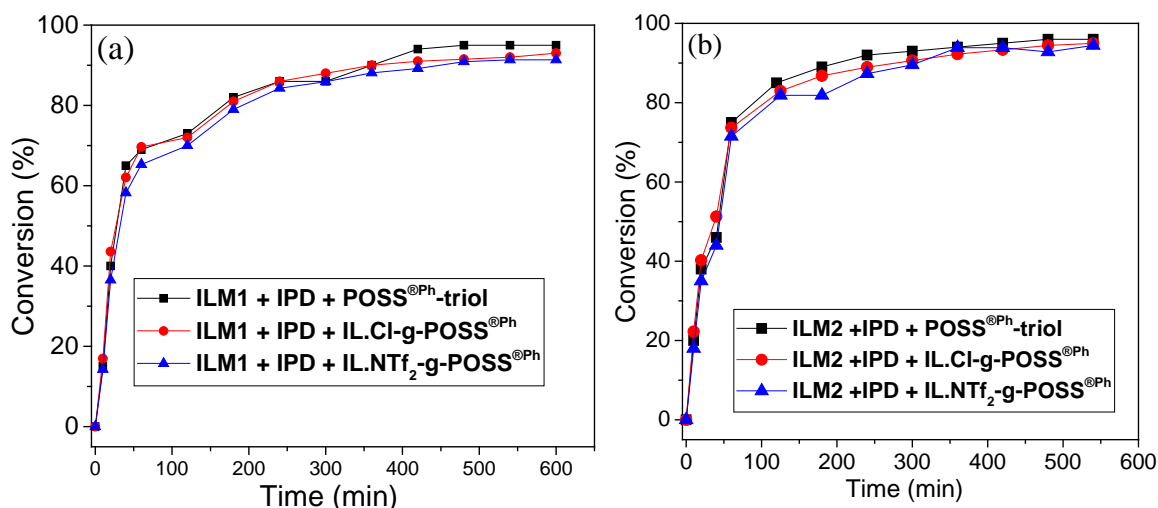
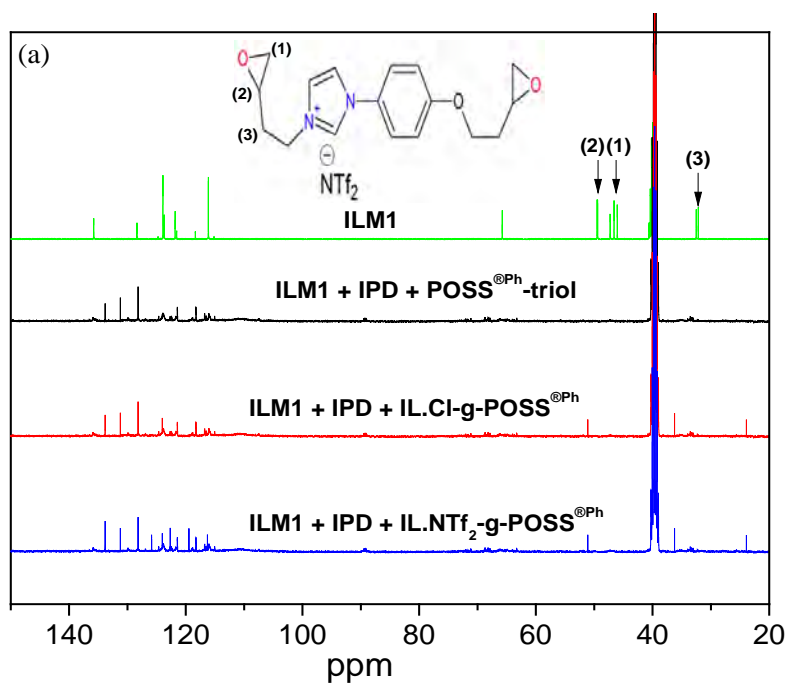


Figure S4.3: Epoxy group conversion as a function of the reaction time from FT-IR spectra for the epoxy hybrid O/I networks containing POSS^{®Ph}-triol, IL.Cl-g-POSS^{®Ph} and IL.NTf₂-g-POSS^{®Ph} respectively, (prepared based on epoxy monomers a) ILM1, and b) ILM2).



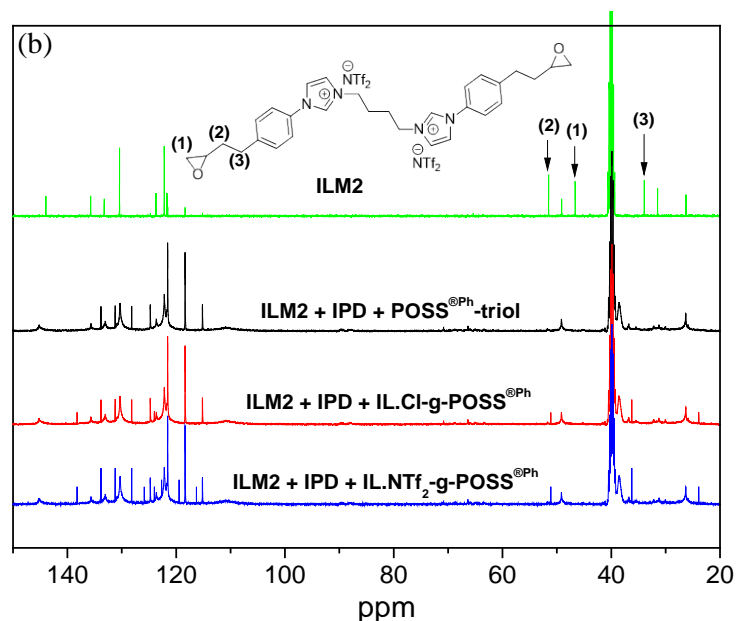
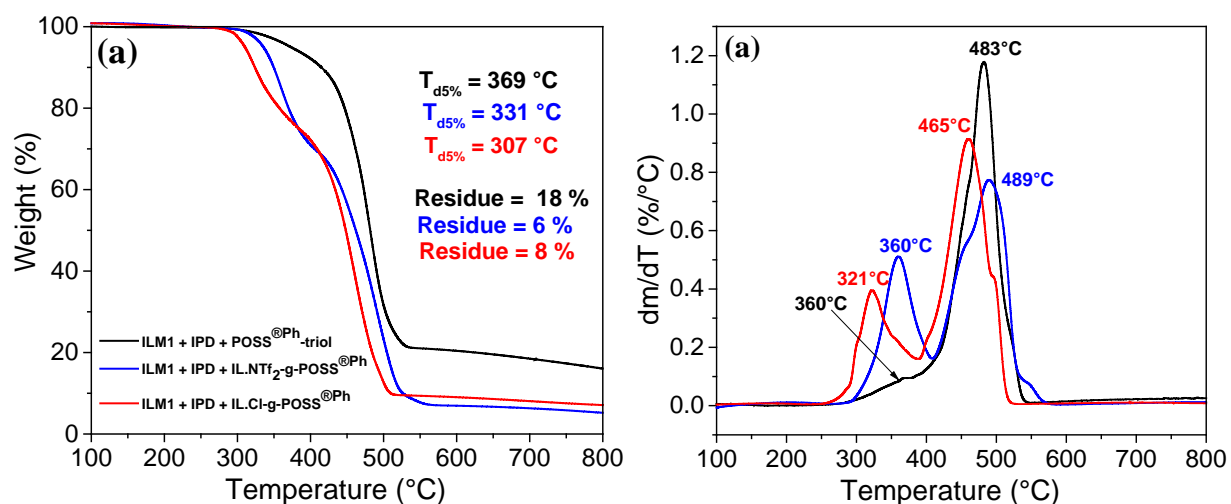


Figure S4.4: HR-MAS ¹³C-NMR spectrum of the epoxy hybrid O/I networks containing POSS^{®Ph}-triol, IL.Cl-g-POSS^{®Ph} and IL.NTf₂-g-POSS^{®Ph} respectively, prepared based on epoxy monomers a) ILM1, and b) ILM2 (DMSO-d₆; 400 MHz).



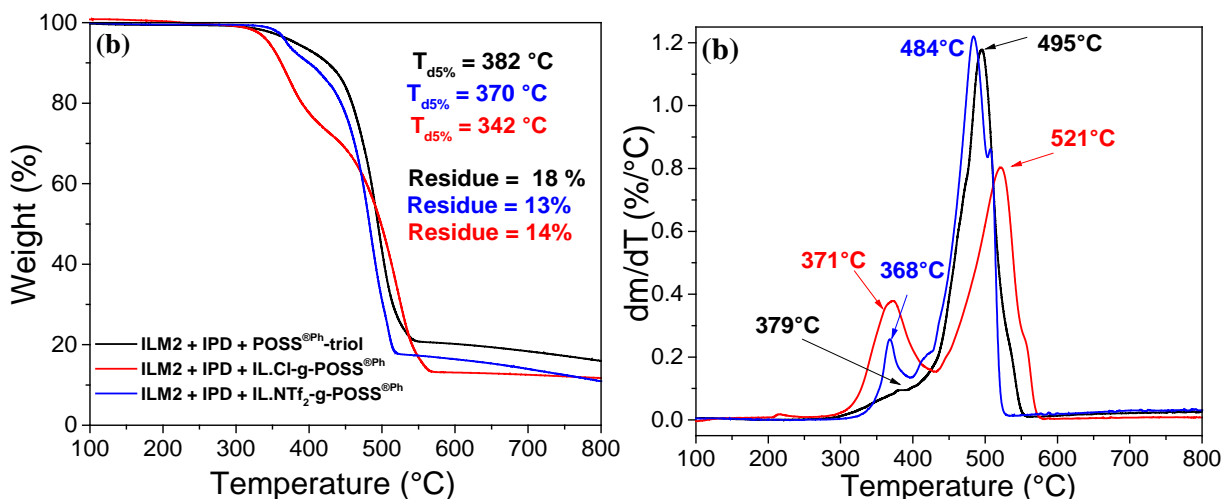


Figure S4.5: Evolution of weight loss in function of temperature (TGA) and derivative of TGA curves (DTG) for the epoxy hybrid O/I networks containing POSS^{®Ph}-triol, IL.Cl-g-POSS^{®Ph} and IL.NTf₂-g-POSS^{®Ph} respectively, prepared based on epoxy monomers a) ILM1, and b) ILM2 (heating rate: 10 K.min⁻¹; atmosphere: nitrogen flow).

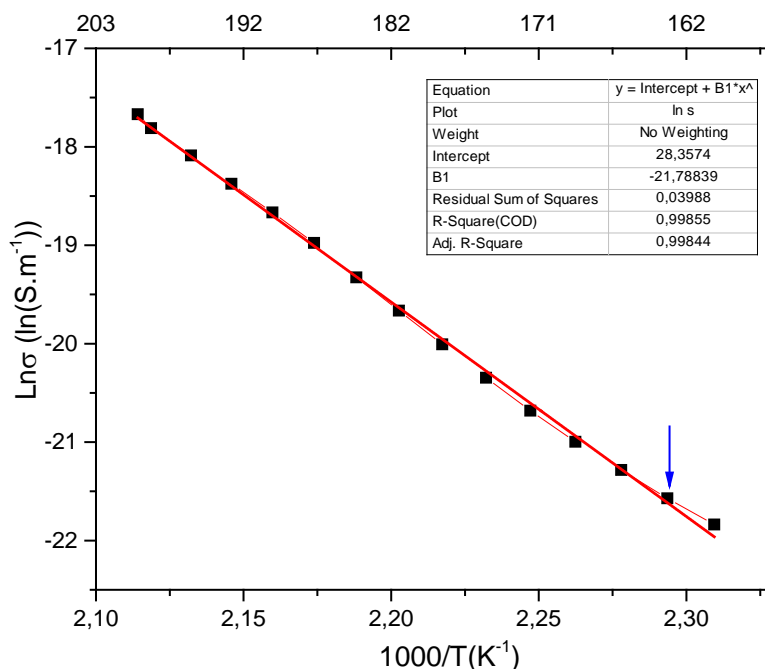


Figure S4.6: Evolution of the DC conductivity as a function of temperature extrapolated from AC conductivity values at 0.1 Hz for DGEBA/IPD network (Solid red line represents a regression to the Arrhenius equation).

References of chapter IV

- (1) Livi, S.; Duchet-Rumeau, J.; Gérard, J. F.; Pham, T. N. Polymers and ionic liquids: a successful wedding. *Macromolecular Chemistry and Physics* **2015**, *216*, 359-368.
- (2) Livi, S.; Silva, A. A.; Thimont, Y.; Nguyen, T. K. L.; Soares, B. G.; Gérard, J. F.; Duchet-Rumeau, J. Nanostructured thermosets from ionic liquid building block-epoxy prepolymer mixtures. *RSC Advances* **2014**, *4*, 28099-28106.
- (3) NGuyen, T. K. L.; Livi, S.; Pruvost, S.; Soares, B. G.; Duchet-Rumeau, J. Ionic liquids as reactive additives for the preparation and modification of epoxy networks. *Journal of Polymer Science Part A: Polymer Chemistry* **2014**, *52*, 3463-3471.
- (4) Sonnier, R.; Dumazert, L.; Livi, S.; NGuyen, T. K. L.; Duchet-Rumeau, J.; Vahabi, H.; Laheurte, P. Flame retardancy of phosphorus-containing ionic liquid based epoxy networks. *Polymer Degradation and Stability* **2016**, *134*, 186-193.
- (5) Nguyen, T. K. L.; Livi, S.; Soares, B. G.; Benes, H.; Gérard, J. F.; Duchet-Rumeau, J. Toughening of epoxy/ionic liquid networks with thermoplastics based on poly (2, 6-dimethyl-1, 4-phenylene ether)(PPE). *ACS Sustainable Chemistry & Engineering* **2017**, *5*, 1153-1164.
- (6) Nguyen, T. K. L.; Livi, S.; Soares, B. G.; Pruvost, S.; Duchet-Rumeau, J.; Gérard, J. F. Ionic liquids: A new route for the design of epoxy networks. *ACS Sustainable Chemistry & Engineering* **2016**, *4*, 481-490.
- (7) Bara, J. E.; Lessmann, S.; Gabriel, C. J.; Hatakeyama, E. S.; Noble, R. D.; Gin, D. L. Synthesis and performance of polymerizable room-temperature ionic liquids as gas separation membranes. *Industrial & Engineering Chemistry Research* **2007**, *46*, 5397-5404.
- (8) Druvari, D.; Koromilas, N. D.; Lainioti, G. C.; Bokias, G.; Vasilopoulos, G.; Vantarakis, A.; Baras, I.; Dourala, N.; Kallitsis, J. K. Polymeric quaternary ammonium-containing coatings with potential dual contact-based and release-based antimicrobial activity. *ACS Applied Materials & Interfaces* **2016**, *8*, 35593-35605.
- (9) Livi, S.; Lins, L. C.; Capeletti, L. B.; Chardin, C.; Halawani, N.; Baudoux, J.; Cardoso, M. B. Antibacterial surface based on new epoxy-amine networks from ionic liquid monomers. *European Polymer Journal* **2019**, *116*, 56-64.

- (10) Cui, J.; Nie, F. M.; Yang, J. X.; Pan, L.; Ma, Z.; Li, Y. S. Novel imidazolium-based poly (ionic liquid) s with different counterions for self-healing. *Journal of Materials Chemistry A* **2017**, *5*, 25220-25229.
- (11) Matsumoto, K.; Endo, T. Confinement of ionic liquid by networked polymers based on multifunctional epoxy resins. *Macromolecules* **2008**, *41*, 6981-6986.
- (12) Matsumoto, K.; Endo, T. Synthesis of ion conductive networked polymers based on an ionic liquid epoxide having a quaternary ammonium salt structure. *Macromolecules* **2009**, *42*, 4580-4584.
- (13) Dimitrov-Raytchev, P.; Beghdadi, S.; Serghei, A.; Drockenmuller, E. Main-chain 1, 2, 3-triazolium-based poly (ionic liquid) s issued from AB+ AB click chemistry polyaddition. *Journal of Polymer Science Part A: Polymer Chemistry* **2013**, *51*, 34-38.
- (14) Chabane, H.; Livi, S.; Benes, H.; Ladavière, C.; Ecorchard, P.; Duchet-Rumeau, J.; Gérard, J. F. Polyhedral oligomeric silsesquioxane-supported ionic liquid for designing nanostructured hybrid organic-inorganic networks. *European Polymer Journal* **2019**, *114*, 332-337.
- (15) Zheng, Z.; Xu, Q.; Guo, J.; Qin, J.; Mao, H.; Wang, B.; Yan, F. Structure-antibacterial activity relationships of imidazolium-type ionic liquid monomers, poly (ionic liquids) and poly (ionic liquid) membranes: effect of alkyl chain length and cations. *ACS Applied Materials & Interfaces* **2016**, *8*, 12684-12692.
- (16) Adzima, B. J.; Taylor, S. C.; He, H.; Luebke, D. R.; Matyjaszewski, K.; Nulwala, H. B. Vinyl-triazolium monomers: Versatile and new class of radically polymerizable ionic monomers. *Journal of Polymer Science Part A: Polymer Chemistry* **2014**, *52*, 417-423.
- (17) Cope, A. C.; Mehta, A. S. Mechanism of the Hofmann elimination reaction: an ylide intermediate in the pyrolysis of a highly branched quaternary hydroxide. *Journal of the American Chemical Society* **1963**, *85*, 1949-1952.
- (18) McDanel, W. M.; Cowan, M. G.; Carlisle, T. K.; Swanson, A. K.; Noble, R. D.; Gin, D. L. Cross-linked ionic resins and gels from epoxide-functionalized imidazolium ionic liquid monomers. *Polymer* **2014**, *55*, 3305-3313.
- (19) McDanel, W. M.; Cowan, M. G.; Chisholm, N. O.; Gin, D. L.; Noble, R. D. Fixed-site-carrier facilitated transport of carbon dioxide through ionic-liquid-based epoxy-amine ion gel membranes. *Journal of Membrane Science* **2015**, *492*, 303-311.

- (20) Demberelnyamba, D.; Yoon, S. J.; Lee, H. New epoxide molten salts: Key intermediates for designing novel ionic liquids. *Chemistry letters* **2004**, *33*, 560-561.
- (21) Dai, Z.; Ansaloni, L.; Gin, D. L.; Noble, R. D.; Deng, L. Facile fabrication of CO₂ separation membranes by cross-linking of poly (ethylene glycol) diglycidyl ether with a diamine and a polyamine-based ionic liquid. *Journal of Membrane Science* **2017**, *523*, 551-560.
- (22) Lou, Z.; Xing, S.; Xiao, X.; Shan, W.; Xiong, Y.; Fan, Y. Selective adsorption of Re (VII) by chitosan modified with imidazolium-based ionic liquid. *Hydrometallurgy* **2018**, *179*, 141-148.
- (23) Ly Nguyen, T. K.; Obadia, M. M.; Serghei, A.; Livi, S.; Duchet-Rumeau, J.; Drockenmuller, E. 1, 2, 3-triazolium-based epoxy-amine networks: Ion-conducting polymer electrolytes. *Macromolecular Rapid Communications* **2016**, *37*, 1168-1174.
- (24) Chardin, C.; Rouden, J.; Livi, S.; Baudoux, J. Dimethyldioxirane (DMDO) as a valuable oxidant for the synthesis of polyfunctional aromatic imidazolium monomers bearing epoxides. *Green Chemistry* **2017**, *19*, 5054-5059.
- (25) Chardin, C.; Rouden, J.; Livi, S.; Baudoux, J. 3-[2-(Oxiran-2-yl) ethyl]-1-{4-[(2-oxiran-2-yl) ethoxy] benzyl} imidazolium bis (trifluoromethane) sulfonimide. *Molbank* **2018**, *2018*, M974.
- (26) Livi, S.; Chardin, C.; Lins, L. C.; Halawani, N.; Pruvost, S.; Duchet-Rumeau, J.; Gérard, J. F.; Baudoux, J. r. m. From Ionic Liquid Epoxy Monomer to Tunable Epoxy-Amine Network: Reaction Mechanism and Final Properties. *ACS Sustainable Chemistry & Engineering* **2019**, *7*, 3602-3613.
- (27) Aboudzadeh, M. A.; Munoz, M. E.; Santamaria, A.; Fernandez-Berridi, M. J.; Irusta, L.; Mecerreyes, D. Synthesis and rheological behavior of supramolecular ionic networks based on citric acid and aliphatic diamines. *Macromolecules* **2012**, *45*, 7599-7606.
- (28) Aboudzadeh, M. A.; Muñoz, M. E.; Santamaría, A.; Marcilla, R.; Mecerreyes, D. Facile synthesis of supramolecular ionic polymers that combine unique rheological, ionic conductivity, and self-healing properties. *Macromolecular Rapid Communications* **2012**, *33*, 314-318.
- (29) Aboudzadeh, M. A.; Muñoz, M. E.; Santamaría, A.; Mecerreyes, D. New supramolecular ionic networks based on citric acid and geminal dicationic ionic liquids. *RSC Advances* **2013**, *3*, 8677-8682.

- (30) Owens, D. K.; Wendt, R. Estimation of the surface free energy of polymers. *Journal of Applied Polymer Science* **1969**, *13*, 1741-1747.
- (31) Zhang, Y.; Li, L.; Nie, K.; Zheng, S. Thermomechanical, surface and shape memory properties of thermosetting blends of epoxy with Poly (ethylene oxide): An impact of POSS[®] microdomain formation. *Materials Chemistry and Physics* **2020**, *240*, 122183.
- (32) Cai, H.; Li, P.; Sui, G.; Yu, Y.; Li, G.; Yang, X.; Ryu, S. Curing kinetics study of epoxy resin/flexible amine toughness systems by dynamic and isothermal DSC. *Thermochimica Acta* **2008**, *473*, 101-105.
- (33) Garcia, F. G.; Soares, B. G.; Pita, V. J.; Sánchez, R.; Rieumont, J. Mechanical properties of epoxy networks based on DGEBA and aliphatic amines. *Journal of Applied Polymer Science* **2007**, *106*, 2047-2055.
- (34) Mounif, E.; Bellenger, V.; Mazabraud, P.; Nony, F.; Tcharkhtchi, A. Chemorheological study of DGEBA/IPD system for reactive rotational molding (RRM). *Journal of Applied Polymer Science* **2010**, *116*, 969-976.
- (35) Won, Y. g.; Galy, J.; Gérard, J. F.; Pascault, J. P.; Bellenger, V.; Verdu, J. Internal antiplasticization in copolymer and terpolymer networks based on diepoxides, diamines and monoamines. *Polymer* **1990**, *31*, 1787-1792.
- (36) Yang, G.; Fu, S. Y.; Yang, J. P. Preparation and mechanical properties of modified epoxy resins with flexible diamines. *Polymer* **2007**, *48*, 302-310.
- (37) Yang, G.; Zheng, B.; Yang, J. P.; Xu, G. S.; Fu, S. Y. Preparation and cryogenic mechanical properties of epoxy resins modified by poly (ethersulfone). *Journal of Polymer Science Part A: Polymer Chemistry* **2008**, *46*, 612-624.
- (38) Silva, A. A.; Livi, S.; Netto, D. B.; Soares, B. G.; Duchet, J.; Gérard, J. F. New epoxy systems based on ionic liquid. *Polymer* **2013**, *54*, 2123-2129.
- (39) Zhang, C.; Mi, X.; Tian, J.; Zhang, J.; Xu, T. Supported ionic liquid silica as curing agent for epoxy composites with improved mechanical and thermal properties. *Polymers* **2017**, *9*, 478.
- (40) Maka, H.; Spychaj, T.; Pilawka, R. Epoxy resin/ionic liquid systems: the influence of imidazolium cation size and anion type on reactivity and thermomechanical properties. *Industrial & Engineering Chemistry Research* **2012**, *51*, 5197-5206.

- (41) Rahmathullah, M. A. M.; Jeyarajasingam, A.; Merritt, B.; VanLandingham, M.; McKnight, S. H.; Palmese, G. R. Room temperature ionic liquids as thermally latent initiators for polymerization of epoxy resins. *Macromolecules* **2009**, *42*, 3219-3221.
- (42) Soares, B. G.; Livi, S.; Duchet-Rumeau, J.; Gerard, J. F. Preparation of epoxy/MCDEA networks modified with ionic liquids. *Polymer* **2012**, *53*, 60-66.
- (43) Soares, B. G.; Livi, S.; Duchet-Rumeau, J.; Gerard, J. F. Synthesis and characterization of epoxy/MCDEA networks modified with imidazolium-based ionic liquids. *Macromolecular Materials and Engineering* **2011**, *296*, 826-834.
- (44) Radchenko, A. V.; Grange, J.; Vax, A.; Jean-Baptiste-dit-Dominique, F.; Matmour, R.; Grelier, S.; Peruch, F. Facile synthesis of 1, 4-cis-polyisoprene–polypeptide hybrids with different architectures. *Polymer Chemistry* **2019**, *10*, 2456-2468.
- (45) Zhao, W.; Gnanou, Y.; Hadjichristidis, N. Organocatalysis by hydrogen-bonding: a new approach to controlled/living polymerization of α -amino acid N-carboxyanhydrides. *Polymer Chemistry* **2015**, *6*, 6193-6201.
- (46) Galy, J.; Sabra, A.; Pascault, J. P. Characterization of epoxy thermosetting systems by differential scanning calorimetry. *Polymer Engineering & Science* **1986**, *26*, 1514-1523.
- (47) Brun, N.; Hesemann, P.; Laurent, G.; Sanchez, C.; Birot, M.; Deleuze, H.; Backov, R. Macrocellular Pd@ ionic liquid@ organo-Si (HIPE) heterogeneous catalysts and their use for Heck coupling reactions. *New Journal of Chemistry* **2013**, *37*, 157-168.
- (48) McDanel, W. M.; Cowan, M. G.; Barton, J. A.; Gin, D. L.; Noble, R. D. Effect of monomer structure on curing behavior, CO₂ solubility, and gas permeability of ionic liquid-based epoxy-amine resins and ion-gels. *Industrial & Engineering Chemistry Research* **2015**, *54*, 4396-4406.
- (49) Berruet, R.; Vinard, E.; Calle, A.; Tighzert, H.; Chabert, B.; Magloire, H.; Eloy, R. Mechanical properties and biocompatibility of two polyepoxy matrices: DGEBA-DDM and DGEBA-IPD. *Biomaterials* **1987**, *8*, 162-171.
- (50) Ochi, M.; Okazaki, M.; Shimbo, M. Mechanical relaxation mechanism of epoxide resins cured with aliphatic diamines. *Journal of Polymer Science: Polymer Physics Edition* **1982**, *20*, 689-699.

- (51) Ochi, M.; Shimbo, M.; Saga, M.; Takashima, N. Mechanical and dielectric relaxations of epoxide resins containing spiro-ring structure. *Journal of Polymer Science Part B: Polymer Physics* **1986**, *24*, 2185-2195.
- (52) Sindt, O.; Perez, J.; Gerard, J. Molecular architecture-mechanical behaviour relationships in epoxy networks. *Polymer* **1996**, *37*, 2989-2997.
- (53) Williams, J. G. The beta relaxation in epoxy resin-based networks. *Journal of Applied Polymer Science* **1979**, *23*, 3433-3444.
- (54) Awad, W. H.; Gilman, J. W.; Nyden, M.; Harris Jr, R. H.; Sutto, T. E.; Callahan, J.; Trulove, P. C.; DeLong, H. C.; Fox, D. M. Thermal degradation studies of alkyl-imidazolium salts and their application in nanocomposites. *Thermochimica Acta* **2004**, *409*, 3-11.
- (55) Huddleston, J. G.; Visser, A. E.; Reichert, W. M.; Willauer, H. D.; Broker, G. A.; Rogers, R. D. Characterization and comparison of hydrophilic and hydrophobic room temperature ionic liquids incorporating the imidazolium cation. *Green Chemistry* **2001**, *3*, 156-164.
- (56) Anderson, J. L.; Ding, J.; Welton, T.; Armstrong, D. W. Characterizing ionic liquids on the basis of multiple solvation interactions. *Journal of the American Chemical Society* **2002**, *124*, 14247-14254.
- (57) Busi, S.; Lahtinen, M.; Kärnä, M.; Valkonen, J.; Kolehmainen, E.; Rissanen, K. Synthesis, characterization and thermal properties of nine quaternary dialkyldiaralkylammonium chlorides. *Journal of Molecular Structure* **2006**, *787*, 18-30.
- (58) Kosmulski, M.; Gustafsson, J.; Rosenholm, J. B. Thermal stability of low temperature ionic liquids revisited. *Thermochimica Acta* **2004**, *412*, 47-53.
- (59) Ngo, H. L.; LeCompte, K.; Hargens, L.; McEwen, A. B. Thermal properties of imidazolium ionic liquids. *Thermochimica Acta* **2000**, *357*, 97-102.
- (60) Tokuda, H.; Hayamizu, K.; Ishii, K.; Susan, M. A. B. H.; Watanabe, M. Physicochemical properties and structures of room temperature ionic liquids. 2. Variation of alkyl chain length in imidazolium cation. *The Journal of Physical Chemistry B* **2005**, *109*, 6103-6110.
- (61) Tokuda, H.; Ishii, K.; Susan, M. A. B. H.; Tsuzuki, S.; Hayamizu, K.; Watanabe, M. Physicochemical properties and structures of room-temperature ionic liquids. 3. Variation of cationic structures. *The Journal of Physical Chemistry B* **2006**, *110*, 2833-2839.

- (62) Ohtani, H.; Ishimura, S.; Kumai, M. Thermal decomposition behaviors of imidazolium-type ionic liquids studied by pyrolysis-gas chromatography. *Analytical Sciences* **2008**, *24*, 1335-1340.
- (63) Baranyai, K. J.; Deacon, G. B.; MacFarlane, D. R.; Pringle, J. M.; Scott, J. L. Thermal degradation of ionic liquids at elevated temperatures. *Australian Journal of Chemistry* **2004**, *57*, 145-147.
- (64) Patil, R. A.; Talebi, M.; Berthod, A.; Armstrong, D. W. Dicationic ionic liquid thermal decomposition pathways. *Analytical and Bioanalytical Chemistry* **2018**, *410*, 4645-4655.
- (65) Behniafar, H.; Nazemi, M. K. Effect of amine-functionalized silica nanoparticles on thermal and mechanical behaviors of DGEBA/IPD epoxy networks. *Polymer Bulletin* **2017**, *74*, 3739-3749.
- (66) Almeida, H. F.; Lopes-da-Silva, J. A.; Freire, M. G.; Coutinho, J. A. Surface tension and refractive index of pure and water-saturated tetradecyltriethylphosphonium-based ionic liquids. *The Journal of Chemical Thermodynamics* **2013**, *57*, 372-379.
- (67) Carvalho, P. J.; Neves, C. M.; Coutinho, J. A. Surface tensions of bis (trifluoromethylsulfonyl) imide anion-based ionic liquids. *Journal of Chemical & Engineering Data* **2010**, *55*, 3807-3812.
- (68) Kaur, M.; Singh, G.; Kumar, S.; Kang, T. S. Thermally stable microemulsions comprising imidazolium based surface active ionic liquids, non-polar ionic liquid and ethylene glycol as polar phase. *Journal of Colloid and Interface Science* **2018**, *511*, 344-354.
- (69) Badey, J.; Espuche, E.; Sage, D.; Chabert, B.; Jugnet, Y.; Batier, C.; Duc, T. M. A comparative study of the effects of ammonia and hydrogen plasma downstream treatment on the surface modification of polytetrafluoroethylene. *Polymer* **1996**, *37*, 1377-1386.
- (70) Włoch, J.; Terzyk, A. P.; Wiśniewski, M.; Kowalczyk, P. Nanoscale water contact angle on Polytetrafluoroethylene surfaces characterized by molecular Dynamics-Atomic force microscopy imaging. *Langmuir* **2018**, *34*, 4526-4534.
- (71) Yang, B. X.; Pramoda, K. P.; Xu, G. Q.; Goh, S. H. Mechanical reinforcement of polyethylene using polyethylene-grafted multiwalled carbon nanotubes. *Advanced Functional Materials* **2007**, *17*, 2062-2069.
- (72) Parameswaranpillai, J.; Siengchin, S.; George, J.; Jose, S. in *Shape memory polymers, blends and composites*; Springer, **2020**, chapter 1, 1-13.

- (73) Santo, L.; Quadrini, F.; Bellisario, D.; Iorio, L. Applications of Shape-Memory Polymers, and Their Blends and Composites. in *Shape Memory Polymers, Blends and Composites*; Springer, **2020**, 311-329.
- (74) Liu, Y.; Leng, J. Applications of shape-memory polymers in aerospace. in *Shape-memory polymers and multifunctional composites*; © by Taylor @ Francis group, LLC, **2010**, 233-266.
- (75) Beloshenko, V.; Beigelzimer, Y. E.; Borzenko, A.; Varyukhin, V. Shape-memory effect in polymer composites with a compactible filler. *Mechanics of composite materials* **2003**, 39, 255-264.
- (76) Beloshenko, V.; Beygelzimer, Y. E.; Borzenko, A.; Varyukhin, V. Shape memory effect in the epoxy polymer-thermoexpanded graphite system. *Composites Part A: Applied Science and Manufacturing* **2002**, 33, 1001-1006.
- (77) Zhu, J.; Fang, G.; Cao, Z.; Meng, X.; Ren, H. A self-folding dynamic covalent shape memory epoxy and its continuous glass fiber composite. *Industrial & Engineering Chemistry Research* **2018**, 57, 5276-5281.
- (78) Parameswaranpillai, J.; Ramanan, S. P.; George, J. J.; Jose, S.; Zachariah, A. K.; Siengchin, S.; Yorseng, K.; Janke, A.; Pionteck, J. r. PEG-ran-PPG modified epoxy thermosets: a simple approach to develop tough shape memory polymers. *Industrial & Engineering Chemistry Research* **2018**, 57, 3583-3590.
- (79) Xie, T.; Rousseau, I. A. Facile tailoring of thermal transition temperatures of epoxy shape memory polymers. *Polymer* **2009**, 50, 1852-1856.
- (80) Arnebold, A.; Hartwig, A. Fast switchable, epoxy based shape-memory polymers with high strength and toughness. *Polymer* **2016**, 83, 40-49.
- (81) Lützen, H.; Gesing, T. M.; Kim, B. K.; Hartwig, A. Novel cationically polymerized epoxy/poly (ϵ -caprolactone) polymers showing a shape memory effect. *Polymer* **2012**, 53, 6089-6095.
- (82) Rousseau, I. A. Challenges of shape memory polymers: A review of the progress toward overcoming SMP's limitations. *Polymer Engineering & Science* **2008**, 48, 2075-2089.
- (83) Feldkamp, D. M.; Rousseau, I. A. Effect of the deformation temperature on the shape-memory behavior of epoxy networks. *Macromolecular Materials and Engineering* **2010**, 295, 726-734.

- (84)Jing, X.; Liu, Y.; Liu, Y.; Liu, Z.; Tan, H. Toughening-modified epoxy-amine system: Cure kinetics, mechanical behavior, and shape memory performances. *Journal of Applied Polymer Science* **2014**, *131*, 40853 (1-7).
- (85)Wu, X. L.; Kang, S. F.; Xu, X. J.; Xiao, F.; Ge, X. L. Effect of the crosslinking density and programming temperature on the shape fixity and shape recovery in epoxy-anhydride shape-memory polymers. *Journal of Applied Polymer Science* **2014**, *131*, 40559 (1-10).
- (86)Ponyrko, S.; Donato, R.; Matějka, L. Tailored high performance shape memory epoxy-silica nanocomposites. Structure design. *Polymer Chemistry* **2016**, *7*, 560-572.
- (87)Yuan, C.; Guo, J.; Yan, F. Shape memory poly (ionic liquid) gels controlled by host-guest interaction with β -cyclodextrin. *Polymer* **2014**, *55*, 3431-3435.
- (88)Du, H.; Liu, X.; Yu, Y.; Xu, Y.; Wang, Y.; Liang, Z. Microwave-Induced Poly (ionic liquid)/Poly (vinyl alcohol) Shape Memory Composites. *Macromolecular Chemistry and Physics* **2016**, *217*, 2626-2634.
- (89)Leng, J.; Wu, X.; Liu, Y. Effect of a linear monomer on the thermomechanical properties of epoxy shape-memory polymer. *Smart Materials and Structures* **2009**, *18*, 095031.
- (90)Xiao, X.; Kong, D.; Qiu, X.; Zhang, W.; Liu, Y.; Zhang, S.; Zhang, F.; Hu, Y.; Leng, J. Shape memory polymers with high and low temperature resistant properties. *Scientific Reports* **2015**, *5*, 1-12.
- (91)Xiao, X.; Kong, D.; Qiu, X.; Zhang, W.; Liu, Y.; Zhang, S.; Zhang, F.; Hu, Y.; Leng, J. Shape memory polymers with high and low temperature resistant properties. *Scientific Reports* **2015**, *5*, 14137.
- (92)Ni, Y.; Zheng, S. Epoxy resin containing octamaleimidophenyl polyhedral oligomeric silsesquioxane. *Macromolecular Chemistry and Physics* **2005**, *206*, 2075-2083.
- (93)Ni, Y.; Zheng, S.; Nie, K. Morphology and thermal properties of inorganic-organic hybrids involving epoxy resin and polyhedral oligomeric silsesquioxanes. *Polymer* **2004**, *45*, 5557-5568.
- (94)Greaves, T. L.; Drummond, C. J. Solvent nanostructure, the solvophobic effect and amphiphile self-assembly in ionic liquids. *Chemical Society Reviews* **2013**, *42*, 1096-1120.
- (95)He, Z.; Alexandridis, P. Nanoparticles in ionic liquids: interactions and organization. *Physical Chemistry Chemical Physics* **2015**, *17*, 18238-18261.

- (96) Ueno, K.; Watanabe, M. From colloidal stability in ionic liquids to advanced soft materials using unique media. *Langmuir* **2011**, 27, 9105-9115.
- (97) Fonseca, G. S.; Machado, G.; Teixeira, S. R.; Fecher, G. H.; Morais, J.; Alves, M. C.; Dupont, J. Synthesis and characterization of catalytic iridium nanoparticles in imidazolium ionic liquids. *Journal of Colloid and Interface Science* **2006**, 301, 193-204.
- (98) Zhou, Y.; Antonietti, M. Synthesis of very small TiO₂ nanocrystals in a room-temperature ionic liquid and their self-assembly toward mesoporous spherical aggregates. *Journal of the American Chemical Society* **2003**, 125, 14960-14961.
- (99) Shim, Y.; Kim, H. J. Solvation of carbon nanotubes in a room-temperature ionic liquid. *Acs Nano* **2009**, 3, 1693-1702.
- (100) Donato, R.; Perchacz, M.; Ponyrko, S.; Donato, K.; Schrekker, H.; Beneš, H.; Matějka, L. Epoxy-silica nanocomposite interphase control using task-specific ionic liquids via hydrolytic and non-hydrolytic sol-gel processes. *RSC Advances* **2015**, 5, 91330-91339.
- (101) Perchacz, M.; Donato, R. K.; Seixas, L.; Zhigunov, A.; Konefał, R.; Serkis-Rodzeń, M.; Beneš, H. Ionic Liquid-Silica Precursors via Solvent-Free Sol-Gel Process and Their Application in Epoxy-Amine Network: A Theoretical/Experimental Study. *ACS Applied Materials & Interfaces* **2017**, 9, 16474-16487.
- (102) Wu, Q.; Zhang, C.; Liang, R.; Wang, B. Combustion and thermal properties of epoxy/phenyltrisilanol polyhedral oligomeric silsesquioxane nanocomposites. *Journal of Thermal Analysis and Calorimetry* **2010**, 100, 1009-1015.
- (103) Laik, S.; Galy, J.; Gérard, J. F.; Monti, M.; Camino, G. Fire behaviour and morphology of epoxy matrices designed for composite materials processed by infusion. *Polymer Degradation and Stability* **2016**, 127, 44-55.
- (104) Li, G. Z.; Wang, L.; Toghiani, H.; Daulton, T. L.; Koyama, K.; Pittman, C. U. Viscoelastic and mechanical properties of epoxy/multifunctional polyhedral oligomeric silsesquioxane nanocomposites and epoxy/ladderlike polyphenylsilsesquioxane blends. *Macromolecules* **2001**, 34, 8686-8693.
- (105) Liu, H.; Zheng, S.; Nie, K. Morphology and thermomechanical properties of organic-inorganic hybrid composites involving epoxy resin and an incompletely condensed polyhedral oligomeric silsesquioxane. *Macromolecules* **2005**, 38, 5088-5097.

- (106) Deng, Y.; Bernard, J.; Alcouffe, P.; Galy, J.; Dai, L.; Gérard, J. F. Nanostructured hybrid polymer networks from in situ self-assembly of RAFT-synthesized POSS[®]-based block copolymers. *Journal of Polymer Science Part A: Polymer Chemistry* **2011**, *49*, 4343-4352.
- (107) Abad, M. J.; Barral, L.; Fasce, D. P.; Williams, R. J. Epoxy networks containing large mass fractions of a monofunctional polyhedral oligomeric silsesquioxane (POSS[®]). *Macromolecules* **2003**, *36*, 3128-3135.
- (108) Zucchi, I. A.; Galante, M. J.; Williams, R. J.; Franchini, E.; Galy, J.; Gérard, J. F. Monofunctional epoxy-POSS dispersed in epoxy-amine networks: Effect of a prereaction on the morphology and crystallinity of POSS[®] domains. *Macromolecules* **2007**, *40*, 1274-1282.
- (109) Cartier, H.; Chopin, A.; Perego, C. Radiation crosslinking of halogen-free flame retardant polymer. US 7423,080 B2, **2008**.
- (110) Wang, X.; Hu, Y.; Song, L.; Xing, W.; Lu, H. Thermal degradation behaviors of epoxy resin/POSS[®] hybrids and phosphorus-silicon synergism of flame retardancy. *Journal of Polymer Science Part B: Polymer Physics* **2010**, *48*, 693-705.
- (111) Zanetti, M.; Camino, G.; Canavese, D.; Morgan, A. B.; Lamelas, F. J.; Wilkie, C. A. Fire retardant halogen-antimony-clay synergism in polypropylene layered silicate nanocomposites. *Chemistry of Materials* **2002**, *14*, 189-193.
- (112) Bizet, S.; Galy, J.; Gérard, J. F. Structure-property relationships in organic-inorganic nanomaterials based on methacryl-POSS[®] and dimethacrylate networks. *Macromolecules* **2006**, *39*, 2574-2583.
- (113) Hirata, T.; Kashiwagi, T.; Brown, J. E. Thermal and oxidative degradation of poly (methyl methacrylate): weight loss. *Macromolecules* **1985**, *18*, 1410-1418.
- (114) Mantz, R.; Jones, P.; Chaffee, K.; Lichtenhan, J.; Gilman, J.; Ismail, I.; Burmeister, M. Thermolysis of polyhedral oligomeric silsesquioxane (POSS[®]) macromers and POSS[®]-siloxane copolymers. *Chemistry of Materials* **1996**, *8*, 1250-1259.
- (115) Tomczak, S. J.; Marchant, D.; Svejda, S.; Minton, T. K.; Brunsvold, A. L.; Gouzman, I.; Grossman, E.; Schatz, G. C.; Troya, D.; Sun, L. Properties and improved space survivability of POSS[®] (polyhedral oligomeric silsesquioxane) polyimides. *MRS Online Proceedings Library (OPL)* **2004**, 851.

- (116) Kim, K.; Lichtenhan, J. D.; Otaigbe, J. U. Facile route to nature inspired hydrophobic surface modification of phosphate glass using polyhedral oligomeric silsesquioxane with improved properties. *Applied Surface Science* **2019**, 470, 733-743.
- (117) Guo, Q.; Han, Y.; Wang, H.; Xiong, S.; Sun, W.; Zheng, C.; Xie, K. Flame retardant and stable Li_{1.5}Al_{0.5}Ge_{1.5}(PO₄)₃-supported ionic liquid gel polymer electrolytes for high safety rechargeable solid-state lithium metal batteries. *The Journal of Physical Chemistry C* **2018**, 122, 10334-10342.
- (118) Liu, Q.; Geng, Z.; Han, C.; Fu, Y.; Li, S.; He, Y. b.; Kang, F.; Li, B. Challenges and perspectives of garnet solid electrolytes for all solid-state lithium batteries. *Journal of Power Sources* **2018**, 389, 120-134.
- (119) Pandian, A. S.; Chen, X. C.; Chen, J.; Lokitz, B. S.; Ruther, R. E.; Yang, G.; Lou, K.; Nanda, J.; Delnick, F. M.; Dudney, N. J. Facile and scalable fabrication of polymer-ceramic composite electrolyte with high ceramic loadings. *Journal of Power Sources* **2018**, 390, 153-164.
- (120) Wang, A.; Liu, X.; Wang, S.; Chen, J.; Xu, H.; Xing, Q.; Zhang, L. Polymeric ionic liquid enhanced all-solid-state electrolyte membrane for high-performance lithium-ion batteries. *Electrochimica Acta* **2018**, 276, 184-193.
- (121) Pal, P.; Ghosh, A. Investigation of ionic conductivity and relaxation in plasticized PMMA-LiClO₄ solid polymer electrolytes. *Solid State Ionics* **2018**, 319, 117-124.
- (122) Obadia, M. M.; Mudraboyina, B. P.; Serghei, A.; Montarnal, D.; Drockenmuller, E. Reprocessing and recycling of highly cross-linked ion-conducting networks through transalkylation exchanges of C-N bonds. *Journal of the American Chemical Society* **2015**, 137, 6078-6083.
- (123) Obadia, M. M.; Mudraboyina, B. P.; Serghei, A.; Phan, T. N.; Gimes, D.; Drockenmuller, E. Enhancing properties of anionic poly (ionic liquid)s with 1, 2, 3-triazolium counter cations. *ACS Macro Letters* **2014**, 3, 658-662.
- (124) Porcarelli, L.; Vlasov, P. S.; Ponkratov, D. O.; Lozinskaya, E. I.; Antonov, D. Y.; Nair, J. R.; Gerbaldi, C.; Mecerreyes, D.; Shaplov, A. S. Design of ionic liquid like monomers towards easy-accessible single-ion conducting polymer electrolytes. *European Polymer Journal* **2018**, 107, 218-228.

- (125) Wang, X.; Zhu, H.; Girard, G. M.; Yunis, R.; MacFarlane, D. R.; Mecerreyes, D.; Bhattacharyya, A. J.; Howlett, P. C.; Forsyth, M. Preparation and characterization of gel polymer electrolytes using poly (ionic liquids) and high lithium salt concentration ionic liquids. *Journal of Materials Chemistry A* **2017**, *5*, 23844-23852.
- (126) Jung, G. Y.; Choi, J. H.; Lee, J. K. Thermal behavior and ion conductivity of polyethylene oxide/polyhedral oligomeric silsesquioxane nanocomposite electrolytes. *Advances in Polymer Technology* **2015**, *34*, 21499(1-6).
- (127) Lu, Q.; Dong, L.; Chen, L.; Fu, J.; Shi, L.; Li, M.; Zeng, X.; Lei, H.; Zheng, F. Inorganic-organic gel electrolytes with 3D cross-linking star-shaped structured networks for lithium ion batteries. *Chemical Engineering Journal* **2020**, *393*, 124708.
- (128) Heux, L.; Halary, J.; Lauprêtre, F.; Monnerie, L. Dynamic mechanical and ¹³C nmr investigations of molecular motions involved in the β relaxation of epoxy networks based on DGEBA and aliphatic amines. *Polymer* **1997**, *38*, 1767-1778.
- (129) Halawani, N.; Augé, J. L.; Morel, H.; Gain, O.; Pruvost, S. Electrical, thermal and mechanical properties of poly-etherimide epoxy-diamine blend. *Composites Part B: Engineering* **2017**, *110*, 530-541.
- (130) Dyre, J. C.; Schrøder, T. B. Universality of ac conduction in disordered solids. *Reviews of Modern Physics* **2000**, *72*, 873.
- (131) Psarras, G. Hopping conductivity in polymer matrix-metal particles composites. *Composites Part A: Applied Science and Manufacturing* **2006**, *37*, 1545-1553.
- (132) Emmert, S.; Wolf, M.; Gulich, R.; Krohns, S.; Kastner, S.; Lunkenheimer, P.; Loidl, A. Electrode polarization effects in broadband dielectric spectroscopy. *The European Physical Journal B* **2011**, *83*, 157-165.
- (133) Chen, H.; Choi, J. H.; Salas-de la Cruz, D.; Winey, K. I.; Elabd, Y. A. Polymerized ionic liquids: the effect of random copolymer composition on ion conduction. *Macromolecules* **2009**, *42*, 4809-4816.
- (134) Hemp, S. T.; Zhang, M.; Allen Jr, M. H.; Cheng, S.; Moore, R. B.; Long, T. E. Comparing ammonium and phosphonium polymerized ionic liquids: thermal analysis, conductivity, and morphology. *Macromolecular Chemistry and Physics* **2013**, *214*, 2099-2107.
- (135) Ye, Y.; Elabd, Y. A. Anion exchanged polymerized ionic liquids: High free volume single ion conductors. *Polymer* **2011**, *52*, 1309-1317.

Chapter V: Conclusions and Perspectives

The aim of this work was to design POSS[®] nanostructures into epoxy networks by using ionic liquids and to study the influence of such nanostructures on the physical properties. POSS[®] is generally not distributed homogeneously and tends to agglomerate. Phase separation could occur between POSS[®] and monomer(s) before and during polymerization depending on the chemical nature and functionality of the organic ligands on the POSS[®] cage. Several POSS[®] carrying one or two ionic liquids were synthesized to prepare *in-situ* nanomaterials from epoxy polymerization leading to “**hybrid**” nanomaterials. The combination of epoxy ionic liquid monomers (ILMs) and IL-modified POSS[®] allows the formation of environmentally friendly epoxy networks with performances induced by both ionic liquid and POSS[®] nanoclusters.

In the first part of this work, polyhedral oligomeric silsesquioxane-supported imidazolium ionic liquid have been synthesized, characterized, and considered as organic-inorganic hybrid nano-objects in order to design nanostructured epoxy-amine networks. Two partially condensed POSS[®]-triol named POSS^{®IB}-triol and POSS^{®Ph}-triol have been covalently grafted with an imidazolium ionic liquid-functionalized silane to get IL-g-POSS^{®IB} and IL-g-POSS^{®Ph} as well as a di-functionalized imidazolium ionic liquid (POSS[®]-N-2IL) starting from POSS[®] bearing two amino-hydrogen functions (POSS[®]-NH₂). The ²⁹Si-NMR and MALDI-TOF mass spectrometry analysis confirmed the obtained different chemical structures, *i.e.*, fully closed and the open cage POSS[®] structure with one IL and two free Si-OH groups. The results of connecting IL with different anions to POSS[®]-triol or POSS[®]-NH₂ showed simultaneously a decrease of the melting temperature and the enhancement of their thermal stability (400 vs 300 °C). The introduction of IL can improve the POSS[®]/epoxy matrix interactions and promote the formation of well-dispersed POSS[®] nanodomains characterized in the case of the mono-functionalized IL POSS[®] by the formation of spherical or ellipsoidal inorganic-rich nanoaggregates with nanometer scale sizes (from 10 to 80 nm). The POSS[®] di-functional IL led to binary morphology composed of nanosized spherical POSS[®]-rich clusters and co-continuous POSS[®]-based phase due to a limit of miscibility generated by the presence of two ionic liquid by POSS[®]. Moreover, all the epoxy networks containing IL-g-POSS[®] or POSS[®]-N-2IL maintain a glass transition temperature close to of the neat epoxy network one.

The second part of this work was dedicated to the incorporation of IL-g-POSS^{®Ph} with two types of counter anions (chloride (Cl⁻) or bis(trifluoromethanesulfonyl)imide (NTf₂⁻)) into epoxy-amine system to improve their properties. The effect of the IL (cation/anion) on the morphology as well as the final properties of IL-g-POSS^{®Ph} modified epoxy networks was investigated. The epoxy networks containing IL-g-POSS^{®Ph} with any nature of anion (Cl⁻ or NTf₂⁻) exhibit high reactivity towards conventional epoxy prepolymers and lead to the formation of polyepoxy networks with epoxy group conversion higher than 90 %. An excellent nanoscale dispersion of POSS^{®Ph} was obtained as spherical nanoscale POSS[®]-rich clusters. The resulting epoxy hybrid O/I networks display excellent properties such as high glass transition (151 - 161 °C), good thermal stability (up than 400 °C), and hydrophobic behavior. Moreover, the combination of IL to POSS^{®Ph}-triol nanoclusters with both types of anion (Cl⁻ or NTf₂⁻) induces a reinforcement effect, *i.e.* an increase of both stiffness and toughness, yield strength, and ability to sustain larger deformation as well as stress at break. In addition, a real synergistic effect between POSS^{®Ph} and ionic liquids take place leading to a systematic improvement of fire retardancy behavior characterized by a significant decrease of the peak of heat release rate (of about 55 %) as well as an enhancement of the ignition time compared to the neat epoxy-amine network.

The final part of this research work is focused on the development of new epoxy thermosets hybrid O/I nanomaterials based on new imidazolum ionic liquid monomers (ILM) and the IL-g-POSS^{®Ph} nanoclusters in order to substitute the conventionally used DGEBA prepolymer which is prepared using toxic and carcinogenic compounds such as bisphenol A and epichlorohydrin. First, ILM monomers display a high reactivity toward amines and the resulting ILM/amine networks possess good thermomechanical properties, higher hydrophobic character, and higher thermal stability. In addition, the mechanical performances of these new epoxy ILM/IPD networks were found to be similar to the reference network (DGEBA/IPD) but such ionic networks demonstrate abilities to have a shape memory behavior with a 100 % recovery in few minutes at moderate temperatures. Secondly, the effect of incorporating IL-g-POSS^{®Ph} nanoclusters with both anions (Cl⁻ or NTf₂⁻) into the epoxy ILM/IPD networks was also investigated. No major difference in morphology with that obtained in the epoxy-amine/IL-g-POSS^{®Ph} networks. In comparison to IL-g-POSS^{®Ph}-modified epoxy/amine networks, a high hydrophobicity close to that of PTFE and an excellent thermal stability with high thermo-oxidative resistance were highlighted for such networks. The networks exhibited a wide broad

temperature rang for their glass transition varying from 45 to 71 °C depending on the nature of the epoxy ILM monomers (ILM1 or ILM2) and POSS^{®Ph}. Finally, high ionic conductivities with excellent electrochemical stability was also obtained with these new ILM/IPD hybrids O/I networks.

These results open new perspectives in the development of a new generation of (multi)functional-dedicated polymer materials for various types of applications such as the ones requiring fire retardancy, high mechanical performances, and shape memory. Moreover, these novel polymers could be investigated more deeply for their ionic conductivities as well as gas barrier properties to be used as solid polymer electrolytes. To evaluate their potential fields of application, several studies must be considered:

- Curing reaction mechanisms between epoxy prepolymer (DGEBA) or epoxy ionic liquid monomers (ILM1, ILM2) and amine in the presence of POSS^{®Ph} require more precise studies in order to obtain a complete understanding about the different reaction steps as well as the state of dispersion of POSS^{®Ph} in the epoxy continuous medium.
- Their excellent hydrophobic behavior is advantageous for coating applications. Corrosion tests are required to really evaluate the potential of such epoxy ionic liquids as well as the epoxy ILM/amine/POSS^{®Ph} systems as protective coatings for metals under various conditions.
- Being well known that the phosphonium ionic liquid presents a high reactivity towards conventional epoxy prepolymers, other associations based on phosphonium ionic liquid cation and phosphinate or phosphate anions with POSS[®] must be studied to investigate their influence on the different properties and especially on the fire behavior.
- Finally, epoxy IL monomers (ILMs) also gained the interests as new components to prepare new generations of epoxies. Thus, it is interesting to have a look to other types of epoxy ILMs prepolymers such as biobased one even with higher epoxy functionality and different natures of anions in order to provide versatile properties to cover a large variety of applications.



FOLIO ADMINISTRATIF

THESE DE L'UNIVERSITE DE LYON OPEREE AU SEIN DE L'INSA LYON

NOM : CHABANE

DATE de SOUTENANCE : 09/07/2021

Prénoms : Houssém

TITRE : INTRODUCTION OF METAL-OXO TYPE NANOSTRUCTURES ASSOCIATED WITH IONIC LIQUIDS FOR THE DESIGN OF MULTI-FUNCTIONAL POLYMER MATERIALS

NATURE : Doctorat

Numéro d'ordre : 2021LYSEI042

Ecole doctorale : Matériaux de Lyon

Spécialité : Matériaux Polymères et Composites

RESUME : Au cours de ces dernières années, des avancées importantes ont été réalisées dans la synthèse, la caractérisation et l'association avec différents polymères, thermoplastiques ou systèmes réactifs (thermodurcissables) de liquides ioniques de nature divers (ammonium, imidazolium ou phosphonium) ouvrent de nouvelles perspectives dans le domaine des matériaux polymères, en particulier celui des réseaux époxyde. En effet, il a été démontré que les liquides ioniques (LI) pouvaient apporter beaucoup aux polymères en se comportant en tant qu'agents nanostructurants, agents interfaciaux de nanocharges (échanges ioniques avec les silicates lamellaires ou greffés sur des nanocharges de silice) ou encore en tant que co-monomères intervenant sur les mécanismes de polymérisation. Des comportements physiques améliorés (mécanique, de surface, de tenue thermique, etc.) peuvent être ainsi obtenus par des approches conventionnelles. Par ailleurs, au cours de nombreuses études, il a été également démontré que des objets organiques-inorganiques (O/I) comme des clusters de type métal-oxo ou POSS® (PolyOligomericSilSexqioxanes) pouvaient être incorporés dans des polymères, en particulier des réseaux de type polyépoxy ou méthacrylates, comme co-monomères et/ou être auto-assemblés sous forme de nanostructures O/I susceptibles de leur conférer des fonctionnalités spécifiques. Ce travail de thèse présente donc la préparation, la caractérisation et la modification de réseaux époxy/amine ou époxy LI/amine avec des POSS® modifiés par des Lis. Dans un premier temps, ce travail est dédié à étudier l'effet du greffage des liquides ioniques d'imidazolium sur des POSS® porteurs de différents ligands organiques (isobutyle ou phényle) sur la formation de nanodomains POSS® uniformément bien dispersés dans des réseaux époxy-amine. Dans la deuxième partie, l'effet de la nanostructuration des LI-g-POSS®^{Ph} sur les propriétés de réseaux époxy/amine, à savoir leur stabilité thermique, leurs propriétés de surface, leur comportement mécanique et leur tenue au feu sera étudié. Dans la dernière section, de nouveaux réseaux époxy-LI hybride O/I ont été mis en œuvre. Pour cela des sels diépoxydés (LIMs) ont été synthétisés puis copolymérisés avec un durcisseur diamine (IPD) avec ou sans la présence de POSS®^{Ph}-triol ou LI-g-POSS®^{Ph} afin de concevoir des réseaux époxy-LI hybride (LIM/amine/LI-g-POSS®^{Ph}) souples présentant des propriétés très intéressantes par rapport des réseaux époxy classiques.

Mots clés : Liquide Ionique; Polyhedral Oligomeric Silsesquioxane (POSS®); Epoxy; Nanomatériaux Organiques-Inorganiques, Réseau Nanostructuré, Mémoire de Forme, Liquide ionique Monomère, Résistance au Feu, Conductivité Ionique

Laboratoire (s) de recherche : Ingenierie des Matériaux Polymères - UMR 5223 INSA de Lyon

Directeur de thèse: GERARD Jean-François

Co-directeurs de these : DUCHET-RUMEAU Jannick - LIVI Sébastien

Président de jury : BONGIOVANNI Roberta

Composition du jury : BONGIOVANNI Roberta, McGRIL Terry, TOURNILHAC François, DUSKOVA-SMRCKOVA Miroslava, GERARD Jean-François, DUCHET-RUMEAU Jannick, LIVI Sébastien.